

**Some pages of this thesis may have been removed for copyright restrictions.**

If you have discovered material in AURA which is unlawful e.g. breaches copyright, (either yours or that of a third party) or any other law, including but not limited to those relating to patent, trademark, confidentiality, data protection, obscenity, defamation, libel, then please read our [Takedown Policy](#) and [contact the service](#) immediately

**BTX EXTRACTION BY SULFOLANE IN A  
MIXER-SETTLER CASCADE**

**by**

**Mohamad Said Hassan Fandary**

**Doctor of Philosophy**

**THE UNIVERSITY OF ASTON IN BIRMINGHAM**

**August 1988**

This copy of the thesis has been supplied on condition that anyone who consults it is understood to recognise that its copyright rests with its author and that no quotation from the thesis and no information derived from it may be published without the author's prior written consent.

The University of Aston in Birmingham

## BTX EXTRACTION BY SULFOLANE IN A MIXER-SETTLER CASCADE

Mohamad Said Hassan Fandary

Doctor of Philosophy

1988

### Summary

The literature relating to the extraction of the aromatics, benzene, toluene and xylene (BTX) using different commercial solvents, and to mixer-settler design and performance, has been reviewed.

Liquid-liquid equilibria of the ternary systems: hexane-benzene-sulfolane, n-heptane-toluene-sulfolane, and octane-xylene-sulfolane were determined experimentally at temperatures of 30°C, 35°C, and 40°C. The work was then extended to a multicomponent system. The data were correlated by using Hand's method and were found to be in a good agreement with theoretical predictions using the UNIFAC method.

A study was made of the performance of a 10-stage laboratory mixer-settler cascade for the extraction of BTX from a synthetic reformat utilizing sulfolane as a solvent. Murphree stage efficiency decreased with stage number but 99% extraction was achievable within 4 stages. The effects of temperature, phase ratio, and agitator speed were investigated. The efficiency increased with agitator speed but >1050 rpm resulted in secondary haze formation. An optimum temperature of 30°C was selected from the phase equilibria; the optimum solvent: feed ratio was 3:1 for 4 stages. The experimental overall mass transfer coefficients were compared with those predicted from single drop correlations and were in all cases greater, by a factor of 1.5 to 3, due to the surface renewal associated with drop break-up and coalescence promoted by agitation.

A similar investigation was performed using real reformat from the Kuwait Oil Company. The phase ratios were in the range 0.5 to 1 to 3.25 to 1, the agitator speed 1050 rpm, and the operating temperature 30°C. A maximum recovery of 99% aromatics was achieved in 4 stages at a phase ratio of 3.25 to 1. A backflow model was extended to simulate conditions in the mixer-settler cascade with this multicomponent system. Overall mass transfer coefficients were estimated by obtaining the best fit between experimental and predicted concentration profiles. They were up to 10% greater than those with the synthetic feed but close agreement was not possible because the distribution coefficient and phase ratio varied with stage number.

Sulfolane was demonstrated to be an excellent solvent for BTX recovery and a mixer-settler cascade was concluded to be a technically viable alternative to agitated columns for this process.

### Key Words

BTX, Liquid-Liquid Extraction, Mixer-Settler Cascade, Sulfolane.

DEDICATED TO

MY COUNTRY

MY PARENTS

MY WIFE

AND

MY CHILDREN



## ACKNOWLEDGMENTS

The author would like to express his thanks to the following people :

Dr. C. J. Mumford for his help, and guidance during his supervision of the research program .

Prof. M. A. Fahim for his help, suggestions, and Supervision.

F. S. Mjalli for his valuable instruction in computing techniques .

Dr. A. H. Salem for his encouragement and constructive criticisms .

## TABLE OF CONTENTS

	Page
Chapter 1: INTRODUCTION	16
Chapter 2: AROMATICS (BTX)-ALIPHATICS SEPARATION	20
2.1 Introduction	21
2.2 Raw Material Sources for Aromatics: Upstream Treatment	21
2.3 Reforming for Specific BTX Compounds	28
2.4 BTX Separation Processes	28
2.4.1 Early Processes	28
2.4.2 The Udex Process	33
2.4.3 Arosolvan Process	37
2.4.4 Tetra Process	40
2.4.5 B.T.X Extraction with Sulfolane	42
2.4.5.1 Extractor	45
2.4.5.2 Extractor Stripper	45
2.4.5.3 Extract Recovery Column	45
2.4.5.4 Water Wash Tower	45
2.4.5.5 Combination of Extraction and Extractive Stripping	46
Chapter 3: SOLVENT PROPERTIES	50
3.1 Solvent Properties	51
3.1.1 Selectivity	52
3.1.2 Capacity "Solvent Power"	53
3.1.3 Optimum Solvent Properties	55
3.1.4 Secondary Solvent Properties	58
3.2 Liquid Liquid Equilibria	60
3.2.1 Equilibrium Data	60
3.2.2 Multicomponent Equilibrium Data	63
3.3 The Distribution Coefficient	64
3.4 Solute and Solvent Recovery	67

<b>Chapter 4:</b>	<b>MASS TRANSFER FUNDAMENTALS</b>	<b>69</b>
4.1	Mass Transfer, into or Out Of, Droplets	70
4.2	Mass Transfer During Drop Formation	73
4.3	Mass Transfer During Drop Travel Through the Continuous Phase	77
4.4	Mass Transfer in the Dispersed Phase	79
4.4.1	Stagnant Droplets.	79
4.4.2	Circulating Droplets	80
4.4.3	Oscillating Droplets	82
4.5	Mass Transfer in the Continuous Phase	84
4.5.1	To, and From, Stagnant Droplets	84
4.5.2	To, and From, Circulating Droplets	87
4.5.3	To, and From, Oscillating droplets	89
4.6	Mass Transfer During Phase Separation	90
4.7	The Driving Force	91
4.8	Mass Transfer and Interfacial Area	93
4.9	Overall Mass Transfer Coefficient	101
<b>Chapter 5:</b>	<b>LIQUID-LIQUID EXTRACTION EQUIPMENT CLASSIFICATION</b>	<b>103</b>
5.1	Equipment Classification	104
5.2	Equipment Selection	104
5.3	Advantages and Disadvantages of Mixer Settlers	107
<b>Chapter 6:</b>	<b>MIXER-SETTLER EQUIPMENT</b>	<b>113</b>
6.1	Mixer Settler Characteristics	114
6.2	Mixer Design	114
6.2.1	Mechanical Mixers	118
6.2.1.1	Paddle Mixers	118
6.2.1.2	Propeller mixers	120
6.2.1.3	Turbine Mixers	120

6.3 Drop Size Distribution	124
6.4 Power Requirement	126
6.5 Dimensional Analysis	127
6.6 Phase Inversion	128
6.7 Dispersion in Mixer	131
6.8 Settler Design Fundamentals	132
6.8.1 Coalescence on Surfaces	137
6.8.2 Coalescence of Secondary Hazes	138
6.9 Mixer-Settler Arrangements	138
6.10 Application of Mixer-Settlers	141
6.11 Stage Efficiency	148
 Chapter 7: MATHEMATICAL MODELS FOR SOLVENT EXTRACTION	153
7.1 Introduction	154
7.2 Diffusion Model	154
7.2.1 Derivation of Equations	155
7.2.1.1 Continuous Phase "Aqueous Phase"	155
7.2.1.2 Dispersed Phase "Organic Phase"	159
7.3 Back Flow Model	162
7.3.1 Model No. 1	163
7.3.1.1 Continuous Phase "Aqueous Phase"	163
7.3.1.2 Dispersed Phase "Organic Phase"	165
7.3.2 Model No. 2	167
7.3.3 Model No. 3, Newly Developed	172
 Chapter 8: EXPERIMENTAL INVESTIGATION AND PHASE EQUILIBRIA	179
8.1 Objectives	180
8.2 Description of Equipment	180
8.3 Material Used	183
8.4 Physical Properties of Materials	185

8.5 Phase Equilibrium Data	187
8.6 Correlation of Data <i>Extraction in a Mixer-Settler</i>	196
8.7 Computation of LLE Data by UNIFAC	199
8.8 Results and Discussion	203
<b>Chapter 9: RESULTS OF LIQUID LIQUID EXTRACTION STUDIES</b>	207
9.1 Introduction	208
9.2 Diffusivities	208
9.3 Interfacial Tension	209
9.4 Calibration Techniques	210
9.5 Operating Procedure	211
9.6 Results and Discussion	213
9.6.1 Hydrodynamics	213
Hold-Up	213
Drop Size	216
Phase Inversion	220
9.6.2 Mass Transfer Results	226
9.6.3 Calculation of Overall Mass Transfer Coefficient	231
<b>Chapter 10: EXTRACTION OF ACTUAL REFORMATE</b>	235
10.1 Introduction	236
10.2 Production of Aromatics	237
10.3 Parameters Investigated	239
10.4 Results and Discussion	240
10.5 Mathematical Modeling Results	249
<b>Chapter 11: CONCLUSIONS AND RECOMMENDATIONS FOR FUTURE WORK</b>	252
11.1 Conclusions	253
11.1.1 Sulfolane as a Solvent	253
11.1.2 Mixer Settler Characteristics	253
11.1.2.1 General	255

11.1.2.2 BTX Extraction in a Mixer- Settler Cascade	254
11.1.3 Prediction and Modelling of Mass Transfer Performance	254
11.2 Recommendations for Future Work	256
Appendicies	259
Nomenclature	289
References	298

## LIST OF FIGURES

- Fig 2.1 Uses of BTX Compounds
- Fig 2.2 Octane Rating as a Function of Aromatics in Reformate
- Fig 2.3 Main Reactions of Catalytic Reforming
- Fig 2.4 Boiling Points of  $C_6 - C_9$  Hydrocarbons
- Fig 2.5 Azeotropy in Nonaromatic Hydrocarbon-Benzene Binary System
- Fig 2.6 Benzene-Heptane-Methylcyclohexane Vapour Pressure vs Temperature
- Fig 2.7 Schematic Flow Diagram of Udex Process
- Fig 2.8 Capacity and Selectivity of Solvents
- Fig 2.9 Arosolvan Process with NMP/Glycol
- Fig 2.10 Arosolvan Process with NMP/Water
- Fig 2.11 Tetra Process
- Fig 2.12 Sulfolane Extractor Unit
- Fig 2.13 Liquid-liquid Equilibrium Relative Solubility of Hydrocarbons in Anhydrous Sulfolane
- Fig 2.14 Vapor Liquid Equilibrium Relative Volatility of Hydrocarbons in Anhydrous Sulfolane.
- Fig 3.1 Survey of Solvents Traverse Through Practical Temperature Range .
- Fig 3.2 Light/Heavy Selectivity Of Solvent Traverse Through Practical Temperature Range
- Fig 3.3 Types of Binary Liquid-liquid Equilibria
- Fig 3.4 Types of Ternary Liquid-liquid Equilibria
- Fig 3.5 Multicomponent System Represented on an Equilateral Triangular Diagram
- Fig 4.1 Specific Area at Vessel Bottom  $O=0.02, m$
- Fig 4.2 Drop size Distribution;  $OD=0.0407, 0.076 m$ , Impeller 325 rpm
- Fig 4.3 Continuous Phase Mass Transfer Coefficient at Different Reynold Numbers

- Fig 4.4 Mean Specific Area : Flow Rate = 0.249 kg/sec  
Re=28500 to 33800 .
- Fig 4.5 Influence of Dispersed Phase Hold-up on  $k_c$ ,  
Flow Rate =0.249 kg/sec, Re= 28500 to 33200
- Fig 4.6 Influence of Baffles and Impeller Power on  $k_c$ ,  
Flow Rate =0.185 to 0.249 kg/sec, 0.065 (Org. /  
Water)
- Fig 4.7 Effect of Baffles on  $k_c$  at Different Impeller  
Power, Flow Rate =0.24 kg/sec, 0.38 (Org. / Water)
- Fig 6.1 Broad Classification of Mixer-Settlers
- Fig 6.2 Propeller with Baffles: Axial Flow Pattern
- Fig 6.3 Flat Blade Turbine with Baffles: Radial Flow  
Pattern
- Fig 6.4 Fundamental Geometric Variables in Agitated Tanks
- Fig 6.5 Flow Patterns for Propeller in Agitated Off-Center  
Position without Baffles
- Fig 6.6 Main Impeller Turbine Designs
- Fig 6.7 Impeller Characteristics and Power
- Fig 6.8 Shape of Actual and Idealized Coalescence Wedges
- Fig 6.9 Baffled Settler
- Fig 6.10 a) Typical Box Type Mixer-Settler  
b) Two-stage Mixer-Settler Extractor  
c) Kemira Mixer-settler  
d) Mensing Design for Mixer-settler Extractor  
e) Schematic Plan of a 4-stage Holley-Mott unit  
f) Three Adjacent stages of Pump-Mix Mixer Settler
- Fig 6.11 Vertical Mixer-Settler
- Fig 6.12 Principal Features of General Mills Mixer-Settler
- Fig 6.13 Stage Efficiency of Single Stage
- Fig 7.1 Diffusion Model: Material Balance Over Differen-  
tial Section
- Fig 7.2 Backflow Model: Material Balance on Finite  
Distance  $dz$
- Fig 7.3 Schematic Diagram of an n-Stage Mixer Settler Unit
- Fig 8.1 Flow Diagram of 10-stage Mixer-Settler Cascade
- Fig 8.2 Typical Settler



- Fig 8.3 Solubility Diagram for System Benzene-Hexane Sulfolane at 30°C
- Fig 8.4 Solubility Diagram for System Toluene-Heptane Sulfolane at 30°C
- Fig 8.5 Solubility Diagram for System Xylene-Octane- Sulfolane at 30°C
- Fig 8.6 Solubility Diagram for System Aromatics Nonaromatic-Sulfolane at 30°C
- Fig 8.7 Solubility Diagram for System Aromatics Nonaromatic-Sulfolane at 35°C, 40°C
- Fig 8.8 Equilibrium Curve for System Aromatics- Non aromatics Sulfolane at 30°C
- Fig 8.9 Hand's Correlation for the System Aromatics- Nonaromatics- Sulfolane at 30°C, 35°C , 40°C
- Fig 8.10 Comparison of Predicted and Experimental Solubility Diagram at 30°C
- Fig 9.1 Variation of Efficiency with Stage Number in the Cascade
- Fig 9.2 Percentage Recovery of Aromatics as a Function of Stage Number in the Cascade
- Fig 9.3 Effect of Mixer Speed on Fractional Holdup in the Mixer (stage No. 4)
- Fig 9.4 Variation of  $d_{32}$  with Holdup at Constant Mixer Speed (Stage No. 4)
- Fig 9.5 Predicted  $d_{32}$  vs Experimental  $d_{32}$
- Fig 9.6 Variation of  $d_{32}$  with Stage No. at Different Phase Ratio
- Fig 9.7 Continuous Phase Throughout vs Dispersed Phase Throughout at Phase Inversion
- Fig 9.8 Total Recovery of Aromatics as a Function of Phase Ratio
- Fig 9.9 The Effect of Mixer Speed on the Recovery of Aromatics at Different Temperatures
- Fig 9.10 Variation of Stage Efficiency with Stage Number at Different Temperatures and Mixer Speeds
- Fig 9.11 Variation of Efficiency with Stage Number at Phase Ratio 3:1
- Fig 10.1 Percentage Aromatics Recovery vs Stage Number at Different Phase Ratios

- Fig 10.2 Percentage Recovery of Aromatics vs Phase Ratio Percentages.
- Fig 10.3 Percentage Recovery of Aromatic Components vs Phase Ratio
- Fig 10.4 Sauter Mean Diameter  $d_{32}$  vs Hold up
- Fig 10.5 Hold up vs Flow Rate of Dispersed Phase
- Fig 10.6 Flow Rate of Dispersed Phase vs Stage Number
- Fig 10.7 Sauter Mean Diameter vs Stage Number for Real and Synthetic Reformate
- Fig 10.8 Experimental Aromatics Recovery vs Model Results at Phase Ratio 2:1
- Fig 10.9 Experimental Aromatics Recovery vs Model Results at Phase Ratio 3:1
- Plate 1 Mixer Settler cascade (10 stages)

## LIST OF TABLES

Table 2.1	Properties of Crude Oil Straight-Run Fractions
Table 2.2	Characteristic Features of BTX Extraction Processes
Table 3.1	Light- HeavySelectivity at 100°C, Solvent;Sulfolane
Table 4.1	Dispersed Phase Mass Transfer Correlations During Drop Travel
Table 5.1	Classification of Extractors Depending Upon The Type of Agitation
Table 5.2	Summary of Features and Fields of Industrial Application of Commercial Extractors
Table 5.3	Design Considerations and Process Parameters of Extractor Selection
Table 6.1	Mixer Settler Geometries
Table 6.2	Comparison of Mixer-Settler Designs
Table 8.1	Physical Properties of Sulfolane
Table 8.2	Experimental LLE Compositions for n-Hexane- Benzene- Sulfolane at 30°C
Table 8.3	Experimental LLE Compositions for n-Heptane- Toluene-Sulfolane at 30°C
Table 8.4	Experimental LLE Compositions for n-Octane- Xylene-Sulfolane at 30°C
Table 8.5	Experimental LLE Compositions for Non- aromatics-Aromatics-Sulfolane at 30°C
Table 8.6	Experimental LLE Compositions for Nonaromatics-Aromatics-Sulfolane at 35°C
Table 8.7	Experimental LLE Compositions for Nonaromatics- Aromatics-Sulfolane at 40°C
Table 8.8	Predicted LLE Compositions at 30°C for Nonaromatics- Aromatics- Sulfolane
Table 9.1	Exponents on Groups Affecting Drop size
Table 9.2	Predicted and Experimental Overall Mass Transfer Coefficients
Table 10.1	Reformate Composition

## APPENDICES

- (I) Refractive Indices, and Densities of Hydrocarbon Components
- (II) UNIFAC Computer Program
- (III) Diffusivities
- (IV) Concentration Calibration Curves
- (V) Rotameter Calibration Curve
- (VI) Reformate GLC Analysis Results
- (VII) Model (3) Results
- (VIII) 'Correlation of Phase Equilibrium of Naphtha Reformate with Sulfolane', Hassan, M.S., Fahim, M.A., Mumford, C.J., Jnl. of Chem. & Eng. Data, 32, 2, 1988, 162-165

## CHAPTER 1

---

### INTRODUCTION

The aromatic hydrocarbons; benzene, toluene and xylene (BTX), are amongst the most important raw materials in the petrochemical industry. The greatest demand is for benzene, of which 40% is processed to styrene, 20% to caprolactam and to phenol, and the remainder to maleic anhydride, aniline and a number of other chemical compounds. The consumption of xylene, which is almost exclusively processed to o-phthalic acid and tetraphthalic acid, takes second place. The considerably lower demand for toluene is reflected by its distinctly lower price. Toluene is used for many syntheses in the pharmaceutical and dyestuff industries but the majority is converted to benzene by dealkylation.

The development of liquid-liquid extraction for separation of aromatics, as a class, from other hydrocarbon types permitted the simultaneous extraction of BTX aromatics, substantially free of non-aromatic impurities, from broad-boiling range, reformed naphthas. The first efficient method was the Udex process, using a glycol-based solvent. This was introduced in 1952 and was superior because, for the first time, a wide-boiling feed-stock could be treated directly to yield BTX products of high purity without expensive pre-fractionation.

The Udex process used aqueous solutions of diethylene glycol (DEG) or triethylene glycol (TEG). In 1968, Union Carbide selected tetraethylene glycol as

the best glycol for this process. The high selectivity and high capacity of this solvent were demonstrated by the low solvent to feed ratio, and low reflux to feed required and by the high recoveries of all aromatics, high purity of aromatics, and low operating costs achieved. Several other aromatic extraction solvents are also available to the industry, e.g., the Arosolvan process used N-methyl pyrrolidone (NMP) which has a low solidification point of  $-24^{\circ}\text{C}$ . NMP has a sufficiently high density to facilitate gravity separation, it has a low viscosity, and very high capacity but a low selectivity.

In 1959, Shell patented a new BTX aromatic extraction process based on 'Sulfolane' solvent, (tetrahydro-thiophene 1, 1-dioxide). The success of the Sulfolane process is demonstrated by the fact that since 1965 more than 65 units, representing over 430,000 barrels/day of aromatic product design capacity, have been licensed. The polar solvent Sulfolane has a very high degree of selectivity. Moreover, its high boiling point permits application on feed-stocks with boiling ranges up to  $250^{\circ}\text{C}$ .

Different designs of extraction column are commonly used in the various extraction processes for the separation of BTX mixtures, e.g., Rotating Disc Contactor. There have been no reports of the use of mixer-settlers. However mixer-settlers have the advantage that the stage efficiency is generally high, so that

the number of stages can be reliably determined in advance, and they can be designed for any number of stages independently of the extractor size. It is also possible to reduce the number of stages in use if required. Therefore the hydrodynamics, mass transfer characteristics, and efficiency of a laboratory-scale, mixer-settler cascade have been investigated for BTX extraction using Sulfolane. As a prerequisite to this, phase equilibria were determined for four systems, namely hexane-benzene-sulfolane, heptane-toluene-sulfolane, octane-xylene-sulfolane and, nonaromatics-aromatics-sulfolane. Experimentation was subsequently performed with a synthetic BTX feed and then with an actual reformat feed obtained from the Kuwait Oil Company. In addition to considering the practical significance of the hydrodynamics and mass transfer data, comparisons were made between experimental overall mass transfer coefficients and those predicted from single drop correlations and from a back-flow mathematical model.

It is hoped that the results of this study will assist in the more-efficient utilization of Sulfolane for BTX recovery and increase understanding of mixer-settler characteristics.



## CHAPTER 2

---

### AROMATICS (BTX) -ALIPHATICS SEPARATION

## 2.1 Introduction

Benzene, toluene and the xylenes are put to a wide variety of uses and eventually enter the modern household in hundreds of different forms. Figure 2.1 illustrates the transformation of BTX to fabrics, resins, moulded products, etc. The processes by which BTX may be recovered are reviewed below.

## 2.2 Raw Material Sources for Aromatics:

### Upstream Treatment

Crude oil is designated by reference to the location of its sources. Some crude oil properties are listed in Table 2.1. A crude oil is a complex mixture of chemical compounds and may contain all the possible saturated hydrocarbons together with their, even-more-numerous, nitrogen and sulfur derivatives.

Natural crude oil is distilled into different fractions in atmospheric or vacuum distillation columns. BTX precursors are generally in the  $50^{\circ}\text{C}$  -  $175^{\circ}\text{C}$  boiling range and represent <20% of the total crude (straight-run naphtha). The highest boiling stocks may be used as feeds to other refining processes, e.g., fluid catalytic cracking, thermal cracking hydrocracking which break the heavy stocks down into lighter fractions, thus rendering them usable as BTX sources.

In the cracking process, n-paraffins form isoparaffins (naphthenes) which contain fewer ethyl side chains than those in straight-run naphthas. Thus, the BTX precursors, whether from straight-run or cracked stocks, are concentrated in materials with a  $50^{\circ}\text{C}$  -  $175^{\circ}\text{C}$  boiling range.

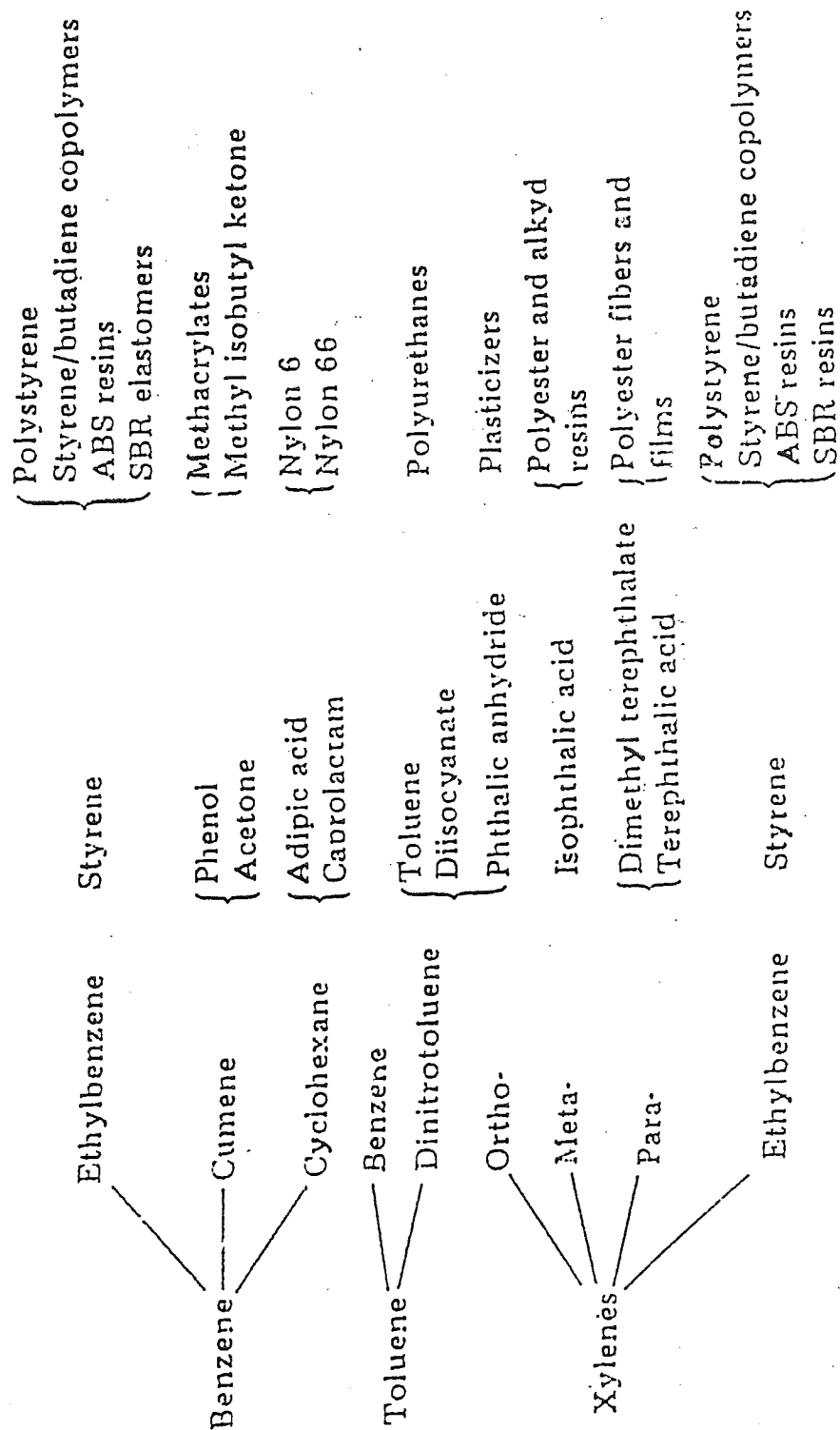


FIG. 2-1 USES OF BTX COMPOUNDS.

Property	Louisiana U.S. Empire Mix	California Huntington Beach	Venezuela Leona	Norway Ekofisk	U.K. Ninian	Libya Sarir	Iran Light	Kuwait	Abu Dhabi
vol %	9.5	12.2	11.9	19.2	19.8	15.0	18.7	17.6	21.9
gravity, °API	59.0	58.0	61.5	63.0	66.0	66.5	65.8	69.7	66.0
octane, F-1 + 3 <sup>a</sup>	82.0	89.6	86.0	80.9	78.0	76.5	79.0	75.3	70.0
paraffins, %	3	43	59	54	57	64	55	78	73
cycloparaffins, %	43	42	20	32	34	33	33	16	17
aromatics, %	9	15	21	14	9	3	10	6	10

<sup>a</sup> F-1 + 3 = a measure of octane rating after addition of 0.79 g tetraethyllead per liter.

Table 2.1 Properties of Crude Oil Straight-Run Fractions

Another classification of crude oils is based upon the PCA (paraffin, cycloparaffins and aromatics) content of the straight-run portion (see Table 2.1). Middle Eastern crude oils are higher in paraffins than most United States crudes. Since the key to BTX processing is the catalytic reforming step (which as a simplification may be considered a  $P \longrightarrow C \longrightarrow A$  conversion), the PCA content of the straight-run naphtha is particularly important because it determines the degree of processing needed to achieve the required aromatics content.

The sulfur and nitrogen contents of a given crude oil affect the preparation of a reformed feed. In catalytic reforming, the feed is treated with a platinum catalyst which is adversely affected by nitrogen, sulfur and oxygen compounds. These elements are therefore removed by pretreating the reformer feed over a nickel-molybdenum, or a cobalt-molybdenum, catalyst in the presence of hydrogen. They are hence converted to ammonia, hydrogen sulfide and water respectively and are readily removed by distillation.

The octane ratings of the various classes of reformer feeds are in the order aromatics > cycloparaffins > isoparaffins > n. paraffins. Thus it is the objective of gasoline refiners and BTX producers to increase the proportion of aromatics. An approximate relationship between the Octane Number and the aromatics content of a reformat is shown in Figure 2.2. The main reactions which occur in a reformer are shown in Figure 2.3; most are reversible indicating the

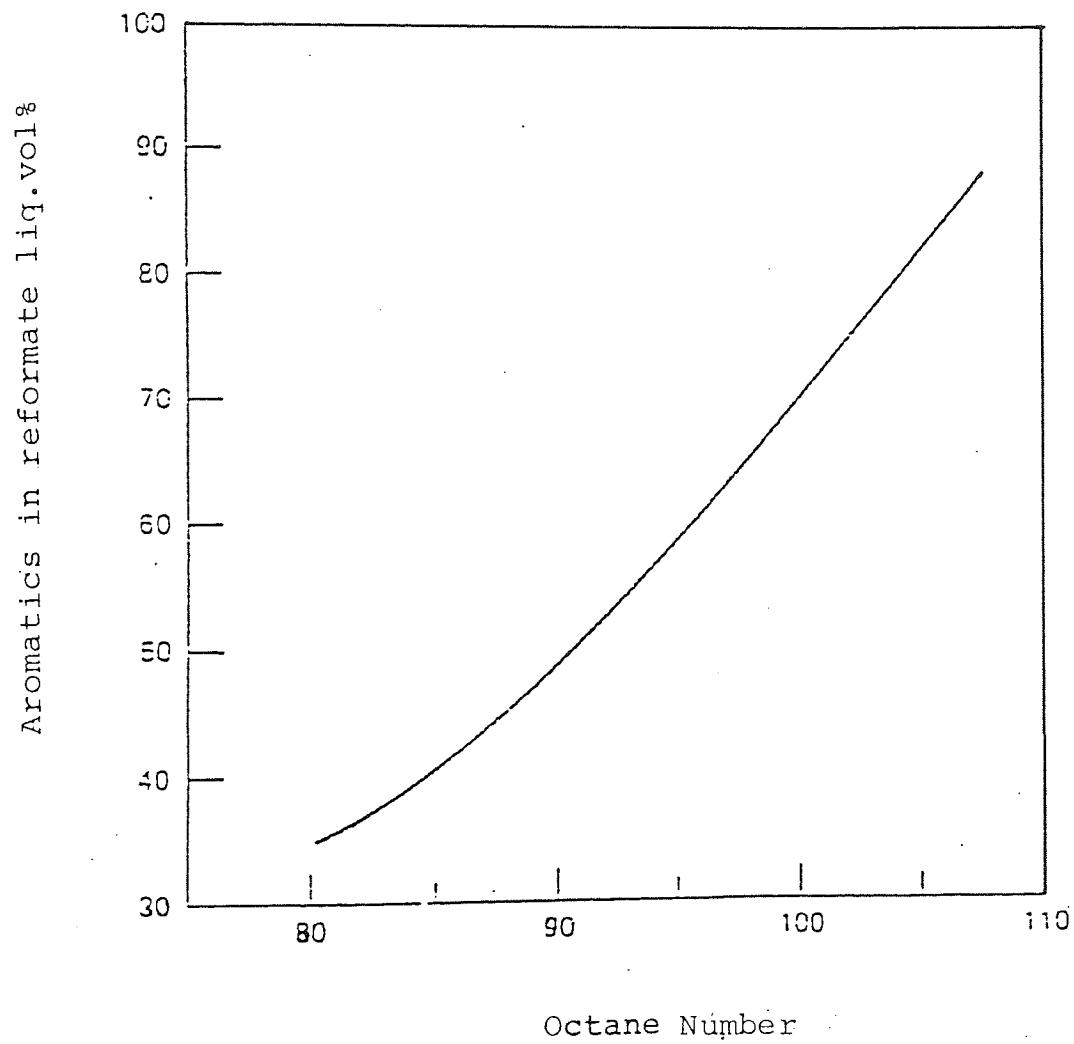


FIG. 2-2 OCTANE RATING AS A FUNCTION OF AROMATICS IN REFORMAT

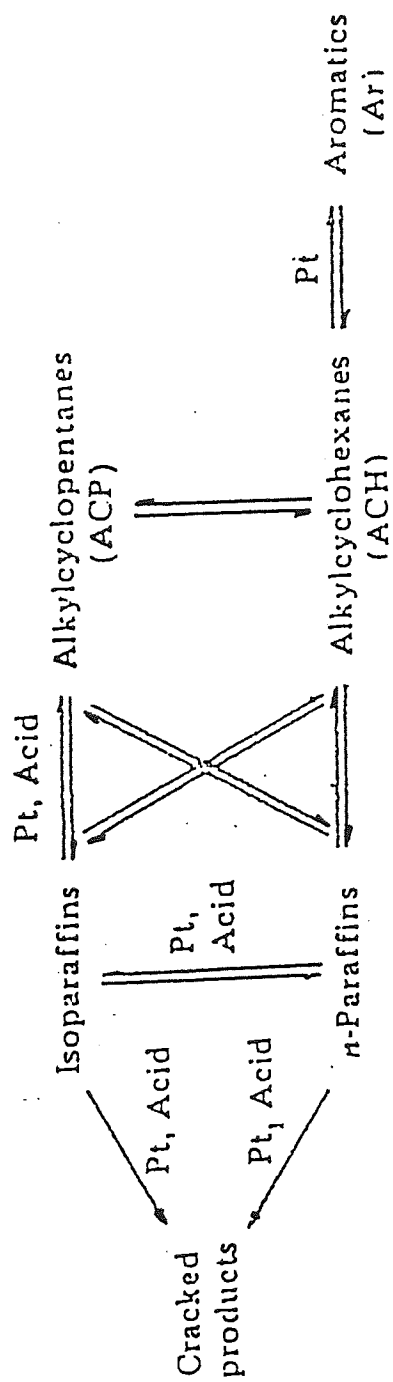


FIG. 2-3 MAIN REACTIONS OF CATALYTIC REFORMING.

importance of reaction equilibrium. In the alkylcyclohexane to aromatics equilibrium  $\text{ACH} \rightarrow \text{Ar}$ , aromatics are favored by high temperature and low pressure. Reforming conditions promote rapid ACH dehydrogenation with high conversion to aromatics (1) The alkylcyclopentane (ACP) to aromatics process is less efficient than ACH dehydrogenation ( $\text{ACP} \rightarrow \text{ACH} \rightarrow \text{Ar}$ ), owing to the slowness of the first step and ACP ring opening, and it requires an acidic platinum catalyst. Cyclohexane is converted to benzene at  $\leq 100\%$  efficiency, whereas only 50-75% of methylcyclopentane is converted to benzene.

Reformer feeds of high aromatics and cycloparaffins content produce high octane reformates using only the cycloparaffins to aromatics reactions. Cyclization of paraffins is generally more difficult.

Comparing the reforming under the same mild conditions of two straight-run fractions with different PCA, the feed with the high C + A content achieves a much higher octane rating (and aromatics content) than that with a low C + A content.

Pyrolysis gasoline is another raw material source for aromatics. It is a by-product from ethylene production and occurs in about the same proportion as the ethylene, i.e., 50%. Before aromatics recovery the low boiling fraction, the  $\text{C}_4$  and  $\text{C}_5$  cut, must be separated and the pyrolysis gasoline treated by low temperature hydrogenation to remove diolefins and by high temperature hydrogenation to remove sulfur compounds.



### 2.3 Reforming for Specific BTX Compounds

In reforming the majority of benzene is formed from cyclohexane and methylcyclopentane. In order to obtain a good yield the severity of treatment must be raised and, if possible, low pressure should be used.

The use of a broad-range feed is inadvisable because of higher catalyst coking rates. Toluene is less valuable as a chemical, but it is an important octane contributor. Toluene demand may increase if a Mitsubishi patent (2) related to earlier DuPont work (3) finds commercial application as an alternative route to polyester via p-tolualdehyde.

Reforming is very common for xylenes. Examination of Figure 2.4 reveals a big overlap between the boiling ranges of  $C_8$ ,  $C_7$  and  $C_9$  hydrocarbons. Thus, even a sharply cut  $90^{\circ}\text{C}$ - $150^{\circ}\text{C}$  fraction may contain only 40-50%  $C_8$  hydrocarbons. A reformate from such a feed will contain only 30%  $C_8$  aromatics.

Recovery of xylenes, which is always accompanied by ethylbenzene, utilizes the heart-cut. If the reformate was made under severe conditions most of the  $C_9$  paraffins, which boil in the xylene range, will be removed. Then, if the heart-cut is sharp, the xylenes may contain very little non-aromatics and extraction is not necessary. This is another advantage of high-severity reforming, particularly as practiced by the regenerative or continuous reforming process.

### 2.4 BTX Separation Processes

#### 2.4.1 Early processes

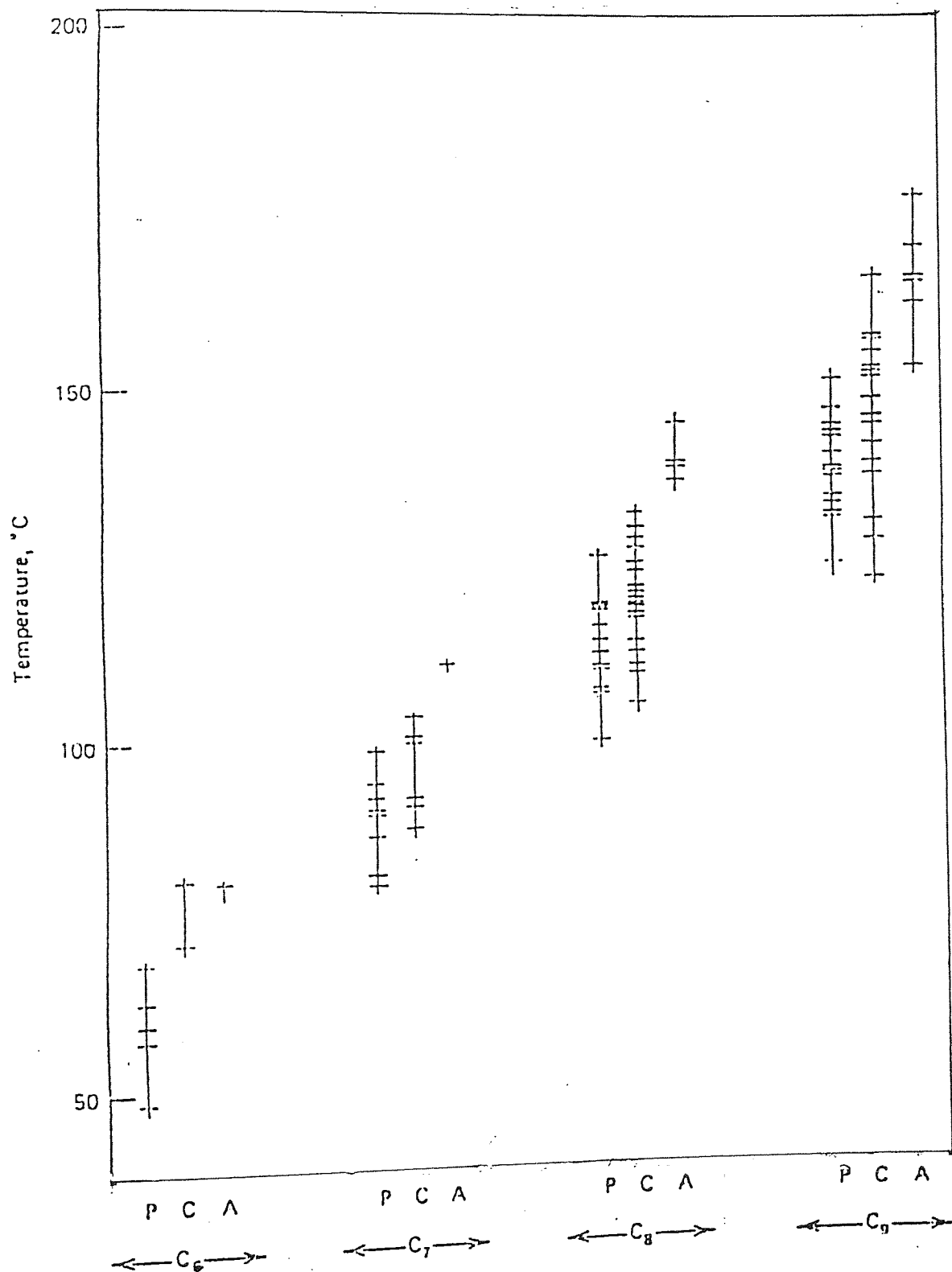


FIG. 2-4 BOILING POINTS OF C<sub>6</sub> - C<sub>9</sub> HYDROCARBONS

P = iso-paraffins, C = Cyclo-Paraffins, A = Aromatics

The earliest large-scale, commercial process for the separation of BTX from aliphatics was straight distillation (4). However, as demonstrated in Figure 2.5, it is impossible to obtain high purity benzene by straight distillation. This Figure shows the boiling points and compositions of the homogeneous binary azeotropes that exist between individual aliphatic compounds and benzene. Thus for each binary (aliphatic-benzene pair) there are three points on the vapour-liquid equilibrium curve, namely the boiling point of each of the two pure components and the boiling point of the azeotrope.

Attempts to improve benzene purity by changing the pressure will be unsuccessful as illustrated in Figure 2.6. The slopes of the vapour pressure curves of benzene and the aliphatics are parallel; thus the relative volatilities are almost unaffected and the compositions of the binary azeotropes will not change significantly.

In the 1940s, extractive distillation was used to increase aliphatic/benzene relative volatilities (5), thereby increasing benzene recovery and purity. Phenol was a preferred solvent for this purpose. However, it was still necessary to distil the whole benzene fraction. Furthermore, for these distillation procedures to be practical, a separate facility was needed to treat each aromatic - containing fraction :  $C_6$ ,  $C_7$  and  $C_8$ .

Extensive commercialization of the BTX processes, however, awaited a resurgence in demand for additional aromatics. Developments in polystyrene plastics, syn-

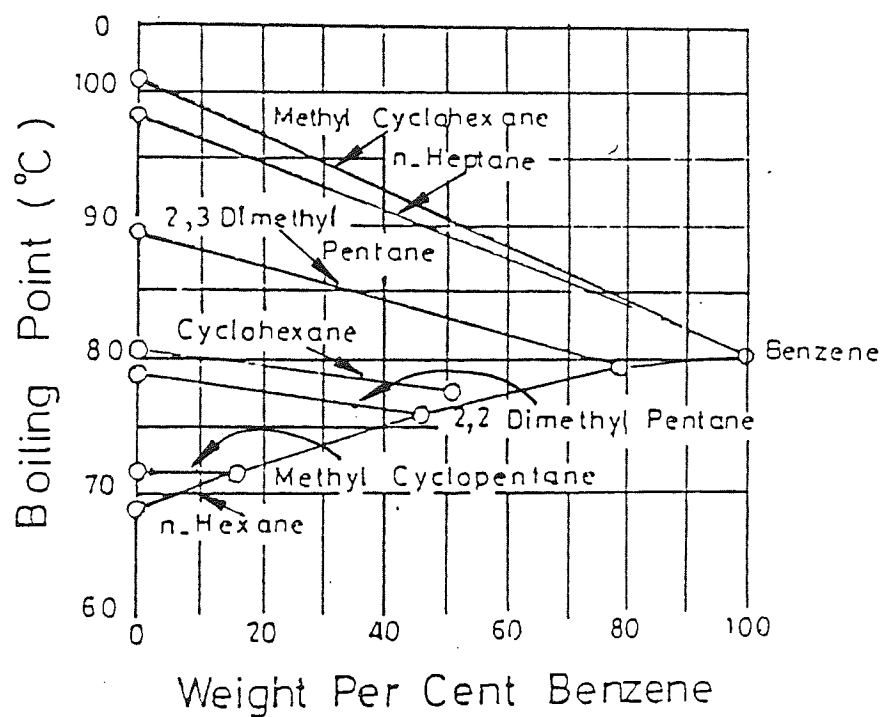


FIG. 2-5 AZEOTROPY IN NONAROMATIC HYDROCARBON-BENZENE BINARY SYSTEMS

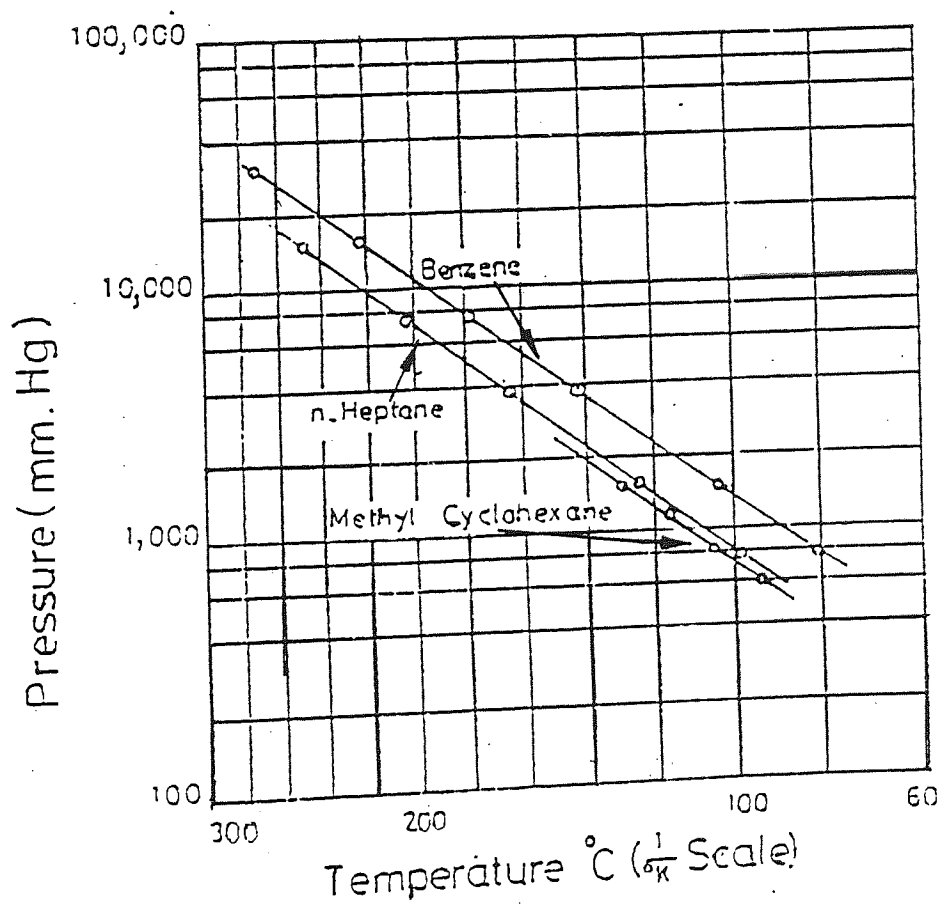


FIG. 2-6 BENZENE-HEPTANE-METHYLCYCLOHEXANE VAPOR PRESSURE VS TEMPERATURE

thetic rubber, nylon fibers and moulding compounds, urethane foams, detergents, resin for coatings, polyester fibers and films, and insecticides were largely responsible for the continuous expansion in production of such aromatic-derived materials. A comprehensive survey of growth in these various applications has been published by Strobaugh (6).

A summary of liquid-liquid extraction processes for BTX recovery is given in Table 2-2.

#### 2.4.2 The UDEX Process (4)

The UDEX extraction process for the separation of aromatic hydrocarbons from petroleum fractions was introduced into commercial operation in the early 1950's. The original solvents used in this process were water solutions with diethylene glycol (DEG) or triethylene glycol (TEG) (4).

Liquid extraction can be used to separate hydrocarbons by type. Thus, benzene as well as toluene and C<sub>8</sub> aromatics, could be recovered from aliphatics in one process by selectively extracting the aromatics and then distilling them from the solvent. Distillation of the aliphatics is avoided so that operating costs are lower than in the fractional and extractive distillation processes. High-purity aromatics can be obtained, because the aromatics are purified in both the extraction step and in the distillation step. The Udex process was, therefore, a significant breakthrough and it has continued to be widely used.

Solvent	Process	Solvent Additives	Operating Temperature	Extractor	Solvent Recovery
Glycol/water mixtures	UDEX process, Universal Oil Products	Solvent can be aqueous diethylene glycol, perhaps with dipropylene glycol, or tetraethylene glycol and water	150°C for diethylene glycol and water	Sieve tray extractor	Distillation
Tetraethylene glycol	Union Carbide Corp.	The solvent is free of water	100°C	Sieve tray extractor	Secondary extraction of BTX into dodecane followed by distillation
Sulfolane	Shell process	None	120°C	RDC or sieve tray	Distillation
N-Methyl pyrrolidone (NMP)	Arosolvan process, Lurgi	Either water or monoethylene glycol added to improve selectivity	NMP/glycol, 60°C	Vertical multistage mixer-settler	Distillation
Dimethyl sulfoxide (DMSO)	Institut Français du Pétrole	Solvent contains up to 9% water to improve selectivity	Ambient	Mechanically agitated contactor, e.g., Kuhni column	Aromatics are displaced from DMSO in a second extraction step. Then recovery of secondary paraffinic solvent is by distillation.
N-Formylmorpholine (FM)	FORMEX process, Snamprogetti	Water addition increases selectivity and also avoids high reboiler temperatures during solvent recovery by distillation	40°C	Sieve tray extractor	Usually by distillation, but if benzene content of feedstock is negligible, a secondary extraction with a hydrocarbon solvent is used to remove BTX from the FM.
Morpholine derivatives	AROMEX process, Krupp-Koppers	4-5 wt.% water content to improve selectivity	Not known	Sieve tray extractor	Distillation

TABLE 2.2 CHARACTERISTIC FEATURES OF BTX EXTRACTION PROCESSES

The flow diagram of the 'Udex' system is shown in Figure 2.7. The distillations are performed in one column and a small percentage of water is also vaporized with the reflux and the BTX product. Water is included in the solvent primarily to reduce the boiling point at the bottom of the distillation column. The vapour-side stream containing the BTX product also includes water and glycol vapours. In the decantation step most of the glycol enters the water phase; therefore a separate distillation column and BTX reflux are not needed. The raffinate and BTX are washed further with small proportions of water to remove the traces of glycol.

With the continuing growth in demand for petrochemicals and high-octane gasoline, increased extraction capacity has been, and will continue to be, needed throughout the years. It has been the trend in industry to employ solvents of increasing solvency( ie, the amount of hydrocarbon which can be contained in the solvent phase) to achieve this capacity increase.

The industry initially used diethylene glycol but improved results were obtained with triethylene glycol. In this case the solvent contains 5% water, so its boiling point is about 140°C. This solvent is also very selective , Benzene distributes in about a 1:2 ratio between extract and raffinate. Triethylene glycol has nearly twice the extraction capacity of diethylene glycol. However, tetraethylene glycol is the best of the glycols that were studied. The solvent contains



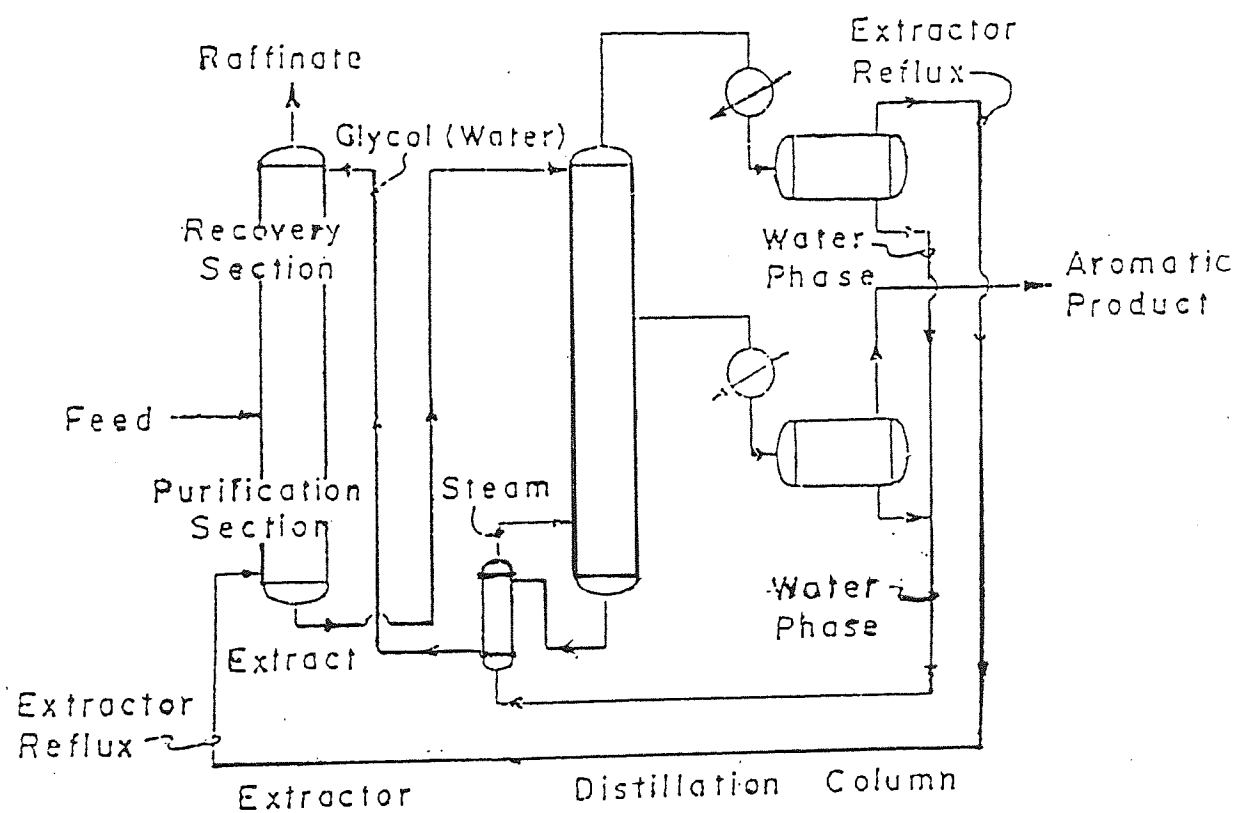


Fig 2.7 SCHEMATIC FLOW DIAGRAM OF UDEX PROCESS

3.9% water so that its boiling point is about 140°C. Benzene distributes very favorably in tetraethylene glycol.

#### 2.4.3 Arosolvan Process (7)

The solvent used in the Arosolvan process N-methyl-pyrrolidone (NMP), has a high capacity discussed further in Chapter 3. Ethylene glycol or water is added to adjust the optimum polarity.

N-methyl-pyrrolidone has proved successful in terms of thermal stability in commercial plant operation. The low solidification points of NMP (-24°C), and of the mixtures of NMP with water or glycol (less than -40°C), are also favorable characteristics. NMP lies in the middle of all solvents with regard to density, i.e., 1040 kg/ m<sup>3</sup>, It also has almost a proper value ~ 1.3 c.St as far as viscosity is concerned, and it is hence easy to separate the two phases. Figure 2.8 shows that NMP has a high capacity and low selectivity.

The operation of the Arosolvan process using NMP-glycol is illustrated in Figure 2.9. The feed is charged to the middle of the extractor and the solvent to the extractor top stage. The raffinate leaves the top of the extraction column saturated with solvent. The extract is withdrawn at the base and fed to the extract recycle column. The column overhead product is recycled to the extractor bottom stage. This recycle contains almost all the non-aromatics. The aromatics and the solvent are separated by vacuum distillation. The glycol dissolved in the aromatics is removed by

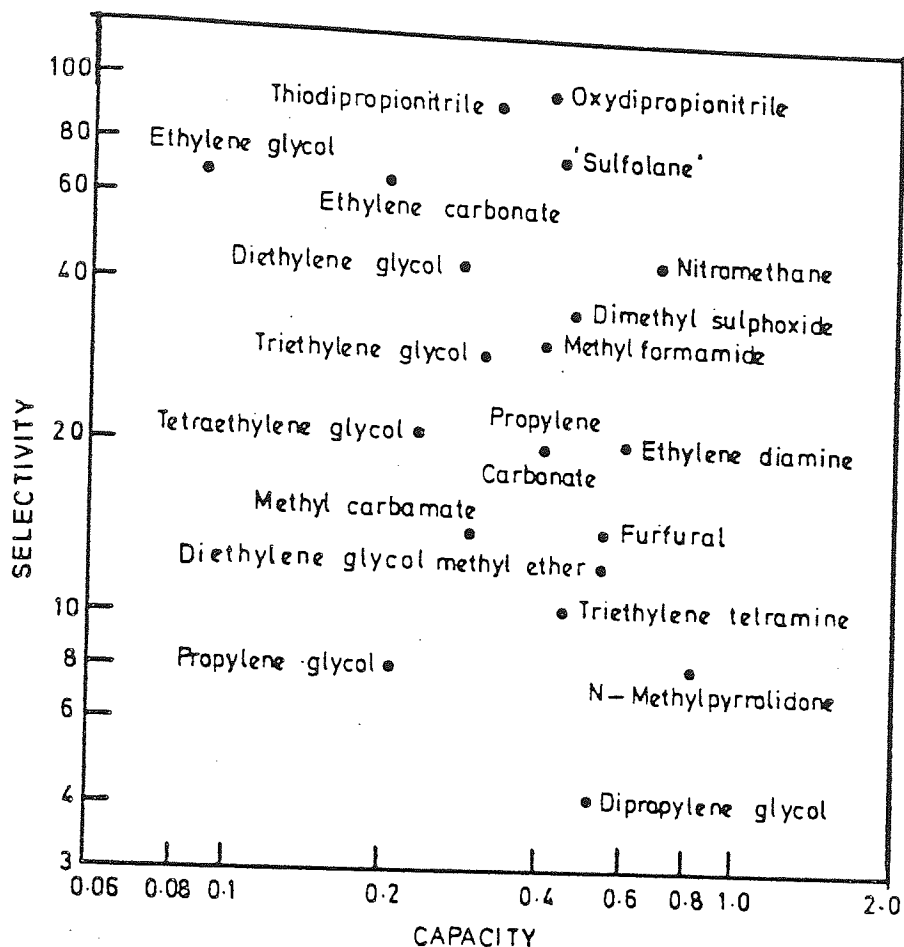


FIG. 2-8 CAPACITY AND SELECTIVITY OF SOLVENTS

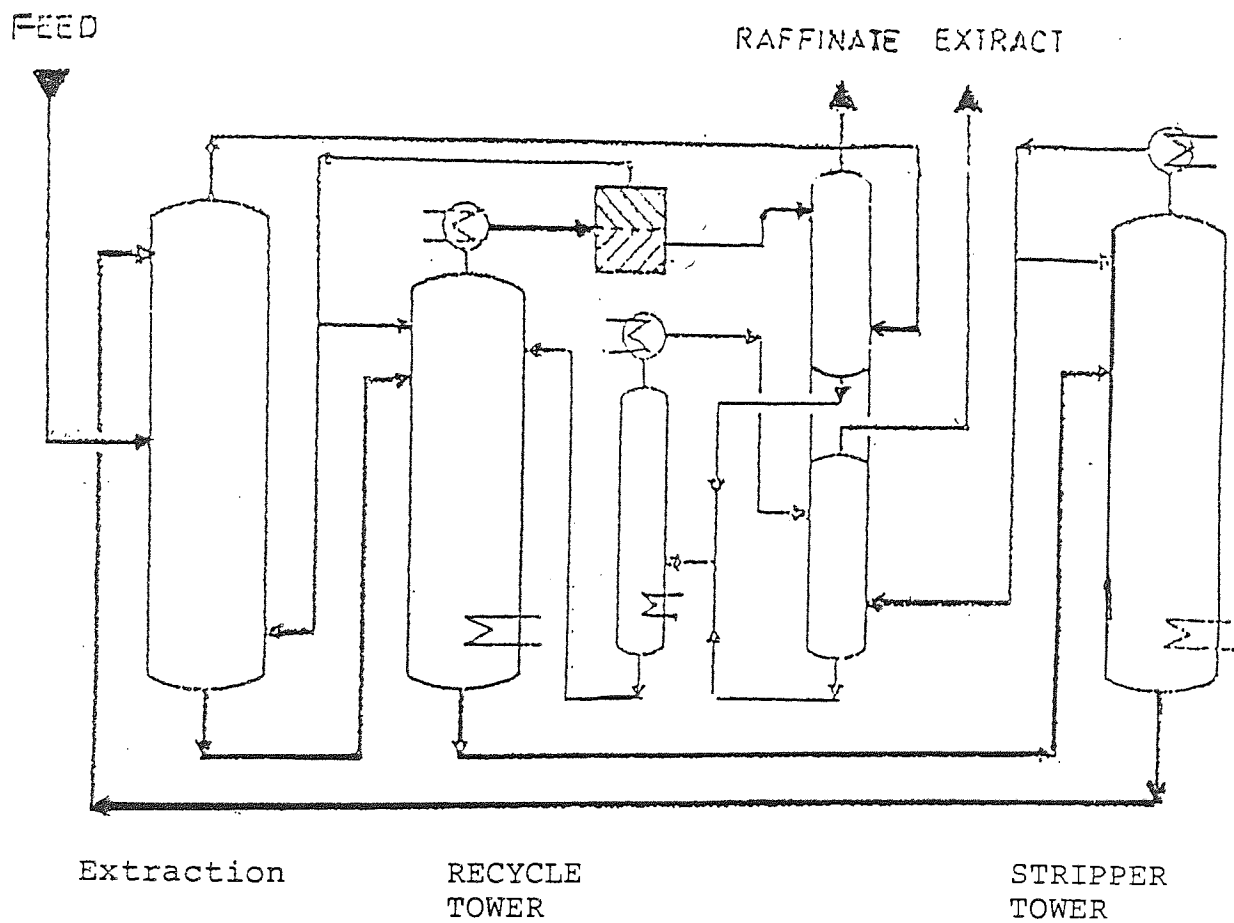


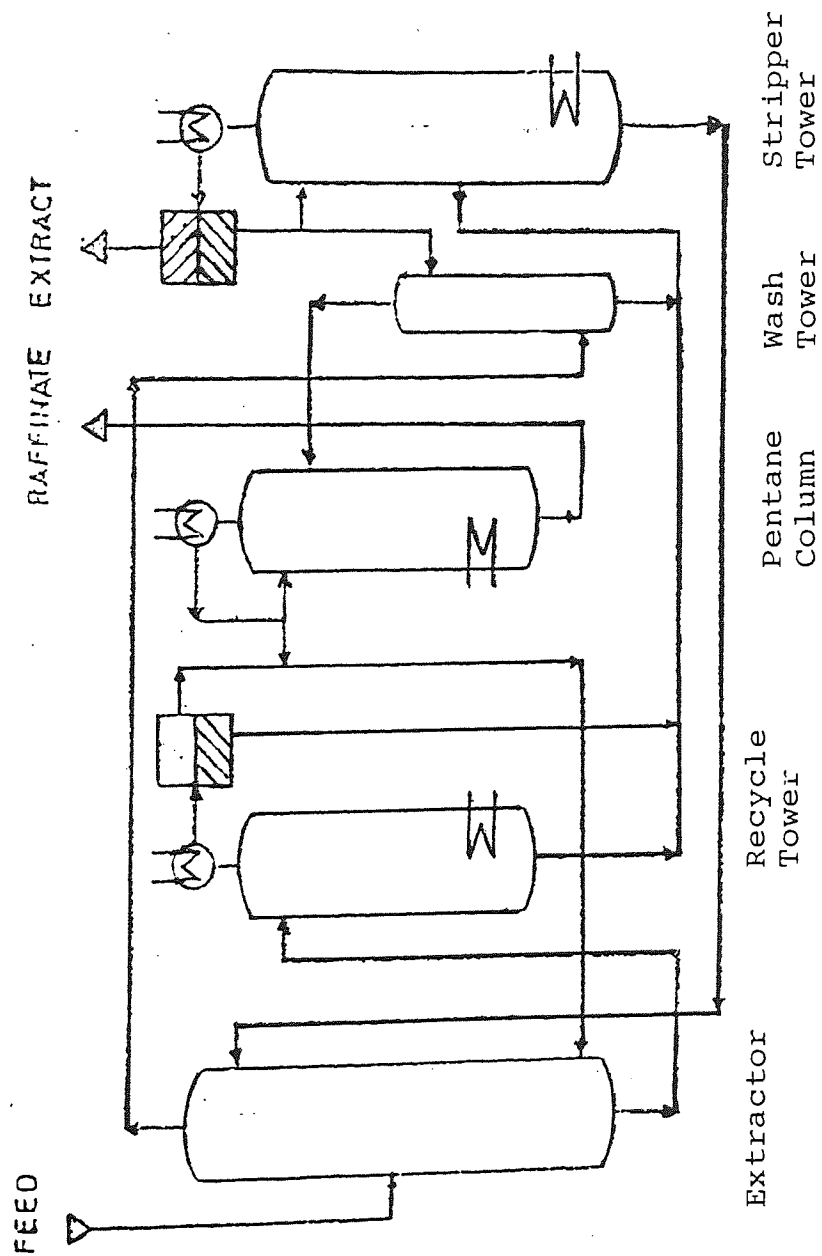
Fig 2.9 AROSOLVAN PROCESS WITH NMP/GLYCOL

counter-current extraction with water. A few percent of solvent returned in the raffinate is washed-out by counter-current contact with water. The bulk of the water in the solvent- laden wash water is removed in a distillation column using a reboiler heated with hot solvent. The remaining water is charged to the extract recycle column where it is removed overhead azeotropically together with hydrocarbon vapour; the solvent is combined with the main solvent stream in the column bottom. Pure aromatics and raffinate are recovered from the top of the two water extractors.

Operation of the Arosolvan process by the use of NMP-water is illustrated in Figure 2.10 (7). It is similar to that of the NMP-glycol process; the feed stock is charged to the middle, with the solvent to the top and the extract recycle to the bottom of the extraction column. The extraction temperature is about 35°C ( compared with 60°C for NMP-glycol). The raffinate, after water washing, is fed to a distillation column where a pentane recycle is produced. This recycle stream flows to the extractor together with the recycle from the extract recycle column. A water distillation column is not required in this process since the water from the solvent stripper top is free of solvent and can be used direct for raffinate washing; thus a water-wash is not required for the aromatics.

#### 2.4.4 Tetra Process

In the Tetra process [tetraethylene glycol] the feed is charged to the middle of the extraction column (1). It flows upward and is contacted by the tetra



2-10 AROSOLVAN PROCESS WITH NMP/WATER

solvent flowing downward. The non-aromatics are removed from the top as the raffinate phase. The aromatics-rich extract leaves from the base of the extraction column and is sent to the top of the stripper. An extractive distillation occurs in the upper part of the stripper. Here light aliphatics are stripped from benzene. Light overhead distillate, consisting of hydrocarbon and water, is condensed and decanted. The hydrocarbon layer with a composition of approximately 60% aromatics and 40% light aliphatics is recycled back to the extractor as reflux. The lower part of the column is operated as a steam distillation unit with injection of stripping water to remove aromatics from the solvent. The pure aromatics are withdrawn as a side product from the stripper. The stripper bottom stream is lean tetra solvent which is recycled back to the top of the column. Both the raffinate and aromatics product streams are sent to a water-wash system, where any dissolved tetra is recovered and returned to the extraction unit. Figure 2.11 illustrates the process.

#### 2.4.5 BTX Extraction with Sulfolane

A simplified flow diagram of the Sulfolane process is shown in Figure 2.12. For illustrative purposes, it will be assumed that fresh feed containing  $C_6-C_8$  aromatics, naphthenes and paraffins is to be extracted. The presence of pentane does not interfere with operation, but, for simplicity, it is assumed to be absent. Similarly, mono-olefins do not interfere, but are neglected in the discussion, since they will behave similarly to naphthenes.

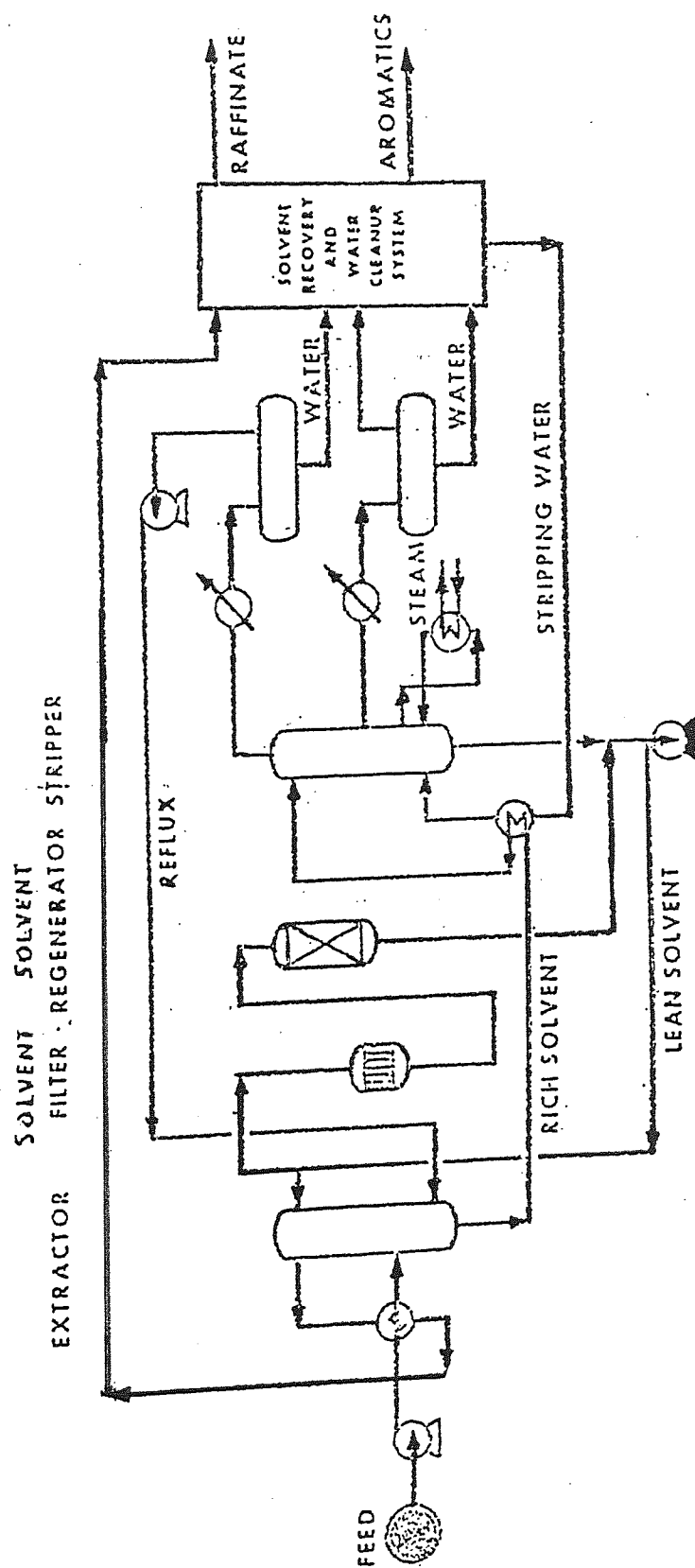


FIG. 2-11 TETRA PROCESS



Flow 30.1. 10000 lb/hr, inward,  
Flow 30.2. 10000 lb/hr, outward

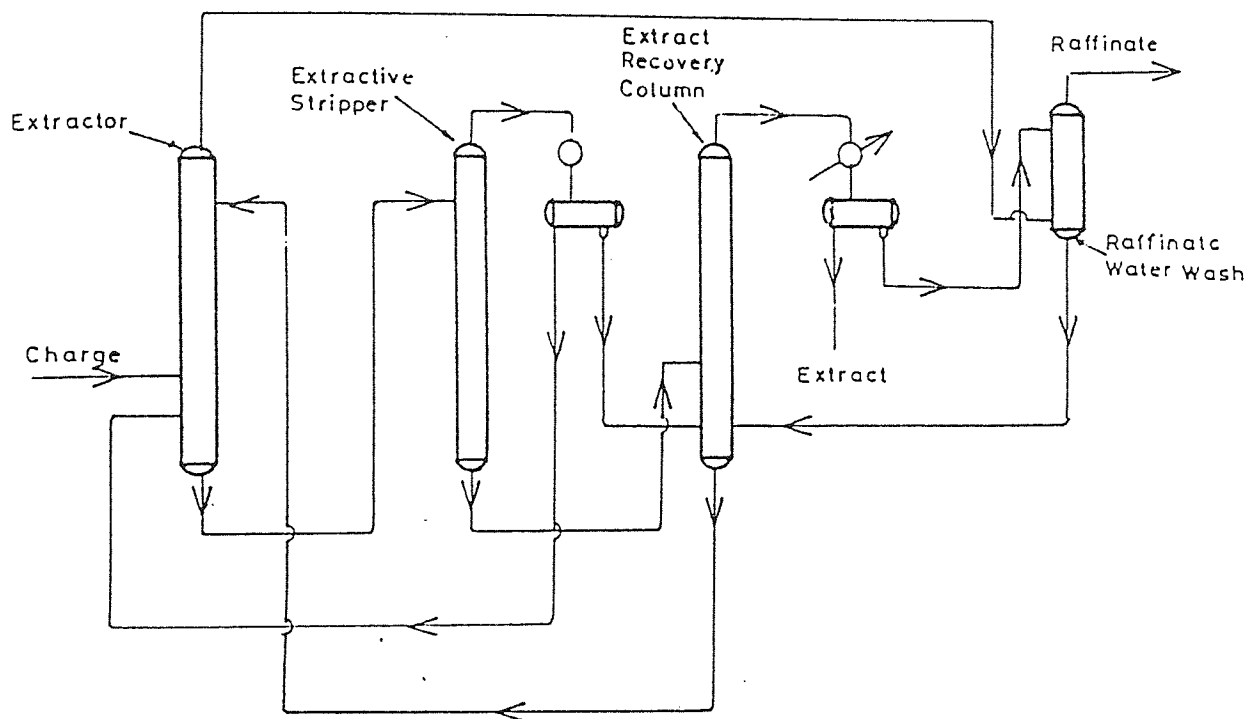


FIG. 2-12 SULFOLANE EXTRACTOR UNIT

#### 2.4.5.1 Extractor

Fresh feed enters the extractor and flows upward, countercurrent to a stream of lean solvent. As the feed flows through the extraction column, aromatics are selectively dissolved in the solvent, and raffinate is withdrawn from the top.

#### 2.4.5.2 Extractor Stripper

Rich solvent from the extractor enters the extractive stripper, in which partial stripping of hydrocarbon from the rich solvent takes place. The non-aromatic components which have volatilities higher than that of benzene under the prevailing conditions, are substantially completely stripped from the solvent and removed in the overhead stream. This stream is returned to the extractor as reflux. The bottoms stream consists of solvent and aromatic components, substantially free of non-aromatics.

#### 2.4.5.3 Extract Recovery Column

Solvent from the extractive stripper enters the recovery column, in which the aromatic product is separated from the solvent stream. Because of the large difference in boiling point between sulfolane and the heaviest desired aromatic product, this separation is readily accomplished. Lean solvent from the column bottom is returned to the extractor.

#### 2.4.5.4 Water Wash Tower

Raffinate from the extractor is contacted with water to remove dissolved Sulfolane, and the water-rich stream is returned to the extract recovery column to reclaim its sulfolane content.

#### 2.4.5.5 Combination of Extraction and Extractive Stripping

It is clear from the sulfolane process flow sheet that separation of non-aromatics from aromatics is accomplished partly by liquid extraction and partly by extractive stripping. In this respect, the process employs a flowsheet similar to that used in the earlier Udex process. The advantages of this mode of operation are discussed in the following paragraphs.

Figure 2.13 demonstrates that in liquid-liquid systems, light non-aromatic components are more soluble in the solvent than are heavy non-aromatics. It follows therefore that liquid-liquid extraction is more effective in separating aromatics from the heavy contaminants than from the light.

In contrast, as shown in from Figure 2.14, light non-aromatics are more readily stripped from the solvent by extractive stripping than are the heavy non-aromatics. It follows that extractive stripping is more effective in separating aromatics from the light contaminants than from the heavy non-aromatics.

Liquid-liquid extraction and extractive stripping thus provide complementary features. Contaminants which are the most difficult to eliminate in one section are the easiest to eliminate in the other. The combination, as employed in the Sulfolane process, permits effective treatment of feed-stocks of much broader boiling range than would be possible by either technique singly.

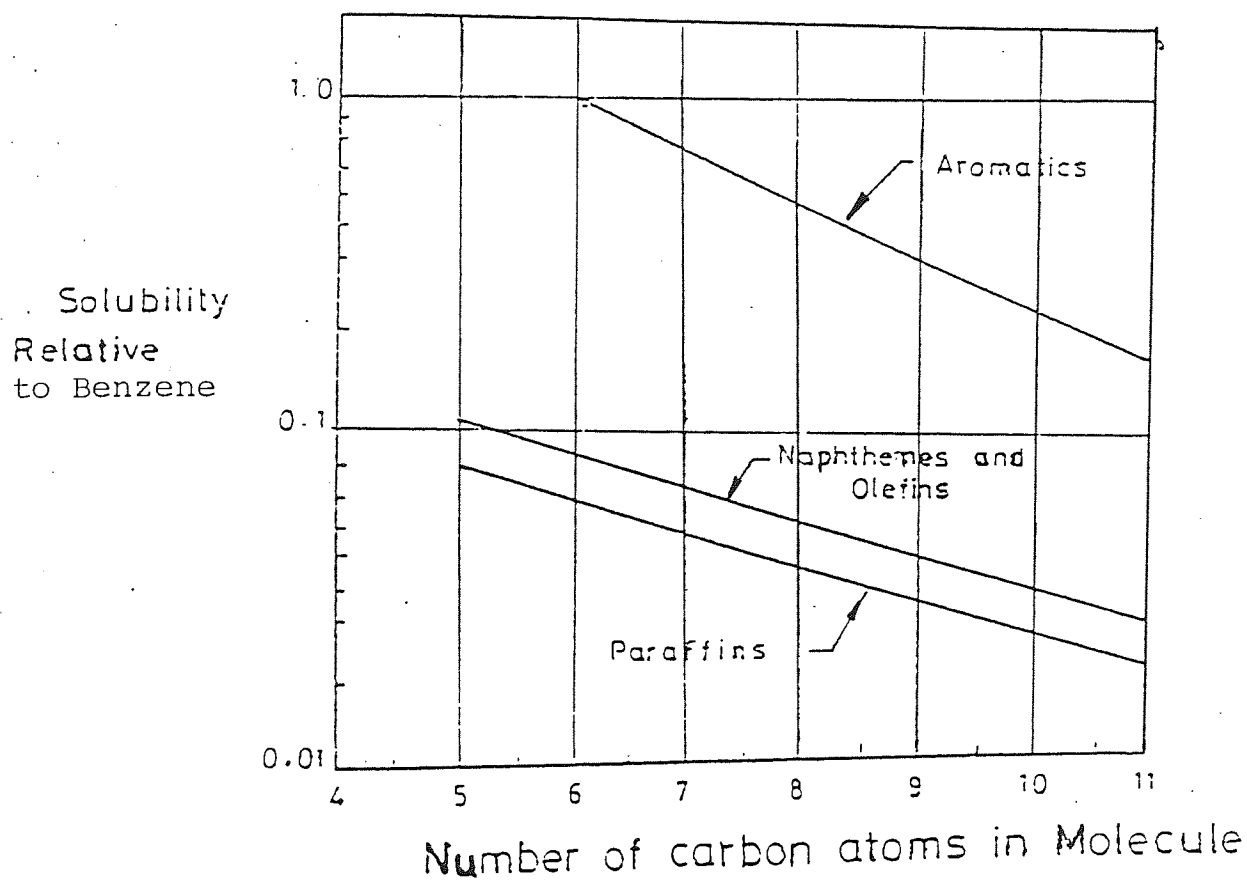


FIG. 2-13 LIQUID-LIQUID EQUILIBRIUM RELATIVE SOLUBILITY  
OF HYDROCARBONS IN ANHYDROUS SULFOLANE

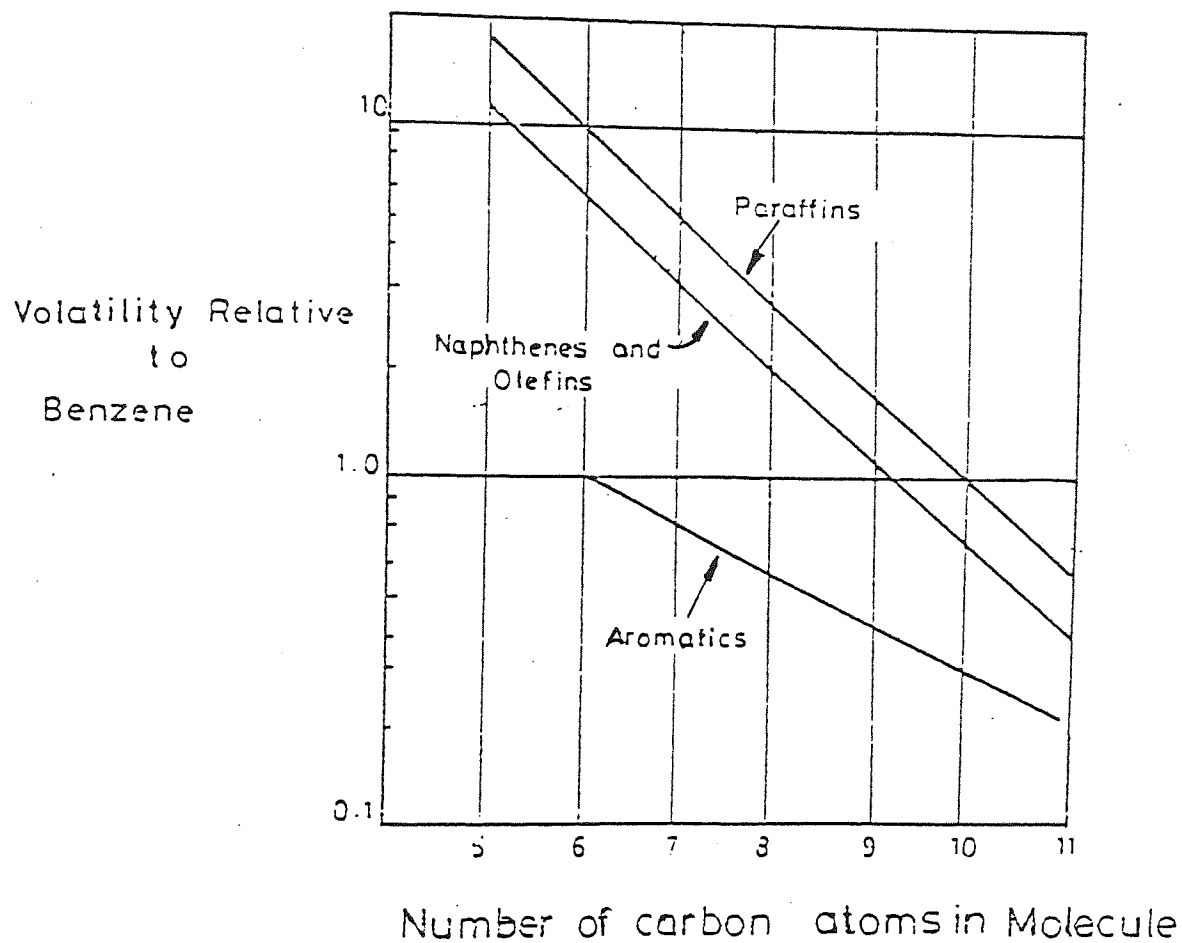


Fig 2.14 VAPOR LIQUID EQUILIBRIUM RELATION VOLATILITY OF HYDROCARBONS IN ANHYDROUS SULFOLANE.

The above review has outlined the major processes available for BTX extraction. The trend over the last 20 years however has been a shift towards the use of sulfolane. Therefore this process was considered most appropriate for study.

## CHAPTER 3

---

### SOLVENT PROPERTIES

### 3.1 Solvent Properties

In liquid-liquid extraction one important characteristic of any solvent is the relationship established with the second phase in physical equilibrium.

A solvent must form non-ideal solutions with the mixture to be separated if two liquid phases are to form. For any solvent used in aromatic/non-aromatic separations these deviations are positive, i.e., hydrocarbons are repulsed by the solvent, some necessarily more than others if the solvent is to be useful. The repulsion of one hydrocarbon relative to another is some measure of the ability of the solvent to discriminate between them and thus to achieve a separation. The relative repulsion is the selectivity of the solvent.

The repulsion forces are expressed as activity coefficients (  $\gamma$  ) ,

$$\gamma_X = \bar{\gamma}_Y \quad 3-1$$

where  $\bar{\gamma}$  activity coefficient of a component in the liquid solvent phase.

$\gamma$  activity coefficient of the same component in the liquid hydrocarbon phase.

$x$  mole fraction in the liquid hydrocarbon phase.

$y$  mole fraction in the liquid solvent phase.

For solutions which obey Raoult's law, i.e., ideal solutions, the activity coefficient is unity. Some non-



ideality exists for mixtures of aromatics with non-aromatics in the hydrocarbon phase but these are so slight, compared with those which exist in the solvent phase, that for the purposes of comparing solvents,  $\gamma$  may be taken as unity for all the hydrocarbons present.

### 3.1.1 Selectivity

Group selectivity,  $\beta$ , for solvents such as dimethyl sulfoxide (DMSO), n-formyl morpholine (NFM), dimethyl formamide (DMF), n-methyl pyrrolidone (NMP), diethylene glycol (DEG) and Sulfolane (S) depends on the polarity of the solvent molecule and the order of affinity for various groups of hydrocarbons is the same for all solvents. The affinity decreases ( $\gamma$  increases) in the order: bicyclic aromatics, monocyclic aromatics, bicyclic paraffins, monocyclic paraffins (naphthenes), olefins, and paraffins. Although group selectivity may be expressed in several ways, the selectivity for aromatics relative to paraffins,  $\beta(A/P)$ , of a solvent for aromatics is conveniently defined as the ratio of the activity coefficient of a particular non-aromatic to that of an aromatic whose recovery is of importance. As an illustration, for consideration of the selectivity of a broad range of solvents, n-heptane and toluene have conventionally been chosen as representative aliphatic and aromatic compounds. Methylcyclopentane and benzene are also used to compare group selectivity for a more limited number of solvents of particular commercial interest.

The light-heavy selectivity,  $\beta$  (L/H), is the relative affinity of a solvent for members of an homologous hydrocarbon series. The selectivity for the light component relative to the heavy component may be defined as the ratio of the activity coefficient of the heavy component to that of the light component. The pair conventionally chosen for numerical illustrations is hexane/heptane. Another definition could be the ratio of the activity coefficients of n-octane and n-heptane; a suitable measure would be the logarithm of this ratio (8).

In general a good solvent should have low light-heavy selectivity in order to allow group separations with a wide boiling range feedstock.

In the different physical separation processes such as distillation, extractive distillation, and extraction, the light-heavy selectivity shows markedly differing behaviour. Data for the system n-octane/n-heptane are given in Table 3.1. This demonstrates that the light-heavy selectivity in extraction as compared to that in normal distillation has a smaller absolute value and is reversed in sign. The combination of the two, extractive distillation, exhibits the overriding influence of distillation of light-heavy selectivity.

### 3.1.2 Capacity, "Solvent Power"

The amount of solute which can be taken-up in the solvent phase is a major factor determining the solvent circulation rate and hence inventory required in a given plant. A quantitative measure for the solvent power could be the reciprocal value of the activity

TABLE 3.1 LIGHT-HEAVY SELECTIVITY AT 100 °C SOLVENT; SULFOLANE

Process		n-octane	heptane	$\log \left[ \frac{\gamma_{n.oct.}}{\gamma_{n.hep.}} \right]$
Distillation	$P_o$ , vapour pressure, mmHg	430	910	-0.33
Extraction	$\gamma$ , activity coefficient	51	41	0.1
Extractive distillation	$(P_o)(\gamma)$	21900	37300	-0.23

coefficient of the solute at infinite dilution. The term "hydrocarbon loading" of a solvent (HCL) is also used and denotes the fraction of total hydrocarbons actually present in a solvent/hydrocarbon mixture. This is not the same as solvent power, which is a somewhat hypothetical solubility of toluene assuming a pure toluene phase could exist in equilibrium with a solvent phase.

The "K value" is the ratio of the concentration of a component in an equilibrated non-solvent phase to its concentration in the solvent phase. In summary the relevant definitions are,

$$\text{A. Group selectivity} \quad \beta \text{ (A/P)} = \frac{v_{\text{heptane}}}{v_{\text{toluene}}}$$

$$\text{B. Light/Heavy selectivity} \quad \beta \text{ (L/H)} = \frac{v_{\text{heptane}}}{v_{\text{hexane}}}$$

$$\text{C. Solvent power} \quad sp = \frac{1}{v_{\text{toluene}}}$$

$$\text{D. Hydrocarbon loading} \quad \text{HCL} = z_{\text{HC}}$$

$$\text{E. K value} \quad K = y/x$$

### 3.1.3 Optimum Solvent Properties

High group selectivity is clearly a desirable property of a solvent in any situation.

Light/heavy selectivity is not germane to the processing of narrow boiling feedstocks. For wide range stocks, a low value is advantageous for extraction and a high value is desirable for extractive distillation. For processes such as the Udex, sulfolane and others which utilize a combination of extraction and

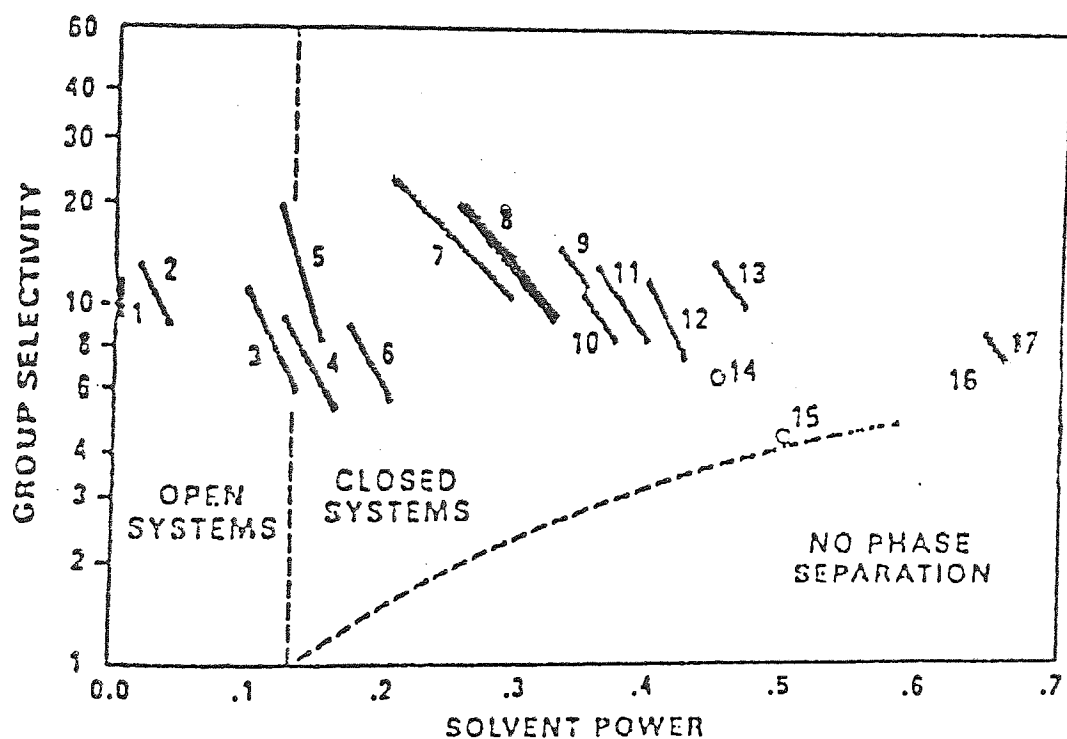
extractive distillation, an intermediate value somewhat greater than unity seems appropriate and is, in fact, displayed by most solvents.

The preferred solvent power, or hydrocarbon loading, is more difficult to state from the outset. With any given solvent, group selectivity decreases with increasing hydrocarbon loading. Further, when the group selectivity of a large number of solvents is plotted against solvent power, the same general sacrifice of selectivity for solvency is observed.

It is concluded that an intermediate range of solvent power is the most desirable, but all known solvents with very high solvent power have such low group selectivities that they cannot in practice be used at very high hydrocarbon loadings.

Figure 3.1 shows the relationship between group selectivity between toluene and heptane and solvent power for toluene for a wide range of solvents, including those used commercially. To the left lie those which are not completely miscible with aromatics. At the lower right would be those which are miscible with paraffins. It can be seen that glycol type solvents [2-6] tend to form one band which, if extrapolated to higher solvent power, would fall below the band formed by the other solvents [7-17].

The best solvent should lie near the upper limit of this band and within a suitable range of solvent power. Several solvents in addition to sulfolane are so suited. However, properties other than the primary solvency/selectivity are also important. Unless a sol-



- |                         |                          |
|-------------------------|--------------------------|
| 1. Water                | 10. Furfural             |
| 2. Ethylene Glycol      | 11. N-Formyl Morpholine  |
| 3. Diethylene Glycol    | 12. Dimethyl Sulfolane   |
| 4. Triethylene Glycol   | 13. Dimethyl Formamide   |
| 5. Diglycol Amine       | 14. Phenol               |
| 6. Tetraethylene Glycol | 15. Methyl Ethyle Ketone |
| 7. Dimethyl Sulfoxide   | 16. Nitro Benzene        |
| 8. Sulfolane            | 17. N-Methyl Pyrrolidone |
| 9. Acetonitrile         |                          |

FIG.3-1 Survey Of Solvents Traverse Through  
Practical Temperature Range

vent has reasonably good secondary properties, as discussed below, it cannot form the basis of successful commercial process.

Figure 3.2 shows the light/heavy selectivity for similar solvents. Here there appears to be only one band instead of two. Of those solvents with reasonable solvent power, sulfolane has one of the larger light/heavy selectivities.

#### 3.1.4 Secondary Solvent Properties

In addition to the primary selectivity/solvency properties a satisfactory commercial solvent should meet minimum standards for a number of other, secondary properties including :

- A. Price and availability
- B. Toxicity
- C. Thermal stability
- D. Chemical Inertness
- E. Boiling point
- F. Specific gravity
- G. Specific heat
- H. Ease of separation from products.

Whilst it is desirable that a solvent possesses favorable properties in all of these categories, some compromises are possible.

Lack of thermal stability or of chemical inertness disqualifies some solvents with excellent properties, e.g., sulfolene (a similar molecule to sulfolane but with one double bond in the ring) is superior to sulfolane at comparable hydrocarbon loadings, but it is not thermally stable.

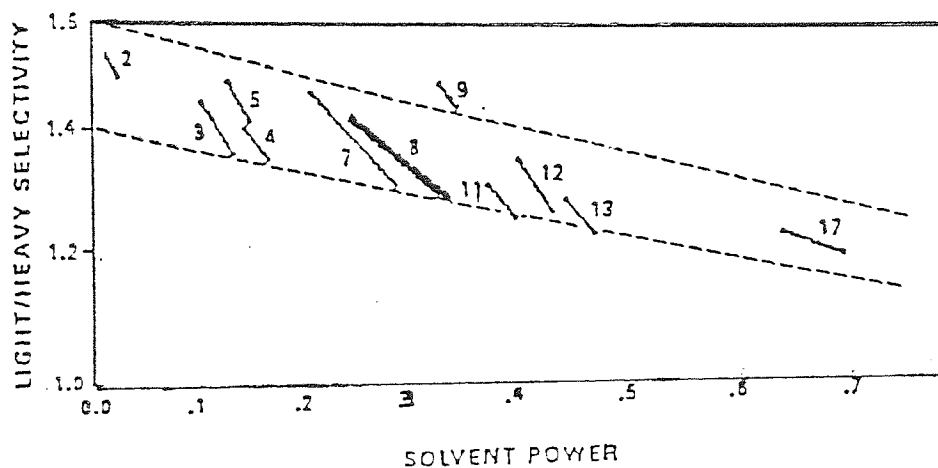


Fig 3-2 LIGHT/HEAVY SELECTIVITY OF SOLVENT  
TRAVERSE THROUGH PRACTICAL TEMPERATURE RANGE.

NOTE:

NUMBERS DENOTE SOLVENTS  
AS GIVEN WITH FIG. 3.1



Solvents are generally organic chemicals and, consequently, have limited thermal stability. The standards for stability of practical solvents must be extraordinarily high, since they are circulated continuously and exposed to heating, cooling and shearing, and are required to survive for a significant period. Sulfolane is outstanding in this regard. Under non-oxidizing conditions, virtually no decomposition is detectable below 200°C. Most organic molecules containing those polar groups able to impart a group selectivity as high as sulfolane are not this stable.

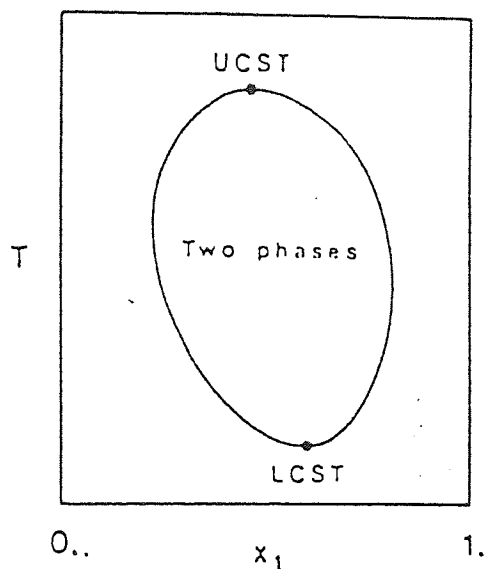
Chemical inertness is important, because a solvent will be exposed to aromatics, paraffins and naphthenes. Sulfolane is most inert compared to the other solvents; it is also resistant, but not immune, to oxidative attack by dissolved molecular oxygen or peroxides in the feedstock.

### 3.2 Liquid-Liquid Equilibria

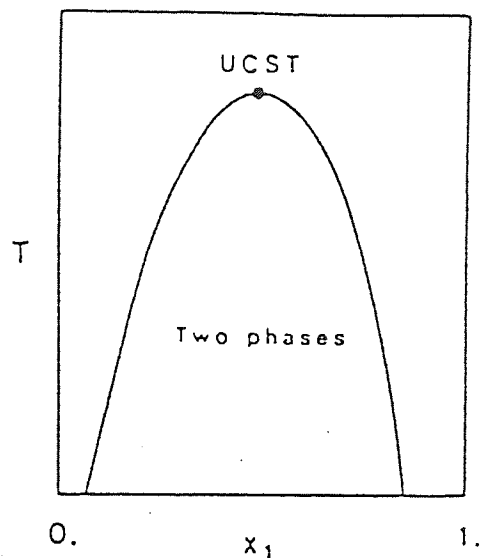
#### 3.2.1 Equilibrium Data

Binary liquid-liquid equilibria data may be presented as T-X diagrams giving the mutual solubilities X as a function of temperature (T). Figure 3.3 represents the most general T-X diagrams. More than 90% of the mixtures are covered by phase diagrams of the types shown in Figure 3.3b, and 3.3d.

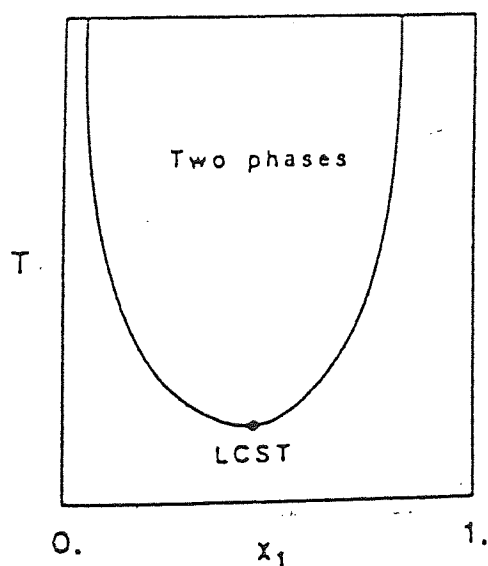
Ternary liquid-liquid equilibrium data are usually recorded at constant temperature. The data may be portrayed on triangular diagrams as shown in Figure 3.4. Each apex represents one of the pure components, the binoidal curve separates the one-phase region from



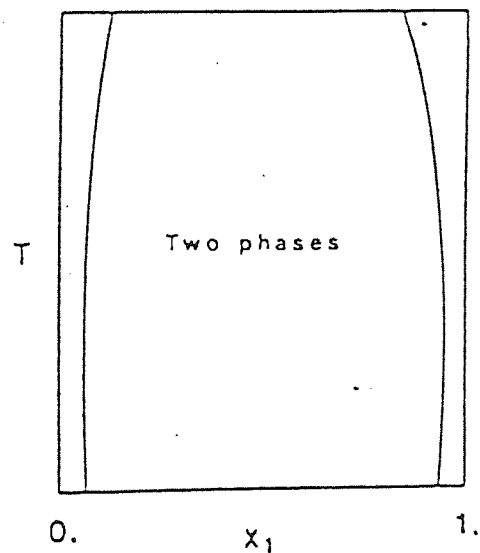
a: Lower (LCST) and upper (UCST) critical solution temperature  
Frequency: 4%



b: Upper critical solution temperature  
Frequency: 41%

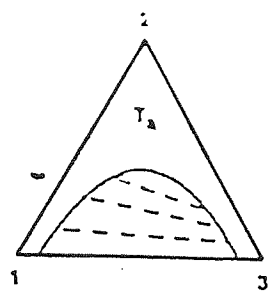


c: Lower critical solution temperature  
Frequency: 2%

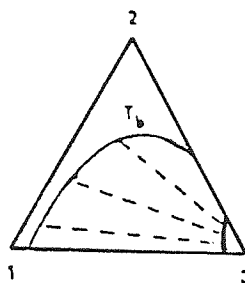


d: Two-phase region in the whole temperature range  
Frequency: 53%

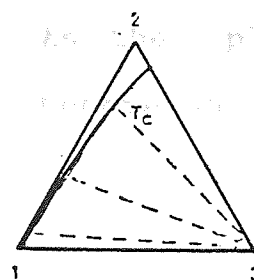
Fig3.3 Types of binary liquid—liquid equilibria.



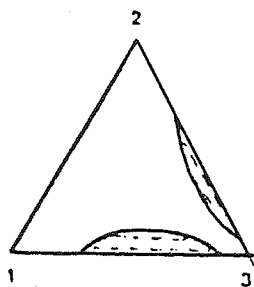
a: Type one  
Frequency: 75%



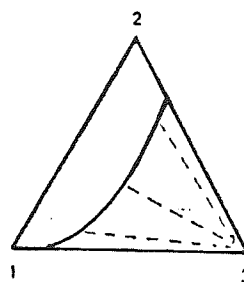
b: Type two (Trans-  
ient between  
type one and two)  
Frequency: 2%



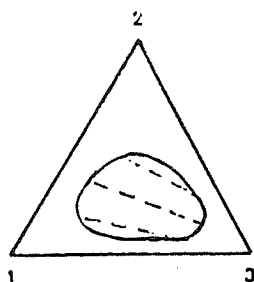
c: Type two  
Frequency: 20%



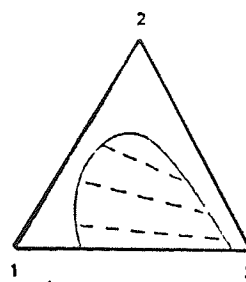
d: Type two (Con-  
structed from two  
type one diagrams)  
Frequency: <1%



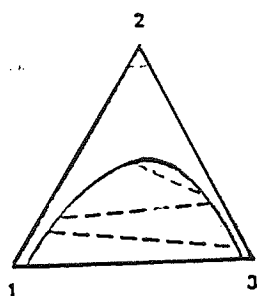
e: Type two (The  
two curves from  
3d have merged)  
Frequency: <1%



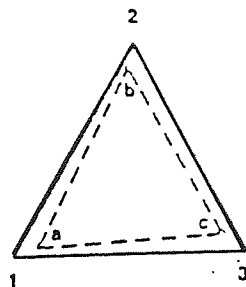
f: Island curve  
Frequency: <1%



g: Type one (Evolved  
from f by a temper-  
ature change)  
Frequency: <1%



h: Type one (Tie  
lines with  
negative slopes)  
Frequency: <1%



i: Three coexist-  
ing liquid  
phases (a, b  
and c)  
Frequency: <1%

FIG. 3-4 TYPES OF TERNARY LIQUID-LIQUID EQUILIBRIA

the two-phase region, and a tie line inter-connects the two liquid phase in equilibrium. As the plait point 'P' is approached, the tie lines become shorter and shorter; finally at the plait point only one liquid phase exists. The different types of ternary diagrams are shown in Figure 3.4. The most common ternary diagram is that corresponding to Figure 3.4a.

The conventional method of measuring the solubility of a solute in a solvent is to place a known amount of solvent in an open vessel controlled at a set temperature and, while agitating, add the solute by titration until the binary mixture becomes turbid. A glass Smith Bonner cell is an apparatus used for such measurements (9). A similar experiment may be carried out in a closed vessel, from which air has been evacuated. In this case, the system will contain two liquid phases and one vapour phase in equilibrium. A device has been developed in Sweden, the AKUFVE Contactor (10), which greatly increases the rate of generation of data. This unit comprises a highly efficient mixing chamber followed by a centrifugal separator. The separated phases are recirculated to the mixing chamber. Provision is made on the return lines for instrumental analysis .

### 3.2.2 Multicomponent Equilibrium Data

In practice, the feed to an extractor often contains more than two-components. However it is difficult to take proper account of the individual action of each component in calculations, and this is rarely attempted. It is usually possible to divide the multicom-

ponent mixture into two groups of like components, one group being extracted and the other group remaining as the raffinate. The calculations may then be performed as if the multicomponent mixture were a binary mixture.

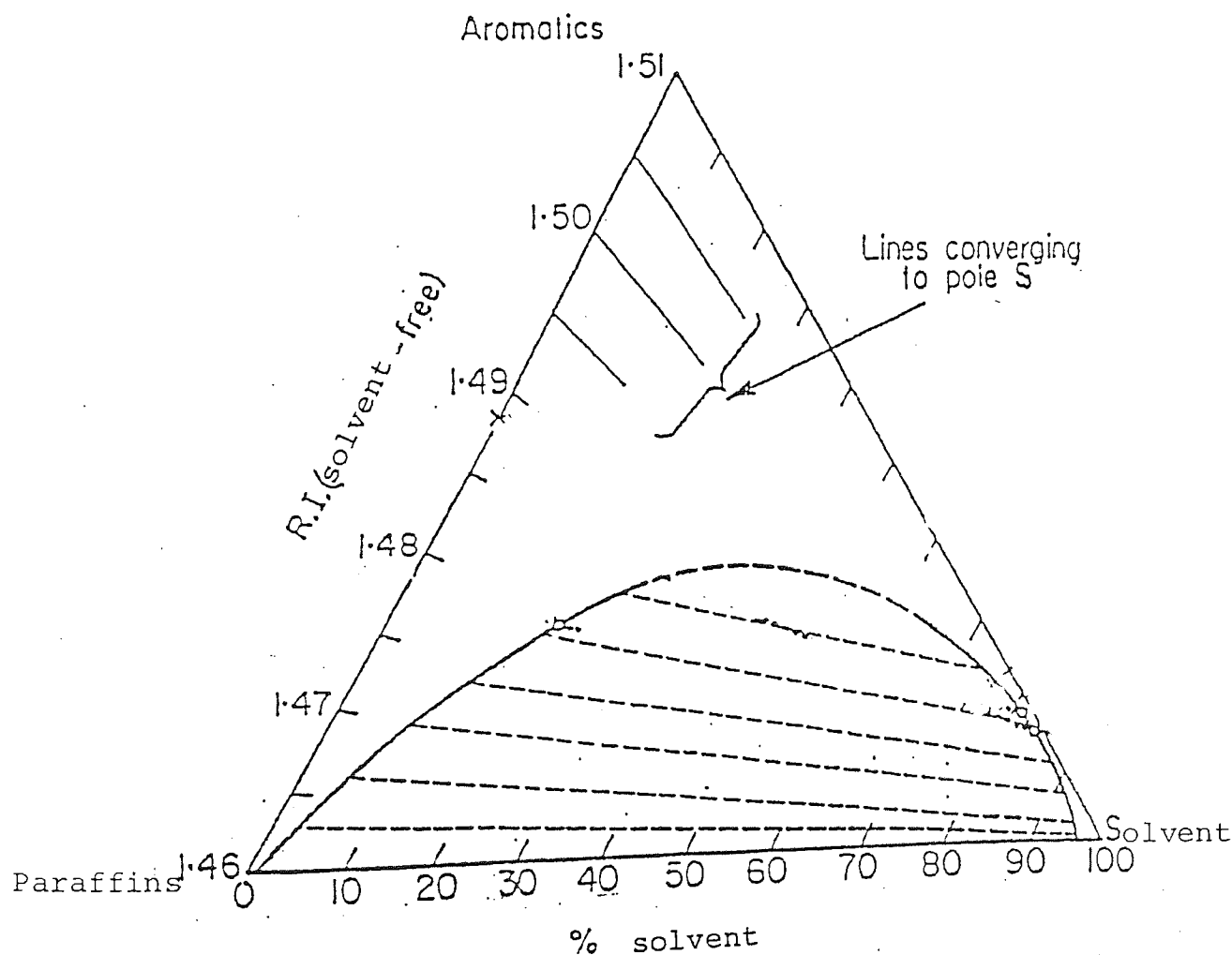
In petroleum refining the multicomponent stream is split into two groups of components, the aromatics and the paraffins, the object of the extraction being to remove aromatics from the oil feed. Several physical properties can be used to differentiate the mixture into aromatic/paraffinic groups. The equilibrium data and the graphical calculations are usually drawn on an equilateral triangular diagram, Figure 3.5 .

### 3.3 The Distribution Coefficient

The Nernst Distribution Law (11) is limited to cases in which the molecular weight of the solute is the same in each phase and when the two solvents remain immiscible even after the addition of the common solute. Nernst subsequently expanded his distribution law to include cases of association or dissociation. One of the first systems investigated was the distribution of acetic acid between water and benzene. The expression  $(C_1^2 / C_2)$  was found to be more constant than  $(C_1 / C_2)$  in concentrated solutions. Neither ratio was found to be constant for the low concentrations studied. The distribution of acetic acid in different solvents was studied by many workers (12,13,14,15,16,17) and there is a general agreement that it varies with concentration due to association

molecules. According to

... or dissociation.



3-5 MULTI-COMPONENT SYSTEM REPRESENTED ON AN EQUILATERAL TRIANGULAR DIAGRAM.

and splitting- up of the acid molecules. According to Farmer (18) the degree of association, or dissociation, of the acid differs from one solvent to the other.

The distribution coefficient can be determined from an accurate knowledge of phase-equilibria relationships. These data can also serve for the determination of the quantities of solvent required and the driving forces determining the rates of mass transfer.

If the activities can be correctly expressed as functions of concentration, the equilibria can be predicted. However with the present state of knowledge (19), it is not generally possible to do this well enough to rely upon the predicted data for extractor design. Nevertheless for the purpose of choosing possible solvents, and in the absence of adequate data, it is possible to make useful predictions of the general trend of the equilibria and to check the reliability of any available data.

Generally, very good agreement should not be expected between data predicted from thermodynamics and experimental data for every system. Joy and Kyle (20) stated that reasonable predictions of liquid-liquid equilibria for type I ternary systems from binary data alone cannot be expected when the ordinary two-parameter activity coefficient equations are used. Kenny (7) also found his calculated results were not in agreement with experimental data. Some other workers (21,22,23) reported poor agreement between calculated and experimental results for type I systems but for type II systems the data may be in good agreement.

The activity coefficients can be determined by using an equation derived by integration of the Gibbs-Duhem equation (24). The recommended equations for liquid-liquid systems are the NRTL equation (25), UNIQUAC equation (26) and UNIFAC equation (27).

Distribution coefficients for a given system can be expected to change with temperature because of the change in the solubility and tie line compositions. For some systems the effect of temperature on distribution may be slight (28). Treybal (29) attempted to regularize the change in distribution coefficient with temperature by assuming that the change in mutual solubility of the solvents is negligible.

#### 3.4 Solute and Solvent Recovery

The removal of solvent from the products of an extraction is nearly always necessary, both to enable recycle of the solvent for reuse, and to provide solvent-free products. In many instances, the solvent recovery operation is the most costly part of the entire separation scheme. Consequently, it must be given special consideration when choosing between alternative solvents. The solvent chosen should provide the least costly overall operation, including both extraction and recovery, even though the extraction operation alone is not the least costly possible. Frequently the solvent recovery operation also has an important influence on the extraction because it determines the purity of the recycled solvent.



Distillation is by far the most commonly-used method of solvent recovery, but less costly schemes can be devised. Distillation is used for the recovery of the solvent when the constituents of the solutions are all volatile; clearly however the relative volatility of the various constituents of the ultimate products and the solvent must be suitable.

If the extracted solute is non-volatile, the solvent may be evaporated from the extract without rectification and distilled from the raffinate. For such cases, the solvent should be relatively low-boiling and have a small latent heat of vaporization.

If the relative volatility of the solvent and solute is poor, or if troublesome azeotropes form, extracting the solvent into another solvent which is more amenable to separation may be possible.

Of the solvent properties discussed above, as demonstrated in Chapter 8, sulfolane has a very good balance of properties for BTX extraction from aromatics.

## CHAPTER 4

---

### MASS TRANSFER FUNDAMENTALS

#### 4.1 Mass Transfer Into, or Out Of , Droplets :

Mass transfer of a solute between a dispersed phase and a continuous phase can, in its simplest form, be considered similar to transfer between a swarm of spheres and the surrounding liquid. Thus a basis for analysis is the theory for mass transfer between a single sphere and surrounding liquid, since the rate expression for mass transfer to, or from, an isolated sphere may in some cases, e.g. with low hold-up and in the absence of interdrop coalescence, be extended to predict approximately the rate for a sphere in a multi- sphere system (30).

Mass transfer rate is generally expressed in terms of an overall mass transfer coefficient  $K$  , defined by

$$N = K A \Delta C$$

4.1

The concentration difference  $\Delta C$  represents the total difference from the beginning to the end of the diffusion path. The coefficient therefore includes the characteristics of the laminar and turbulent flow regions of the fluid and the molecular eddy diffusion. When a fluid is in turbulent flow past a solid surface, since the fluid velocity is zero at the surface itself, there must be a viscous layer or film in the fluid adjacent to the surface . The effective film would have to be very thin so that the quantity of solute within it is small relative to the amount passing through it, or the concentration gradient would have to be set up

quickly (31). The resistance to mass transfer in each phase is represented by the reciprocal of the individual film coefficient and the resistances are additive :

$$\frac{1}{K_d} = \frac{1}{k_d} + \frac{m}{k_c} \quad 4.2$$

or

$$\frac{1}{K_c} = \frac{1}{k_c} + \frac{1}{mk_d} \quad 4.3$$

Equilibrium at the interface requires equal values of chemical potential in the liquids at the interface and consequently no resistance to transfer at the interface.

Mass transfer into, or out of, drops in a solvent extraction column occurs during three distinct stages :

- i) Drop formation at the nozzles or distributor,
- ii) Drop movement through the continuous phase
- iii) Drop coalescence at the interface.

In practical columns, particularly those involving rotary agitation or pulsing, mass transfer during stages (i) and (iii), which are termed end effects, is sometimes neglected. The following equations define the end effects.

$$E_{t1} = \frac{C_1 - C_2}{C_1 - C_0} \quad 4.4 \text{ a}$$

$$E_m = \frac{C_2 - C_3}{C_2 - C_0} \quad 4.4 \text{ b}$$

$$E_{t2} = \frac{C_3 - C_4}{C_3 - C_0} \quad 4.4 \text{ c}$$

where  $E_{t1}$ ,  $E_m$ , and  $E_{t2}$  are the fractional approach to equilibrium in the formation, steady fall (or rise), and coalescence periods respectively .

and

$C_1$  = Concentration of dispersed phase (uniformly mixed) at the nozzle,

$C_2$  = Concentration of dispersed phase (uniformly mixed) at the beginning of transfer in the steady-fall period,

$C_3$  = Concentration of dispersed phase (uniformly mixed) in the plane at which a drop strikes the coalesced dispersed phase interface .

$C_4$  = Concentration of dispersed phase (uniformly mixed) at column outlet .

$C_0$  = Concentration of dispersed phase (uniformly mixed) at equilibrium with respect to transfer of solute to, or from, dispersed phase.

In practical situations only  $C_1$ , and  $C_4$  are directly measurable; therefore the only accurately measured efficiency is the overall, or total , efficiency .  $E_r$  given by ,

$$E_r = \frac{C_1 - C_4}{C_1 - C_0} \quad \text{4.5}$$

By simple algebraic manipulation of equations 4.4 a, 4.4b, 4.4c, and 4.5 the following equation results:

$$E_m = \frac{E_r - E_{t1} - E_{t2} + E_{t1} \times E_{t2}}{1 - E_{t1} - E_{t2} + E_{t1} \times E_{t2}} \quad 4.6$$

$$E_m = \frac{E_r - E_f}{1 - E_f} \quad 4.7$$

where  $E_f$  is a combined end effect.

In a mixer-settler stage however drop formation and travel through the mixer are indistinguishable and, because of the higher hold-up and intense turbulence, a coalescence-redispersion mechanism causes drops to rapidly lose their identity. This mechanism also produces high mass transfer rates by surface renewal, together with large values of interfacial area per unit volume.

#### 4.2 Mass Transfer During Drop Formation

Sherwood, et.al. (32, 33) attempted to measure the amount of solute extracted as a drop formed before detachment from a nozzle in a gravity column. They reported that 40% - 45% of the solute was extracted before the drop left the nozzle. Robinson (34) reported that only 14-20% extraction occurred during drop formation. However direct comparison is not meaningful

since the amount is likely to be a function of the system, solute concentration, direction of solute transfer, drop size and rate of drop formation. Johnson and Hamielec (35), and Nadi and Viswanathan (36) reported comprehensive studies on end effects in an extraction column. They concluded that for a specific system the use of end-effect efficiencies permits comparison of the magnitude of the combined end effect ( i.e. due to formation and eventual coalescence ) and of the correlation factor with values predicted by various mechanisms in the literature.

The conditions under which solute transfer occurs during the formation of a single drop from a submerged nozzle in a stationary solvent phase are probably explained as follows: While the drop is being formed the interior must be in rapid motion and of relatively uniform concentration. The surrounding continuous phase undergoes viscous displacement due to expansion of the drop. Here, there is no significant film resistance in the continuous phase surrounding the drop. Mathematical analysis of this mechanism is given in reference (34) . Heertjes et.al. (38), by assuming Higbie's equation (39) for transient diffusion into the surface of drop as it is formed, developed the following equation for mass transfer during formation,

$$\frac{C_0 - C_1}{C_0 - C^*} = \frac{20.6}{d_p} (Dt)^{0.5} \quad 4.8$$

while Licht and Pensing (12) proposed the following expression:

$$\frac{C_0 - C_1}{C_0 - C^*} = \frac{2.9}{md_p} (Dt) \quad 4.9$$

While these two models indicate that the extraction during drop formation depends on the drop size and time of formation, Licht and Conway (40) and Marsh and Heideger(37) found that the percent solute extracted in three systems; acetic acid extracted from water by methyl-isobutyl-ketone, from perchloro-ethylene by water, and from carbon tetrachloride by water, in a spray column 30 cm high, and 4.7 cm inside diameter, was independent of drop size and drop formation time. However, they concluded that the amount of extraction occurring during drop formation was so small that the experimental results did not detect the variation with drop formation time and drop size. Experiments carried out with other systems in other apparatus indicated that 10% of the mass transfer occurred during drop formation (41).

The following conditions generally have been assumed to hold in the derivation of equations relating to mass transfer during drop formation,

1. The interfacial concentration is that at saturation.

2. Mass is transferred by diffusion perpendicular to the interface.



3. The process of diffusion is slow compared with the process of drop growth.

4. Variation in the diffusion coefficient in the direction of flow may be neglected.

An expression was proposed by Skelland and Minhas (42) for the mass transfer coefficient :

$$\frac{k_{df} t_f}{d_p} = 0.0432 \left[ \frac{V_n^2}{c_p g} \right]^{0.089} \left[ \frac{d_p^2}{t_f D_d} \right]^{-0.334} \left[ \frac{\mu_d}{\sqrt{\rho_d c_\sigma}} \right]^{-0.601} \quad 4.10$$

This correlation represents the overall mass transfer occurring during formation, which includes mass transfer during drop growth, during the detachment of the drop and the influence of the rest drop remaining on the nozzle. Around 25% deviation was obtained from the experimental values. This model did not however consider the rate of formation as one of the variables affecting mass transfer, whereas Heertjes et.al.(43) and Coulson and Skinner (44) observed increased mass transfer at higher frequencies of drop formation, which would be expected because of the higher degree of internal turbulence.

The rate of mass transfer to a forming droplet can be expressed in terms of the Higbie Penetration Theory (39), allowing for the increase of area during growth. From the Penetration Theory :

$$J = -D \left( \frac{dc}{dz} \right)_{z=0} = (C_i - C_b) \sqrt{\frac{D}{\pi}} \quad 4.11$$

which induces intense mixing  
 The amount transferred during time  $dt$  is given  
 by high mass transfer rate

$$dM = \Delta C A \left( \frac{D}{\pi} \right)^{0.5} t^{0.5} dt \quad 4.12$$

where

$\Delta C$  is the driving force

$A$  is the area of contact defined for a full grown droplet by:

$$A = A_f (t/t_f)^{2/3} \quad 4.13$$

and the dispersed phase mass transfer coefficient  $k_{df}$  is correlated by :

$$k_{df} = \frac{6}{7} \left[ \frac{D_d}{\pi t_f} \right]^{0.5} \quad 4.14$$

#### 4.3 Mass Transfer During Drop Travel

##### Through The Continuous Phase

There are three different conditions for mass transfer to, or from, drops in motion, namely those of

i) rigid drops, normally less than 2mm diameter for which as an approximation

$$Re = \frac{\rho V_d d_p}{\mu_c} < 10$$

- ii) circulating drops, or,
- iii) oscillating drops.

Circulation and oscillation induces intense mixing inside the drop resulting in a high mass transfer rate to, or from, the drop. Conversely a stagnant drop has a lower mass transfer rate due to the inhibition of the internal mixing.

A wide variety of correlations have therefore been proposed for either  $k_d$  or  $k_c$  depending on the drop hydrodynamics. These are reviewed below. However it is relevant to note that correlations may be restricted to the systems for which they were evaluated and for the specific direction of mass transfer studied. Also since different apparatus was used, and different temperatures, the predicted values of  $k$  are not strictly comparable.

Although mass transfer is dependent on the hydrodynamic state of the drops, the presence of a wake behind the moving drop may affect the overall transfer rate (45). Few attempts have been made to quantify this effect, which may be pronounced in quiescent flow. Kinard (46) developed an equation to modify the driving force due to entrainment of a wake behind the drop. Laddha (47) studied the effect of a wake in spray columns.

In turbulent flow the wake effect is small since, because of renewal of the continuous phase, the wake is not allowed to develop. Thus wake effects are of no relevance to mass transfer within an agitated vessel.

#### 4.4 Mass Transfer in the Dispersed phase

The hydrodynamic state of the drop moving through the continuous phase is correlated approximately by the Reynolds number. Hadamard (48) showed that the liquid inside the droplet would circulate at droplet's Reynolds number  $(d_p V \rho_c / \mu_c)$  greater than 1, and it has been found that oscillations commence in regimes of flow for which droplet  $Re > 200$  (49). Al Hassan (50) showed that Reynolds number is insufficient to explain the hydrodynamics of the drop; this is not surprising since important physical properties e.g.  $\sigma$ ,  $\rho_c$ ,  $\mu_d$  are not accounted for.

##### 4.4.1 Stagnant Droplets

A small drop may be considered to approximate to a rigid sphere in behaviour. Newman (51) has put forward a relation for the prediction of transfer rates in such drops;

$$E_m = 1 - \frac{6}{\pi^2} \sum_{n=1}^{\infty} \frac{1}{n^2} \exp \left[ \frac{-n^2 \pi^2 D_d t_f}{r^2} \right] \quad 4.15$$

from which

$$k_d \frac{-d}{6t} \ln \frac{6}{\pi^2} \sum_{n=1}^{\infty} \frac{1}{n^2} \exp \left[ \frac{-n^2 \pi^2 D_d t_f}{r^2} \right] \quad 4.16$$

Vermeulen (52) found that Newman's model could be closely approximated by the empirical expression

$$E_m = 1 - \exp -\pi^2 \left[ \frac{R D_d t_f}{r^2} \right]^{0.5} \quad 4.17$$

which for values of  $E_m$  less than 0.5 can be expressed by

$$E_m = \pi \left[ \frac{R D_d t_f}{r^2} \right]^{0.5} \quad 4.18$$

Treybal (29) proposed a correlation based on a linear concentration difference driving force;

$$k_d = \frac{2 \pi^2 D_d}{3 d_p} \quad 4.19$$

#### 4.4.2 Circulating droplets

The liquid inside a drop moving in a viscous continuous phase tends to circulate due to the shear stress applied at its interface (53,54). As a result of this circulation the transfer rate is increased by a factor proportional to the Schmidt number (55). Kronig and Brink (56) made an analysis of mass transfer inside a circulating droplet with laminar circulation. Their relation can be applied for the case when resistance to mass transfer in the continuous phase is zero.

$$E_m = 1 - \frac{3}{8} \sum_{n=1}^{\infty} A_n^2 \exp \left[ -\lambda_n^2 \frac{16 D_d t_f}{r^2} \right] \quad 4.20$$

Where  $A_n, \lambda_n$  are Eigen values

The mass transfer coefficient becomes:

$$k_d = \frac{d_p}{6t} \ln \left[ 6 \sum_{n=1}^{\infty} A_n^2 \exp \left( -\lambda_n^2 \frac{4D_d t}{d_p^2} \right) \right] \quad 4.21$$

A correction for the calculated mass transfer coefficient, was proposed by Olander (57), for cases involving short contact times:

$$k_d = 0.972 k_{HB} + 0.075 \frac{d_p}{t} \quad 4.22$$

where  $k_d$  = actual transfer coefficient

$k_{HB}$  = coefficient calculated from Handlos and Baron's model, which is:

$$E = 1 - 2 \sum_{n=1}^{\infty} (A_n)^2 \exp \left( - \frac{\lambda_n^2 U_t}{128 \left( 1 + \frac{\mu_D}{\mu_c} \right) d_p} \right) \quad 4.23$$

Heertjes et al (43) present a value for  $A_n$  and  $\lambda_n$  for values of  $n$  from one to seven. Calderbank et.al. (58) proposed an empirical approximation to equation 4.20,

$$E_m = 1 - \exp \left[ - \frac{2.25 D_d t}{r^2} \right] \quad 4.24$$

Kronig and Brink (56) proposed an equation for circulating droplets (laminar circulation)

$$K_d = \frac{17.9 D_d}{d_p} \quad 4.25$$

Handlos and Baron (59), who assumed that the liquid between streamlines became really mixed after one circuit, proposed a correlation for mass transfer coefficient for droplets under turbulent circulation as:

$$k_d = \frac{3.75 \times 10^{-3} u_t}{(1 + (\mu_d/\mu_c))} \quad 4.26$$

Skelland and Wellek (60) and Johnson and Hamielec (35) verified this correlation using experimental data.

#### 4.4.3 Oscillating droplets

Garner and Haycock, mentioned in (50), found that the period of oscillation was dependent on the physical properties of the liquid-liquid system, particularly the densities. Johnson and Hamielec (35) reported that once oscillations were set-up in drops the diffusivities were 52 times greater than the molecular values. Kinter (61) proposed a model for mass transfer from vigorously oscillating, single liquid drops moving in a liquid field based on the concept of interfacial stretch and internal droplet mixing. The proposed model gives:

$$E_m = 1 - \exp \frac{2\pi D_E}{v} \int_{t_0}^{t_f} \frac{1}{f_1(t)} \left[ \left( \frac{3v}{4\pi W} \right)^2 + \frac{1}{2\alpha} \ln \left( \frac{1+\alpha}{1-\alpha} \right) + W \right] dt \quad 4.27$$

where:

$$\alpha = \frac{W - (3v/4\pi W)^2}{W} \quad 4.28$$

and,

$$W = (a_0 + a_p / \sin \bar{\omega} t)^2 \quad 4.29$$

$$X = \frac{[a_0^2 b_0 - (a_0 - X_0)^2 (b_0 - X_0)] - 2abX_0 + bX_0^2}{a^2 - 2aX_0 + X_0^2} = f_1(t) \quad 4.30$$

$$a = a_0 + a_p [\sin 0.5\omega t] \quad 4.31$$

Rose and Kinter (61) developed a mass transfer coefficient model for the case of oscillating drops:

$$k_d = 0.45 (D_d \omega)^{0.5} \quad 4.32$$

where the frequency of oscillation is predicted from Schroeder and Kinter's equation, later modified by Lamb (62).

$$\omega^2 = \frac{n \sigma b_1}{r_{dp}^3} \left[ \frac{(n+1)(n-1)(n+2)}{[(n+1)\rho_d + n\rho_c]} \right] \quad 4.33$$

where

$$b_1 = \frac{de^{0.225}}{1.242} \quad 4.34$$

and  $n$  is the mode of oscillation, when  $n = 0.1$  corresponding to rigid body motion. The fundamental mode corresponds to  $n = 2$ .

Another model for oscillating droplets was proposed by Ellis based on the assumption that oscillating droplets could be divided into different regions of mass transfer. This division of the droplet is not in agreement with the physical phenomena of drop oscillation and also the shape of the drop is not a sphere during oscillation (62).



A summary of the best-known correlations is given in Table 4-1 .

#### 4.5 Mass Transfer in the Continuous phase

Griffith (66) has reported data on mass transfer from stationary liquid drops of isobutanol, ethylacetate, cyclohexanol, and isobutyl acetate to a flowing water stream under forced convection conditions. The mass transfer rate coefficients of the continuous water phase were correlated by the equation:

$$Sh_C = 2 + B (Re)^{0.5} (Sc)^{0.33} \quad 4.35$$

The value of B varied from 0.63 to 0.7 specifically dependent upon the droplet-phase liquid .

Many investigators have attempted to derive a theoretical or empirical correlation for the continuous phase-mass transfer coefficient. Summaries of these investigations have been presented by Linton (67). The different mechanisms of mass transfer in the continuous phase to, or from, a droplet depend on the hydrodynamic state of the droplets. They are divided into the three classes stagnant, circulating, and oscillating as already discussed .

##### 4.5.1 To, and From, Stagnant Droplets

Garner and Jenson (68) used the boundary layer theory to propose an equation for mass transfer to or from, rigid spheres :

$$Sh_C = A + B Re_C^{1/2} Sc_d^{1/3} \quad 4.36$$

Table 4.1 Dispersed phase mass transfer correlations during drop travel

Author and Reference	Correlation	State of Drops	Remarks
Newman (51)	$E_m = \frac{C_1 - C_0}{C_1 - C^*} = \pi \left( \frac{D_d t_f}{r^2} \right)^{0.5}$	Stagnant	For small drop size
Calderbank et al (58)	$E_m = \frac{C_1 - C_0}{C_1 - C^*} = \pi \left( \frac{R D_d t}{r^2} \right)^{0.5}$	Laminar Circulation	R is the ratio of effective diffusivity to molecular diffusivity = 2.25
Kronig and Brink (56)	$E_m = 1 - \frac{3}{8} \sum_{n=1}^{\infty} A_n^2 \left[ \frac{-\lambda_n 16 D_d t}{r^2} \right]$	Laminar Circulation	Values of $A_n$ and $\lambda_n$ for (n) from 1-7 presented by (54)
Handlos and Baron (59)	$Sh_d = 3.75 \times 10^{-3} Pe_d / \left( 1 + \left( \frac{\mu_d}{\mu_c} \right) \right)$	Turbulent Circulation	Recommended when resistance to mass transfer exists in continuous phase
Skelland and Wellek (60)	$Sh_d = 31.4 T_m^{-1.338} Sc_d^{-0.125} We^{0.371}$	Circulating	Drops falling in a stationary continuous phase
Rose and Kintner (61)	$k_d = 0.45 (D_d \omega)^{0.5}$	Oscillating	For symmetrical spheroid droplet, widely accepted
Angelo et al (63)	$k_d = \left[ \frac{4 D_d \omega (1 - \epsilon + \frac{3}{8} \epsilon^2)}{\pi} \right]^{0.5}$	Oscillating	For integral number of completed oscillations

Table 4.1 continued

frequently determined

Author and Reference	Correlation	State of Drops	Remarks
Brunson et al (64)	$Sh_d = \frac{2}{\pi} \frac{d^2 \omega}{2D} \left[ \frac{1}{1 + 0.687 \epsilon^2} \right]^{0.5}$	Oscillating	With 26% absolute deviation
Yamaguchi et al (65)	$Sh_d = 1.14 (Re')^{0.56} (Sc_d)^{0.5}$	Oscillating	For transfer of low solute concentration from aqueous drop to organic continuous phase
Al-Hassan (60)	$k_d = 4.3 \epsilon^{2.69} E_o^{1.62} (D_d w)^{0.5}$	Oscillating	

where A, B, c, d are constants, subsequently determined experimentally .

Linton et.al.(69) proposed a similar equation for stagnant droplets in the system; water-acetone-toluene, as follows :

$$Sh_C = 0.0582 (Re)^{0.5} (Sc)^{0.33} \quad 4.37$$

This ignored the wake effect. However, Rowe et.al.(70) proposed an equation which included a term accounting for the diffusion process:

$$Sh_C = 2 + 0.76 (Re)^{0.5} (Sc)^{0.33} \quad 4.38$$

Kinard (46) proposed another equation to include the wake effect as follows:

$$Sh_C = 2 + (Sh)_n + 0.45 (Re)^{0.5} (Sc)^{0.33} + 0.0484 (Re) (Sc)^{0.33} \quad 4.39$$

#### 4.5.2 To, and from, Circulating Droplets

Heertjes and de Nie (43) recommended the following correlation for circulating drops, when  $Re > 10$

$$Sh_C = 1.13 (Re)^{0.5} (Sc)^{0.5} \quad 4.40$$

For a baffled vessel with a flat-blade, turbine impeller Kinard (46) proposed a correlation of single drop data for the systems: benzoic acid-kerosene-water, benzoic acid-toluene-water by the equation

$$Sh_C = 0.0924 (Re)^{0.071} (Sc)^{0.5} \quad 4.41$$

which implies a surprisingly low dependence on velocity. Tayeban (79) proposed an equation with the constant as 0.6.

$$Sh_C = 0.6 (Re)^{0.5} (Sc)^{0.5} \quad 4.42$$

but this correlation is inapplicable to  $Re > 450$ .

Friedlander (72) has proposed the following equation for the continuous phase film coefficient in laminar motion for  $Pe > 10^3$

$$Sh_C = 0.99 (Pe)^{0.33} \quad 4.43$$

while Gaffney (73) has recommended the following relationship:

$$Sh_C = 2 + 1.13 (Pe)^{0.5} (k_v)^{1/3} \quad 4.44$$

where  $k_v$  is a function of  $(\mu_d/\mu_c)$  and Reynolds number  $Re$ .

For fully circulating drops, Equation (4.44) reduces to the Boussinesq equation (74) based on potential flow. Boussinesq's proposed correlation did not consider the existence of a wake under practical conditions, although the constant was still 1.13. This correlation is claimed to be valid for many systems.

From a consideration of the surface velocity distribution and a general expression for short range diffusion from a circulating sphere , Baird and Hamielec (75) have suggested the following equation for viscosity ratio  $\mu_d / \mu_c$  less than 2.

$$Sh = \frac{2}{\pi} Pe \left( \frac{40 + 8A_1}{24 + 9/\mu_d/\mu_c} \right) \quad 4.45$$

where  $A_1$  is a function of  $Re$  and  $(\mu_d / \mu_c)$  .

#### 4.5.3 To, and From, Oscillating Droplets

Oscillation commences in regimes of flow for which droplet Reynolds number  $Re > 200$ . Below this circulation predominates. Garner et.al. (76) observed that mass transfer data for liquid drops and gas bubbles demonstrated increased transfer in the continuous phase due to oscillation. Hughmark (77) suggested the following correlation for oscillating liquid drops

$$Sh_c = 2 + 0.084 \left[ (Re)^{0.489} (Sc)^{0.339} \left( \frac{d_p g^{0.33}}{D_c^{0.67}} \right)^{0.072} \right]^{1.5} \quad 4.46$$

Garner and Skelland (78) suggested that the continuous phase coefficients when oblate-prolate oscillations are present can be calculated from the Higbie equation,

$$k_c = 2 \left( \frac{D_c}{\pi t_e} \right)^{0.5} \quad 4.47$$

where  $t_e$  is the time of contact for solute transfer.

Garner and Tayeban (79) reported a Schmidt number exponent greater than 0.5 because, for oscillating drops, there is less dependence on diffusivity. Their correlation is:

$$Sh_C = 50 + 0.0085 (Re)(Sc)^{0.7} \quad 4.48$$

Yamaguchi (80) proposed an equation with a modified Reynolds number  $\hat{Re} = \rho \omega d_e^2 / \mu_C$  for oscillating drops, which neglects the drop velocity, as follows:

$$Sh_C = 1.40 (\hat{Re})^{0.56} (Sc)^{0.5} \quad 4.49$$

Finally Mekasut et.al.(81) correlated the Sherwood number with Galileo number for oscillating drops of 0.2 to 0.4 cm ,

$$(Sh)_C = 6.74 (Ga)^{0.34} \quad 4.50$$

They ignored the effect of the frequency of oscillation of the drop, so that their correlation would be expected to be strictly limited to the experimental conditions covered (82).

#### 4.6 Mass Transfer during phase separation :

Skelland and Menhas's (42) observed that insignificant mass transfer occurred during coalescence under gravity. This has been confirmed by Heertjes and deNie (43). Further since coalescence on impact with an interface is almost instantaneous (with a time of the order of  $3 \times 10^{-2}$  sec), very little mass transfer would be expected .

#### 4.7 The Driving Force

Most theoretical interpretations of interface mass transfer presume that the process can be adequately described by the Ohm's law type of rate expression, given earlier in which the transfer resistance is independent of both the concentration level and the direction and magnitude of the concentration driving force (83). This assumption is invalid with very large driving forces when the effects of property variations (e.g. interfacial tension) and interfacial velocity begin to affect the mass transfer coefficient.

Some investigators (83,84,85) suggested that activities rather than concentrations should be used as a measure of the driving force. Nevertheless, since activities are difficult to evaluate accurately in extraction equipment, concentration is usually used to estimate the driving force.

Other investigators (80, 81, 86) have noted a change in mass transfer rate with a change of solute concentration and have attributed this to a change in the interfacial tension. Olander and Redd (83) reported that the overall mass transfer coefficient for three systems increased sharply by factors of 1.5 - 4 as the driving force was increased. In addition to high solute concentrations causing greater interfacial turbulence and hence higher rates of mass transfer (31), Licht and Conway (40) reported that, for equal concentration driving forces the rate of mass transfer of a common solute, such as acetic acid, depends upon whether the solute is transferred from the organic phase to the



water phase or vice versa. This phenomenon is presumed to be the result of hydrogen bonding forces being more intense when acetic acid is being extracted from water than when it is being extracted from an organic phase. Overcashier et. al. (86) found that the average mass transfer driving force itself was affected by the degree of baffling in a mixer, comprising a vessel 36.5cm diameter with either propellers, spiral turbines, or flat blade turbines from 10 to 25cm diameter. They stated that when baffles are present, axial flow is increased, especially with propellers, and the entering feed streams are diluted with solutions closer to equilibrium, thus reducing the average mass transfer driving force. In the absence of baffles, end-to-end mixing is diminished and a swirling plug-type flow results which utilizes the driving force better and permits mass transfer at a lower agitation level.

The driving force in an extraction process is measured (87), as with any diffusion process, by the deviation of the system from equilibrium. The difference between the actual concentration of solute in one phase and the concentration which should be in equilibrium with that in the other phase is the force tending to dissolve (or release from solution) the solute. The algebraic sum of these differences of concentrations causes the process to proceed. Jeffreys et. al. (88) used Simpson's rule to estimate the mean concentration driving force over a column but if both the

equilibrium curve and the operating line are straight lines, the mean driving force is best determined by the logarithmic mean.

#### 4.8 Mass Transfer and Interfacial Area

The hydrodynamic conditions on both sides of the interface affect the mobility of the interface. Thus the hydrodynamic conditions in the interface have an important effect on the mass transfer rate. The phenomena of the Marangoni effect (89), is due to momentum transfer caused by surface tension driving force. Additional phenomena can affect the mass transfer rate other than by a change in the hydrodynamic conditions, e.g., by diminished diffusivity across the interface due to the presence of surface-active agents which form a barrier to solute diffusion.

Sterling and Scriven (90) studied the relation between Marangoni effect and mass transfer. They reported that some systems may be stable with solute transfer in one direction but unstable with transfer in the opposite direction.

They suggested that interfacial turbulence is usually promoted by

- i) Solute transfer out of the phase of higher viscosity ;
- ii) Solute transfer out of the phase in which its diffusivity is lower ;
- iii) Large differences in kinematic viscosity and solute diffusivities between the two phases ;
- iv) Steep concentration gradients near the interface;

v) A system in which the interfacial tension is highly sensitive to solute concentrations ;

vi) Low viscosities and diffusivities in both phases;

vii) Absence of surface active agent, and ,

viii) Interfaces of large extent.

Schindler and Treybal (91) measured the area-free continuous phase mass-transfer coefficients for continuous flow of ethyl acetate (dispersed) and water (continuous) in a  $24.13 \times 10^{-2}$  m diameter baffled vessel, agitated with either  $7.62 \times 10^{-2}$  m or  $12.7 \times 10^{-2}$  m diameter flat-blade turbines, and in the absence of baffles using the  $7.62 \times 10^{-2}$  m turbine. Their experimental data were based on drop sizes measured at the bottom of the vessel. However despite this and their determination under batch conditions, the distributions are claimed to be applicable to positions throughout the vessel and for continuous flow. The specific area at the bottom was however in general substantially smaller than that predicted from the correlations of Calderbank (92). Vermeulen's correlation (93), is for  $a_{av}$  and gives results roughly in agreement with observed areas, but indicates a more rapid increase with impeller speed than that observed. Figure 4.1 shows that the areas produced by the  $7.62 \times 10^{-2}$  m turbine in baffled and unbaffled vessels were similar for the same impeller power and  $\phi_D$ , which is in agreement with the findings of Fick (94). Figure 4.2 illustrates the drop-size distribution for the same conditions and impeller speed in both batch and continuous flow runs. The only impor-

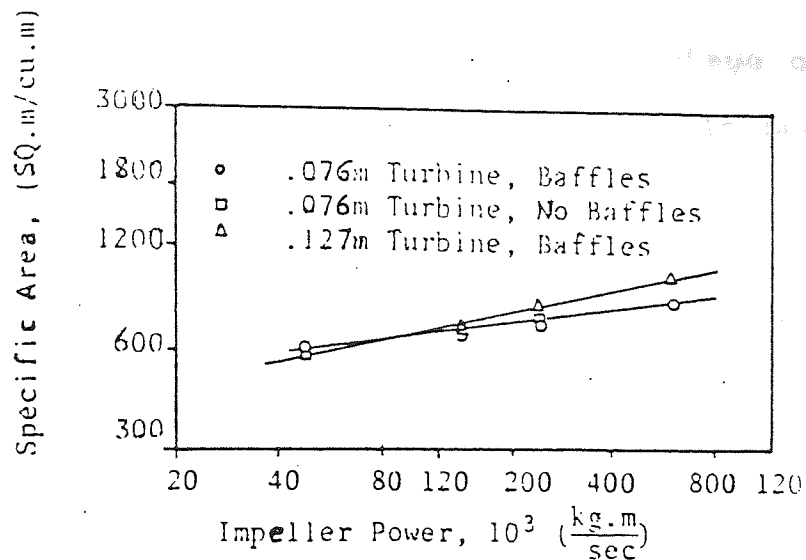


FIG. 4-1 SPECIFIC AREA AT VESSEL BOTTOM OD=0.02m (92)

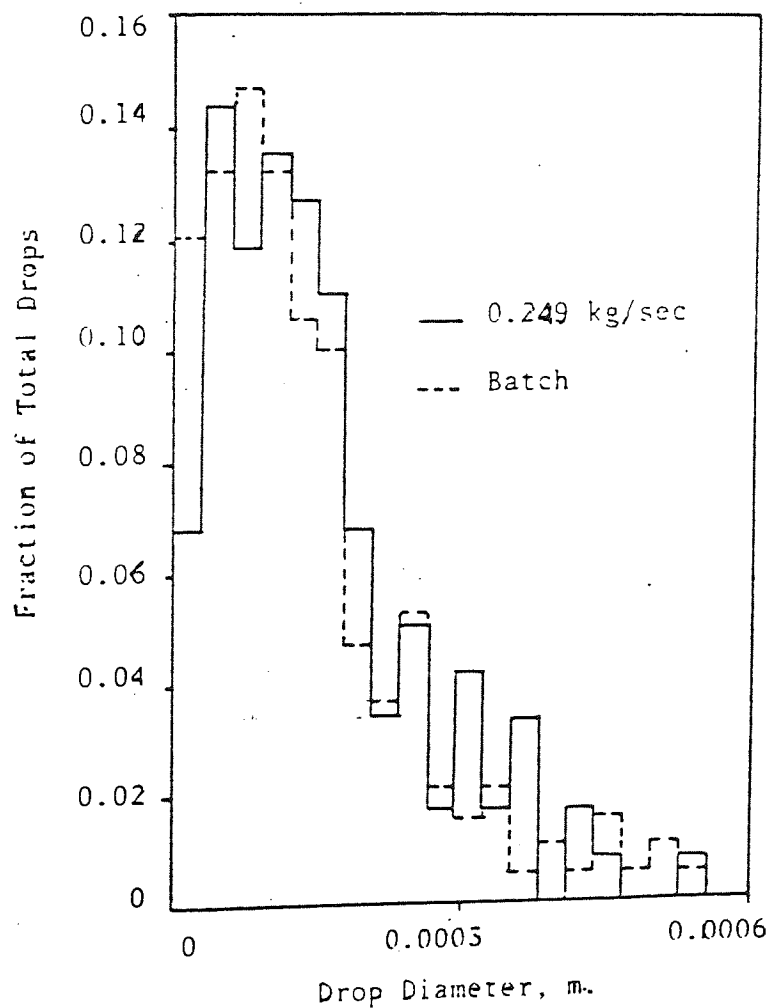


FIG. 4-2 DROP-SIZE DISTRIBUTION; OD = 0.0407 m  
0.076m impeller, 325 r.p.m. (92)

tant difference is in the percentage of small drops, which may be completely dissolved in continuous operation.

According to Schindler and Treybal (91), the concentrations of ethyl acetate in the bulk continuous liquid  $X_{A2}$  were the same at all three levels of sampling for the baffled vessel; but the difference between  $X_{A2}$  at the top and bottom was approximately 2% in the unbaffled vessel. Thus both vessels were essentially completely backmixed. The driving force,  $X_{A1} \rightarrow X_{A2}$ , was therefore essentially constant throughout the vessel. Three different mass transfer coefficients were used (95), defined for the backmixed vessel by,

$$W_A = k_1 a_{av} (X_{A1} - X_{A2}) \quad 4.51$$

$$W_A = k_2 a_{av} \ln \frac{W_A / (W_A + W_B) - X_{A2}}{W_A / (W_A + W_B) - X_{A1}} \quad 4.52$$

$$W_{A1} - X_{A1} (W_A + W_B) = k_3 a_{av} (X_{A1} - X_{A2}) \quad 4.53$$

Since both ester and water were extracted, only  $k_2$  and  $k_3$  are really applicable, but they differed by less than 2%. They were therefore reported as  $k_C$ , whose units permit more direct comparison with the work of others;

$$k_1 = k_2 = k_3 = k_C (\rho/M)_{av} \quad 4.54$$

Figure 4.3 illustrates how the typical volumetric coefficients  $k_c a_{av}$ , were influenced by impeller Reynolds number, for comparison with other data (96). The specific area corresponding with the data in Figure 4-5 is shown in Figure 4.4. It varies less rapidly with  $\phi_{Dav}$  than does  $k_c a_{av}$ , so that hold-up also influences  $k_c$ . The data of Schindler and Treybal (91) reproduced in Figure 4.5 illustrates the influence of dispersed - phase hold-up on  $k_c$ .

Figure 4.6 indicates that  $k_c$  for the unbaffled vessel was roughly 2.5 times larger than that for the baffled vessel at the same impeller speed. It was suggested that if two drops of ethyl acetate of diameter  $0.03 \times 10^{-2} \text{ m}$  and interfacial tension  $6.4 \times 10^{-3} \text{ kg/sec}^2$  coalesce, the energy release due to reduction in surface is equivalent to a kinetic energy for the resulting large drop corresponding to a velocity of about  $0.245 \text{ m/sec}$ . Hence the violence of the coalescence action may be sufficient to renew the shell of continuous liquid surrounding the drop, thus enhancing the rate of mass transfer.

In a study (41) of mass transfer in a laboratory scale mixer-settler using the system acetic acid - toluene-water at different temperatures it was concluded that the overall mass transfer coefficient increased as the number of stages increased as shown in Figure 4.7. Average values of dispersed phase holdup and droplet diameter were considered.

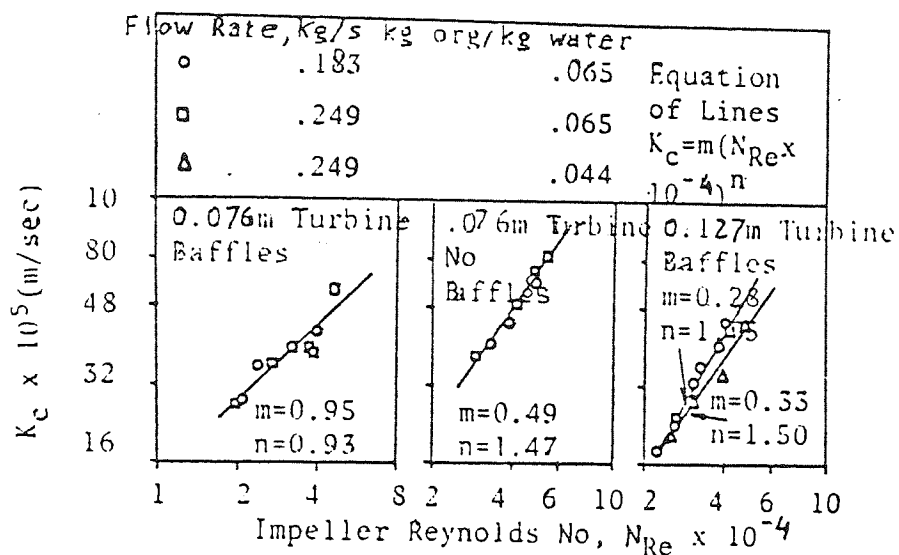


FIG. 4-3 CONTINUOUS PHASE MASS TRANSFER COEFFICIENT  
AT DIFFERENT REYNOLDSNO'S (92)

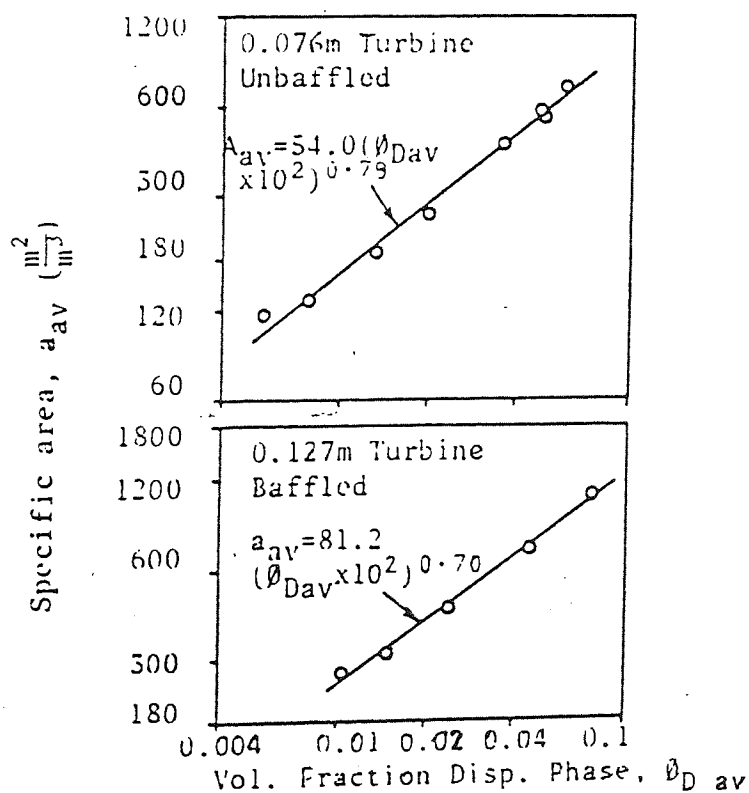


FIG. 4-4 MEAN SPECIFIC AREA : FLOW RATE 0.249 kg/sec.  
Re = 28,500 to 33,800 (92)

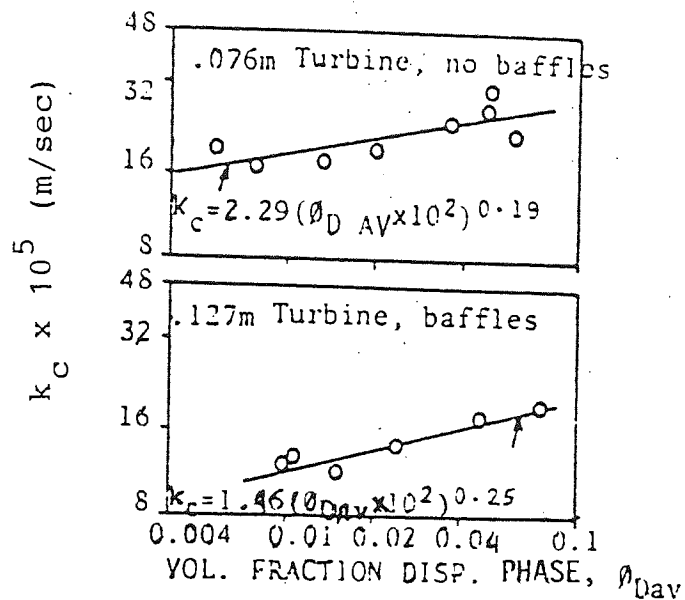


FIG. 4-5 INFLUENCE OF DISPERSED PHASE HOLD-UP ON  $k_c$ , FLOW RATE 0.249 kg/sec  
 $N_{Re} = 28,500$  to  $33,200$ . (92)

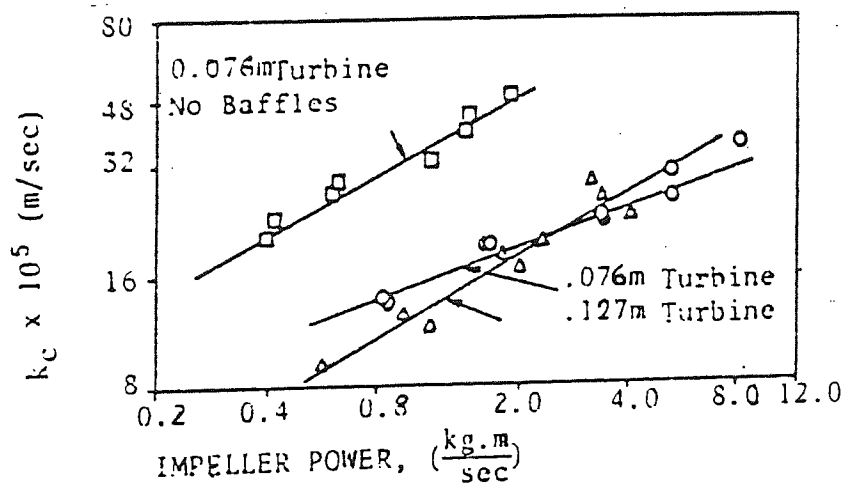


Fig. 4-6 INFLUENCE OF BAFFLES AND IMPELLER POWER ON  $k_c$ ; FLOW RATE 0.185 to 0.249 kg/sec., 0.065 kg. org./kg. water (92)



Efficient

Efficiencies may be deter-

mined by the following

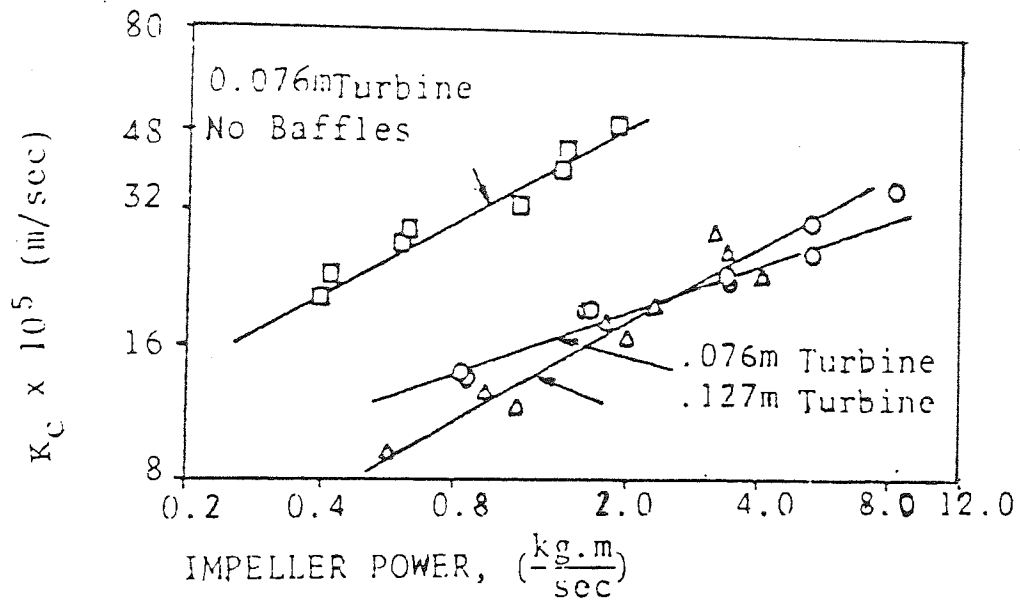


FIG. 4-7 EFFECT OF BAFFLES ON  $K_c$  AT DIFFERENT IMPELLER POWER, FLOW RATE 0.24g kg /sec., 0.38 kg/sec. org phase/ 1kg/sec. of water

#### 4.9 Overall Mass Transfer Coefficient

Overall mass transfer coefficients may be determined by the additivity of individual resistances. Thus:

$$\frac{1}{K_{OC}} = \frac{1}{k_C} + \frac{1}{mk_d} \quad 4.55$$

$$\frac{1}{K_{Od}} = \frac{1}{k_d} + \frac{m}{k_C} \quad 4.56$$

The individual phase coefficients need to be evaluated by taking into account whether the drops formed are of the circulating, oscillating or rigid type.

Patel and Wellek (97) have suggested that if  $k_C$  is estimated by Garner and Tayeban's equation (79) given below:

$$Sh = 50 + 0.0085 (Re) \left( \frac{\mu_c}{\rho_c D_c} \right)^{0.7} \quad 4.57$$

$k_d$  should be estimated by the Handlos and Baron equation (4.26). Patel and Wellek also tested the effect of circulation within the drop in the Handlos and Baron (59) models for the determination of  $k_C$  and  $k_d$  by equation (4.26). Overall coefficients in terms of  $K_{Od}$  taking the values of  $k_C$  and  $k_d$  by equations (4.41) and (4.26) have shown good agreement with experimental

data for a wide range of systems. The above analysis illustrated how overall mass transfer performance can be predicted from single drop mass transfer data. However in the real situation, as discussed in Chapter 6, a distribution of drop sizes will exist in any swarm within an extractor. Coalescence and redispersion may also occur, generally resulting in enhanced mass transfer. Furthermore in some contactors, but not in a conventional mixer-settler cascade, the driving force is modified by back-mixing effects.

Equipment may be clas-

## CHAPTER 5

---

### LIQUID-LIQUID EXTRACTION EQUIPMENT CLASSIFICATION

### 5.1 Equipment Classification

Liquid-liquid extraction equipment may be classified as:

- i. Stage-wise (discrete stage) contactors, which include mixer-settler units;
- ii. Continuous (differential) contactors, which include the different types of packed, rotary agitated or pulsed columns.

In the first category the liquids are mixed, extracted and separated in discrete stages. In the second category the immiscible phases are contacted counter-currently and the equivalent of several stages are accommodated in one shell. Table 5.1 provides a typical classification for the most common units, depending upon the type of any agitation applied. Table 5.2 summarizes the features and fields of industrial application of commercial extractors.

### 5.2 Equipment Selection

The important considerations in selecting a contactor for a specific duty are:

- i. the number of stages or transfer units required
- ii. the volumetric throughput
- iii. the residence time.

Although each contactor possesses advantages and disadvantages, the choice for any particular extraction depends largely upon experience. Continuous extractors are, in general, preferable to mixer-settlers when large throughputs are needed since they offer economies in agitation power cost, floor space and solvent inventory. They can operate with relatively low phase

<i>Mechanical</i> Type of agitation		Stage wise contactors	Continuous contactors
None			1. Wetted-wall towers (29) 2. Spray columns (98, 29) 3. Baffle plate columns (29) 4. Packed towers (29)
Rotary devices		1. Simple mixer-settler (101) 2. Pump-mix settler (102) 3. Stacked-stage mixer settler (98) 4. Individual stage centrifuges (98, 29)	1. Scheibel column (99) 2. Oldshue-Rushton column (100) 3. Multistage mixer columns (29) 4. Podbielniak extractor (98) 5. Luwesta (98) 6. Rotating disc contactor (98, 29)
Pulsed		Pulsed mixer settler (98)	Pulsed columns (98, 29)

TABLE 5.1 CLASSIFICATION OF EXTRACTORS DEPENDING UPON THE TYPE OF AGITATION

Types of extractor	General features	Fields of industrial application
unagitated columns e.g. spray, packed, sieve plane mixer-settlers	low capital cost, low operating and maintenance cost, simplicity in construction, handles corrosive material	petrochemical, chemical
	high-stage efficiency, handles wide solvent ratio, high capacity, good flexibility, reliable scale-up, handles liquids with high viscosity	petrochemical, nuclear, fertilizer, metallurgical
pulsed columns e.g. pulsed plate, pulsed packed columns	low HETS, no internal moving parts, many stages possible	nuclear, petrochemical, metallurgical
rotary agitated columns e.g. RDC, Scheibel, Oldshue-Rushton	reasonable capacity, reasonable HETS, many stages possible, reasonable construction cost, low operating and maintenance cost	petrochemical, metallurgical, pharmaceutical, fertilizer
Reciprocating-plate columns	high throughput, low HETS, great versatility and flexibility, simplicity in construction, handles liquids containing suspended solids, handles mixtures with emulsifying tendencies	pharmaceutical, petrochemical, metallurgical, chemical
centrifugal extractors stage wise or differential	short contacting time for unstable material, limited space required, handles easily- emulsified material, handles systems with little liquid density difference	pharmaceutical, nuclear, petrochemical

TABLE 5.2 SUMMARY OF FEATURES AND FIELDS OF INDUSTRIAL APPLICATION OF COMMERCIAL EXTRACTORS

ratios, and their flexibility of operation also enables extraction to be performed with systems likely to form fine dispersions (102), e.g., by operating with low rates of agitation.

Mixer-settlers are inherently simple in design and in construction and are easy to operate. Therefore they have found widespread use. The most important design considerations, and the process parameters to consider in extractor selection, are summarized in Table 5.3.

### 5.3 Advantages and Disadvantages of Mixer-Settlers

The main advantages of mixer-settlers are:

1. In contrast with counter-current continuous contact extractors, which are usually gravity operated towers, the degree of dispersion or intensity of turbulence in mixer-settlers may be established at any level through mechanical agitation without the risk of "flooding" or reducing the flow capacity of the equipment. However the formation of fine emulsions can result in excessive settling / coalescence times and hence large settling vessels

2. Any proportion of two liquids may be handled easily, with either phase dispersed, and the ratio of the two liquids in the mixer may be controlled independently of the ratio of the flow through the cascade as a whole.

3. Suspended solids are handled more successfully by a mixer-settler than by most other types of extractor.

4. The common horizontal arrangement of a multi-stage cascade is particularly useful when headroom is



TABLE 5.3 DESIGN CONSIDERATIONS AND PROCESS PARAMETERS  
FOR EXTRACTOR SELECTION

Factor	Contactors
1. Number of stages required:	
i) Few (2-3) stages	all types
ii) (10-20) stages	spray towers (33 m height) mixer-settlers
2. Capacity (throughput):	
i) Low or moderate	spray or packed columns
ii) Intermediate and high	RDC, pulsed columns, or mixer-settlers
3. Residence time:	
i) Short	centrifugal types
ii) Longer	1. Mixer-settlers (settling and phase separation depend on the rate of coalescence of the dispersed phase)  2. Differential contactors (the residence time is a function of the mean drop- let velocity and not on the coalescence rate)
4. Phase flow ratio:	
i) $\phi$ d less than 0.1 of the flow	mixer-settlers (96)
ii) $\phi$ d greater	other types
5. Physical properties:	
i) Small ( $\frac{\sigma}{\Delta\rho}$ )	Non-agitated contactors
ii) Large ( $\frac{\sigma}{\Delta\rho}$ )	Mechanically agitated con- tactors
iii) High viscosities	Mechanically agitated con- tactors

Continue TABLE 5 - 3

6. Direction of mass transfer:

- |   |                                  |
|---|----------------------------------|
| i) From solvent to aqueous phase          | Mechanically agitated contactors |
| ii) From the aqueous phase to the solvent | Little information is available  |

7. Phase dispersion and hold-up:

- |  |  |
|--|--|
| i) If the phase of the highest throughput is to be dispersed | Difficulties may be encountered in column contactors |
| ii) If a low hold-up of one phase is required                | Centrifugal contactors                               |

8. Slow reactions:

Mixer-settlers

9. Presence of solids in one or both feeds

Pulsed plate column, Luwesta centrifugal extractor, and Graesser contactor

10. Overall performance:

i) Performance index =

$$\frac{\text{mass of superficial flow rates at flooding}}{\text{HTU}}$$

For continuous differential contactors

ii) Performance index =

$$\frac{\text{sum of the volumetric phase flow rates at flooding}}{\text{Total volume of one stage}}$$

For stage wise contactors

low.

5. The horizontal arrangement also makes it possible to add additional stages to the cascade at any time, should that be necessary.

6. Continuously operated mixer-settlers may easily be shut-down for relatively long periods of time. On start-up there is no delay in reaching steady-state concentrations and on-specification product may be withdrawn almost immediately. This is not possible with gravity-operated columns in which the liquids settle out by gravity for the full length of the column on shut-down, necessitating recycle of off-specification products on start-up until steady-state conditions again arise. This advantage is particularly important for small scale processes operated intermittently.

7. A high degree of approach to equilibrium (i.e. a high stage efficiency) is almost always possible, and this makes for reliable design and more readily established guarantees of performance.

8. Reasonably reliable scale-up from small to industrial size is possible, at least for the simpler designs.

9. Mixer-settlers are free of interstage backmixing.

10. In the "pump mix" design the only moving parts are in the mixing pumps. These are very resistant to mechanical damage since they operate at low rev/min. and generally handle clean product, e.g., the mixing

pumps in an Aerosolvan plant, which has been in operation for nearly ten years, are claimed to have been completely trouble-free (103).

11. In the case of a vertical mixer-settler its tower construction is compatible with equipment used in the chemical and petroleum industries. Further improvements in mixer-settlers are likely to relate to improved settler design (104). This is clearly right and with modern plants emphasis should be on reducing the inventory of materials in process, i.e. reducing rate of the settler to mixer volumes possibly using mechanically-assisted separation.

Mixer-settlers may have the disadvantages that,

1. A secondary dispersion containing drops  $< 100 \mu\text{m}$  may be formed owing to high mixing efficiencies; this dispersion will not separate, and settle out in a reasonable time in a simple gravity settler.

2. Interstage pumping of either, or both, of the liquids is required in most designs.

3. Independent agitation equipment for each stage involves additional capital cost.

4. The horizontal arrangement occupies valuable floor space.

5. The high hold-up of the liquids in the settler increases the solvents inventory and hence the working capital requirements. It may also increase the hazard if highly flammable liquids are involved, or in nuclear fuels reprocessing.

The detailed arrangements of mixer-settler cascades are described in Chapter 6.

## CHAPTER 6

---

### MIXER-SETTLER EQUIPMENT

## 6.1 Mixer-Settler Characteristics

In its simplest form each stage of a mixer-settler, consists of a mixing vessel followed by a gravity settling chamber. The mixer may sometimes comprise only a centrifugal pump. Usually however it is a vessel provided with a propeller, or turbine, agitator and baffles. The settling chamber may be simply a tank or it may be provided with elaborate baffles, or contain packing to serve as a coalescing aid. A detailed discussion of settler design is given in section 6.5.

Figure 6.1 represents a simple classification of mixer-settlers depending on the type of mixing used and the settler characteristics.

Many mixer-settler geometries have been described in the literature. Some are summarized in Table 6.1.

## 6.2 Mixer Design

The function of the mixer is to provide an adequate combination of agitation to provide a homogeneous dispersion of large interfacial area, and sufficient residence time, for the desired degree of extraction to occur. Many mixers also incorporate a pumping action to avoid the need for separate pumps for interstage liquid transport. Agitation serves to create a homogeneous primary dispersion of drops with a distribution of sizes generally between 0.1 and 3mm. This facilitates mass transfer without subsequently introducing phase separation problems. Liquid-liquid mixers may therefore be classified into four types:

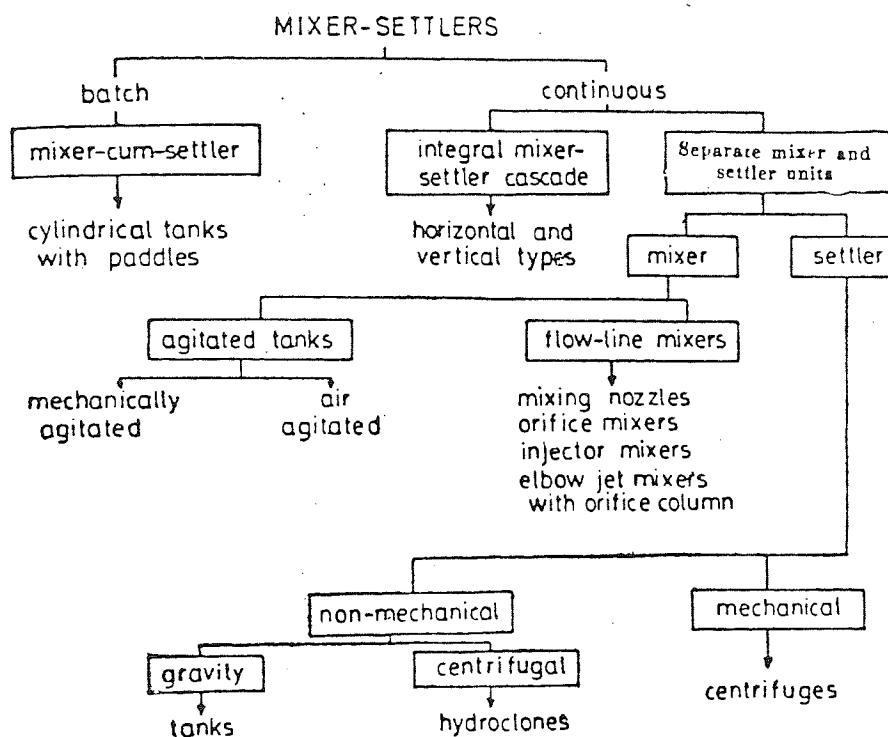


FIG. 6-1 BROAD CLASSIFICATION OF MIXER SETTLERS



TABLE 6.1 MIXER-SETTLERS GEOMETRIES

Title	Type	Recirculation	Type of Impeller	Interface Control	Mixing section design
Argonne Laboratory (1948)	Box contactor	Not designed for recirculation but probably occurred to a slight degree from settler back to mixer	Simple vertical paddles	Automatic between stages, but heavy phase off-take control on last stage	Feeds in and out via slots in walls but interposition of ante-chamber before mixer compartment
Standard Oil Co.Ltd. (1949)	-Ditto-	Similar to Argonne contactor	-Ditto-	-Ditto-	-Ditto-
Pump-Mix (1954)	Separate stages; pumps used as mixer	Not designed for recirculation	Centrifugal pumps as mixing section	Imps control	The mixing section is a centrifugal pump in a conventional casing. The combination produces excellent mixing.

Continue TABLE 6.1

A.E.R.E. Cylindrical stages; type (1954)	Separate mixers inside settlers	Circulation only within the mixers	Up-thrust type stirrers	Stirrer automatically controls each inter-face except final one	Phase feed into chamber in similar fashion to Mensing
Holley-Mott (1934)	Separate mixers and settlers	Both phases can be re-recycled from settler to mixer, via pipes, valve control	Simple vertical diamond shaped paddles	Probably automatic between stages and final heavy phase weir adjustable	Simple tanks, ports in walls
I.M.I. (1974)	Hydraulically independent battery of mixer settlers	Both phases can be recycled from settler to mixer	Turbine pump mixer	Pump control	Simple cylindrical tanks, posts in walls and draft tube

- i) Air-agitated vessels
- ii) Vessels with mechanical agitators  
(Mechanical mixers)
- iii) In-line mixers
- iv) Pump mixers

#### 6.2.1 Mechanical mixers:

Whilst vessels with mechanical agitators are widely used, the other three groups find only limited application in liquid-liquid extraction (99). The mechanical agitators are classified according to their shape, viz, as paddles, propellers, turbines or special mixers. These are mainly rotary mixers and can be subdivided into high speed and low speed impellers. Low speed mixers include paddles with a maximum speed of 60 rpm whilst high speed mixers include turbines and propellers. Mixing equipment may also be classified according to the type of flow pattern produced, e.g. tangential, radial, axial and/or compound flow. The basic flow patterns in agitated vessels are illustrated in Figures 6.2 and 6.3.

##### 6.2.1.1 Paddle mixers:

Paddle mixers are one of the oldest types of impeller. They have two blades, horizontal or vertical, with a high  $d_i/d_T$  ratio. The main advantages are simplicity and low cost, but their use is limited to liquids with a viscosity  $< 1.0$  kg/m sec, and axial flow of liquid from the impeller is small. Paddles are usually of large diameter,  $d_i/d_T = 0.66-0.9$ , and relatively slow speed, usually 15-45 rpm. They are used without baffles, due to their small pumping action, and

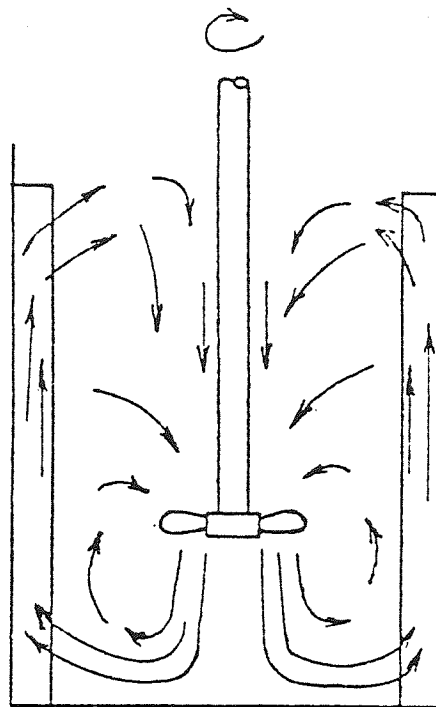


FIG. 6-2 PROPELLER WITH BAFFLES:AXIAL FLOW PATTERN

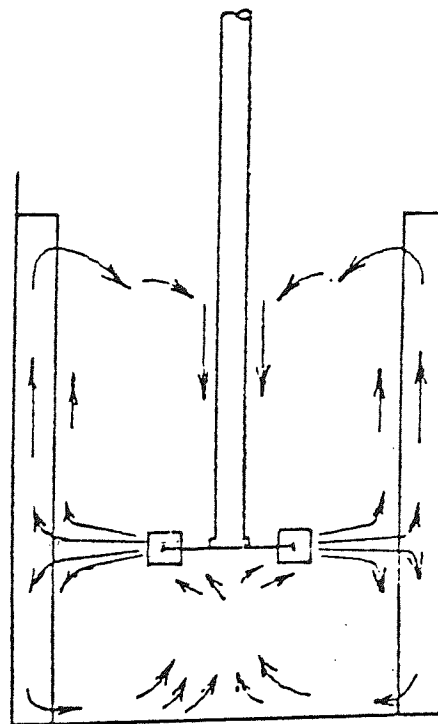


FIG. 6-3 FLAT BLADE TURBINE WITH BAFFLES : RADIAL FLOW PATTERN

there is no significant vortex formation. The relative dimensions of a single paddle on a shaft are defined in Figure 6.4.

#### 6.2.1.2 Propeller mixers:

Propellers are often used for agitation in tanks smaller than  $3.8 \text{ m}^3$  and less than 1.8m in diameter when less than 2.2kW is satisfactory for obtaining the desired process results.

Propeller mixers may be clamped on the side of an open vessel in the angular, off-center position as shown in Fig. 6-5. Two basic speed ranges are available: 1150 or 1750 rpm with direct drive and 350 or 420 rpm, or any other value, with a gear drive. Propellers may also be mounted near the bottom of the cylindrical wall of a vessel.

#### 6.2.1.3 Turbine Mixers:

The A.I.Ch.E. Standard Test Procedure for Impeller Type Mixing Equipment (107) defines a turbine as an impeller with an essentially constant angle with respect to a vertical plane, over its entire length or over finite sections having blades either vertical or set at an angle less than  $90^\circ$  with the vertical. The number of blades can be two or more, and they may be curved or flat. Figure 6.6 shows various shapes of turbine impeller. Their main advantage is their adaptability for liquids of high viscosity and density, e.g., viscosities up to 60 kg/m sec are allowable.

For effective dispersion the dimensional ratios of a turbine mixer are:

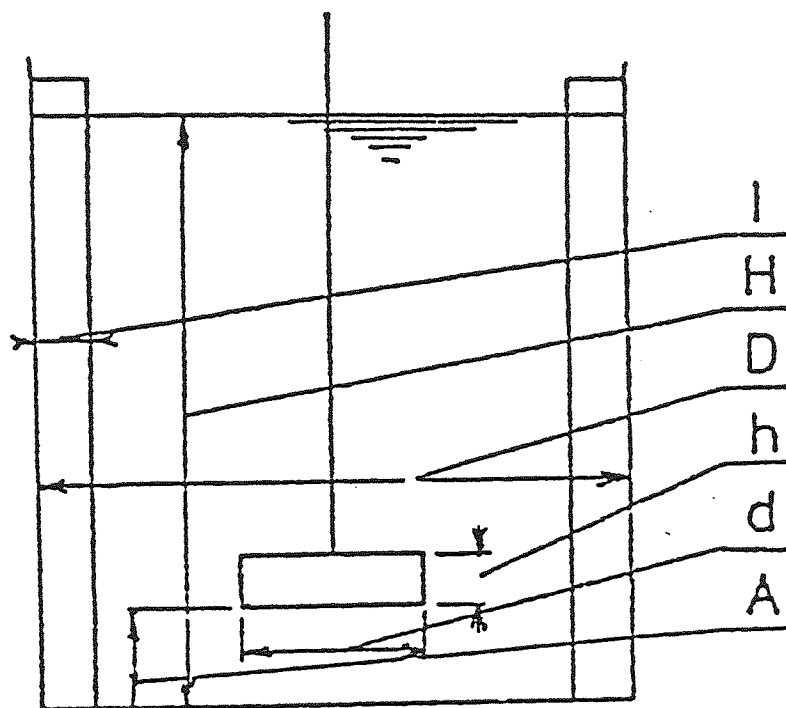


FIG. 6-4 FUNDAMENTAL GEOMETRIC VARIABLES  
IN AGITATED TANK

A	H
— = 0.0- 0.3	— = 0.8-1.3
D	D
d	h
— = 0.66-0.9	— = 0.1-0.2
D	D

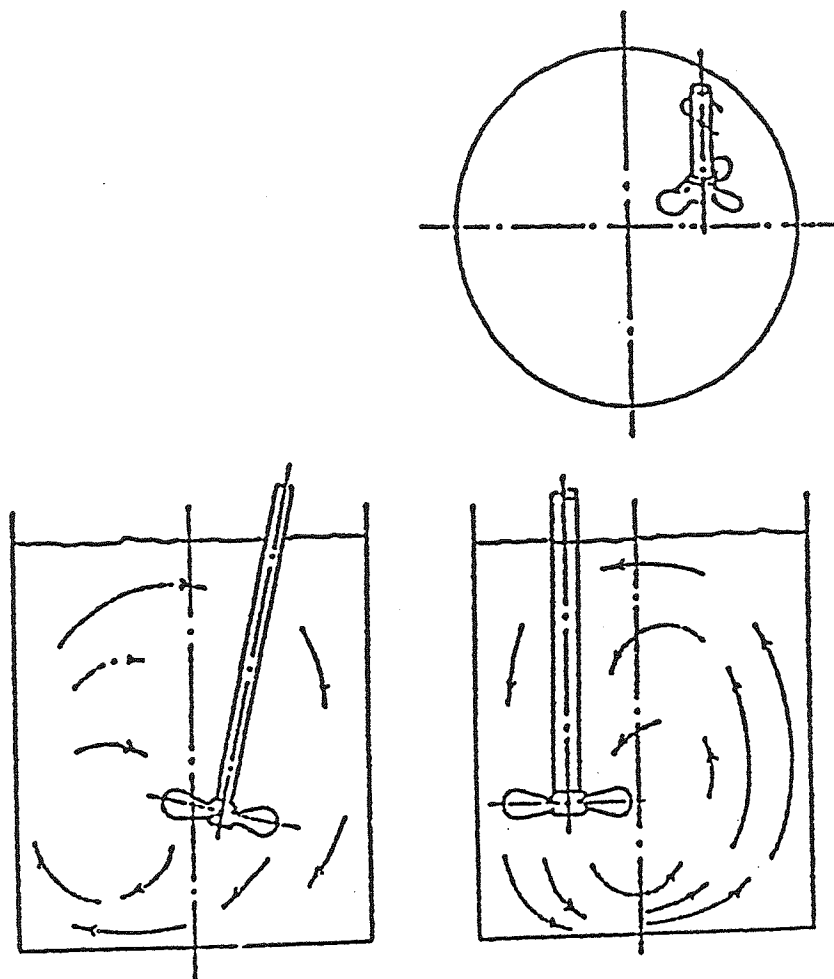


FIG. 6-5 FLOW PATTERN FOR PROPELLER IN  
AGITATED OFF-CENTRE POSITION WITHOUT BAFFLES

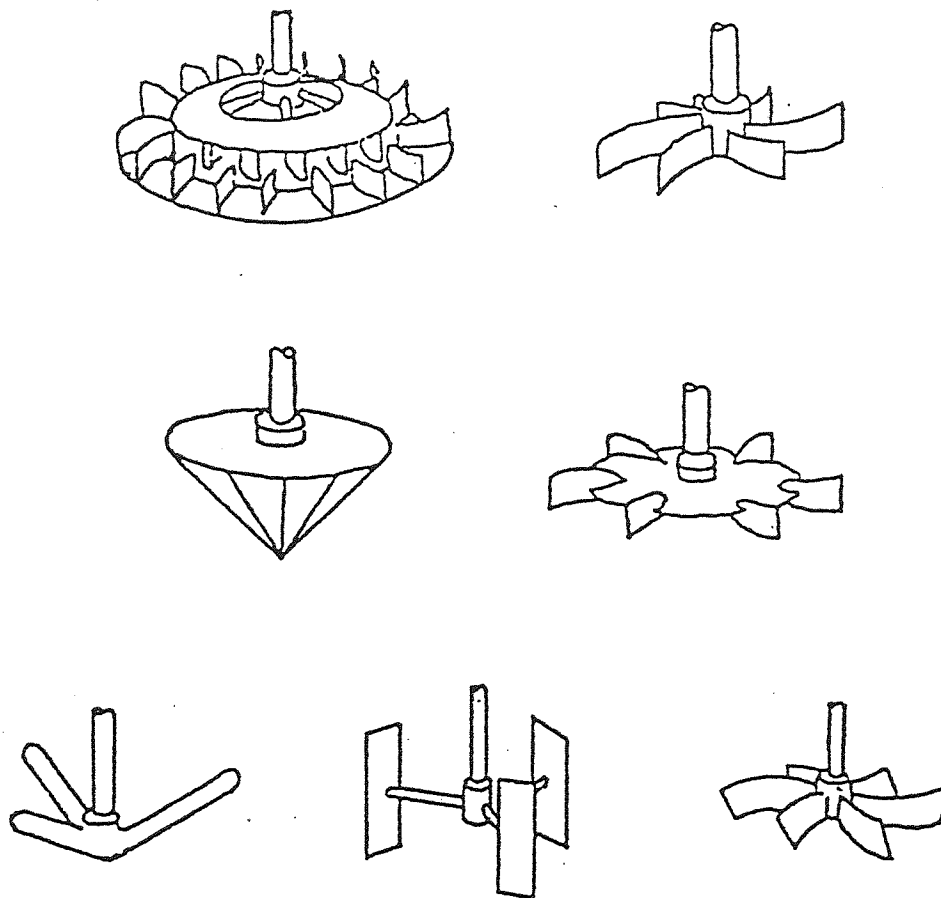


FIG. 6-6 MAIN IMPELLER TURBINE DESIGNS



$$\frac{d_T}{d_i} = 3-3.5, \quad \frac{H}{d_i} = 1.0-2.0$$

The tip speed of the blade ranges between 3.3m/s to 8.3 m/s

### 6.3. Drop Size Distribution.

It is desirable to be able to predict the drop size of a dispersion since a knowledge of this, and the dispersed phase hold up, enables the interfacial area of contact to be estimated. Generally, the maximum drop size that can be developed in a turbulent liquid is governed by the ratio of the dynamic pressure of the liquid that tends to break-up the drop and the interfacial tension forces that tend to counteract this.

In the case where the drops are large relative to the scale of turbulence, the ratio becomes:

$$We_{crit} = \frac{\rho_c \bar{U}^2 d_p}{\sigma} \quad 6.1$$

which defines a critical drop Weber number. The following equation for drop size has been derived on the basis of isotropic homogeneous turbulence, (29).

$$d_p = c_1 (N_{we})_{crit}^{0.6} \left( \frac{\sigma}{\rho_c} \right)^{0.6} \left( \frac{v \rho_m}{p} \right)^{0.2} \quad 6.2$$

Defining an impeller Weber number as,

$$We = \frac{d_i^3 N^2 \rho_c}{\sigma} \quad 6.3$$

This may be substituted into equation 6-2, with the various constant terms gathered together, to produce:

$$d_p = \frac{C_2 v^{0.4}}{We^{0.6} d_i^{0.2}} \quad 6.4$$

It is well-known that the turbulence in a mixing vessel generates a rather wide distribution of drop size. Moreover, there are the competing effects of the generation of new drops due to shear through turbulence in the bulk flow and droplet coalescence due to drop interaction effects. Depending upon the characteristics of the particular contactor there will be a balance of these processes so that at a distance considerably removed from the feed inlet, two limiting situations may arise; a distribution of drop size and drop residence times, or a size distribution of drops all essentially of the same age. This size distribution may be considered to be bounded by an upper limit and a minimum stable size (105) depending upon the break-up processes prevailing.

The Weber number governs the maximum drop size. Thus when two immiscible liquids are agitated a dispersion is formed in which continuous break-up and coalescence of droplets occur until, after a short time, a dynamic equilibrium is established between the break-up and coalescence processes. This results in a distribution of drop sizes which together with the mean

drop size, depends on the type and extent of agitation and the physical properties of the liquids. If the extent of agitation is sufficient to maintain a uniform level of turbulence throughout the vessel the mean drop size and drop size distribution will be the same throughout; otherwise clusters of drops of different sizes will exist in different parts of the vessel.

However, for every physical system and set of conditions there must be a stable drop size. Drops larger than this will tend to break-up whereas small drops will tend to coalesce (108).

#### 6.4. Power Requirement

Treybal (29) suggested that the following equation may be used for a four-bladed paddle in an unbaffled vessel to estimate the minimum impeller speed  $N$  for mixing the liquid phases.

$$N = \frac{30600}{d_T^{0.67}} \left( \frac{\mu_c}{\rho_c} \right)^{0.111} \left( \frac{\Delta p}{\rho_c} \right)^{0.26} \quad 6.5$$

Miller and Mann (109) who studied the power characteristics of a variety of impeller designs in a cylindrical mixing chamber observed slight variations in power consumption among the various impellers at any specific mixing index. For continuous operation in a baffled vessel mixing index,  $I_M$ , could be defined in terms of the ratio of the hold up of the dispersed phase to the fraction of the dispersed phase in the feed, as indicated by,

x

on the type of im-

$$I_M = \frac{x}{U_d / (U_d + U_c)} \quad 6.6$$

A mixing index of unity indicates complete uniformity in mixing. Miller and Mann (109) have observed that in the case of an unbaffled vessel with batch operation, uniform dispersions were developed by the application of impeller power input of 285 to 570 mN/S : m<sup>3</sup>. For baffled vessels with continuous operation a plot of mixing index versus agitator power based on data for kerosene-water dispersions indicates approximately a mixing index of 0.95 corresponding to input power of 455 mN/S : m<sup>3</sup> (29)

### 6.5 Dimensional Analysis

Dimensional analysis can be applied to derive the equation for agitator power. The dimensionless relationship

$$f\left(\frac{d_i^2 \rho N}{\mu}, \left(\frac{N^2}{g d_i}\right), \left(\frac{P}{d_i^5 \rho N^3}\right)\right) = 0 \quad 6.7$$

This can be written as :

$$N_p = K (Re)^a (Fr)^b \quad 6.8$$

for a fully-baffled tank  $b = 0$

$$N_p = K (Re)^a \quad 6.9$$

At high Reynolds numbers the power can be obtained

from:

$$P = K N^3 d_i^5 \rho \quad 6.10$$

where  $K$  is a constant depending on the type of impeller.

Marten (110) and Brown et.al. (111) collected data on all types of impellers. The data collected for turbine impellers are shown in Figures 6.7.

#### 6.6 Phase Inversion

Under certain hydrodynamic conditions the phases in an extractor may spontaneously invert. This may have an important effect on mass transfer efficiency and coalescence rates.

Phase inversion studies in agitated tanks can be divided into two parts:

- 1) Batch Mixing Tank
- 2) Continuous mixer-settler

In batch mixing tanks Quinn and Sigloh (112) found that for a fixed impeller speed the inversion concentration  $\phi_i$  expressed as a volume fraction in the organic phase was given by:

$$\phi_i = \phi_o + a/p \quad 6.11$$

Where  $\phi_o$  is the constant asymptotic inversion concentration,  $a$  is a system constant and,  $P$  is the power input given by:

$$P = K \rho N^3$$

Where  $K$  is a constant.

Chen (113) studied phase inversion at high rotor speed and found after phase inversion, secondary droplets of the continuous phase in the primary drops.

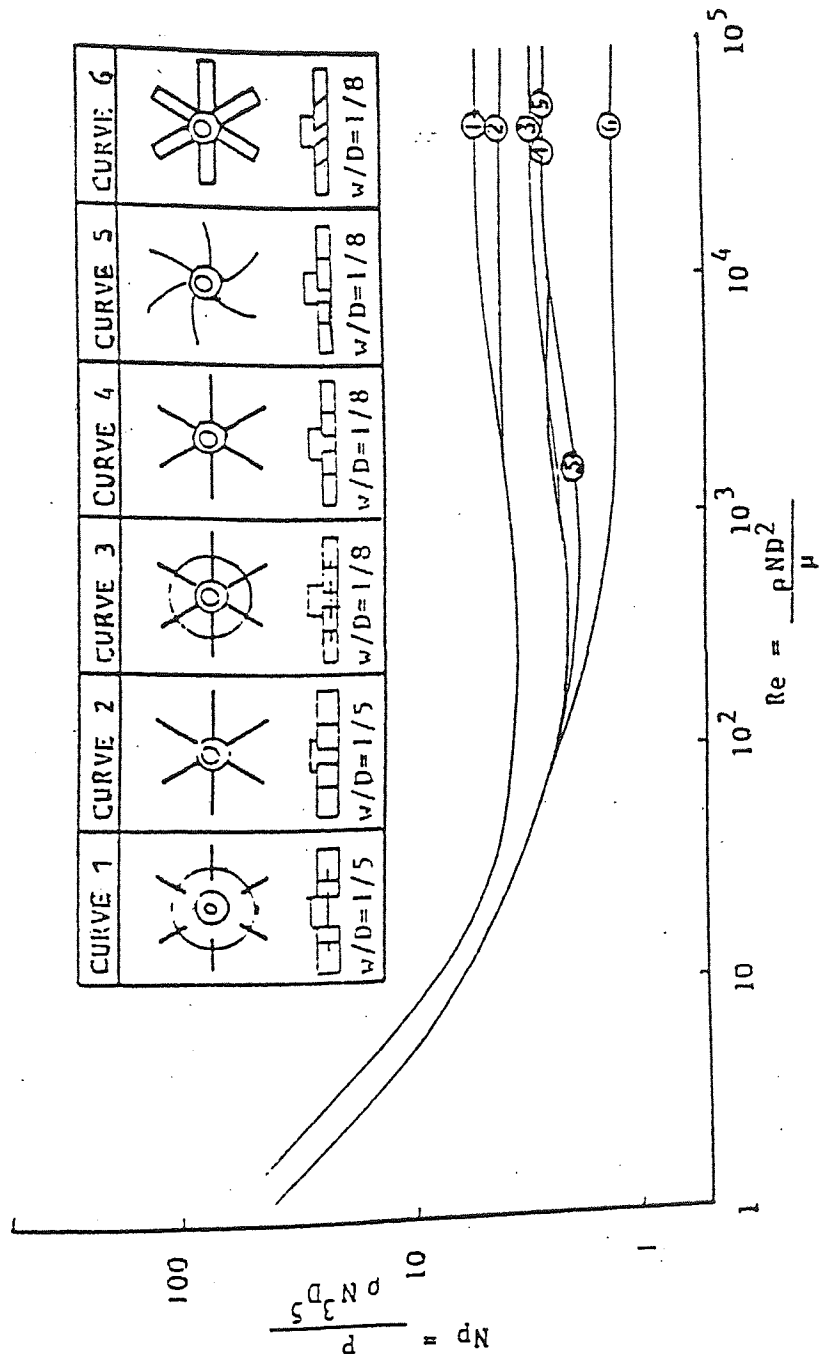


FIG.6-7 IMPELLER CHARACTERISTICS AND POWER

Ali (114) confirmed the position of the impeller as the determinant of the nature of the dispersed phase. If the impeller is placed in the organic phase, the aqueous phase will become dispersed and vice versa. If the impeller is placed at the interface, either phase can be dispersed. Yeh et.al.(115) studied the effect of temperature, interfacial tension and density and concluded that there was no general correlation applicable to all systems.

In a continuous mixer-settler, which phase is dispersed is clearly of importance since the mass transfer efficiency is dependent on the direction of transfer of solute; the wedge length in the settler is also dependent on which phase is dispersed. Phase inversion is accompanied by either a decrease or an increase in wedge length. A mathematical model has therefore been derived to characterize phase inversion (116).

McClarey and Mansoori (117) confirmed the factors which affected phase inversion in a mixer-settler; they found viscosity ratio of the phases, interfacial tension and, to a lesser extent, the stirrer speed were the relevant factors. However no attempt was made to quantify their findings. Hossain (116) was the first to report this phenomena in a cascade of laboratory mixer-settler units. The following correlation was proposed:

$$\frac{V_c}{V_d} = 1 - \left(\frac{\quad}{3X}\right)^4 + \left(\frac{\quad}{9X^2}\right)^1 + \left(\frac{\quad}{27X^3}\right)^2 + \left(\frac{\quad}{81X^4}\right)^4$$

where  $V_c$ ,  $V_d$  are the characteristic velocities of the continuous and dispersed phases respectively and  $X$  is the inversion holdup. However the above model appears to be restricted to a very limited range of physical properties and a particular mixer-settler unit.

#### 6.7 Dispersion in a Mixer

The steady state drop size is a function of both the agitator speed and the dispersed phase hold-up, and the effects of hold-up on drop size have been the subject of a large number of research studies. These were summarized by Tavlarides and Coualaloglou (118) who stated that the different correlations proposed are equally valid, within the limits of their derivation. The correlation of Thornton and Bouyatiotis (119) can be applied to estimate the mean drop size at different dispersed phase hold-ups. Thornton and Bouyatiotis showed that the droplet size may be expressed by an equation of the form

$$d_p = d_o + m \Phi \quad 6.13$$

where  $m$  is related to the physical properties by:

$$m = K_2 \left( \frac{\sigma}{\mu_c^2 g} \right) \left( \frac{\Delta \rho \sigma^3}{\mu_c^4 g} \right)^{-0.062} \left( \frac{\Delta \rho}{\rho_c} \right)^{0.05} \quad 6.14$$

where  $K_2$  is a geometric constant.

These authors further showed that the drop size at substantially zero hold-up, could be correlated by the expression:



first approach each other

zone between the

$$\frac{d_o \rho_c^2 g}{\mu_c^2} = 31.2 \left( \frac{P_o^3 g_c^3}{\rho_c^2 \mu_c g^4} \right)^{-0.32} \left( \frac{\rho_c \sigma^3}{\mu_c^4 g} \right)^{0.14} \quad \text{droplets are} \quad 6.15$$

Replacing  $P_o$  by  $(K_1 \rho_c N^3)$  and converting to SI units and rearranging equation 6.15 gives :

$$d_o = K_3 m_1 \cdot N^{-2.88} \quad 6.16$$

where  $m_1$  is correlated to be,

$$m_1 = \left( \frac{\mu_c^2}{\rho_c^2 g} \right) \left( \frac{\rho_c \sigma^3}{\mu_c^4 g} \right)^{0.14} \left( \frac{\rho_c}{\mu_c g^4} \right)^{-0.32}, \quad 6.17$$

Combining equations 6.17, 6.13 leads to

$$d_p = K_3 m_1 N^{-2.88} + m \phi \quad 6.18$$

When the dispersion is agitated, the drops will collide and some will coalesce. If the disperse phase hold-up is increased at constant agitator speed, the proportion of the pairs of drops coalescing at each collision will increase until, at phase inversion, coalescence will occur at every collision.

#### 6.8. Settler Design Fundamentals

The stability of the dispersed phase is an important property in liquid-liquid extractor operation. It represents the resistance offered by the dispersion to coalescence of the dispersed phase droplets. In any

gravity-settler the droplets first approach each other and form a close-packed heterogeneous zone between the two phases. The initial velocities of the droplets are thus reduced and they move towards the interface in a close-packed arrangement. Inter-droplet coalescence occurs amongst the densely-populated droplets before they reach the two phase-interface, and drop-interface coalescence occurs. An undesirable secondary dispersion may sometimes be produced if there is intense agitation in the mixer particularly if the system has a low interfacial tension. This secondary haze comprises a large number of secondary drops. Stable emulsions are normally characterized by small droplet sizes  $<100 \times 10^{-6}\text{m}$  diameter, which require an excessive residence time to settle out. Stepwise coalescence of primary drops may also result in small secondary drops at the interface in the settler (120).

Settlers may be classified as :

1. gravity settlers (vertical or horizontal)
2. centrifugal (cyclones)

The above types are non-mechanical, in comparison with mechanical types, e.g., centrifuges.

The earliest design procedures for gravity settlers were all either related to a mean residence time, usually determined empirically (120), or to a hydraulic balance of the flows of the liquid phases. Neither of these procedures deals with the physical processes governing the separation of a droplet dispersion; that is no account is taken of system interfacial tension, or drop size distribution.

The first attempt to take account of the physical processes governing separation was proposed by Davies et.al. (121) Figure 6.8 shows that in a single mixer settler the flocculation - coalescence band was found to be wedge shaped. The length of the band increased with increase in the dispersed phase flow and decrease in inlet drop diameter. The drop size was found to increase with distance from the inlet and was dependent upon the agitator speed and flow rate. Jeffreys, et. al. (122) concluded that the mean axial velocity of the phases in a horizontal gravity settler should not exceed 0.01m/s. Above this value a significant amount of secondary haze would be formed in the settler. It has been shown that the design and position of the entrance line into the settler is of prime importance. A vertical baffle should preferably be located centrally immediately opposite the phase inlet of the settler. The ratio of the phase inlet point diameter to the settler diameter should be less than 0.16 and should not be so large as to reduce the mixing efficiency.

IMI proposed a design of a compact settler in which dispersion bands of practically constant thickness, 0.05 to 2 m were claimed to occur. Under these conditions, and with all other parameters held constant, the relationship between dispersion band thickness and settler loading can be expressed approximately by (123) :

$$\Delta H = K (Q/A)^Y$$

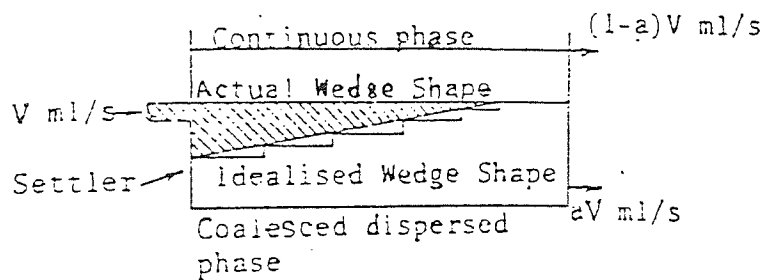


FIG. 6-8 SHAPE OF ACTUAL AND IDEALISED COALESCENCE WEDGES

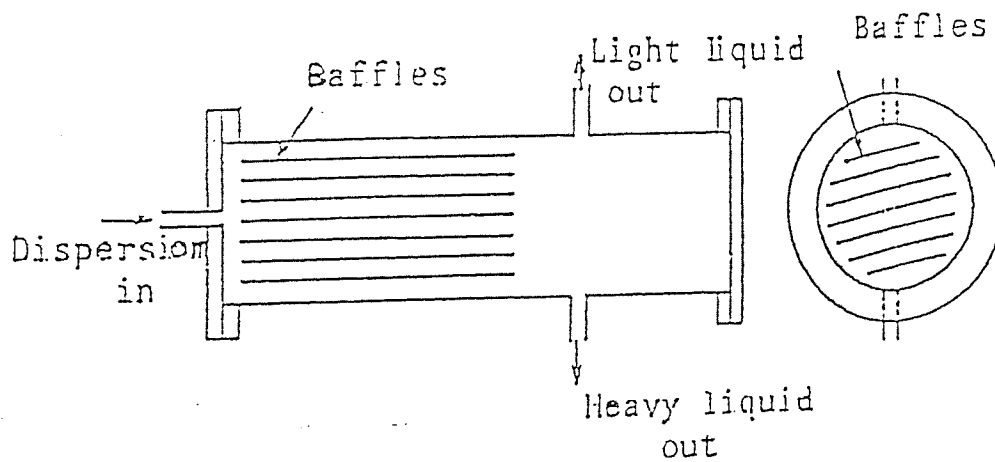


FIG. 6-9 BAFFLED SETTLER

where  $\Delta H$  is dispersion band thickness,  $K$  is a constant,  $Q$  is the dispersion throughput,  $A$  is the horizontal cross-sectional area of the settler, and  $y$  is constant. Equation (6.19) can be modified as follows

$$Q / (A \Delta H) = Q/V = 1/(K^{1/y} \Delta H^{1-1/y}) \quad 6.20$$

where  $Y > 2.5$

Vijayan et.al.(124) studied the different models of Jeffreys et.al.(125) and usefully analyzed the relative contributions of the drop/drop and drop/interface modes of coalescence.

Coalescers, separating membranes, and electrical devices, may sometimes be used as settler auxiliaries. Coalescing aids may be added, e.g. vertical baffles are used in settling tanks to reduce turbulence introduced from the mixer. Horizontal baffles are also used to reduce the depth through which droplets must settle and to ensure laminar flow. As would be expected, baffles produce no significant improvement with secondary dispersions. Different types of baffles are used to influence the direction of flow; sometimes the aim is to cause impingement of the dispersion on the baffles and enhance coalescence. Figure 6.9 shows the types of baffles which may be used in a settler.

A baffle design used by Power Gas Corporation enables the mixed phase to be introduced at the coalescing interface by providing a passage down which

the mixed phases flow after they have been discharged from the top of the mixing chamber. The baffle runs full of dispersed phase and eliminates turbulence and re-entrainment of the settled phases in the region of the settler inlet. Another feature is the picket fence baffle, placed across the final width of the settler at intervals along its length to damp-out wave motions which otherwise occur at the fluid interfaces and which may result in phase carry-over at the weirs. The picket fence plays a part in increasing the coalescing rate and is therefore made of material which is wetted by the dispersed phase.

#### 6.8.1. Coalescence on Surfaces

Solid surfaces influence the rate of coalescence of dispersed phase depending upon the solid properties, e.g., the wettability. Thus as discussed, baffles can improve the rate of coalescence in settlers.

Other coalescence aids such as knitted mesh pads (126) or settling rafts (127) also increase the rate of coalescence by increasing the frequency of impact between drops by interfacial tension effects, or by improving the drainage paths for coalesced fluid.

In a study of the coalescence of toluene droplets in water on a wetted plate (128) it was observed that the contact angle with a plate decreased as the drop volume increased and increased with an increase in initial drop size. It has also been observed that for non-wetted plates the contact angle increased as further drops were added.

### 6.8.2 Coalescence of Secondary Hazes

Secondary hazes may be formed due to the excessive turbulence in the mixer or due to partial coalescence taking place within a dispersion in a settler (129). Secondary hazes with droplet sizes of the order of  $<500 \times 10^{-7}$  m diameter require an excessive time to separate into two layers. The physical properties of the system also affect the ease of separation of the haze. Coalescers may be used to assist separation. Fibrous beds which are sometimes used to assist separation should possess a high ratio of surface area to volume (130). The efficiency of separation is improved with a high surface roughness and small fiber diameter. It was confirmed by Jeffreys and Davies (131) that the reduction of separation velocity with increase in bed depth beyond an optimum value was due to primary droplet breakup within the packing. The use of such beds is limited by the pressure drops involved and their sensitivity to deposited solids.

### 6.9 Mixer-Settler Arrangements

Davis, et. al. (132) discussed the advantages and disadvantages of various mixer-settler arrangements. The main design features for twelve types of mixer settler are summarized in Table 6.2. Hanson and Kaye (133) considered horizontal mixer-settlers more versatile and obtained efficiencies as high as 93 % with the system nitric acid-water-tri-n-butyl acetate. Coplan (24) discussed the advantages and the disad-

TABLE 6.2. COMPARISON OF MIXER-SETTLER DESIGNS

Inventor	Type of stirring	Type of settling	Arrangement	Driving force for flow	Relation of phase ratio to overall flow ratio	Ref
McKittrick (1939)	Common shaft	Cocurrent	Vertical	Gravity	Independent	135
Schoneborn (1934)	Common shaft	Cocurrent	Vertical	Gravity	Dependent	136
McConnell (1937)	Common shaft	Cocurrent	Vertical	Heavy phase by gravity	Independent	137
Scheibel (1946)	Common shaft	Cocurrent	Vertical	Gravity	Dependent	138
Bottaro (1940)	Common shaft	Counter current	Near Vertical	Gravity	Dependent	139
Othmer (1935)	Common shaft	Counter current	Vertical	Gravity	Independent	140
Van Dijk (1941)	Common shaft or individual stirrers	Counter current	Near Horizontal	Gravity	Either dependent or independent	141
Holley (1934)	individual stirrers	Counter current	Near Horizontal	Gravity	Independent	142



TABLE 6.2 continue

Mensing (1947)	individual stirrers	Counter current	Horizontal	Both phase pumped by mixer	Independent	143
Edeleanu (1927)	individual stirrers	Cocurrent	Horizontal	Light phase pumped, heavy phase pumped by gravity	Dependent	144
Standard oil development (1949)	individual stirrers	Cocurrent	Near Horizontal	Gravity	Independent	145
Gordon (1939)	individual stirrers	Cocurrent	Horizontal	Both phase pumped by mixer	Dependent	146
Hanson et al (1964)	Common Shaft	Counter Current	Vertical	Gravity	Independent	133
I.M.I. (1974)	Individual Stirrers	Counter Current	Horizontal	Gravity	Independent	147
Hartland et al	Common Shaft	Counter Current	Vertical	Gravity	Independent	134

vantages of this type of equipment. Figure 6.10 (a,b,c,d,e,f) illustrate some mixer-settler arrangements.

Hanson et.al.(98) attempted to reduce the energy requirements inherent in a conventional mixer settler by arranging the stages vertically above one another as shown in Figure 6.11. A vertical arrangement of the stages also features in contactors described by Treybal (29) and in another new glass extractor . Hartland et.al. (134) reported a new design of a mixer-settler column with mean stage efficiencies up to 100% for solute transfer from the continuous to the dispersed phase and up to 170% for the opposite direction. with the system toluene-acetone-water.

#### 6.10 Application of Mixer-Settlers

Some of the earliest liquid-extraction plants employed mixer settlers that involved separate mixing and settling vessels.

Holley-Mott (142) was the first mixer-settler unit used in the petroleum industry, viz., in oil refineries, and was also used for radioactive materials processing. The Windscale mixer-settler (148) is used for the extraction of uranium and plutonium from irradiated nuclear fuel. A multi-stage unit is built as one box, with partitions to create the different stages, thus eliminating all interstage piping. This design is simple, without mechanical complexity and has proved very reliable in operation.

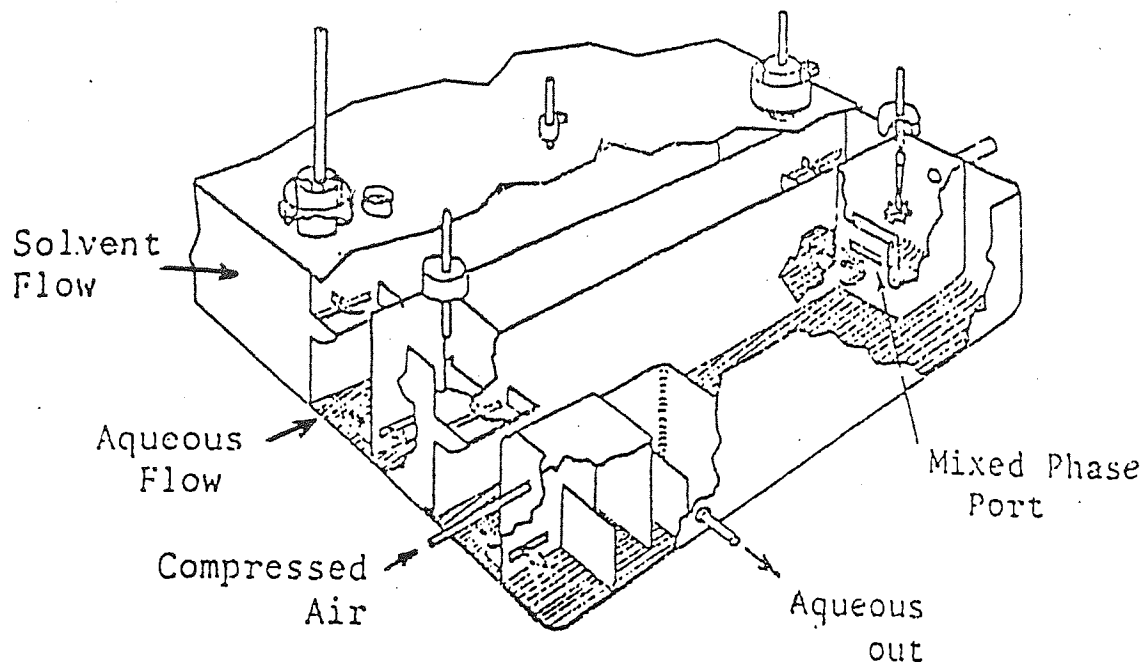


FIG. 6-10 a TYPICAL BOX TYPE MIXER SETTLER

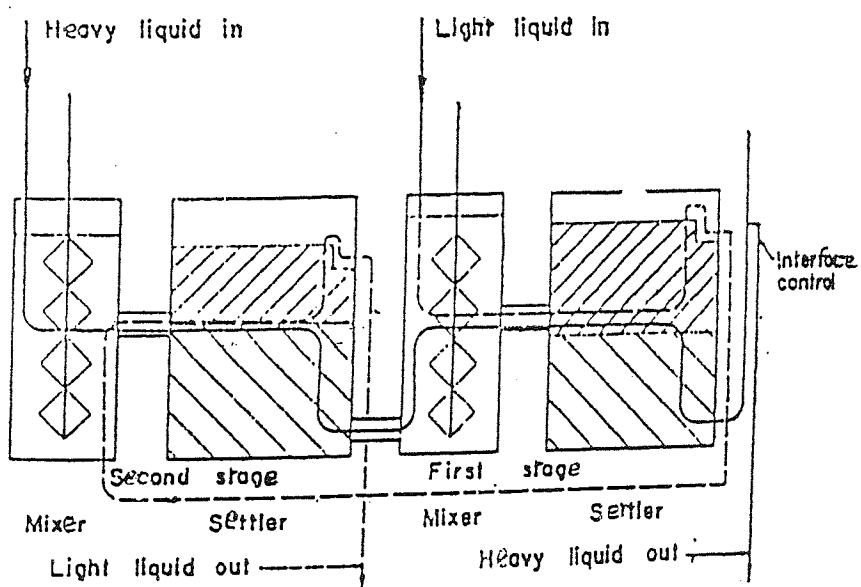
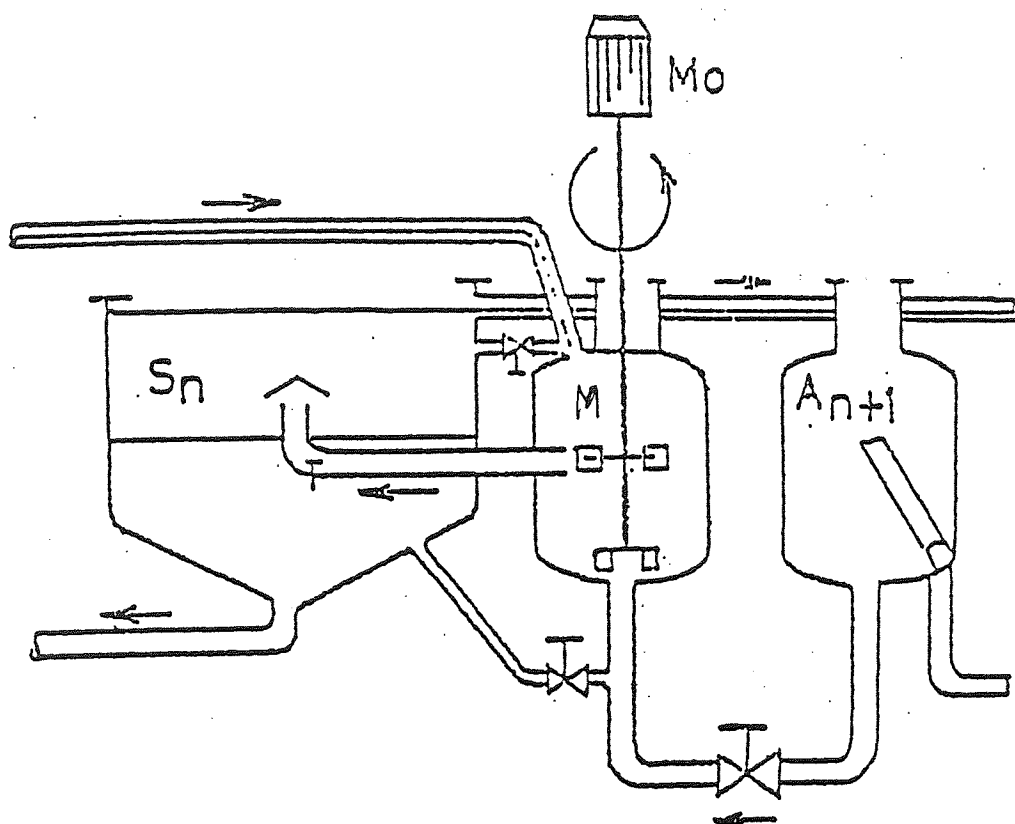


FIG. 6-10 b TWO STAGE MIXER SETTLER EXTRACTOR



M MIXING SPACE

S SETTLER SPACE

A AUXILIARY SPACE

6-10 C KEMIRA MIXER SETTLER

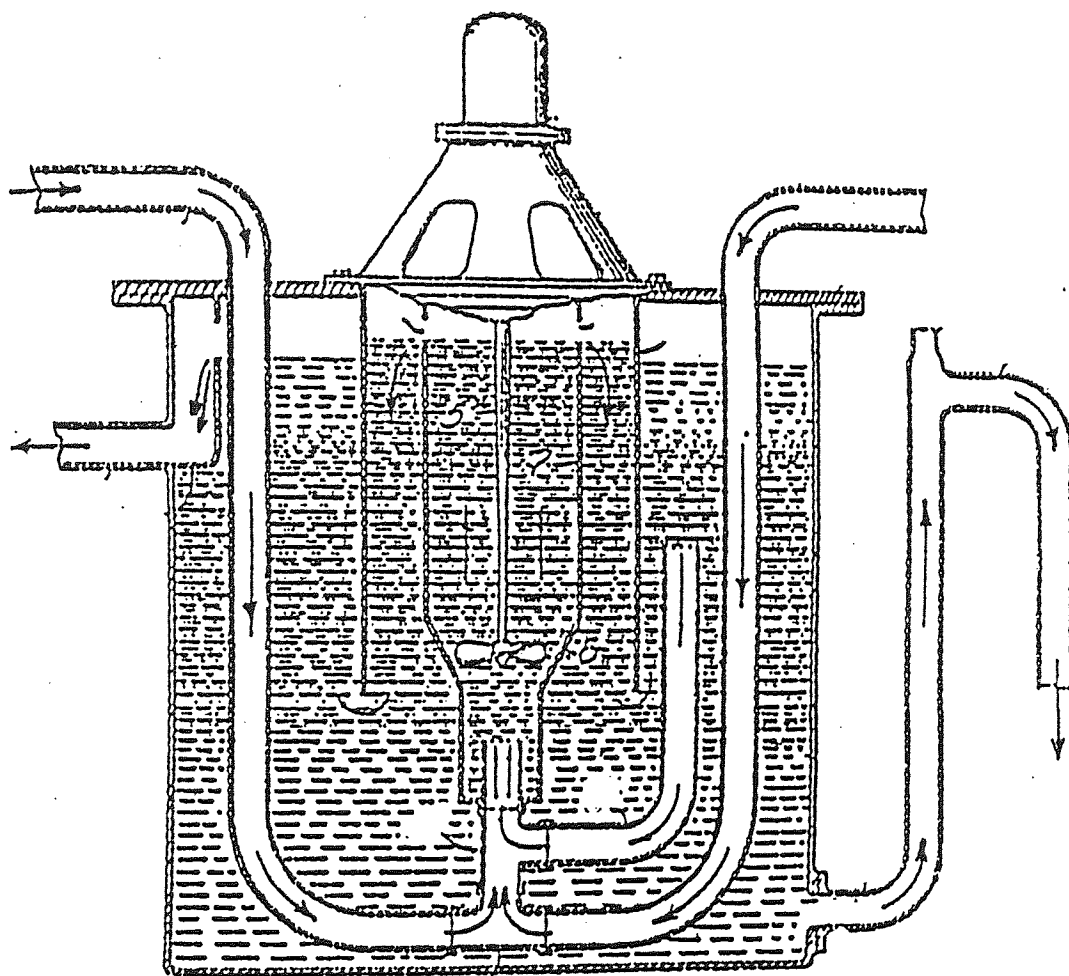


FIG. 6-10 D MENSING DESIGN OF MIXER SETTLER EXTRACTOR

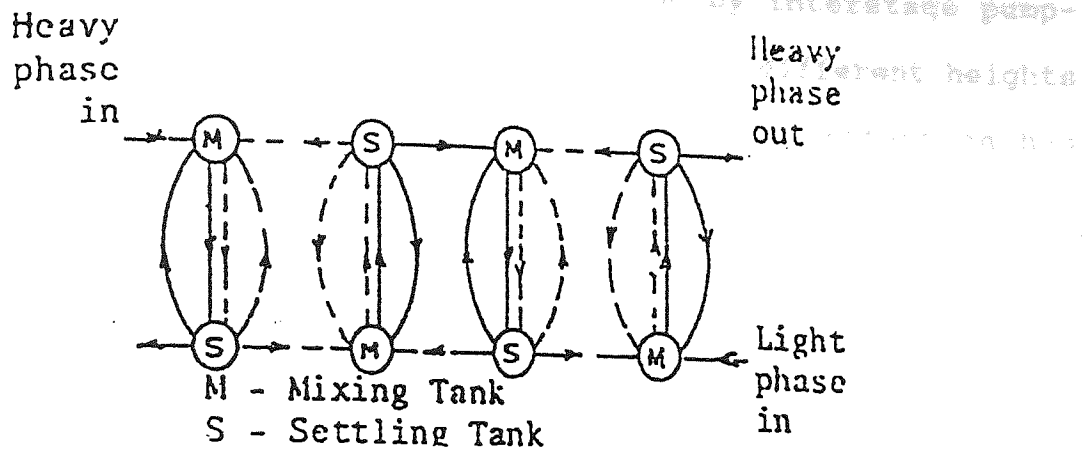


FIG. 6-10e SCHEMATIC PLAN OF FOUR STAGE HOLLEY MOTT-UNIT

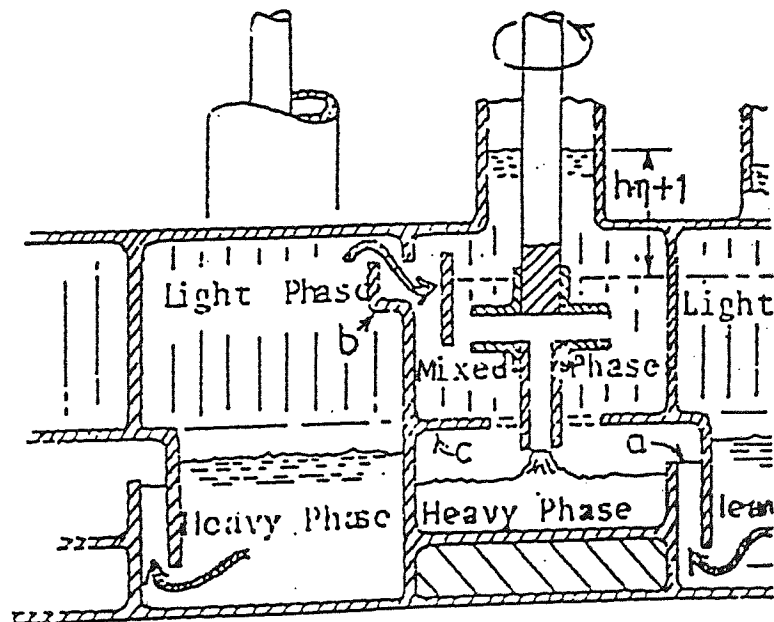


FIG. 6-10f THREE ADJACENT STAGES OF PUMP-MIX MIXER  
SETTLER

Flow limitations of the simple gravity mixer-settler can obviously be overcome by interstage pumping. Rather than having the stages at different heights with the heavy phase pumped 'up hill', attention has focused on devices that can be used to both mix and pump the two phases at the same time. The first-widely recognized design to achieve this object was the Pump-Mix extractor (149). This was primarily developed for nuclear fuel processing and has been widely used for this purpose.

The General Mills unit, designed by the manufacturers of the first commercially-used copper extractant, has a baffled cylindrical mixer fitted in the base with a top shrouded turbine that both mixes and pumps the incoming phases as shown in Figure 6.12.

The mixer-settler designed by Ryan et.al. (150) is used in the Dupex (151) solvent extraction process for the recovery of uranium from sulphuric acid leaching of ores.

For the recovery of metals, Power Gas Corporation Ltd., (149) designed a mixer-settler which is mainly used for copper. The IMI mixer-settler (147) was developed for commercial use in uranium extraction and phosphoric acid purification.

The Kermira mixer-settler (152) is used mainly for inorganic extractions. It is particularly flexible, especially where there are great variations in the flow rate from stage to stage.

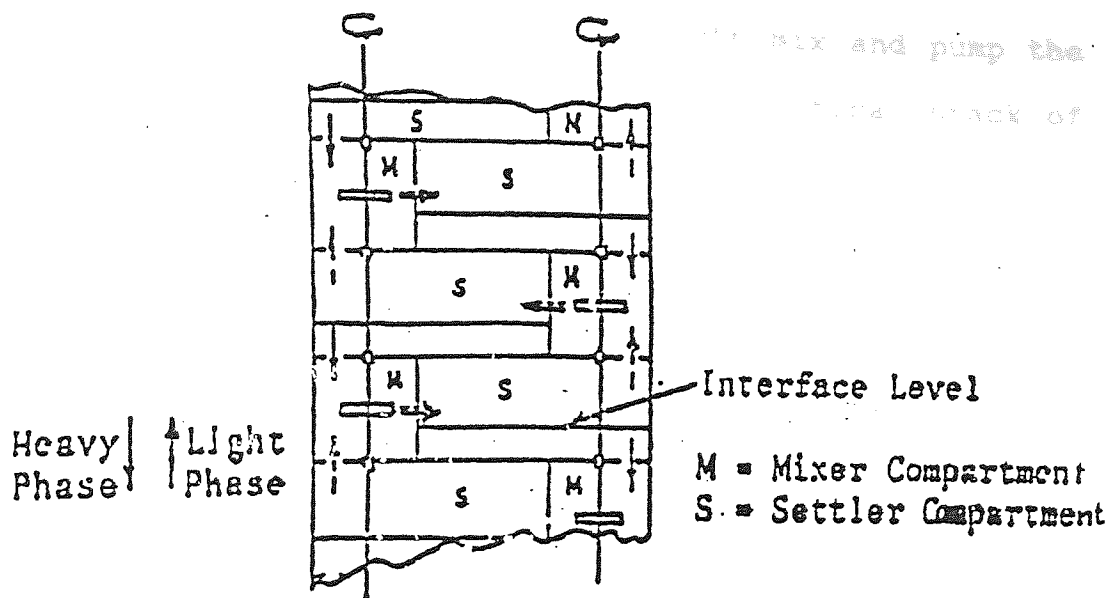


FIG 6-11 VERTICAL MIXER SETTLER

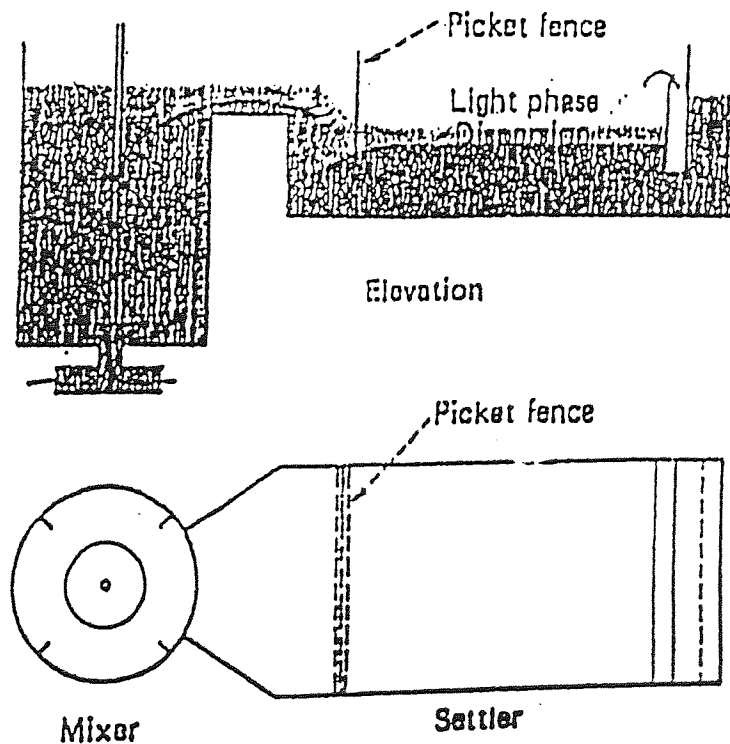


FIG. 6-12 PRINCIPLE FEATURES OF GENERAL MILLS MIXER SETTLER



Two distinct types of mixer-settler are marketed by Lurgi of West Germany. The horizontal type (153) uses an axial-flow impeller to both mix and pump the phases. The other type comprises a vertical stack of stages and takes the form of a column (154).

#### 6.11 Stage Efficiency

Extraction efficiencies are calculated on the basis of either raffinate, or the extract phase composition. A number of definitions of these coefficients are used. The Murphree efficiency based on the extract phase or dispersed phase is most commonly used. In Figure 6.13 the Murphree efficiency in a single stage, is in terms of the extract phase,

$$E_{ME} = \frac{Y_2 - Y_1}{Y_2^* - Y_1} = \frac{BF}{DF} \quad 6.21$$

where  $Y_2^*$  is the extract in equilibrium with raffinate at  $X_2$ . Similarly in terms of the raffinate phase

$$E_{MR} = \frac{X_1 - X_2}{X_1 - X_2^*} = \frac{FA}{FG} \quad 6.22$$

where

$X_2^*$  : the raffinate in equilibrium with extract at  $Y_2$ .

The stage efficiency can be derived as

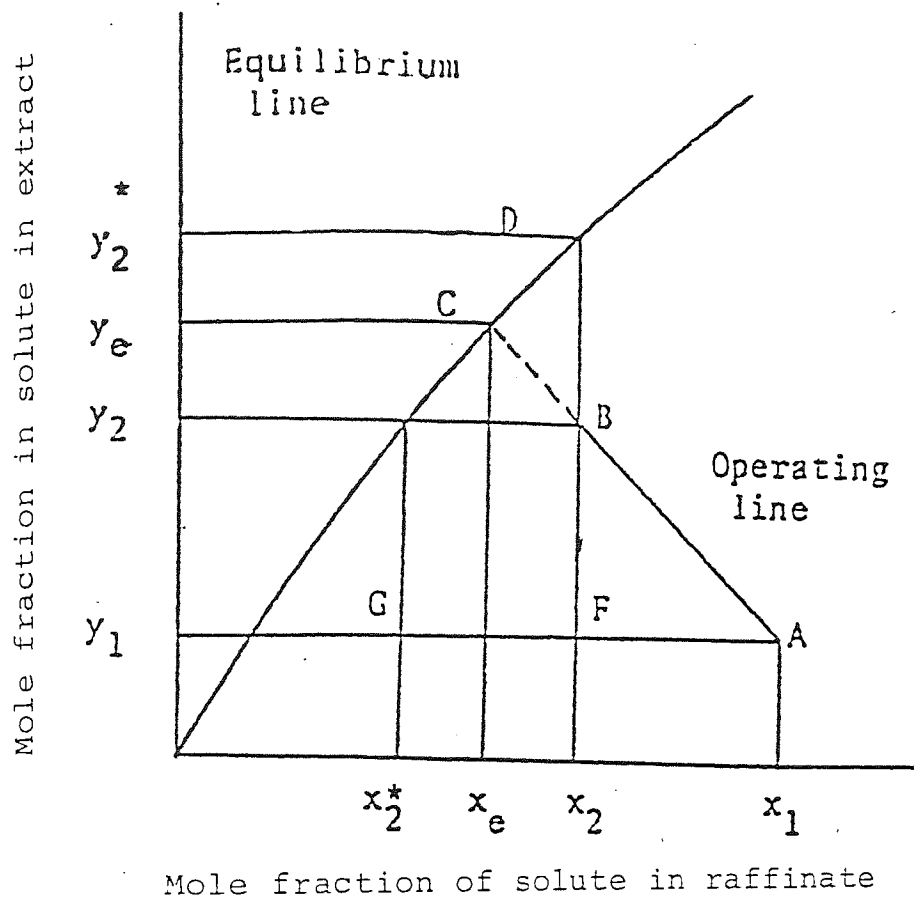


FIG. 6-13 STAGE EFFICIENCY OF SINGLE STAGE

$$E = \frac{X_1 - X_2}{X_1 - X_e} = \frac{Y_2 - Y_1}{Y_e - Y_1} = \frac{AB}{AC} \quad 6.23$$

where  $X_1, Y_1$  are the initial solute concentrations and  $X_2, Y_2$  the final concentrations in the raffinate and extract phases respectively. The overall efficiency of a mixer settler unit is defined as the ratio of the number of ideal to real stages required for a given concentration change.

Treybal (29) has recommended the following equation for estimation of Murphree stage efficiency for baffled or well-stirred vessels which exhibit complete mixing in the continuous phase.

$$E_{MC} = E_{Md} = 1 - \exp(-K_{od}Z_c/U_d) \quad 6.24$$

$$= 1 - \exp(-K_{od}a \frac{\theta}{X_i}) \quad 6.25$$

where  $\theta$  is the average residence time for the total liquid in the vessel,  $X_i$  is the volume fraction of the dispersed phase in the initial charge to the vessel,  $(V_d/V_c + V_d)$ , and  $K_{od}a$  is the overall mass transfer coefficient based on the dispersed phase. Treybal (29) has presented a detailed calculation procedure for estimation of Murphree stage efficiency in a mixer-settler. The overall stage efficiency for any completely-mixed stage could then be defined by

$$\xi_0 = \frac{\xi_{Md} \left[ 1 - \frac{m U_d}{U_c} \right]}{1 + \xi_{Md} \frac{m U_d}{U_c}} \quad (6-26)$$

where  $m U_d / U_c$  is the extraction factor involving the superficial velocities  $U_d$  and  $U_c$ . For continuous flow in several such mixer units, each having a stage efficiency of the combined over all efficiency for  $n$ -stage may be obtained by

$$\xi_n = \xi_0 [1 + (1-\xi_0) + (1-\xi_0)^2 + (1-\xi_0)^3 + \dots + (1-\xi_0)^{n-1}] \quad (6.27)$$

Sleicher (155) studied the effect of entrainment, which occurs if the dispersed phase is not completely separated. A portion of one of the liquids is entrained in the other.

Brown and Souder (111) reported an complex relationships solved by computer program for stage efficiency, applicable with the following restrictions:

- i) The degree of entrainment of one phase in the other is constant for all stages except that the effluents from the end stages of the cascade are completely settled and free of entrainment ;
- ii) Complete back mixing of each phase in the mixers;
- iii) A similar mass transfer coefficient for each stage ;
- iv) All mass transfer occurs in the mixers.

Overcashier et. al. (86) used the following relationship for the counter current stage efficiency

$$E = \frac{\log\left(\frac{mY_2 - x_2 + b}{mY_1 - x_1 + b}\right)}{\log\left(\frac{m(Y_2 - Y_1)}{(x_2 - x_1)}\right)}$$

6.28

Flynn and Treybal (156) investigated the effect of vessel size, rate of flow, agitator speed or power and phase ratio on the stage efficiency of agitated extractors. The stage efficiency increased exponentially with the speed of agitation. The increase of agitation speed over its optimum value not only decreased the efficiency but also increased the degree of dispersion so that settling was more difficult and volumetric capacity decreased. More stagnant drops were generated so that the reduced mass transfer coefficients counteracted the effect of increased area.

It is clear from this review that a wide range of mixer-settlers is available, each of which may be more suited to a specific application, depending upon the physical properties of the system, the permissible residence time, the volumetric throughput etc. For the purpose of the present work a simple laboratory mixer-settler, described in Chapter 8, was considered suitable to typify the general characteristics of a mixer-settler cascade.

## CHAPTER 7

---

### MATHEMATICAL MODELS FOR SOLVENT EXTRACTION

## 7.1 Introduction

Two distinct types of model have been proposed to simulate mass transfer in liquid-liquid contactors, namely the diffusion model, which assumes a turbulent back diffusion of solute superimposed on plug flow of the phases (157), and the back flow model with well mixed non ideal stages between which back flow occurs (158). These two models represent limiting cases; thus the diffusion model is approached in practice by differential extractors such as packed and baffle plate columns and the back flow model, by mixer-settler or cocurrent settler type with heavy entrainment in the separated phases.

Between these two extremes there is a variety of multicompartment extractors of both the non-coalescing types (e.g. multi impeller and pulsed plate columns) and the counter current mixer-settler type (e.g. mixer-settler) which do not conform closely to either model. However, a relationship exists between the two models that becomes closer as the number of compartments is increased, allowing the performance of such contactors to be expressed in terms of either model with reasonable accuracy.

## 7.2 The Diffusion Model

The assumptions in this model are: (157)

1. The turbulent diffusion coefficient  $E_x$  is constant.
2. The mean velocity and concentration of each phase is constant through every cross section.
3. The volumetric mass transfer coefficient  $K_{Ox}a$  is constant through the column.
4. The concentration profiles of the solute are continuous in each phase.
5. The raffinate and the extract are effectively immiscible.
6. Volumetric flow rate of solvent and feed phases are constant throughout.
7. The equilibrium relationship is assumed to be linear.

### 7.2.1 Derivation of Equations

Material balances over a differential length of contactor in the two phases as shown in Figure 7.1 can, assuming the dispersed phase is the organic phase, be divided into:-

#### 7.2.2.1 Continuous Phase (Aqueous Phase)

$$U_x c_x + E_x \left( \frac{dc_x}{dz} + \frac{d^2 c_x}{dz^2} dz \right) = E_x \frac{dc_x}{dz} + U_x \left( c_x + \frac{dc_x}{dz} dz \right) + K_{ox} a (c_x - c_x^*) dz$$

7.1

where the terms are as defined in Figure 7.1 and the Nomenclature.

$$U_x c_x + E_x \frac{dc_x}{dz} + E_x \frac{d^2 c_x}{dz^2} dz = E_x \frac{dc_x}{dz} + U_x c_x + U_x \frac{dc_x}{dz} dz + K_{ox} a (c_x - c_x^*) dz$$

7.2

$$E_x \frac{d^2 c_x}{dz^2} dz = U_x \frac{dc_x}{dz} dz + K_{ox} a (c_x - c_x^*) dz$$

7.3

$$E_x \frac{d^2 c_x}{dz^2} dz - U_x \frac{dc_x}{dz} dz - K_{ox} a (c_x - c_x^*) dz = 0$$

7.4

by defining a dimensionless group

$$\xi = \frac{c_x - c_x^*}{c_{ox} - c_{ox}^*}$$

7.5



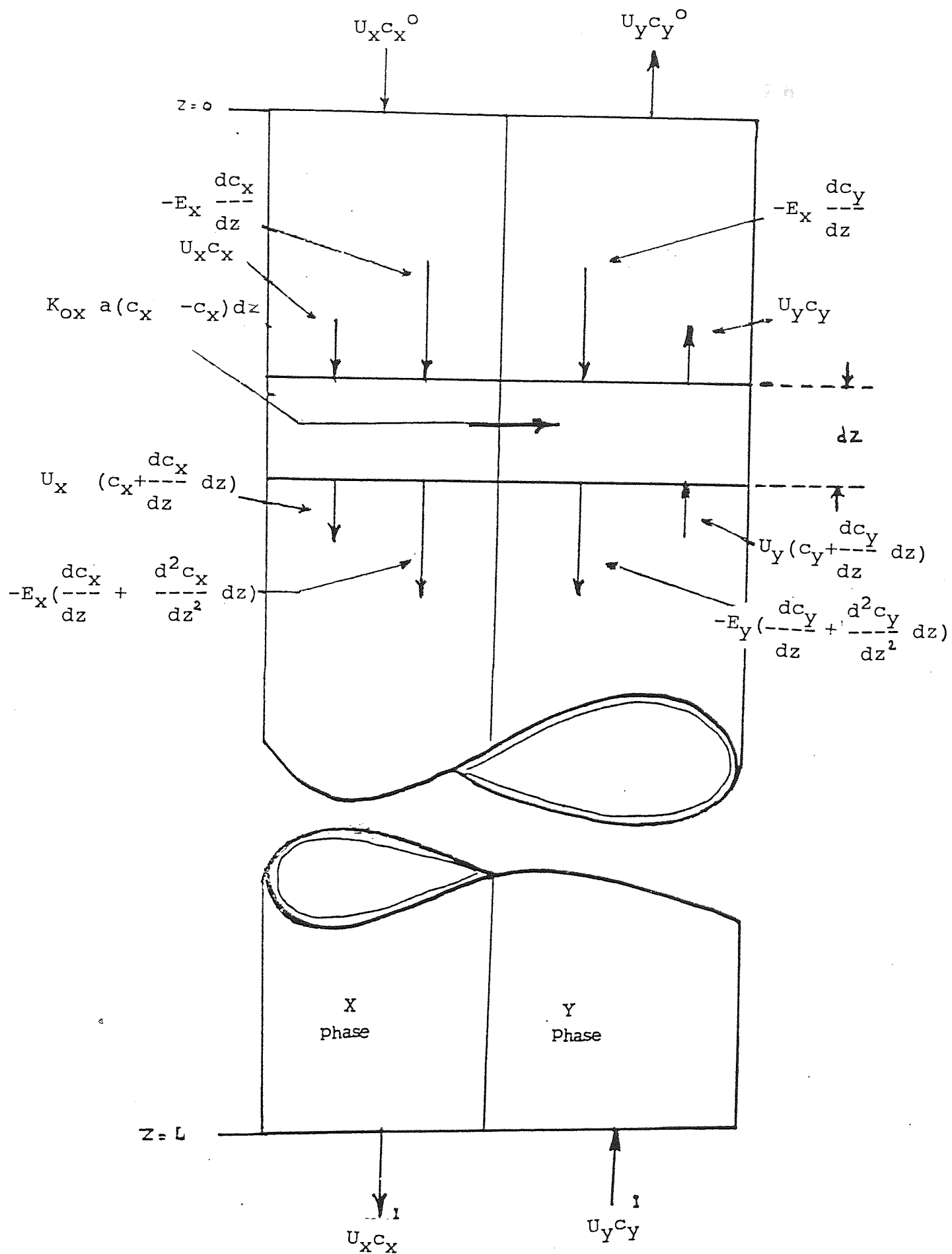


FIG.7-1 DIFFUSION MODEL: MATERIAL BALANCE ON FINITE DISTANCE  $dz$

$$c_x = \xi c_{ox} - \xi c_{ox}^* + c_x^* \quad 7.6$$

by differentiating equation 7.5

$$\frac{dc_x}{dz} = \xi \frac{dc_{ox}}{dz} + c_{ox} \frac{d\xi}{dz} - \xi \frac{dc_{ox}^*}{dz} - c_{ox}^* \frac{d\xi}{dz} + \frac{dc_{ox}^*}{dz} \quad 7.7$$

but

$$\frac{dc_{ox}}{dz} = \frac{dc_x}{dz} = \frac{dc_x^*}{dz} = 0 \quad 7.8$$

$$\therefore \frac{dc_x}{dz} = \frac{d\xi}{dz} (c_{ox} - c_{ox}^*) \quad 7.9$$

differentiation of equation 7.9 yields,

$$\frac{d^2c_x}{dz^2} = c_{ox} \frac{d^2\xi}{dz^2} + \frac{d\xi}{dz} \frac{dc_{ox}}{dz} - c_{ox}^* \frac{d^2\xi}{dz^2} - \frac{d\xi}{dz} \frac{dc_{ox}^*}{dz} \quad 7.10$$

but

$$\frac{dc_{ox}}{dz} = \frac{dc_{ox}^*}{dz} = 0 \quad 7.11$$

equation 7.10 will be

$$\therefore \frac{d^2c_x}{dz^2} = \frac{d^2\xi}{dz^2} (c_{ox} - c_{ox}^*) \quad 7.12$$

By substitution from equation 7.9, 7.10 into equation 7.4

$$E_x \frac{d^2 \xi}{dz^2} (c_{ox} - c_{ox}^*) dz - U_x \frac{d\xi}{dz} (c_{ox} - c_{ox}^*) dz - K_{ox} a (c_x - c_x^*) dz = 0 \quad 7.13$$

Dividing equation 7.13 by  $U_x$

$$\frac{E_x}{U_x} \frac{d^2 \xi}{dz^2} (c_{ox} - c_{ox}^*) dz - \frac{d\xi}{dz} (c_{ox} - c_{ox}^*) dz - \frac{K_{ox} a}{U_x} (c_x - c_x^*) dz = 0 \quad 7.14$$

By defining  $Pc = \frac{U_x}{E_x}$ ,  $(No)_x = \frac{K_{ox} a}{U_x}$

$$\therefore \frac{1}{(Pc)_x} \frac{d^2 \xi}{dz^2} (c_{ox} - c_{ox}^*) dz - \frac{d\xi}{dz} (c_{ox} - c_{ox}^*) dz - (No)_x (c_x - c_x^*) dz = 0 \quad 7.15$$

multiplying by  $Pc$  yields,

$$\frac{d^2 \xi}{dz^2} (c_{ox} - c_{ox}^*) dz - Pc \frac{d\xi}{dz} (c_{ox} - c_{ox}^*) dz - (No)_x Pc (c_x - c_x^*) dz = 0 \quad 7.16$$

dividing by  $(c_{ox} - c_{ox}^*) dz$  yields

$$\frac{d^2 \xi}{dz^2} - Pc \frac{d\xi}{dz} - (No)_x Pc \frac{c_x - c_x^*}{c_{ox} - c_{ox}^*} = 0 \quad 7.17$$

$$\therefore \frac{d^2 \xi}{dz^2} - Pc \frac{d\xi}{dz} - (No)_x (Pc) \xi = 0 \quad 7.18$$

#### 7.2.1.2 Dispersed phase (organic phase)

$$U_y (c_y + \frac{dc_y}{dz} dz) + E_y \frac{dc_y}{dz} = U_y c_y + E_y \left( \frac{dc_y}{dz} + \frac{d^2 c_y}{dz^2} dz \right) - K_{oy} a (c_y - c_y^*) \quad 7.19$$

By using the same procedure as the X-phase the following equation is obtained: for the y-phase,

$$E_y \frac{d^2 c_y}{dz^2} dz + U_y \frac{dc_y}{dz} dz + K_{oy} a (c_y - c_y^*) dz = 0 \quad 7.20$$

By difining a dimensionless group

$$\phi = \frac{m(c_x - c_x^*)}{(c_{ox} - c_{ox}^*)} \quad 7.21$$

$$\frac{\phi}{m} c_{ox} - \frac{\phi}{m} c_{ox}^* = c_x - c_x^* \quad 7.22$$

$$c_x = \frac{\phi}{m} c_{ox} - \frac{\phi}{m} c_{ox}^* + c_x^* \quad 7.23$$

Differentiation of equation 7.23 with respect to  $z$  yields

$$\frac{dc_x}{dz} = \frac{1}{m} \left( \phi c_{ox} - \phi c_{ox}^* \right) \quad 7.24$$

$$= \frac{1}{m} \left( \frac{d\phi}{dz} c_{ox} - c_{ox}^* \frac{d\phi}{dz} \right) \quad 7.25$$

but  $\frac{dc_x^*}{dz} = \frac{dc_{ox}^*}{dz} = \frac{dc_{ox}}{dz} = 0$  7.26

$\therefore$  equation 7.24 will be

$$\frac{dc_x}{dz} = \frac{1}{m} \frac{d\phi}{dz} (c_{ox} - c_{ox}^*) \quad 7.27$$

Differentiation of equation 7.27 yields,

$$\frac{d^2 c_x}{dz^2} = \frac{1}{m} \frac{d^2 \phi}{dz^2} (c_{ox} - c_{ox}^*) \quad 7.28$$

$$c_y = m c_x \quad 7.29$$

$$\therefore \frac{dc_y}{dz} = \frac{m dc_x}{dz} \quad 7.30$$

and by differentiation of equation 7.30

$$m \frac{d^2 c_x}{dz^2} = \frac{d^2 c_y}{dz^2} \quad 7.31$$

substitution of these terms in equation 7.27, 7.28 yields

$$\frac{dc_y}{dz} = \frac{d\phi}{dz} (c_{ox} - c_{ox}^*) \quad 7.32$$

$$\frac{d^2 c_y}{dz^2} = \frac{d^2 \phi}{dz^2} (c_{ox} - c_{ox}^*) \quad 7.33$$

By substitution equation 7.32, 7.33 into equation 7.20

$$E_y \frac{d^2 \phi}{dz^2} (c_{ox} - c_{ox}^*) dz + U_y \frac{d\phi}{dz} (c_{ox} - c_{ox}^*) dz + K_{oy} a (c_y - c_y^*) dz = 0 \quad 7.34$$

By dividing equation 7.34 by  $U_y$

$$\frac{E_y}{U_y} \frac{d^2 \phi}{dz^2} (c_{ox} - c_{ox}^*) dz + \frac{d\phi}{dz} (c_{ox} - c_{ox}^*) dz + \frac{K_{oy} a}{U_y} (c_y - c_y^*) dz = 0 \quad 7.35$$

and dividing by  $c_{ox} - c_{ox}^*$

$$\frac{1}{(Pc)_y} \frac{d^2\phi}{dz^2} + \frac{d\phi}{dz} + (No)_y \frac{(c_y - c_y^*)}{c_{ox} - c_{ox}^*} = 0 \quad 7.36$$

On multiplication by  $(Pc)_y$ ,

$$\frac{d^2\phi}{dz^2} + (Pc)_y \frac{d\phi}{dz} + (No)_y (Pc)_y \phi = 0 \quad 7.37$$

Hence by solution of this equation and, subsequently,  $c_x$  leaving any stage can be determined.

### 7.3 Backflow Model (158)

Several versions of the two-phase backflow model have been formulated which differ in the degree of simplification and means of expressing the mass transfer rate in the stages. Algorithms have been proposed allowing for non-linear equilibria, variable flow and back mixing of the phases, multicomponent transfers and different conditions in the settling zones.

Ricker and co-workers (159) have recently proposed a general method for the computation of countercurrent separation processes where the performance is dominated by axial and the phase equilibrium behaviour is complex. A simplified version of this model with phase inlets only to the end stages has been used in this thesis, as described in 7.3.3.

### 7.3.1 Model No.1 (159)

The assumptions of this model are:

1. The back mixing is expressed in terms of the ratio of back mixed to net forward interstage flow and is constant for all stages
2. The volumetric flow rates of feed and solvent phases are constant throughout.
3. The equilibrium relation is linear or can approximately by a straight line.
4. All mass transfer occurs in the mixer.
5. Each stage is well mixed, and back mixing occurs by mutual entrainment of the phases between stages, after coalescence if appropriate.

#### 7.3.1.1 Continuous Phase (Aqueous Phase)

From a material balance on stage  $i$  as shown in Fig 7.2, with again all terms being defined in the Nomenclature.

$$U_x(1 + \alpha_x)X_{i-1} - U_x\alpha_x X_i - U_x(1 + \alpha_x)X_i + U_x\alpha_x X_{i+1} - J_{xi} = 0 \quad 7.38$$



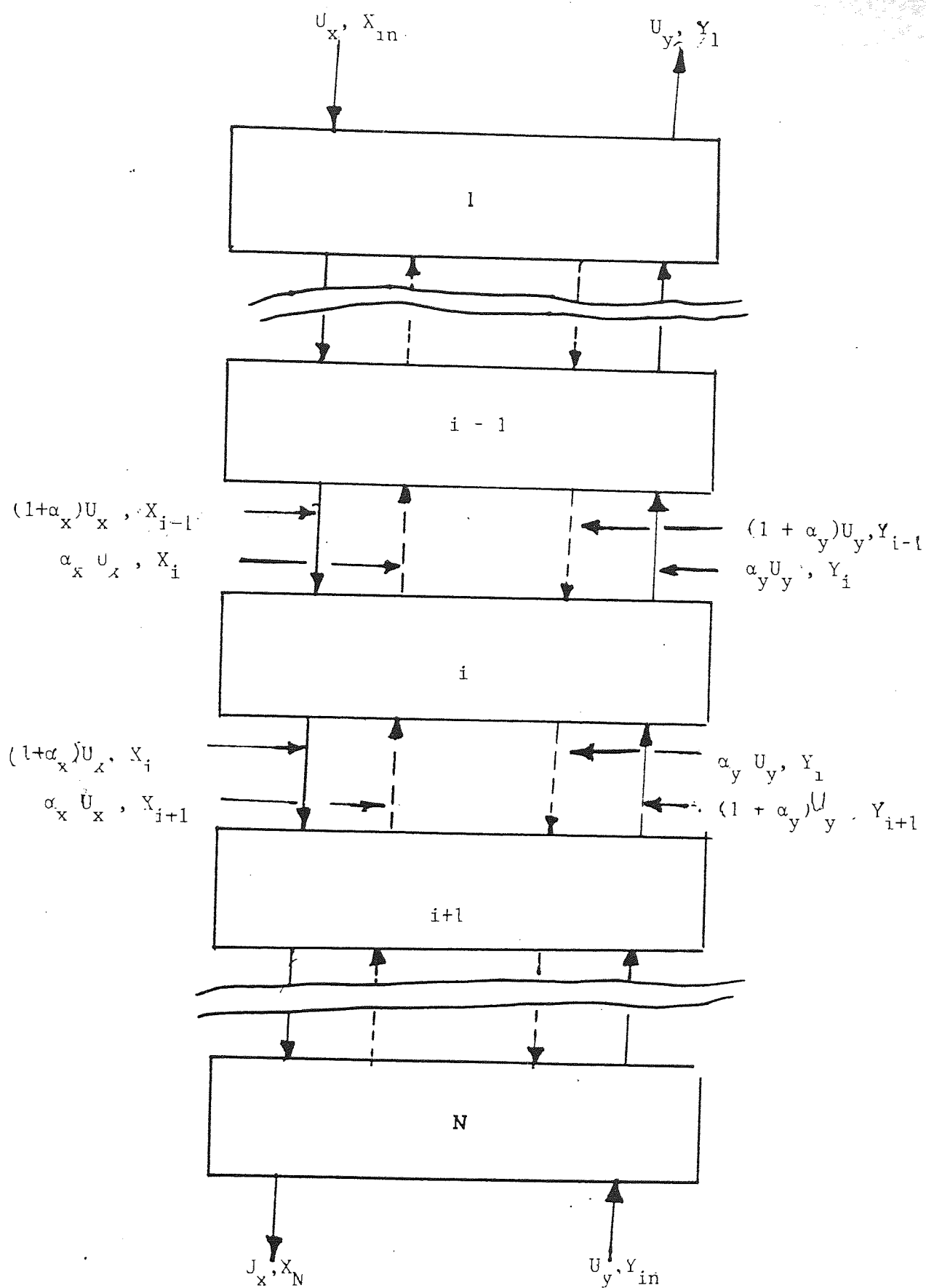


FIG. 7-2 BACKFLOW MODEL : MATERIAL BALANCE ON STAGE  $i$

where  $J_{xi} = (K_x a) h_m (X_i - X_i^*)$

and  $\alpha_x$  = backmixing coefficient

$h_m$  = the height of the stage

$$U_x(1 + \alpha_x)X_{i-1} - U_x\alpha_x X_i - U_x(1 + \alpha_x)X_i + U_x\alpha_x X_{i+1} - J_{xi} = 0 \quad 7.39$$

$$U_x X_{i+1}(1 + \alpha_x) - U_x X_i(1 + 2\alpha_x) + U_x\alpha_x X_{i+1} - J_{xi} = 0 \quad 7.40$$

Dividing equation 7.40 by  $U_x$

$$X_{i+1}(1 + \alpha_x) - X_i(1 + 2\alpha_x) + X_{i+1}\alpha_x - q_{xi} = 0 \quad 7.41$$

where 
$$q_{xi} = \frac{(K_x a)_i h_m}{U_x} (X_i - X_i^*) = \frac{J_{xi}}{U_x}$$

Again solution of equation 7.41 enables  $X_{i-1}$  and  $X_{i+1}$  to be evaluated for any stage

#### 7.3.1.2 Dispersed phase Organic Phase)

By following the same procedure for the organic (dispersed) phase the equation shown below is obtained:

$$\alpha_y Y_{i+1} - (1 + 2\alpha_y)Y_i + (1 + \alpha_y)Y_{i+1} + \lambda q_{yi} = 0 \quad 7.42$$

where  $\lambda$  is the ratio of phase flows.

$$q_{xi} = \lambda q_{yi} \quad 7.43$$

$$Y_i^* - mX_i^* = 0 \quad 7.44$$

$$q_{yi} = \frac{(K_y a)_i h_m}{U_y} (Y_i^* - Y_i) \quad 7.45$$

For equation 7.41, 7.42  $i=2, \dots, N_s-1$   
 For stages  $i, N_s$  equation 7.41, 7.42 will be

$$i=1 \quad X_n - (1 + \alpha_x)X_1 + \alpha_x X_2 - q_{x1} = 0 \quad 7.46$$

$$i = N_s \quad Y_n - (1 + \alpha_y)Y_1 + \alpha_y Y_2 + \lambda q_{y1} = 0 \quad 7.47$$

if constant interfacial area and constant mass transfer coefficients are assumed, the model contains four parameters, viz, two mass transfer terms,  $K_x a$ ,  $K_y a$  and two backmixing coefficients  $\alpha_x$ ,  $\alpha_y$ .

It can be shown that, even in the case of non-linear equilibria, the information in the concentration profiles is not sufficient to allow estimation of the two mass transfer terms with any certainty. Hence it is necessary to have some additional information independent of the profiles. For example, a ratio of the two coefficients may be assumed so that

$$K_y a = R K_x a \quad 7.48$$

Equation 7.48 reduces the number of parameters to be estimated to three.

### 7.3.2 Model No.2 (158)

This is a sample model based on the following assumptions:

- i) The liquid are immiscible
- ii) The phases are mixed uniformly
- iii) The concentration at any time and in any stage is given by a linear equilibrium relationship
- iv) The flow rates are constant
- v) The hold-up and equilibrium relationships are independent of time and stage number

AS shown in Figure 7.3 the mass balance equations for the mixer settler are given by

$$H \frac{dZ_i}{dt} = q_z (Z_{i-1} - Z_i) - S_i \quad i = 1, 2, \dots, N \quad 7.49$$

$$h \frac{dX_i}{dt} = q_x (X_{i+1} - X_i) + S_i \quad i = 1, 2, \dots, N \quad 7.50$$

According to the third assumption

$$X_i = D Z_i + E \quad i = 1, 2, \dots, n \quad 7.51$$

$$Z_i = \frac{X_i - E}{D} \quad 7.52$$

$$\frac{dX_i}{dt} = D \frac{dZ_i}{dt} \quad 7.53$$

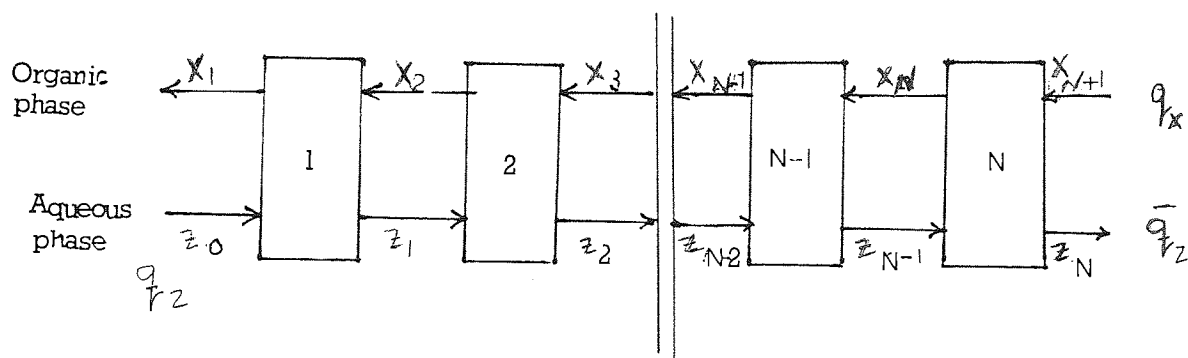


Fig 7.3 SCHEMATIC DIAGRAM OF AN n-STAGE MIXER SETTLER UNIT

By adding equation 7.49 and 7.50

$$H \frac{dZ_i}{dt} + h \frac{dX_i}{dt} = q_z (Z_{i+1} - Z_i) + q_x (X_{i+1} - X_i) \quad 7.54$$

Using equation 7.53 in equation 7.54

$$\frac{H}{D} \frac{dX_i}{dt} + \frac{h dX_i}{dt} = q_z (Z_{i-1} - Z_i) + q_x (X_{i+1} - X_i) \quad 7.55$$

$$\frac{dX_i}{dt} \left( \frac{H}{D} + h \right) = q_z Z_{i-1} - q_z Z_i + q_x X_{i+1} - q_x X_i \quad 7.56$$

Substitution using  $Z_i = \frac{X_i - E}{D}$  yields, for the R.H.S of equation 7.56

$$= q_z Z_{i-1} - q_z \frac{(X_i - E)}{D} + q_x X_{i+1} - q_x X_i \quad 7.57$$

$$= q_z Z_{i-1} - \frac{q_z}{D} X_i + \frac{q_z}{D} E + q_x X_{i+1} - q_x X_i \quad 7.58$$

$$= q_z Z_{i-1} + \frac{q_z}{D} E - X_i \left( \frac{q_z}{D} + q_x \right) + q_x X_{i+1} \quad 7.59$$

$$= \frac{q_z}{D} (D Z_{i-1} + E) - \left( \frac{q_z}{D} + q_x \right) X_i + q_x X_{i+1} \quad 7.60$$

$$\therefore \left( \frac{H}{D} + h \right) \frac{dX_i}{dt} = \frac{q_z}{D} X_{i-1} - \left( \frac{q_z}{D} + q_x \right) X_i + q_x X_{i+1} \quad 7.61$$

Assuming  $Z_0$  is the concentration in the inlet aqueous phase, equation 7.61 can be written in a compact form using matrix notation

$$\frac{d\bar{X}}{dt} = \bar{A}\bar{X} + \bar{B}_1 Z_0 + \bar{B}_2 \quad 7.62$$

Assuming four stages, four equations can be written as follows:

$$\frac{dX_1}{dt} \left( \frac{H}{D} + h \right) = \frac{q_z}{D} X_0 - \left( \frac{q_z}{D} + q_x \right) X_1 + q_x X_2 \quad 7.63$$

$$\frac{dX_2}{dt} \left( \frac{H}{D} + h \right) = \frac{q_z}{D} X_1 - \left( \frac{q_z}{D} + q_x \right) X_2 + q_x X_3 \quad 7.64$$

$$\frac{dX_3}{dt} \left( \frac{H}{D} + h \right) = \frac{q_z}{D} X_2 - \left( \frac{q_z}{D} + q_x \right) X_3 + q_x X_4 \quad 7.65$$

$$\frac{dX_4}{dt} \left( \frac{H}{D} + h \right) = \frac{q_z}{D} X_3 - \left( \frac{q_z}{D} + q_x \right) X_4 + q_x X_5 \quad 7.66$$

about this equilibrium  
number simplified

where

$$\bar{A} = \frac{1}{\left(\frac{H}{D} + h\right)} \begin{vmatrix} -\left(\frac{q_z}{D} + q_x\right) & q_x & 0 & 0 \\ \frac{q_z}{D} & -\left(\frac{q_z}{D} + q_x\right) & q_x & 0 \\ 0 & \frac{q_z}{D} & -\left(\frac{q_z}{D} + q_x\right) & q_x \\ 0 & 0 & \frac{q_z}{D} & -\left(\frac{q_z}{D} + q_x\right) \end{vmatrix} \quad 7.67$$

$$\bar{X} = \begin{vmatrix} X_1 \\ X_2 \\ X_3 \\ X_4 \end{vmatrix}, \quad \bar{B}_1 = \begin{vmatrix} \frac{q_z}{\left(\frac{H}{D} + h\right)} \\ 0 \\ 0 \\ 0 \end{vmatrix}, \quad \bar{B}_2 = \begin{vmatrix} \frac{q_z E/D}{\left(\frac{H}{D} + h\right)} \\ 0 \\ 0 \\ \frac{q_x X_{N+1}}{\left(\frac{H}{D} + h\right)} \end{vmatrix} \quad 7.68$$

for steady state

$$\frac{d\bar{X}}{dt} = 0 \quad 7.69$$

$$-\bar{A}X^0 = \bar{B}_{i1} Z_0 + \bar{B}_2 \quad 7.70$$

$$X^0 = -\bar{A}^{-1} (\bar{B}_{i1} Z_0 + \bar{B}_2) \quad 7.71$$



If we consider only small changes about this equilibrium position, then the model is further simplified to

$$\frac{d\Delta X}{dt} = A\Delta x + B_1 \Delta Z_0 \quad 7.72$$

where  $\Delta X = X - X^0 \quad 7.73$

$$\Delta Z_0 = Z - Z_0^0 \quad 7.74$$

### 7.3.3 Model 3, Newly Developed

The earlier models, 1, 2, suffer from the disadvantage that they rely upon assumption of constant hold-up in each stage; Moreover no account is taken of stage efficiency. Therefore an improved model was developed for the purpose of this work.

The equilibrium relationship is as follows:

$$X_i^* = D_i Z_i + E_i \quad 7.75$$

The Murphree stage efficiency for the organic phase is defined as:

$$\zeta_1 = \frac{X_i - X_{i+1}}{X_i^* - X_{i+1}} \quad 7.76$$

Elimination  $X_i$  from the equation 7.75

$$Z_i = \frac{X_i^* - E_i}{D_i} \quad 7.77$$

$$Z_i = \frac{X_i^*}{D} - \frac{E_i}{D_i} \quad 7.78$$

from equation 7.76

$$X_i^* = \frac{(X_i - X_{i+1})}{\zeta_i} + X_{i+1} \quad 7.79$$

$$Z_i = \frac{1}{D_i} \frac{(X_i - X_{i+1})}{\zeta_i} + X_{i+1} - \frac{E_i}{D_i} \quad 7.80$$

$$= \frac{1}{D_i} \frac{(X_i - X_{i+1} + \zeta_i X_{i+1})}{\zeta_i} - \frac{E_i}{D_i} \quad 7.81$$

$$Z_i = \frac{1}{\zeta_i D_i} [(X_i - X_{i+1}(1 - \zeta_i))] - \frac{E_i}{D_i} \quad i = 1, 2, \dots, N \quad 7.82$$

Differentiation of equation 7.82 yields

$$\frac{dZ_i}{dt} = \frac{1}{\zeta_i D_i} \left[ \frac{dX_i}{dt} - \frac{dX_{i+1}}{dt} (1 - \zeta_i) \right]$$

multiplying by  $H_i$

$$H_i \frac{dZ_i}{dt} = \frac{H_i}{D_i \zeta_i} \left[ \frac{dX_i}{dt} - \frac{dX_{i+1}}{dt} (1 - \zeta_i) \right] \quad 7.84$$

R.H.S. of equation 7.54 equation is

$$q_z Z_{i-1} - q_z Z_i + q_x X_{i+1} - q_x X_i$$

by using equation 7.82 for substituting  $Z_{i-1}, Z_i$

$$\begin{aligned} \text{R.H.S.} &= \frac{q_z}{\zeta_{i+1} D_{i+1}} X_{i-1} - \left( \frac{q_z (1 + \zeta_{i+1})}{\zeta_{i+1} D_{i+1}} + \frac{q_z}{\zeta_i D_i} + q_x \right) X_i \\ &\quad + \left( \frac{q_z (1 - \zeta_i)}{\zeta_i D_i} + q_x \right) X_{i+1} + q_z \left( \frac{E_i}{D_i} - \frac{E_{i-1}}{D_{i-1}} \right) \end{aligned} \quad 7.85$$

L.H.S. of equation 7.54 is

$$H_i \frac{dZ_i}{dt} + h_i \frac{dX_i}{dt}$$

by substituting equation 7.83 this

$$= \frac{H_i}{\zeta_i D_i} \left[ \frac{dX_i}{dt} - \frac{dX_{i+1}}{dt} (1 - \zeta_i) \right] + h_i \frac{dX_i}{dt} \quad 7.86$$

$$\begin{aligned}
\therefore \left( \frac{H_i}{\zeta_i D_i} + h_i \right) \frac{dX_i}{dt} - \frac{H_i (1 - \zeta_i) dX_{i+1}}{D_i \zeta_i dt} &= \left( \frac{q_z}{D_{i-1} \zeta_{i-1}} \right) X_{i-1} \\
&- \left( \frac{q_z (1 - \zeta_{i-1})}{\zeta_{i-1} D_{i-1}} + \frac{q_z}{\zeta_i D_i} + q_x \right) X_i \\
&+ \left( \frac{q_z (1 - \zeta_i)}{\zeta_i D_i} + q_x \right) X_{i+1} + q_z \left( \frac{E_i}{D_i} - \frac{E_{i-1}}{D_{i-1}} \right)
\end{aligned}$$

(for all values of  $i$  except 1)

7.87

for  $i = 1$

$$\left( \frac{H_1}{D_1 \zeta_1} + h_1 \right) \frac{dX_1}{dt} - \frac{H_1 (1 - \zeta_1)}{D_1 \zeta_1} \frac{dX_2}{dt} =$$

$$\frac{q_z}{D_0} X_0 \left( \frac{q_z}{D_1 \zeta_1} + q_x \right) X_1 + \left( \frac{q_z (1 - \zeta_1)}{D_1 \zeta_1} + q_x \right) X_2 + q_z \left( \frac{E_1}{D_1} - \frac{E_0}{D_0} \right)$$

7.88

by using equation 7.75

$$\begin{aligned}
\left( \frac{H_1}{D_1 \zeta_1} + h_1 \right) \frac{dX_1}{dt} - \frac{H_1 (1 - \zeta_1)}{D_1 \zeta_1} \frac{dX_2}{dt} &= q_z Z_0 - \left( \frac{q_z}{D_1 \zeta_1} + q_x \right) X_1 \\
&+ \left( \frac{q_z (1 - \zeta_1)}{D_1 \zeta_1} + q_x \right) X_2 + q_z \frac{E_1}{D_1}
\end{aligned}$$

7.89

It is to be noted that  $X_{n+1}$ , the organic phase inlet concentration, is considered constant, and thus the second term in the L.H.S. of equation 7.89 will vanish for  $i = N$

$$\text{Let} \quad P_i = \left[ \frac{H_i}{D_i \zeta_i} + h_i \right] \quad 7.90$$

$$Q_i = - \left[ H_i (1 - \zeta_i) / D_i \zeta_i \right] \quad 7.91$$

$$R_i = \left[ q_z / D_{i-1} \zeta_{i-1} \right] \text{ for } i \neq 1 \quad 7.92$$

$$R_i = q_z / D_0 \quad \text{for } i = 1 \quad 7.93$$

$$U_i = - \left( \frac{q_z (1 - \zeta_{i-1})}{D_{i-1} \zeta_{i-1}} + \frac{q_z}{D_{i-1}} + q_x \right) \text{ for } i \neq 1 \quad 7.94$$

$$U_i = - \left( \frac{q_z}{D_i \zeta_i} + q_x \right) \text{ for } i = 1 \quad 7.95$$

$$V_i = \left( \frac{q_z (1 - \zeta_i)}{D_i \zeta_i} + q_x \right) \quad 7.96$$

$$W_i = q_z \left( \frac{E_i}{D_i} - \frac{E_{i-1}}{D_{i-1}} \right) \quad 7.97$$

equation 7.89 can be written in compact form using matrix notation 7.104

$$\overline{G} \frac{dX}{dt} = \overline{A}X + \overline{B}_1 Z_0 \overline{B}_2 \quad 7.98$$

Assuming four stages in a mixer settler there are 4 equations as follows:a

$$P_1 \frac{dX_1}{dt} - Q_1 \frac{dX_2}{dt} = R_1 X_0 + U_1 X_1 + V_1 X_2 + W_1 \quad 7.99$$

$$P_2 \frac{dX_2}{dt} - Q_2 \frac{dX_3}{dt} = R_2 X_1 + U_2 X_2 + V_2 X_3 + W_2 \quad 7.100$$

$$P_3 \frac{dX_3}{dt} - Q_3 \frac{dX_4}{dt} = R_3 X_2 + U_3 X_3 + V_3 X_4 + W_3 \quad 7.101$$

$$P_4 \frac{dX_4}{dt} - Q_4 \frac{dX_5}{dt} = R_4 X_3 + U_4 X_4 + V_4 X_5 + W_4 \quad 7.102$$

$$\overline{G} = \begin{bmatrix} P_1 & Q_1 & 0 & 0 \\ 0 & P_2 & Q_2 & 0 \\ 0 & 0 & P_3 & Q_3 \\ 0 & 0 & 0 & P_4 \end{bmatrix}, \quad \overline{A} = \begin{bmatrix} U_1 & V_1 & 0 & 0 \\ R_2 & U_2 & V_2 & 0 \\ 0 & R_3 & U_3 & V_3 \\ 0 & 0 & R_4 & U_4 \end{bmatrix},$$

$$\overline{B}_1 = \begin{bmatrix} q_z \\ 0 \\ 0 \\ 0 \end{bmatrix}, \quad \text{and} \quad \overline{B}_2 = \begin{bmatrix} W_0 \\ W_2 \\ W_3 \\ W_4 + V_4 X_5 \end{bmatrix} \quad 7.103$$

Note that  $W_0 = q_z \frac{E_1}{D_1}$

7.104

For steady estate equation 7.98 will be

where  $\frac{dX}{dt} = 0$

7.105

$$-\bar{A}x = \bar{B}_1 Z_0 + \bar{B}_2$$

7.106

and  $X_0 = -\bar{A}^{-1} (\bar{B}_1 Z_0 + \bar{B}_2)$

7.107

If  $\gamma_i = 1$  (in all stages) Model No.3 will be exactly the same as Model No.2

## CHAPTER 8

---

### EXPERIMENTAL INVESTIGATION AND PHASE EQUILIBRIA



### 8.1 Objectives

The objectives of the experimental investigation were to investigate the efficiency of BTX extraction in a mixer-settler cascade using sulfolane. A horizontal cascade was chosen as an alternative to the agitated columns used commercially in the extraction of aromatics, since there are no comparative data on mixer settler performance.

A synthetic reformat was made-up and used initially. This contained benzene 25.78%, toluene 17.94% and xylene 11.28% as aromatics, and hexane 9.22%, heptane 18.58%, and octane 17.18% as non-aromatics. A real reformat cut used subsequently had the composition given later in Chapter 10. A computer simulation of extraction in a mixer-settler cascade was developed to predict the concentration profile; this was tested with experimental data.

### 8.2 Description of Equipment

The experimental extractor, shown in plate 1, comprised a laboratory mixer-settler unit containing ten stages arranged to operate under counter-current flow conditions. The arrangement is illustrated in Figure 8.1. The mixer was constructed from stainless steel, had an inside diameter of 5 cm and a height of 1.1 m, and also acted as a mixing pump. Each mixer was provided with a stainless steel shaft of 1 cm diameter. Six paddles each 2.1 cm long, 0.9 cm wide and, 0.8 cm high were fitted to the base of each shaft which was mounted in two bearings and coupled to a 5 cm diameter pulley. Every five shafts were driven by

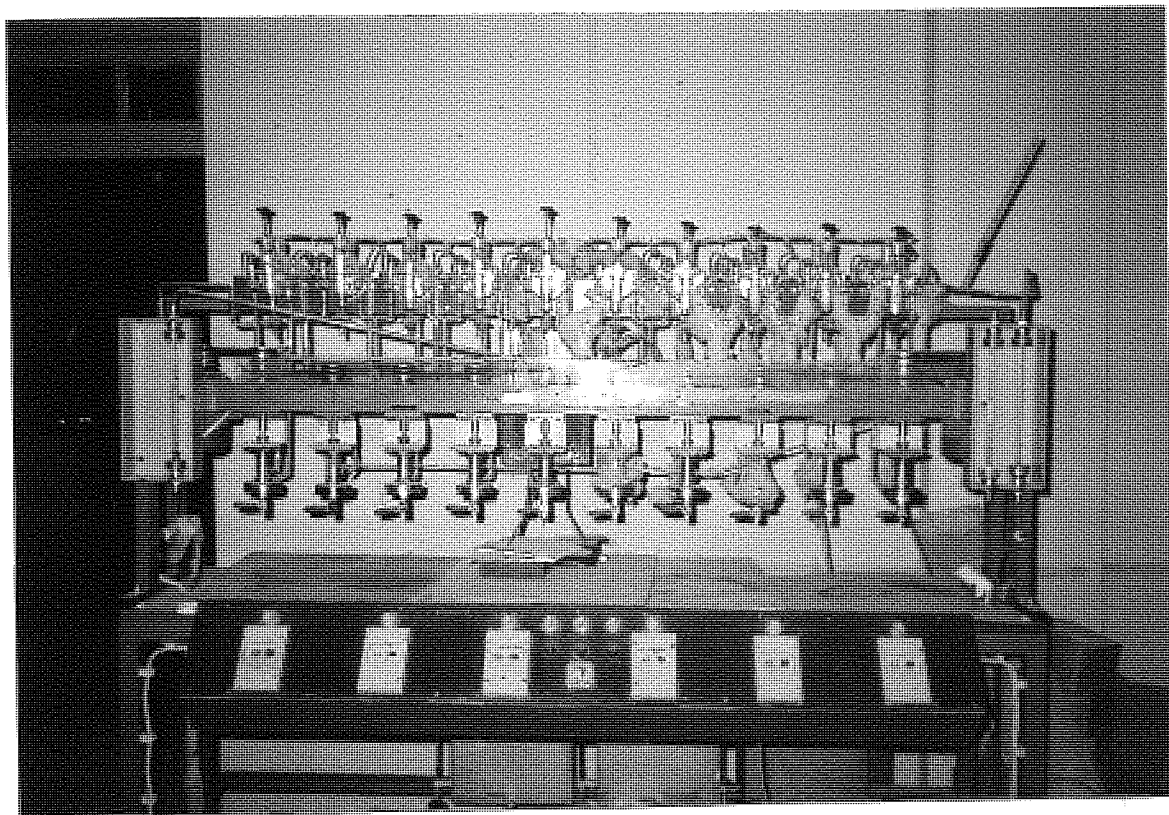


PLATE.1 MIXER-SETTLER CASCADE ( 10 STAGES )

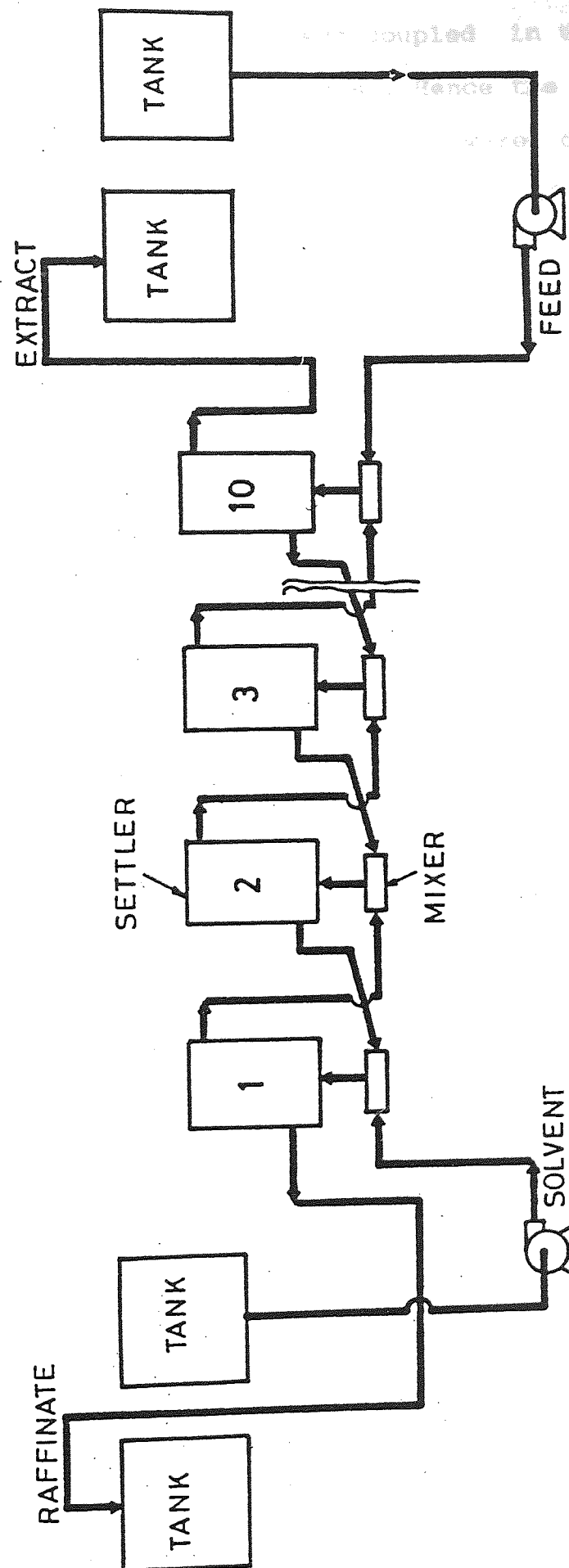


FIG. 8-1 FLOW DIAGRAM OF 10 STAGE MIXER SETTLER CASCADE

three different size pulleys coupled in turn to three pulleys also of different sizes. Hence the speed of the shafts could be varied. The pulleys were driven by a 0.12 kW, 1400 rpm electric motor. Each of the agitator shafts rotated at identical speed.

The settler, shown in Figure 8.2, consisted of a horizontal cylindrical glass vessel 9 cm in diameter and 12 cm long, with a capacity of 750 mls. The ratio of the mixed volume to the available settler volume was approximately 1:50, which was sufficient to ensure efficient coalescence and phase separation. Regulation of the phase separation levels was achieved by a p.t.f.e sleeve, which could be moved up, or down, by means of a sling and wire loop made of stainless steel. This construction allowed adjustment for extremely high or low phase separation levels.

The feed and the solvent were stored in two stainless steel tanks each of twenty-four liters capacity. Flow rates of the feed and the solvent were provided by two feed pumps of similar construction to the mixing pumps, and operating at 2800 rpm in order to reach the necessary pumping head. The flow rates were measured by glass rotameters.

All parts contacting the process liquids including the storage tanks were made of glass or stainless steel.

### 8.3 Materials Used

Sulfolane, obtained from Fluka AG Chemical Fabrican, Switzerland, was first pre-distilled in a packed column, 2 m in height and 10 cm in diameter. The

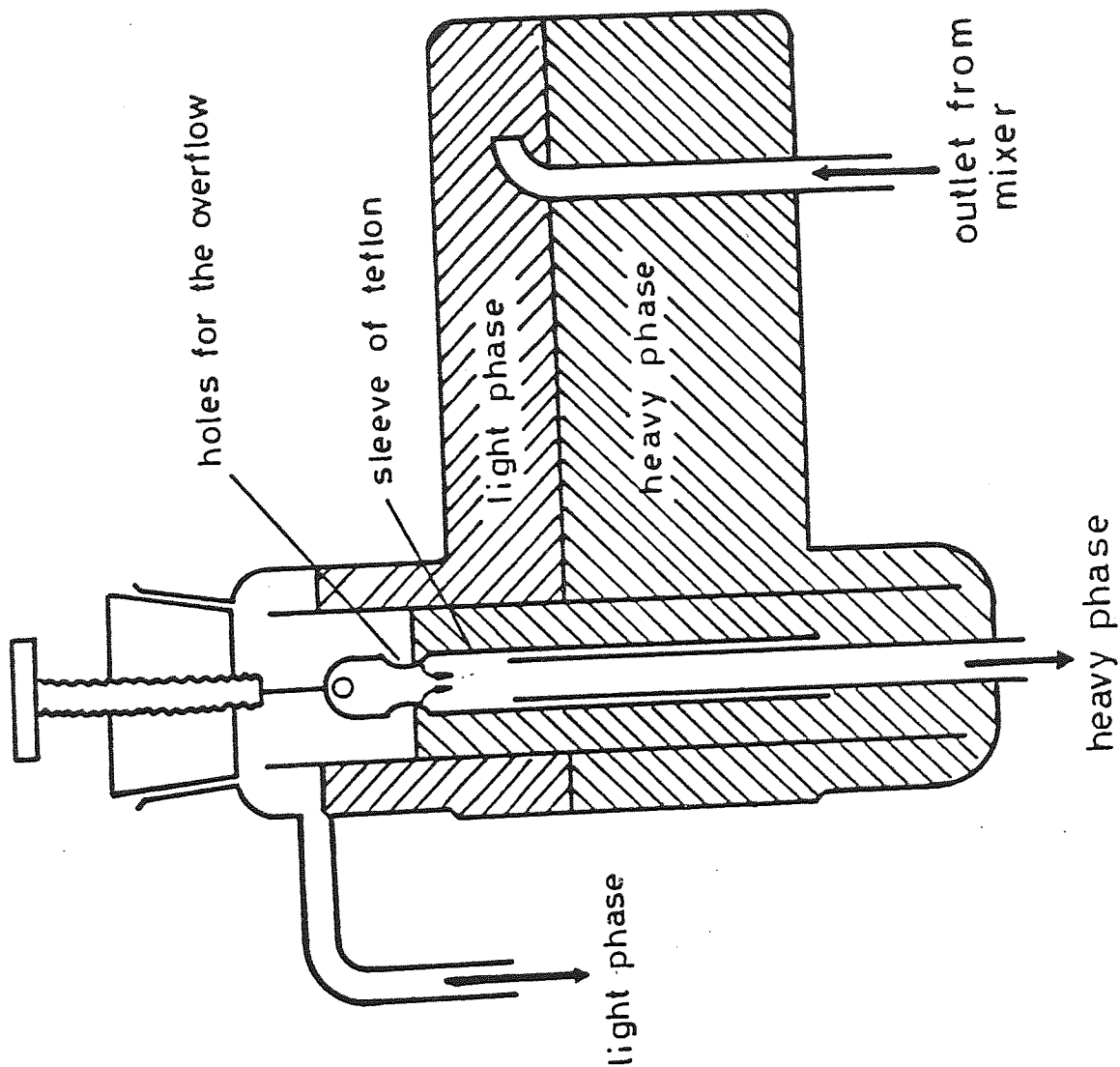


FIG. 8-2 TYPICAL SETTLER

maximum water content after distillation was 0.5%. During recovery of sulfolane by distillation, its color turned dark reddish-brown; therefore purification was necessary prior to use and following recovery. A number of simple procedures have been described in the literature for the purification of sulfolane (160-162). The procedure adopted in this study was developed by Geotzee et.al.(163), and consisted of four main steps. Sulfolane was stirred with 10 g/l decolorising carbon at 80°C for six hours. This step was followed by digestion with 2 g/l calcium permanganate for 3 hours at 90°C followed by filtration as suggested by Spurgeon (164). Vacuum distillation was the final step and was performed in a 2 m high, 10 cm diameter column packed with 1.25 cm Raschig rings. The vacuum was in the range 0.01 to 0.02 torr.

All the hydrocarbons used in this study were obtained from BDH Limited, U.K. Refractive indices and densities were determined for each hydrocarbon and were found in each case to correspond to a purity of 99.5%. as shown in Appendix I.

#### 8.4 Physical Properties of Materials

Selected properties of sulfolane (tetrahydrothiophene - 1, 1-dioxide, tetramethylene sulfolane) are listed in Table 8.1. It offers major advantages as a medium of proton transfer and other reactions. It is one of the most inert of the dipolar solvents with respect to its acid-base properties as well as other types of chemical attack, yet its relative permittivity (dielectric constant) is relatively high. It is a very weak acid,

electrochemical oxide-

chemical attack, even by

tion for many

stably

TABLE 8.1 PHYSICAL PROPERTIES OF SULFOLANE

Chemical formula	$C_4H_8SO_2$
Molecular weight	120.17
Specific gravity at 30/30 °C	1.266
Boiling point	285 °C
Freezing point	27.4-27.8 °C
Viscosity at 25 °C	10.3 cp
Viscosity at 100 °C	2.5 cp
Viscosity at 200 °C	0.97 cp

(165) and is highly resistant to electrochemical oxidation or reduction (166) and to chemical attack, even by the active atoms (167). Its main limitation for many applications is its viscosity, which is approximately ten times that of water. Typical fundamental studies recently carried out on sulfolane included: hydrogen bonding and proton transfer reactions (168) transport properties of electrolytes, and the voltammetry of inorganic compounds (169).

#### 8.5 Phase Equilibrium Data

The phase equilibria data of the ternary systems hexane-sulfolane-benzene, heptane-sulfolane-toluene, octane-sulfolane-xylene, and the multicomponent system aromatics-sulfolane-nonaromatics, were determined using a Smith-Bonner cell (9) controlled at temperatures of 30°C, 35°C or 40°C respectively. A specific amount of B (the non-aromatic) and the solute C (the aromatic) were introduced into the cell and agitated while maintained at a constant temperature by circulation of water through the external jacket from a thermostatic bath. The mixture was then titrated slowly against sulfolane until turbidity appeared and continued until the turbidity disappeared. Repeating this procedure at various compositions, enabled a complete set of curves to be obtained (170).

Analyses were performed by refractive index measurements using an Abbe refractometer supplied by American Optics. The solubility diagrams are shown in Figures 8.3 to 8.7 respectively, and the data are given in Tables 8.2 to 8.7



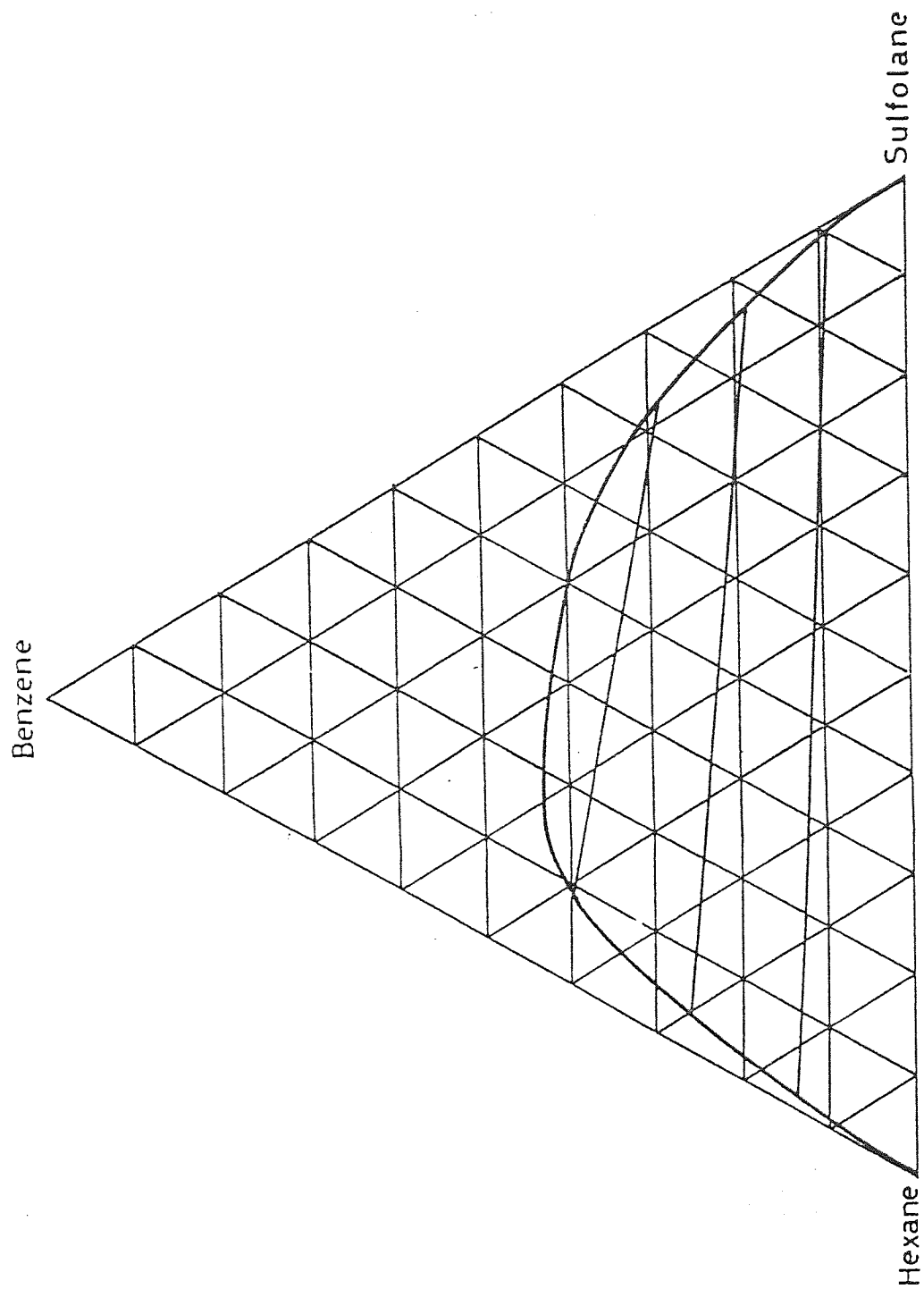


Fig 8.3 SOLUBILITY DIAGRAM FOR SYSTEM BENZENE-HEXANE SULFOLANE AT 30 °C

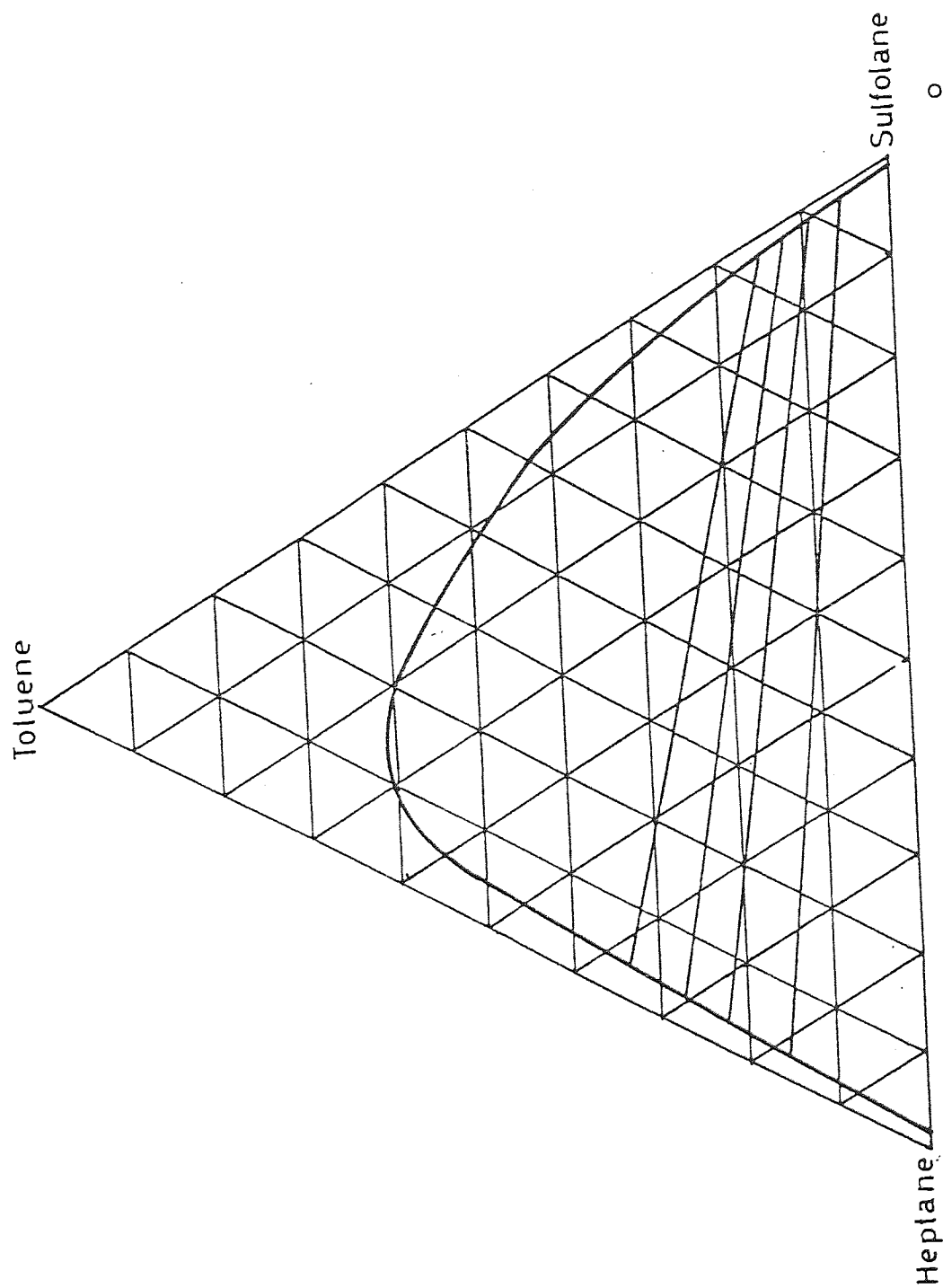


Fig 8.4 SOLUBILITY DIAGRAM FOR SYSTEM TOLUENE-HEPTANE SULFOLANE AT 30 °C

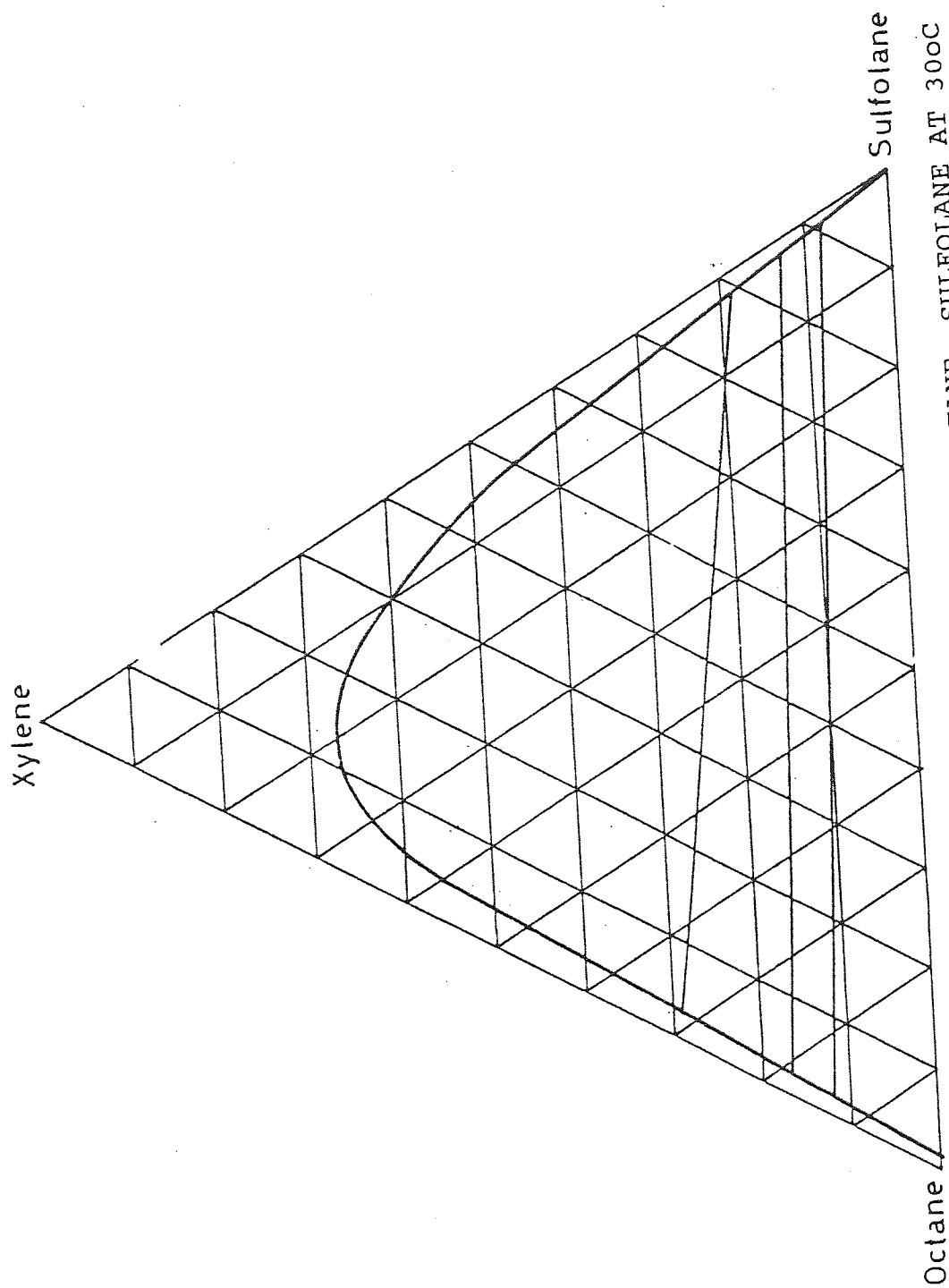


Fig 8.5

SOLUBILITY DIAGRAM FOR SYSTEM XYLENE-OCTANE- SULFOLANE AT 30oC

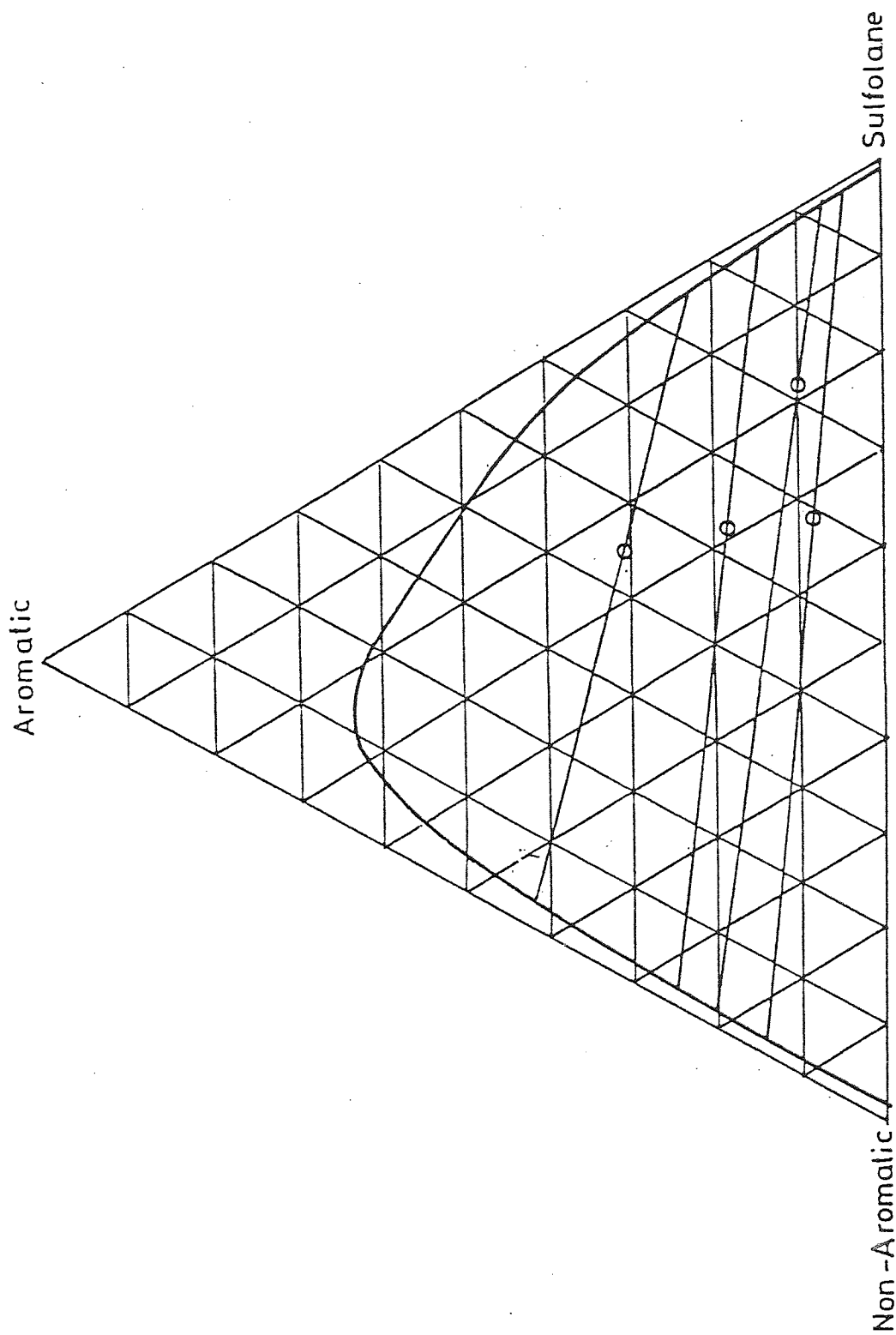


Fig 8.6 SOLUBILITY DIAGRAM FOR SYSTEM AROMATICS-NONAROMATICS-SULFOLANE AT 30 °C

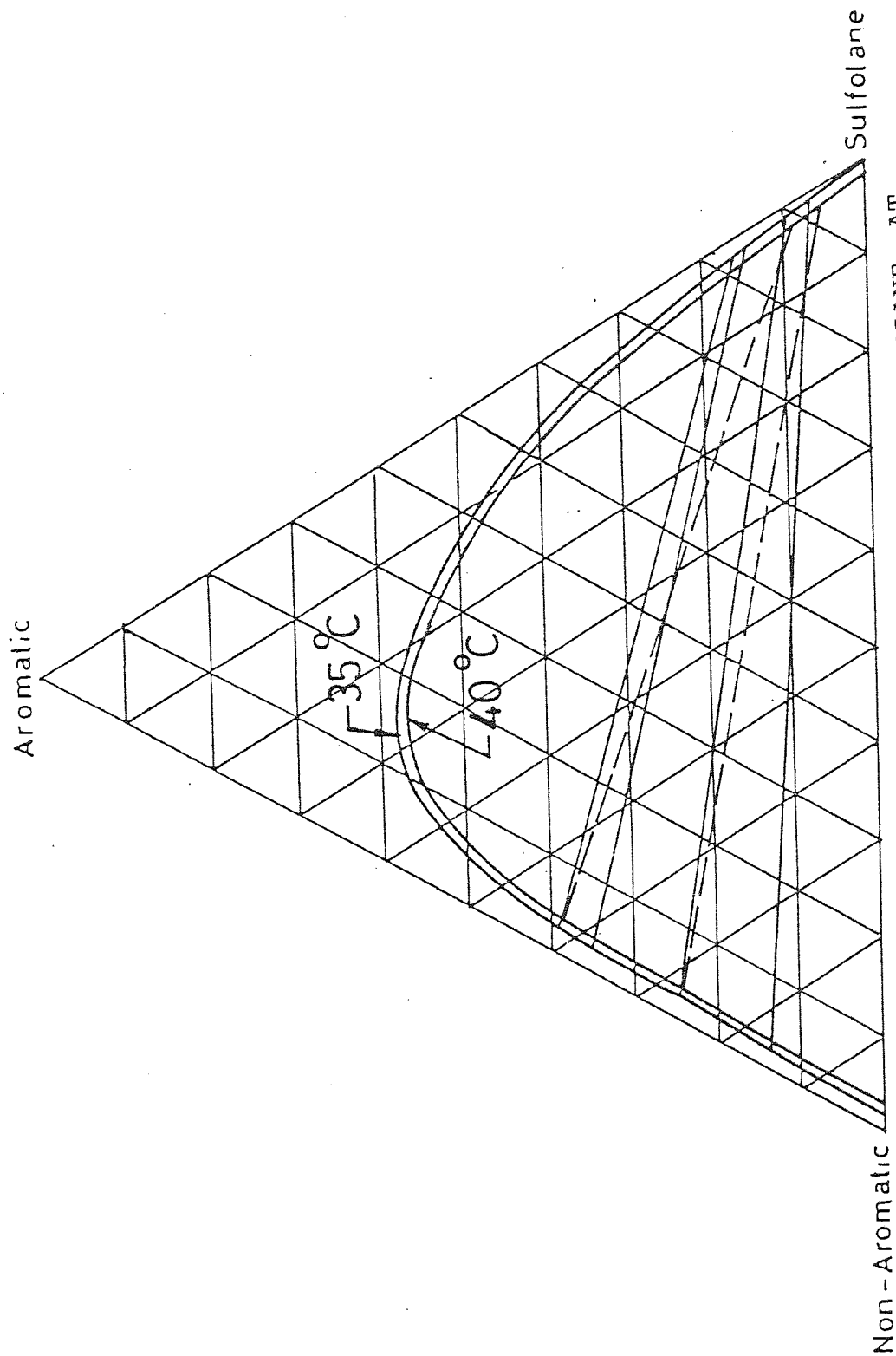


Fig 8.7 SOLUBILITY DIAGRAM FOR SYSTEM AROMATICS-NONAROMATICS-SULFOLANE AT

35 C, 40 C

TABLE 8.2 EXPERIMENTAL L.L.E COMPOSITIONS FOR N-HEXANE

°  
BENZENE-SULFOLANE AT 30 C

Wt fraction in raffinate			Wt fraction in extract		
N-Hexane	Benzene	Sulfolane	N-Hexane	Benzene	Sulfolane
0.990	-	0.009	0.006	-	0.993
0.851	0.131	0.018	0.015	0.083	0.891
0.705	0.26	0.034	0.047	0.181	0.771
0.512	0.392	0.995	0.088	0.281	0.62

TABLE 8.3 EXPERIMENTAL L.L.E COMPOSITIONS FOR N-HEPTANE-

°  
TOLUENE-SULFOLANE AT 30 C

Wt fraction in raffinate			Wt fraction in extract		
N-Heptane	Toluene	Sulfolane	N-Hexane	Toluene	Sulfolane
0.981	-	0.018	0.01	-	0.989
0.025	0.155	0.899	0.012	0.049	0.938
0.029	0.228	0.742	0.015	0.088	0.896
0.031	0.272	0.696	0.017	0.126	0.856

TABLE 8.4 EXPERIMENTAL L.L.E COMPOSITIONS FOR N-OCTANE-

XYLENE-SULFOLANE AT 30 °C

Wt fraction in raffinate			Wt fraction in extract		
N-Octane	Xylene	Sulfolane	N-Octane	Xylene	Sulfolane
0.983	-	0.017	0.005	-	0.994
0.865	0.123	0.021	0.008	0.085	0.907
0.812	0.161	0.026	0.019	0.125	0.855
0.675	0.289	0.036	0.029	0.185	0.785

TABLE 8.5 EXPERIMENTAL L.L.E COMPOSITIONS FOR NONAROMATICS-

AROMATICS SULFOLANE AT 30 °C

Wt fraction in raffinate			Wt fraction in extract		
N-Aromatic	Aromatic	Sulfolane	Nonaromatic	Aromatic	Sulfolane
0.845	0.144	0.012	0.007	0.048	0.994
0.783	0.204	0.013	0.012	0.072	0.916
0.731	0.255	0.014	0.016	0.142	0.842
0.550	0.422	0.029	6.02	0.231	0.749

TABLE 8.6 EXPERIMENTAL L.L.E COMPOSITIONS FOR NONAROMATICS-

AROMATICS-SULFOLANE AT 35 °C

Wt fraction in raffinate			Wt fraction in extract		
N-Aromatic	Aromatic	Sulfolane	Nonaromatic	Aromatic	Sulfolane
0.842	0.135	0.023	0.017	0.06	0.923
0.73	0.245	0.025	0.02	0.09	0.88
0.66	0.313	0.027	0.025	0.115	0.86
0.58	0.39	0.03	0.035	0.145	0.82

TABLE 8.7 EXPERIMENTAL L.L.E COMPOSITIONS FOR NONAROMATICS-

AROMATICS-SULFOLANE AT 40 °C

Wt fraction in raffinate			Wt fraction in extract		
N-Aromatic	Aromatic	Sulfolane	Nonaromatic	Aromatic	Sulfolane
0.912	0.06	0.028	0.015	0.25	0.95
0.822	0.149	0.295	0.022	0.052	0.92
0.675	0.282	0.037	0.027	0.088	0.88
0.6	0.36	0.04	0.03	0.11	0.86



## 8.6 Correlation of Data

Geometrical methods for interpolation and extrapolation of tie line data have been devised by Brancker et.al. (171) Sherwood (32) and Hand (11). Whilst they are entirely graphical, these methods are useful for extrapolation. The first empirical equation describing the distribution of components in a three component, two phase liquid system was due to Bachman (172).

$$X_{BB} = a + b (X_{BB}/X_{AA}) \quad 8.1$$

where  $a$  and  $b$  are constants.

Othmer and Tobias (173) showed that this correlation is of limited use because it is based upon a ternary system composed of practically immiscible non-consolute components in the absence of the consolute component. They, therefore, proposed that

$$\frac{1 - X_{AA}}{X_{AA}} = K \left[ \frac{1 - X_{BB}}{X_{BB}} \right]^n \quad 8.2$$

where  $K$  and  $n$  are constants for any specific system at a fixed temperature.

On logarithmic coordinates this equation gives a straight line. Unfortunately however, the method of Othmer and Tobias is also limited since it does not include the concentration of the distributed component. Therefore, the most useful formula appears to be that

of Hand which correlates the concentration of the solute in the two conjugate solutions. Hand's equation is represented by,

$$\frac{X_{CA}}{X_{AA}} = K \left[ \frac{X_{CB}}{X_{BB}} \right]^r \quad 8.3$$

i.e. the logarithmic plot of  $(X_{CA}/X_{AA})$  against  $(X_{CB}/X_{BB})$  is rectilinear.

A regression analysis of the solubility data for the system aromatics - non aromatics-sulfolane at 30°C based on Hand's correlation resulted in the equation

$$\frac{X_{CA}}{X_{AA}} = 0.414 \left( \frac{X_{CB}}{X_{BB}} \right)^{0.865} \quad 8.4$$

where A, B, and C refer to sulfolane, nonaromatics and aromatics respectively.

Figure 8.8 shows that the results predicted by Hand's correlation gave good agreement when plotted against the experimental values. The results of regression analysis of the data for this system at 35°C, resulted in the equation:

$$\frac{X_{CA}}{X_{AA}} = 0.23 \left( \frac{X_{CB}}{X_{BB}} \right)^{0.64} \quad 8.5$$

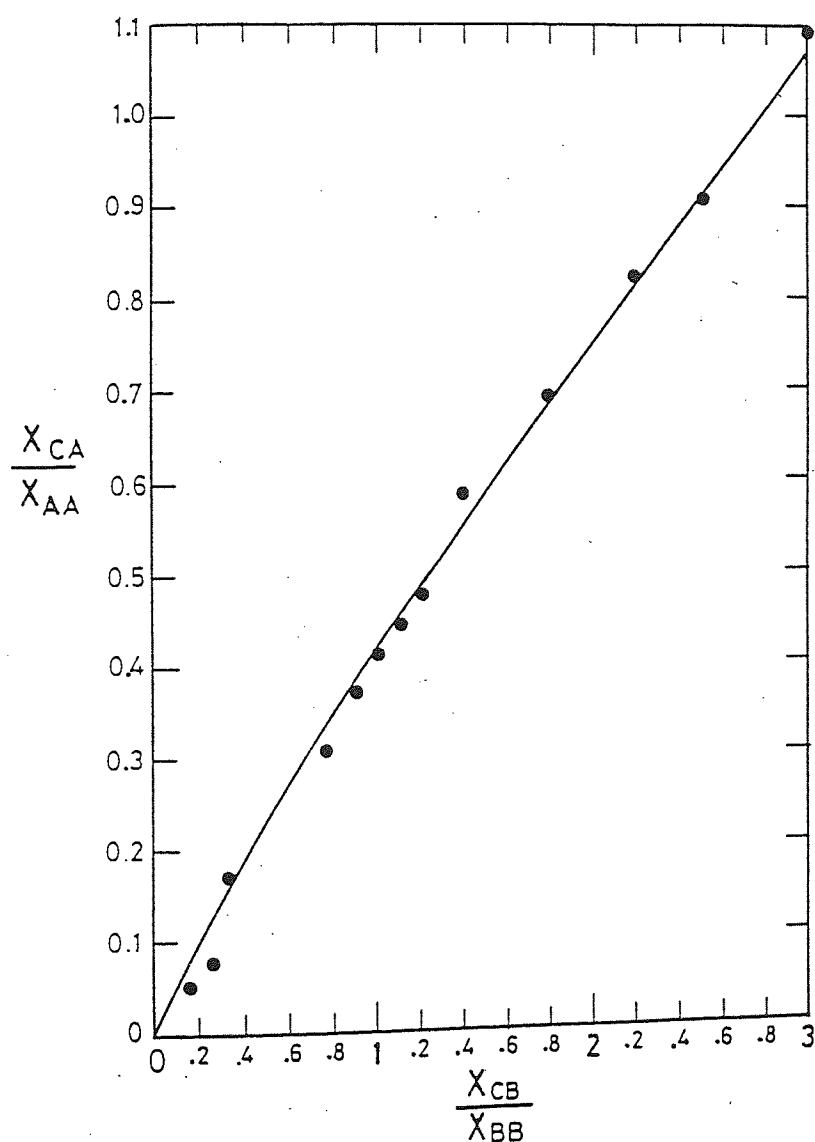


FIG. 8-8 EQUILIBRIUM CURVE OF SYSTEM : AROMATICS-  
NON-AROMATICS - SULFOLANE AT 30°C

and at 40°C

$$\frac{x_{CA}}{x_{BB}} = 0.188 \left( \frac{x_{CB}}{x_{BB}} \right) \quad 8.6$$

Figure 8.9 presents Hand's correlation for the multicomponent system nonaromatics-aromatics-sulfolane at 30°C, 35°C and 40°C.

#### 8.7 Computation of LLE data by UNIFAC

As applied in this work, the UNIFAC group contribution method has been utilized for the prediction of liquid-liquid equilibrium data of multicomponent aromatics extraction systems from the limited knowledge of binary VLE data and mutual solubilities. The UNIFAC model requires two group-interaction parameters ( $a_{mk}$  and  $a_{km}$ ) per pair of groups and the group volumes and surface area of individual groups as follows :

The activity coefficient is expressed as the sum of two parts, namely (i) combinatorial, and (ii) residual. For any component  $i$ , the activity coefficient is expressed as :

$$\ln \gamma_i = \ln \gamma_i^C + \ln \gamma_i^R \quad 8.7$$

The combinatorial contribution  $\gamma_i^C$ , is given by :

$$\ln \left( \frac{\Psi_i}{x_i} \right) + \frac{\bar{Z}}{2} q_i \ln \left( \frac{\theta_i}{\Psi_i} \right) + \ell_i - \frac{\Psi_i}{x_i} \sum_{i=1}^C (x_i \ell_i) \quad 8.8$$

where

$$\ell_i = \left( \frac{\bar{Z}}{2} \right) (r_i - q_i) - (r_i - 1) \quad 8.9$$

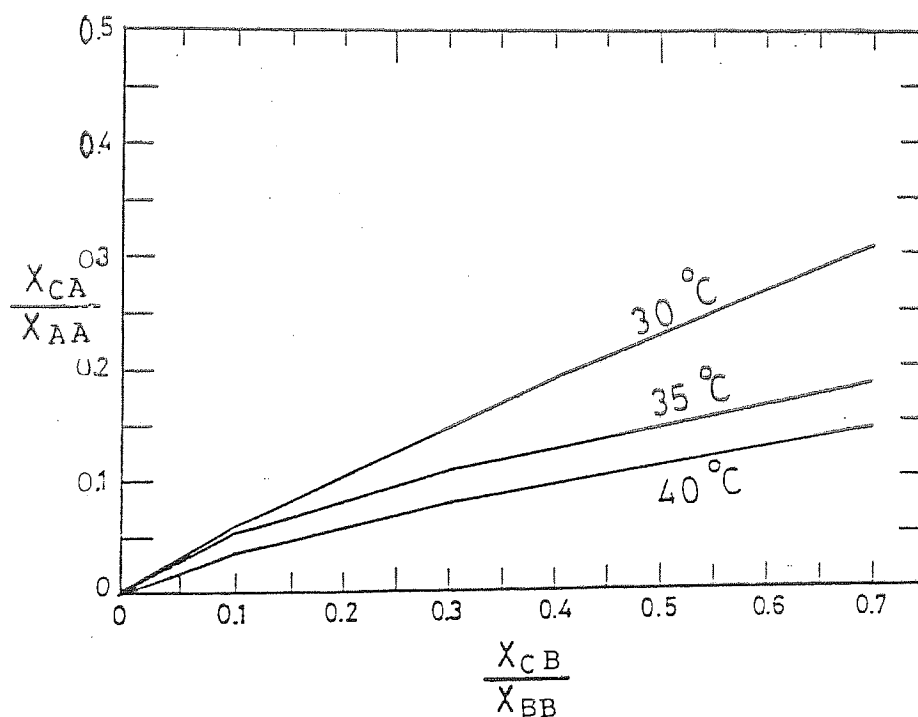


FIG. 8-9 HANDS' CORRELATION OF SYSTEM: AROMATIC-NONAROMATIC  
SULFOLANE AT 30°C, 35°C, 40°C

where  $\bar{z}$  is a co-ordination number normally equal to 10.0 and the segment fraction,  $\psi_i$  and surface area fraction,  $\theta_i$  for component  $i$  are given by :

$$\psi_i = \frac{x_i r_i}{\sum_{i=1}^c x_i r_i} = \text{segment fraction} \quad \theta_i = \frac{x_i q_i}{\sum_{i=1}^c x_i q_i} = \text{area fraction}$$

$$q_i = \sum_k \nu_k^{(i)} Q_k \quad r_i = \sum_k \nu_k^{(i)} R_k \quad 8.10$$

$R_k$  and  $Q_k$  are the group volumes and surface area parameters for group  $k$ . The residual contribution  $\gamma_i^R$ , to the activity coefficient is given by :

$$\ln \gamma_i^R = \sum_{\substack{\text{all functional} \\ \text{groups in the} \\ \text{mixture}}} \nu_k^{(i)} (\ln \Gamma_k - \ln \Gamma_k^{(i)}) \quad 8.11$$

This activity coefficient  $\Gamma_k$  of group  $k$  is given by :

$$\ln \Gamma_k = Q_k \left[ 1 - \ln \left( \sum_m \theta_m T_{mk} \right) - \sum_m \frac{\theta_m T_{mk}}{\sum_n \theta_n T_{nm}} \right] \quad 8.12$$

The mole fraction  $X_m$  for the group  $m$  is expressed as :

$$X_m = \frac{\sum_j \nu_j^{(m)} x_j}{\sum_j \sum_n (\nu_n^{(j)} x_j)} \quad 8.13$$

group surface area fraction,  $\theta_m$  is expressed as :

$$\theta_m = \frac{X_m Q_m}{\sum_n X_n Q_n} \quad 8.14$$

and

$$T_{mk} = \exp \left( - \frac{a_{mk}}{T} \right) \quad 8.15$$

This model requires two group interaction parameters (  $a_{mk}$  and  $a_{km}$  ) per pair of groups , group volumes, and surface areas of individual groups for estimation of the activity coefficient .

Computation of the liquid - liquid equilibrium phase compositions involves solving equation (8.4) with material balance equations (8.17, 8.18, and 8.19), using an iterative procedure based on the Newton Raphson method (174).

$$(\gamma X_i)^I = (\bar{\gamma} X_i)^{II} \quad 8.16$$

$$X_i^F = \theta X_i^I + (1 - \theta) X_i^{II} \quad (i=1, 2, \dots, N) \quad 8.17$$

$$\sum_{i=1}^N X_i^I = 1 \quad 8.18$$

$$\sum_{i=1}^N X_i^{II} = 1 \quad 8.19$$

$\theta$  is the fraction extracted.

The procedure involves estimation for  $\theta$  and  $X_i^I$  and successive iteration until equation (8.16) is satisfied , the  $X_i^I$  and  $X_i^{II}$  are next calculated, using the compositions just obtained from UNIFAC (174). New values of  $X_i^{II}$  and  $X_i^I$  are then calculated from equations 8.20 and 8.21.

$$X_i^{II} = \frac{X_i^F}{1 + (K_i - 1)\theta} \quad 8.20$$

$$X_i^I = K_i X_i^{II}$$

8.21

where  $K_i = X_i^I / X_i^{II}$  and are improved upon successive iteration until  $(X_i^{II\text{ old}} - X_i^{II\text{ new}})^2 < 10^{-8}$ .

### 8.8 Results and Discussion

Figure 8.10 and Table 8.8 demonstrate that the predicted phase compositions were in good agreement with the corresponding experimental values for the system aromatic-nonaromatic-sulfolane. The deviation of the predicted compositions near the plait point is characteristic of any prediction method, but is of little consequence since practical extractions are never carried out near the plait point. The cause of such deviations is that near the plait point the two conjugate phases approach each other in their compositions and other properties such as density, and viscosity; hence the prediction of activity coefficient is difficult.

With regard to the effect of temperature on the selectivity and distribution coefficient, the selectivity of sulfolane will decrease with temperature since the heterogeneous area decreases with temperature. The slope of the tie lines is inclined towards the solvent, but the selectivity is greater than one; thus the extraction is possible.

It is concluded from the above results that the temperature had a modest effect on the miscibility range of the systems studied. On balance considering both capacity and selectivity of sulfolane, better results were achieved at the lowest temperature of 30°C.



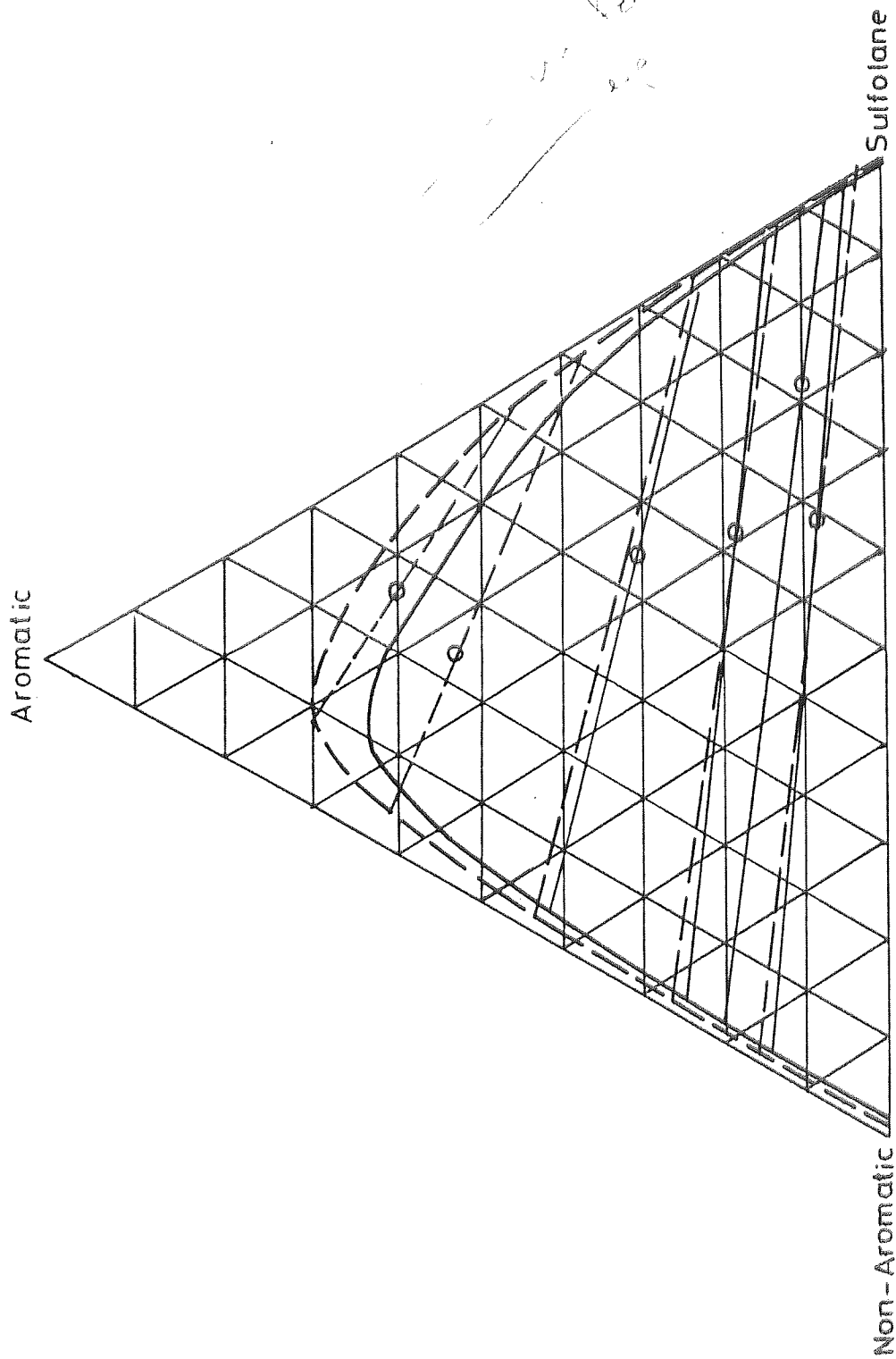


Fig 8.10 COMPARISON OF PREDICTED AND EXPERIMENTAL SOLUBILITY DIAGRAM AT

30 °C

between data predicted

that results as shown

is presented

Table 8.8 PREDICTED L.L.E COMPOSITIONS AT 30 °C FOR  
AROMATICS-NONAROMATICS SULFOLANE

Compositions of Aromatic (Benzene 46.799, Toluene 32.29, xylene 20.91 Vol. %), Nonaromatics (N-hexane 21.47, N-Heptane 40.6, N-octane 37.91 Vol. %)					
Wt fraction in raffinate			Wt fraction in extract		
N-Aromatic	Aromatic	Sulfolane	Nonaromatic	Aromatic	Sulfolane
0.843	0.142	0.015	0.009	0.052	0.938
0.781	0.199	0.019	0.014	0.075	0.910
0.725	0.254	0.020	0.020	0.149	0.840
0.549	0.420	0.035	0.025	0.239	0.735

Good agreement was obtained between data predicted by the UNIFAC method and experimental results as shown in Figure 8.10. The computer program used is presented in appendix II.

## CHAPTER 9

---

### RESULTS OF LIQUID-LIQUID EXTRACTION STUDIES.

## 9.1 Introduction

A study was made of the performance of the 10-stage laboratory mixer-settler cascade for the extraction of benzene-toluene-xylene (BTX) from a synthetic reformat utilizing sulfolane as solvent. Prior to this hydrodynamics of the equipment were established. Relevant physical properties were also measured, or predicted. Subsequently extraction was performed using an actual reformat feed as described in Chapter 10 .

## 9.2 Diffusivities

Diffusivities of aromatics in the non-aromatics and sulfolane phases were predicted from a method given in reference (175). An empirical modification of the Stokes -Einstein relation was used to calculate the diffusivities of the aromatics in both phases at very low concentrations i.e. < 1% .

$$D_{AB}^0 = 7.4 \times 10^{-8} \frac{(xM)^{0.5} T}{\mu V_A^{0.6}} \quad 9.1$$

where  $D_{AB}^0$  = molecular diffusion coefficient of solute A at very low concentrations in solvent B

M = molecular weight of solvent B

T = Absolute temperature K

$\mu$  = Viscosity of solvent B, cP

$V_A$  = Molal volume of solute at its normal boiling temperature, cm<sup>3</sup>/g-mole

x = association factor of solvent

B, dimensionless.

In this calculation the value of  $V_A$  is best estimated at the boiling point  $T_b$ . Wilke and Chang (176) recommend that  $x$  equals 1 for unassociated solvents. Anderson (177) found that for the effect of concentration on the diffusion coefficient, the volume fraction of solute is important.

$$\frac{D_{AB}}{D_{AB}^0} = (1-X)^{6.5} \quad 9.2$$

where  $D_{AB}^0$  = infinite dilution diffusion coefficient  
 $X$  = solute volume fraction.

No activity correction is recommended (177). The predicted diffusivities obtained are presented in Appendix III.

### 9.3 Interfacial Tension

The interfacial tension of the aromatics-nonaromatics-sulfolane system was measured by DuNoy's method at 30°C, 35°C, 40°C. Samples of different concentrations of aromatics were thoroughly mixed in a Smith-Bonner cell for 4 hours, with an agitator speed of about 1400 rpm, at constant temperature, until equilibrium was obtained. The system was then allowed to settle until the phases were clear and the interfacial tension of each phase was then determined.

The interfacial tension of immiscible liquids is less than the larger of the surface tensions of the component liquids. Quantitative prediction may be made with Antonoff's rule which states that for two

saturated-liquid layers in equilibrium the interfacial tension is equal to the difference between the individual surface tensions of the two mutually saturated phases under a common vapour or gas.

$$\sigma = \sigma_{1s} - \sigma_{2s} \quad 9.3$$

The experimental interfacial tension data were in reasonable agreement with predictions using equation 9.3. The interfacial tension data at 30°C were correlated using regression analysis, and the correlation obtained was

$$\sigma = 20.7 X_o^{0.7} \quad 9.4$$

where  $X_o$  is the total concentration in the system.

#### 9.4 Calibration Techniques

Calibration graphs for measurements of the concentration :

The aromatics concentration in each phase was calculated from refractive index measurements using an Abbe refractometer. This method was preferred because samples of small size (0.2-0.3ml) were required. A graph of concentrations vs refractive index was constructed for each phase; these are presented in Appendix IV.

Calibration graphs for measurements of the flow rates : The two rotameters used in the mixer-settler unit were calibrated with water at 20°C. Therefore it was necessary to recalibrate them using the two experimental, phases, namely the feed phase (aromatics 55%, non-aromatics 45%) and the sulfolane phase. The calibration graphs for these fluids are given in Appendix IV.

### 9.5 Operating Procedure

The feed contained 55% w/w of aromatics (benzene, toluene and xylene); a typical composition is shown in Chapter 8. The aromatics concentration was restricted to 55% for the following reasons:

- i) The 55% feed concentration matches the concentration in most reformates.
- ii) Such a feed concentration could be expected to yield a reasonable difference in outlet raffinate and extract concentrations from the different stages, hence minimizing experimental error.
- iii) Such a feed concentration results in a reasonable mass transfer driving force.

The feed was prepared by mixing the requisite amounts of feed components (benzene, toluene, xylene, hexane, heptane, and octane). A sample was withdrawn to check the concentration using the refractive index method.

At the start of each run, the cascade was filled with the continuous solvent phase followed by the feed and the interface was adjusted to correspond with the mid-position in the settler. The agitator speed was set to the desired value; feed and solvent flow rates were then adjusted to give the required phase ratio. This was normally achieved by fixing the feed flow rate (10 ml/min) and changing the solvent flow rate. The range of phase ratios covered was 1:1 to 3:1. Other variables investigated were the mixer speed (400 rpm to 1050 rpm), and the temperature which was maintained in separate experiments at 30°C, 35°C, 40°C ( $\pm 1^\circ\text{C}$ ) respec-



tively by heating the feed tanks thermostatically and by controlling the temperature of the laboratory. In all cases, a time of 30 min was found to be sufficient to reach equilibrium, resulting in homogeneous dispersions , but indicated by a steady concentration profile.

Steady-state holdup in the mixer was measured by both the rapid shut-off and displacement methods (178). In the former the valves in the feed and exit lines were rapidly and simultaneously closed; the fractional volume of the dispersed phase was measured after complete phase separation had occurred. The results agreed in all cases with a deviation of  $<1\%$  , which was not unexpected with a mixer-settler .

Because it was impractical to photograph droplets within the mixer directly, drop sizes were measured using a graduated capillary tube inserted into the mixer through which samples were withdrawn. A graduated microsyringe was used to withdraw the sample and to estimate the volumes of individual drops. The capillary tube was calibrated and the volume of 5 or 6 drops withdrawn at any one time could hence be read accurately and the volumes calculated . Up to 50 drops were counted for any one mixer and operating condition. There were no visual indications of either drop break-up or coalescence occurring in the tube during sampling and measurement. An Abbe refractometer was used to measure the refractive indices of samples of raffinate and extract after steady state was attained; the co-

ncentrations were then determined by reference to the calibration charts obtained previously and checked by material balance calculations .

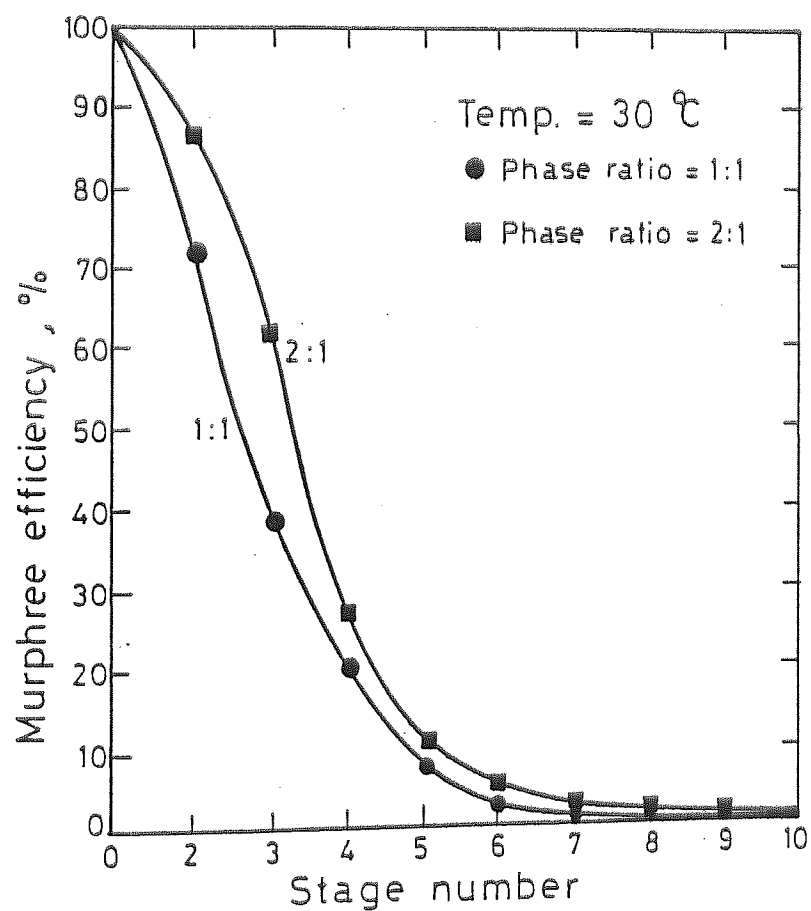
#### 9.6 Results and Discussion

The Murphree stage efficiencies, and recoveries of aromatics were measured in each stage. For this purpose the stage efficiency was defined by equation 6.22 Although the cascade consisted of 10 stages, it was observed in initial experiments that the percentage product recovery, and hence the stage efficiency, both leveled-off after only 4 stages. This is illustrated for example in Figures 9.1 and 9.2. It was concluded that four stages were sufficient to give acceptable values of recovery and efficiency and the remainder of the experimental work was carried out using these only.

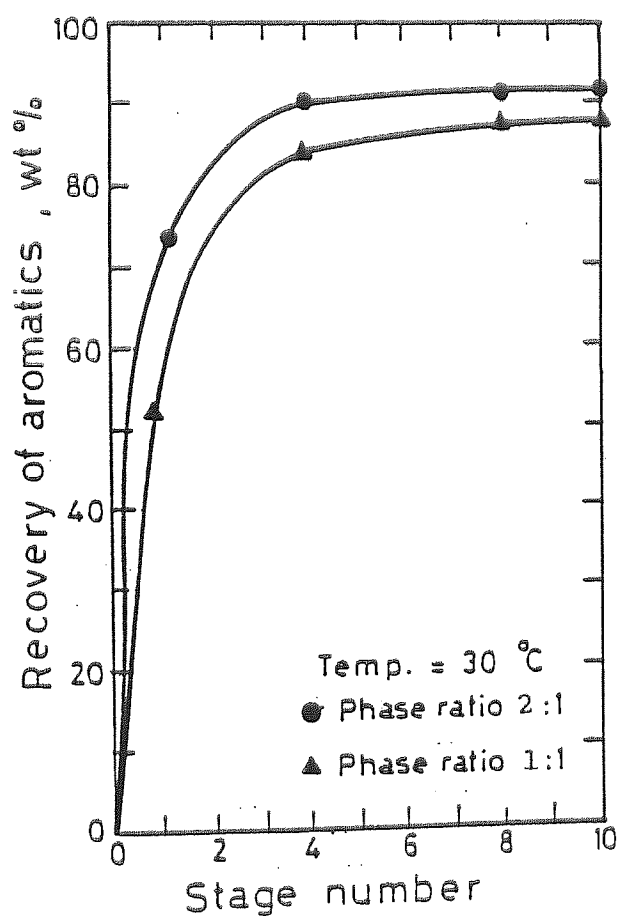
##### 9.6.1 Hydrodynamics

###### Hold-Up

Hold-ups were determined of both mutually-saturated phases and in the presence of mass transfer . The effect of mixer speed on dispersed phase hold-up ( $\phi_D$ ) was studied, by plotting ( $\phi_D/\phi_O$ ) as function of mixer speed, where  $\phi_D$  is the average holdup of the dispersed phase and  $\phi_O$  is the fraction of dispersed phase in the feed. When the agitator speed was varied from 3 rps to 20 rps,  $\phi_D/\phi_O$  varied widely, i.e., from 0.1 to 0.97. Figure 9.3 shows that holdup in stage 4 reached an asymptotic value at an impeller speed of 17.5 rps (1050 rpm), and this value was therefore used in all runs involving mass transfer. The phenomenon itself is in agreement with the observation of Thornton (119) and



9-1 VARIATION OF EFFICIENCY WITH STAGE NO IN THE CASCADE



9-2 PERCENTAGE RECOVERY OF AROMATICS AS A FUNCTION OF STAGE NO IN THE CASCADE.

Treybal (71) that dispersed phase hold-up in a continuous mixer-settler approaches the volume fraction of the dispersed phase in the feed with increasing impeller speed .

The mutually-saturated hydrocarbons were used for the study of hydrodynamics in the absence of mass transfer. This is the conventional means of reducing the amount of experimentation required (180) . However, it is based on an assumption that the concentration of solute and transfer rate does not significantly affect the phase physical properties and hence the drop sizes. The difference in physical properties between the saturated and the original feed containing both saturates and aromatics is reflected in the slight difference in the fractional holdup in stage 4 shown in Figure 9.3.

#### Drop-size

Drop sizes were determined under mass transfer conditions .The range of drop sizes observed in the mixer was generally between 0.41 and 0.67 mm. In all cases some droplets were produced which approached the secondary dispersion size range, i.e.,  $<0.3$  mm, but these created no difficulties in the settler because, at the energy inputs used, they were a small proportion of the dispersed phase.

The mean drop size varied with rotor speed, hold up, and system physical properties. As shown in Figure 9.4 for stage 4 the Sauter mean drop diameter at constant

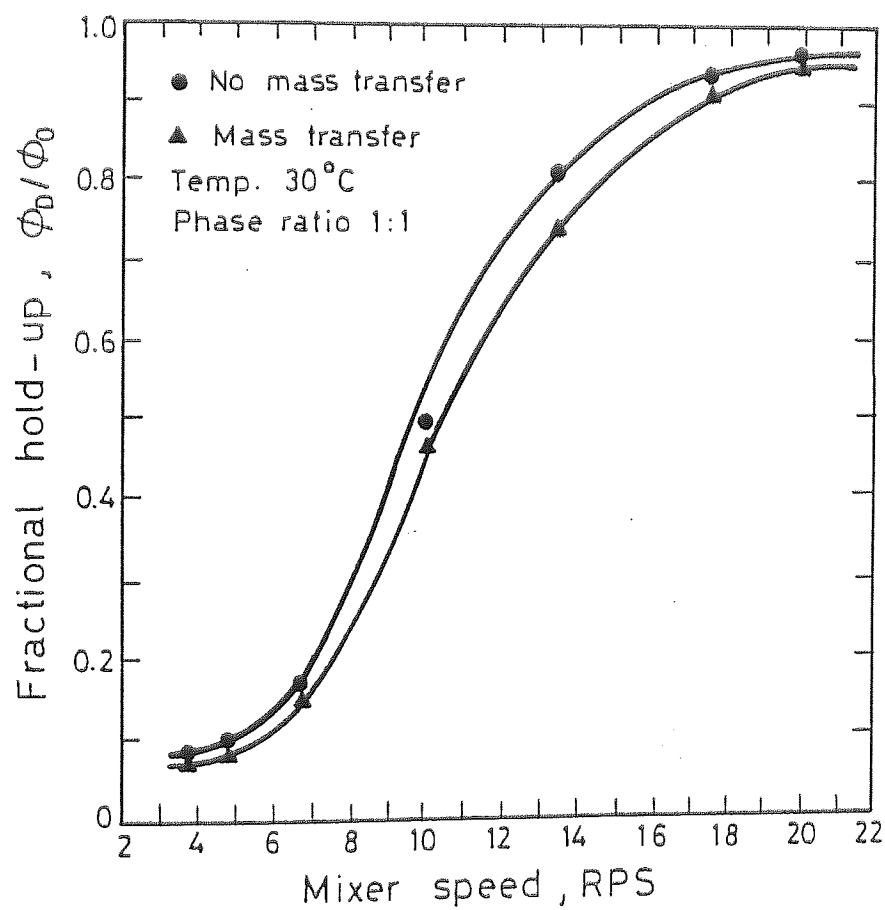


FIG. 9-3 EFFECT OF MIXER SPEED ON FRACTIONAL HOLD UP IN THE MIXER (STAGE 4).

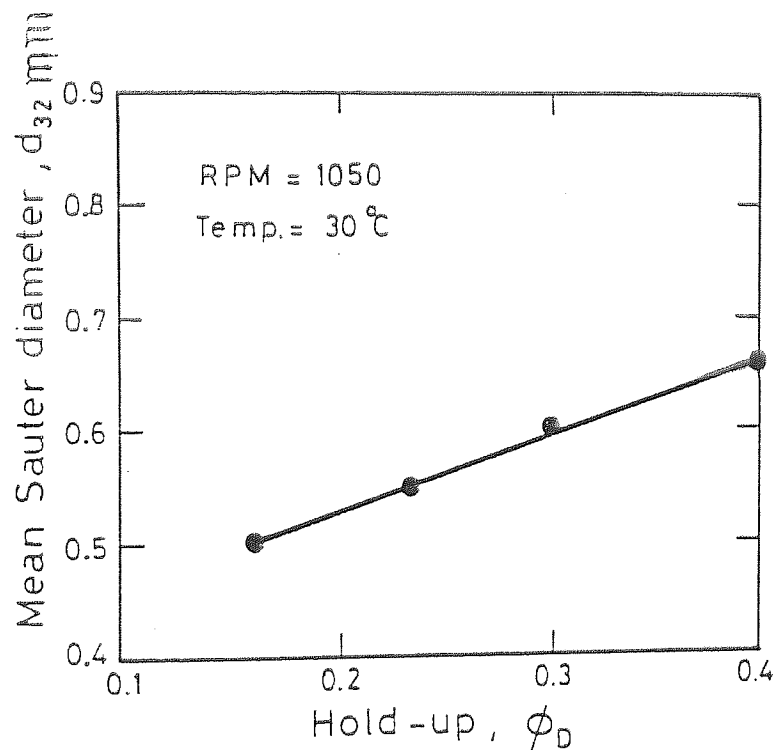


FIG. 9-4 VARIATION OF  $d_{32}$  WITH HOLD-UP AT CONSTANT MIXER SPEED (STAGE 4).

rotor speed increased linearly with hold up due to the change in balance between coalescence effects and droplet break-up.

Experimental values of  $d_{32}$  were compared with the correlation of published data (118). Although such data were carried out without a settler and, more importantly, the ratio of impeller to tank diameter was 0.386 compared to 0.97 in the present work, the average difference between mean drop sizes under corresponding conditions was approximately 20%. The difference is almost certainly due to the different geometric configuration of the mixing systems, and also to the presence of a settler in the present work, which created a back pressure. Only one correlation has previously been published for drop size and hold-up in the mixer of a continuous mixer-settler (4). Such a correlation can be derived by dimensional analysis involving the physical properties of the system, operating conditions, and impeller diameter, to yield,

$$d_{32} = f(N, V_d, V_c, \mu_d, \mu_c, \sigma_i, \rho_m, d_i) \quad 9.5$$

$$\frac{d_{32}}{d_i} = K (We)^\alpha \left(\frac{r}{1+r}\right)^\beta \left(\frac{\mu_d}{\mu_c}\right)^\gamma \quad 9.6$$

where  $r$  is velocity ratio of phases  $V_d/V_c$

$$\frac{d_{32}}{d_i} = K \left(\frac{N^2 d_i^3 \rho_m}{\sigma_i}\right)^\alpha \left(\frac{r}{1+r}\right)^\beta \left(\frac{\mu_d}{\mu_c}\right)^\gamma \quad 9.7$$



Calculation of the exponents  $\alpha$ ,  $\beta$ ,  $\gamma$  and the value of the constant K from the experimental results in the present work yielded;

$$\frac{d_{32}}{d_i} = 0.133(We)^{-0.38} \left(\frac{r}{1+r}\right)^{0.326} \left(\frac{\mu_d}{\mu_c}\right)^{-0.12} \quad 9.8$$

This equation described the data with a correlation coefficient of 0.98. Figure 9.5 shows that the measured experimental values lie within  $\pm 3\%$  of those calculated using equation 9.7. In Table 9.1 the exponents are compared with published results for related, but not identical systems. No data are available for drop size in the mixer section of a mixer-settler cascade. The exponents of N and  $d_i$  agree with reported work to within 24% and that of  $(r/1+r)$  of 0.326 agrees with the reported work to within 67%. The exponent of  $(\mu_d/\mu_c)$  agrees with the reported work to within 42%. The differences in the exponents of  $d_i$ , N,  $(r/1+r)$  and  $(\mu_d/\mu_c)$  may be due to the differences in mixer geometry, impeller size, and position in mixing vessel, and the presence of the settler and the ratio of  $d_i/d_T$ . Moreover although, the interfacial tension were similar (116),  $\mu_c$  and  $\Delta\rho$  were significantly higher in the present work. The change in drop size with stage number at different phase ratios is shown in Figure 9.6.

#### Phase Inversion

Following the procedure used in previous investigations into phase inversion in continuous differential contactors (180), the agitator speed and the con-

Table 9 - 1

## EXPONENTS ON GROUPS AFFECTING DROP SIZE

Group	This work exponents	Published data range of	Reference
We	-0.38	-0.58	Hossain
N	-0.76	-1.0 to -1.5	Arnold
D	-1.14	-1.0 to -2.0	Arnold
$\mu_d/\mu_c$	-0.12	-0.21	Hossain
(r/l+r)	0.326	1 - 1.02	Buoyatidis and Thornton

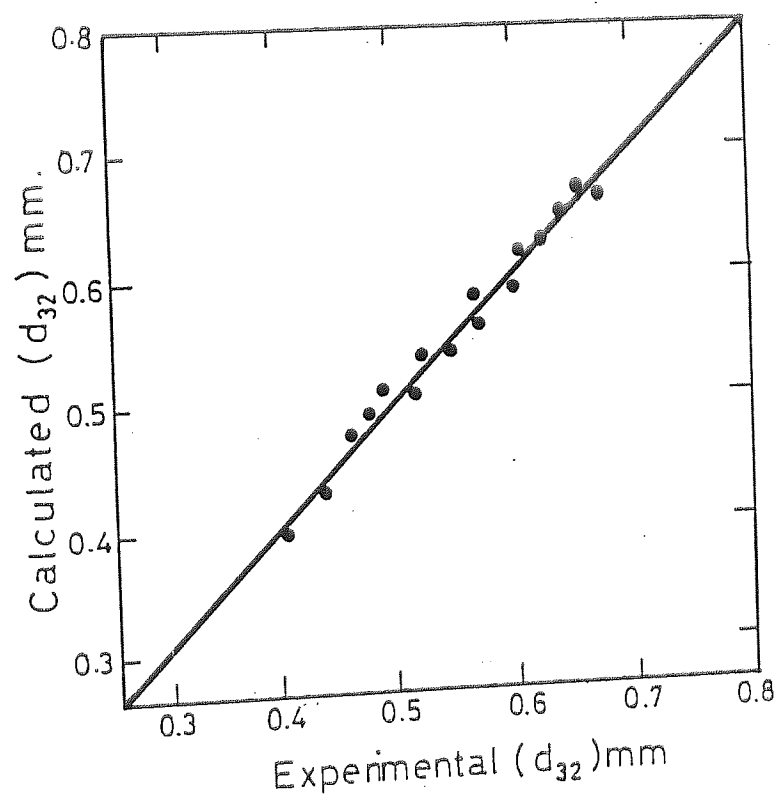


FIG.9- 5 PREDICTION OF  $d_{32}$  VS EXPERIMENTAL  $d_{32}$

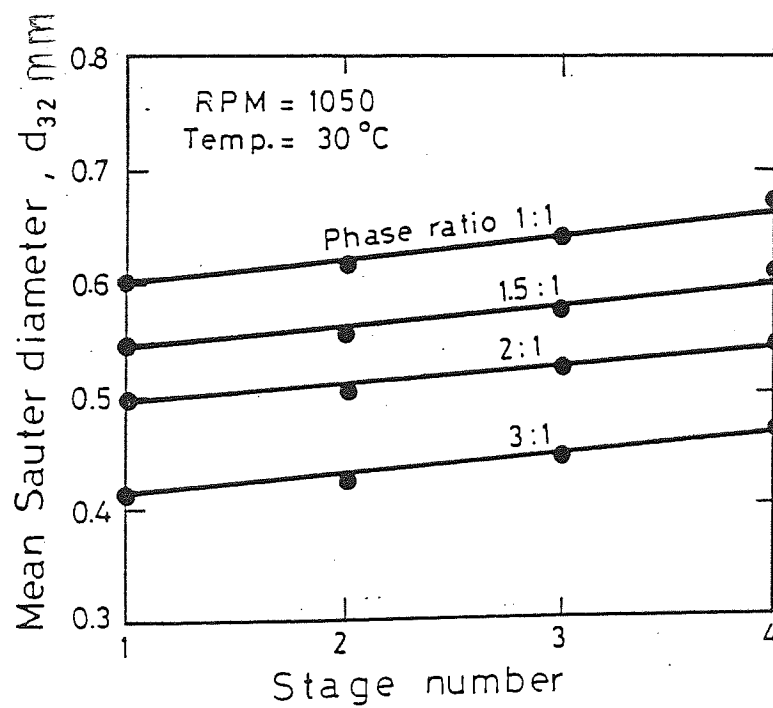


FIG 9-6 VARIATION OF  $d_{32}$  WITH STAGE NO AT DIFFERENT PHASE RATIOS.

tinuous phase flow rate were kept constant and the dispersed phase flow rate was then increased incrementally by between 2% and 5% until phase inversion occurred. A similar procedure was also used but with the dispersed phase flow maintained constant and the continuous phase flow being gradually decreased incrementally. The impeller speeds used were 400, 800, 1050 & 1400 rpm since below 400 rpm dispersion was not uniform and above 1400 rpm effective separation of the phases was not obtained in the settler due to the formation of a secondary haze.

A dispersion was classified as being either non-aromatic or sulfolane phase continuous, by testing with the addition of an organic soluble methyl red dye. The dye was used at a concentration less than 0.01%, at which concentration it had no significant effect on interfacial tension (181).

Conditions in the settler changed when phase inversion occurred in the mixer. The onset of inversion was not instantaneous, and it required of the order of 30-35s to appear in the settler. Similar time scales have been observed by others (116). Phase inversion occurred consecutively in each stage, with a well-defined time lag between successive stages. This time lag was found to be approximately 60s due to the time taken for each downstream stage to reach the point of inversion equilibrium.

Figure (9.7) shows the variation of the inversion point with agitator speed for different dispersed and continuous phase flow rates.

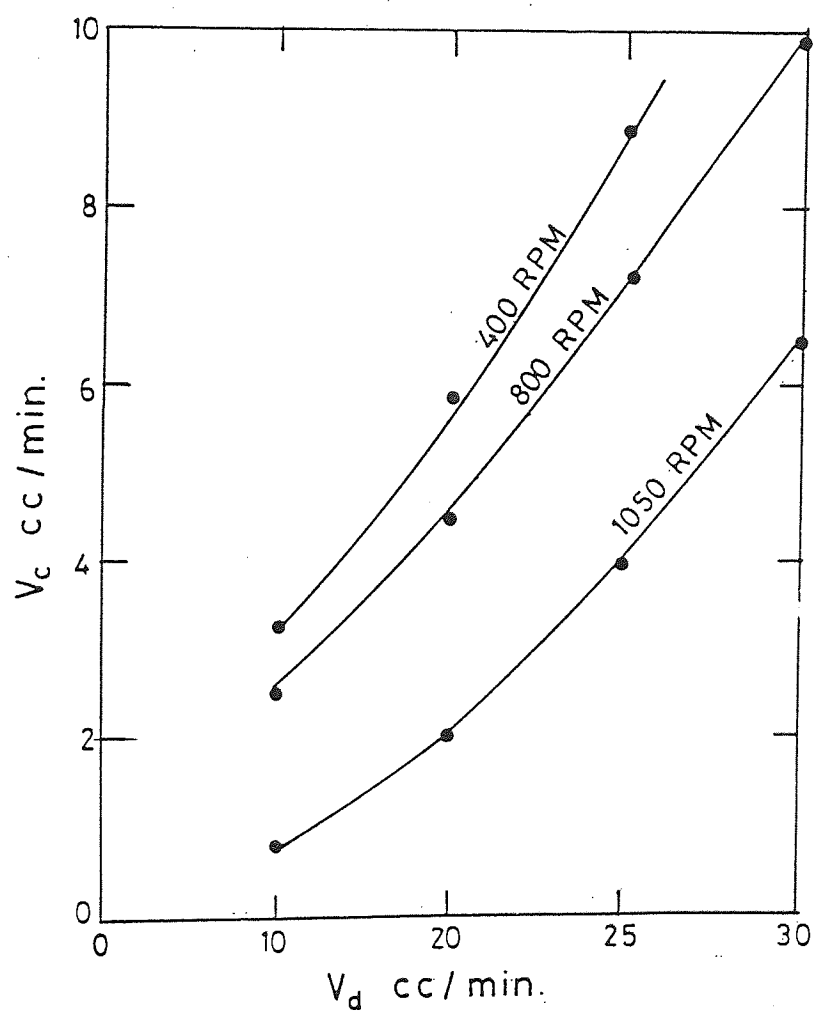


FIG. 9-7 CONTINUOUS PHASE THROUGHPUT VS DISPERSED PHASE THROUGHPUT AT PHASE INVERSION.

### 9.6.2 Mass Transfer Results

Figures 9.8 and 9.9 show the effect of the three variables namely the phase ratio, mixer speed and the extraction temperature on the recovery of aromatics. In Figure 9.8, the percentage recovery increases sharply with the phase ratio until it reached an asymptotic value of 2.5:1 to 3:1. The effect of the mixer speed and extraction temperature on the recovery of aromatics is shown in Figure 9.9. Within the temperature range investigated, the temperature had a considerable impact on the recovery. The mixer speed, had a greater effect on the recovery as the extraction temperature decreased.

At a phase ratio of 1:1 and temperatures of 30°C, 35°C and 40°C respectively the stage efficiency decreased with stage number. Typical results are shown in Figure 9.10. At a phase ratio of 3:1 the stage efficiency decreased more sharply after the first stage as typified by Figure 9.11. For the phase ratio 3:1, the efficiency could exceed 100% as in Figure 9.11. In fact it is possible for Murphree efficiency in mixer-settlers to achieve such a high efficiency as reported earlier by Scheibel (182) and recently by Milos and Stanley (183). The Murfree stage efficiencies, and recoveries of aromatics were measured in each stage. For this purpose the stage efficiency used as defined in equation 6.22. The equilibrium concentrations were predicted for each stage from the comprehensive data published elsewhere (179).

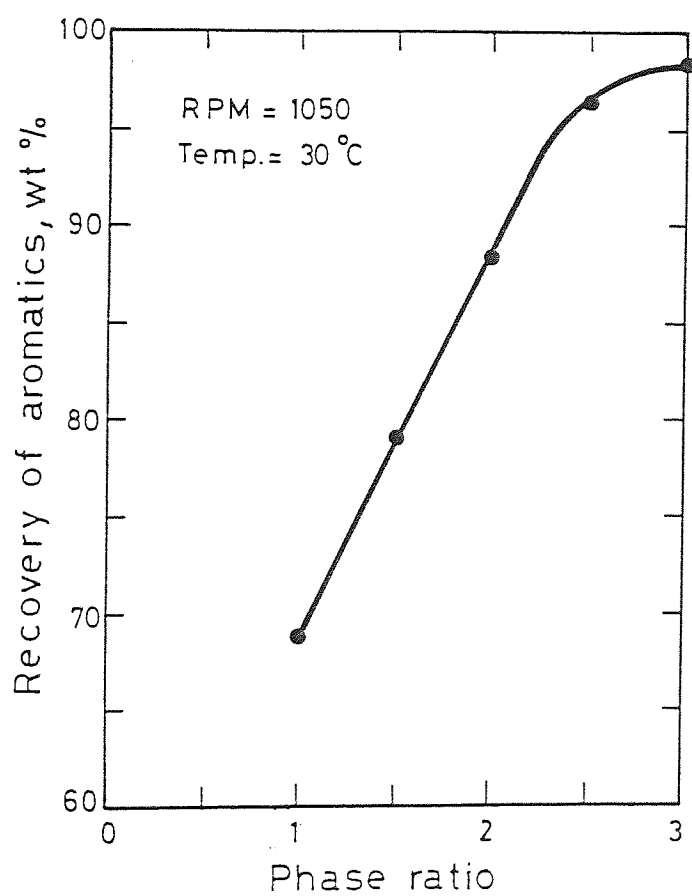


FIG. 9-8 TOTAL RECOVERY OF AROMATICS AS A FUNCTION OF PHASE RATIO.



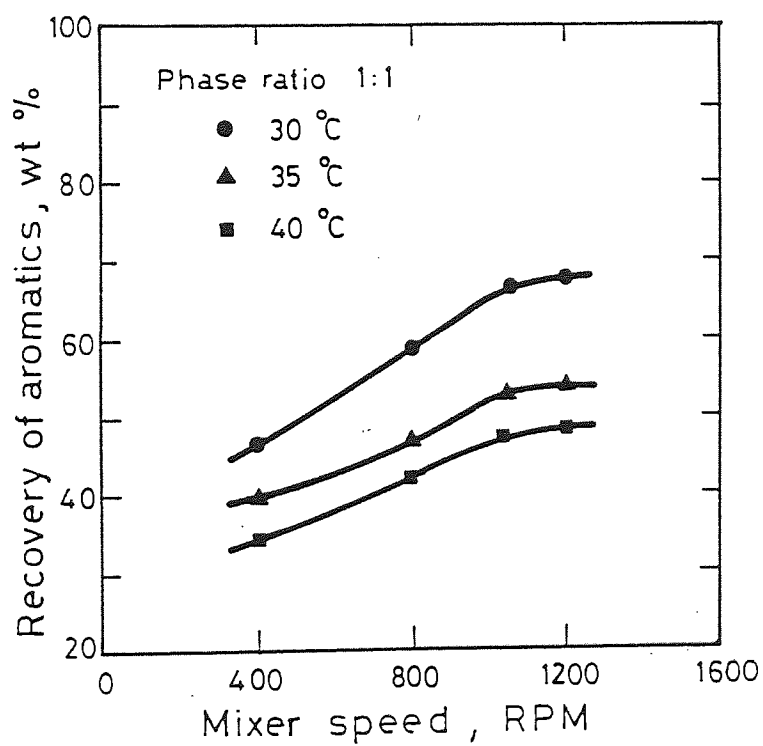


FIG. 9-9 EFFECT OF MIXER SPEED ON RECOVERY OF AROMATICS  
AT DIFFERENT TEMPERATURES

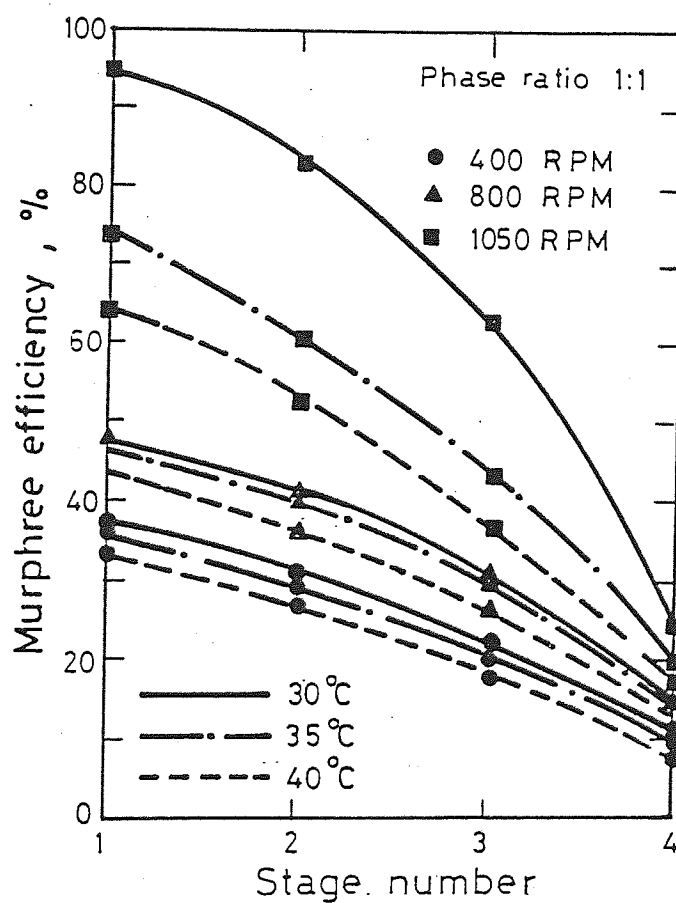


FIG. 9 -10 VARIATION OF STAGE EFFICIENCY WITH STAGE NO AT DIFFERENT TEMPERATURES AND MIXER SPEEDS

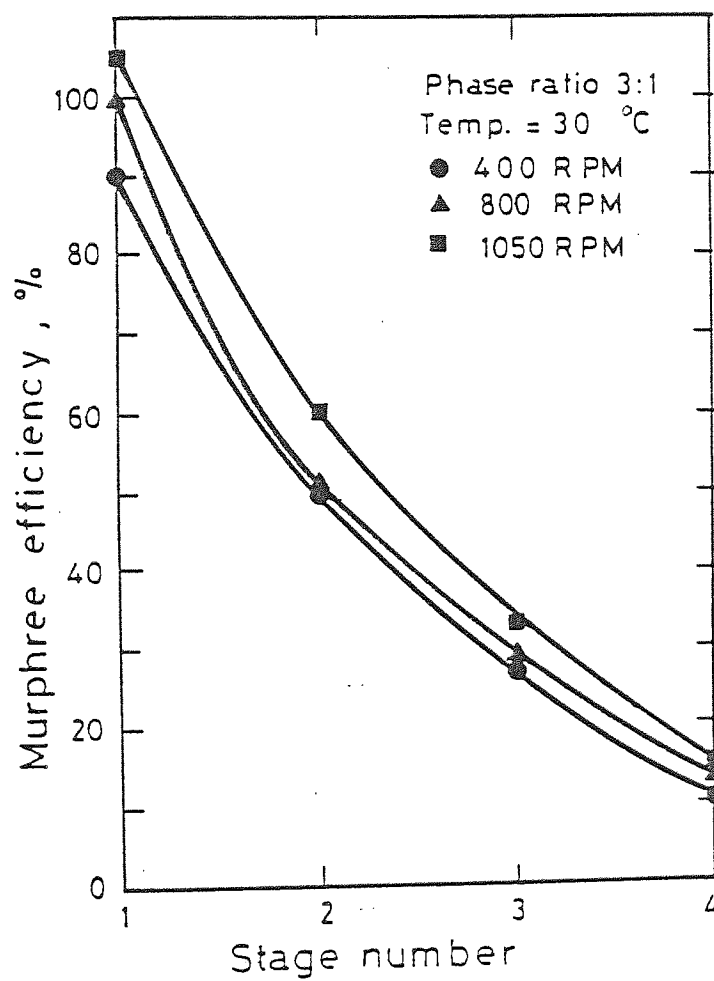


FIG. 9-11 VARIATION OF EFFICIENCY WITH STAGE NO AT  
PHASE RATIO 3:1

### 9.6.3 Calculation of Overall Mass Transfer Coefficient

Calculations of the overall mass transfer coefficient from correlations developed for single drops depend, as discussed in Chapter 4, upon the Reynolds Number. Droplet oscillation commences in regimes of flow with droplet Reynolds Number  $>200$ ; below this until  $Re < 10$  circulation predominates whereas at low values drops are stagnant.

For the purposes of calculation it was assumed that given the mixer geometry with small agitator-wall clearance, and the relatively high agitator speeds, the turbulence would be such that all drops would be in the oscillating mode. Furthermore the local velocity of each drop was equated to the agitator tip speed. Hence for example a typical Reynold's number would be

$$Re = \frac{d_p V \rho}{\mu} = \frac{0.06 \times 3.14 \times 4.85 \times 1050 \times 1.26}{60 \times 103} = 201 \quad 9.9$$

Furthermore recent work in agitated columns (188) has determined that best agreement is a generally obtained with oscillating drop correlations.

The correlation developed by Rose and Kintner for single oscillating drops (61), was applied to predict  $k_{do}$ . since this has been generally recommended (184).

$$k_{od} = 0.45 (D_d \omega)^{0.5} \quad 9.10$$

where

$$\omega = \frac{\sigma b}{r^3} \frac{n(n-1)(n+1)(n+2)}{(n+1)\rho_d + n\rho_c} \quad 9.11$$

and

$$n = 2 \text{ and } b = \frac{d_o^{0.225}}{1.242} \quad 9.12$$

$D_d$  is the diffusion coefficient in the dispersed phase, and  $\omega$  is the oscillation frequency.

Garner and Tayeban's (79) correlation was used for the continuous phase coefficient  $k_{co}$ .

$$\frac{k_{co}d_o}{D_c} = 50 + 0.0085 \text{ Re } Sc^{0.7} \quad 9.13$$

where  $D_c$  is the diffusion coefficient in the continuous phase.

The overall mass transfer coefficient for oscillating drops was estimated from equation 4.55.

The experimental overall mass transfer coefficients are compared with those calculated from single drop correlations in Table 9.2. Clearly there are considerable differences between the values, which can only be interpreted by the phenomena of coalescence-redispersion and associated surface renewal effects which predominate and because the times are short, so that interfacial resistance is not established.

For example a rate of interface generation of 1640 to 3280  $\text{m}^2/\text{m}^3$  has been reported. As has been pointed out

Phase Ratio		1:1				1.5:1			
Stage number		1	2	3	4	1	2	3	4
$K_{exp} \text{ s}^{-1}$		$2.25 \times 10^{-2}$	$1.76 \times 10^{-2}$	$1.6 \times 10^{-2}$	$1.7 \times 10^{-3}$	$3.9 \times 10^{-2}$	$2.2 \times 10^{-2}$	$1.8 \times 10^{-2}$	$1.6 \times 10^{-2}$
$K_{pred} \text{ s}^{-1}$		$1.5 \times 10^{-2}$	$8.8 \times 10^{-3}$	$6.6 \times 10^{-3}$	$5.7 \times 10^{-4}$	$2.0 \times 10^{-2}$	$1.1 \times 10^{-2}$	$7.3 \times 10^{-3}$	$6.3 \times 10^{-3}$
Phase Ratio		2:1				3:1			
Stage Number		1	2	3	4	1	2	3	4
$K_{exp} \text{ s}^{-1}$		$3.9 \times 10^{-2}$	$2.6 \times 10^{-2}$	$2.2 \times 10^{-2}$	$2. \times 10^{-2}$	$5.9 \times 10^{-2}$	$4.4 \times 10^{-2}$	$2.7 \times 10^{-2}$	$2.3 \times 10^{-2}$
$K_{pred} \text{ s}^{-1}$		$2.6 \times 10^{-2}$	$1.3 \times 10^{-2}$	$8.9 \times 10^{-3}$	$7.2 \times 10^{-3}$	$4.0 \times 10^{-2}$	$2.2 \times 10^{-2}$	$1.1 \times 10^{-2}$	$7.8 \times 10^{-3}$

Table 9.2 Predicted and Experimental Overall Mass Transfer Coefficients

by Al-Aswad (184) there is also some doubt regarding the use of  $d_{32}$ , rather than the distribution, in predicting mass transfer in agitated systems .

## Chapter 10

---

### EXTRACTION OF ACTUAL REFORMATE



## 10.1 Introduction

The purpose of reforming is to increase the Octane Number of a sulfur-free feed stock and thereby raise its value as motor gasoline blend stock. If benzene, toluene and xylene are removed for use as basic chemicals, the gasoline reservoir, or pool, has to be compensated for the loss of its more important high-octane components.

The crude oil received by the refiner contains a fraction in the  $65^{\circ}\text{C}$  -  $175^{\circ}\text{C}$  boiling range. It is separated by distillation, but is of little use in gasoline or as a chemical feed-stock because the concentration of aromatics, and thus the Octane Value, are low.

The process of reforming consists of passing a mixture of hydrogen and vaporized hydrocarbons over a catalyst containing platinum and rhenium at controlled temperatures and pressures. The Octane Number improvement results primarily from:

- i) The production of aromatics by dehydrogenation and by dehydrocyclization of paraffins;
- ii) Isomerization of paraffins;
- iii) Hydrocracking of heavy, low octane paraffins to light, higher octane paraffins.

Reforming reactions are typically carried out at a temperature between  $454^{\circ}\text{C}$ - $552^{\circ}\text{C}$  and at a pressure between 34 and  $150\text{kg}/\text{cm}^2$ . These reactions are predominantly endothermic. Therefore heat must be added to keep the reactions going. The heat of reaction is between 110 and 275 Kcal/kg of naphtha feed, depending

on the feed-stock and on the severity of operation. This heat is added by passing the stock through furnaces between the reactors.

Large volumes of hydrogen are circulated with the feed stock. This hydrogen, which is produced by the reforming reactions, plays an important part in the process because its presence helps to control the rate of formation of coke on the catalyst. A high recycle ratio helps to promote a low rate of coke laydown, and correspondingly a low rate of catalyst deactivation.

Reformats usually contain about 50% aromatics, almost half of which are xylenes and a quarter benzene. The nonaromatics proportion contains almost no naphthenes but upto 5% olefins.

## 10.2 Production of Aromatics

The aromatics cannot be separated from the non-aromatics by distillation. The major separation methods are extraction and extractive distillation.

If the heart-cut reformate contains appreciable nonaromatics, extraction may be necessary to prevent the accumulation of nonaromatics in the processing loop. Some isomerization processes are capable of cracking the paraffins but at the expense of additional hydrogen consumption.

The choice of extraction solvent and the advantages of sulfolane are discussed in Chapter 8.

The reformate used in this investigation was obtained from the Kuwait Oil Company (K.O.C.); the details of reformate composition are tabulated in Table 10.1 based upon the GLC analysis given in Appendix VI .

Table 10.1  
REFORMATE COMPOSITION

Component	Wt percent
Pentane	5.12
Hexane	8.81
Heptane	19.72
Octane	10.37
Benzene	1.58
Toluene	14.71
Xylenes	20.42
C - Benzene 3	15.47
C - Benzene 4	3.80

### 10.3 Parameters Investigated

The parameters investigated were similar to those for synthetic reformat as described in Chapter 9. This enabled a direct comparison to be made between the results. The presence of C<sub>9</sub>, C<sub>10</sub> aromatics, and C<sub>5</sub> paraffins in the actual reformat constituted the main difference. There were also differences in percentages of each component as between the actual and synthetic reformat, but this was inevitable given the normal variation in reformat composition even from one refinery (ie. within the 50% to 55% aromatics the variation in actual proportions of benzenes, toluenes, and xylenes is not controlled)

As described in Chapter 9 the agitator speed was set to 1050 rpm to obtain the optimum interfacial area without forming a haze. Consideration of the effect of temperature on the distribution coefficient (Figure 8.5 ), indicated that the maximum value was obtained at 30°C. Therefore a temperature of 30°C was maintained throughout the study. The phase ratios covered were in the range 0.5:1 to 3.25:1. At the start of each run, the cascade was filled with the two phases, as described previously, and the interface was adjusted to correspond with the midposition in the settler. Operation was then as described in Chapter 9 with a feed (dispersed) flowrate of 10 ml/min . Gas chromatography was used to analyze both raffinate and extract fractions for their chemical compositions.

#### 10.4 Results and Discussion

The recovery of aromatics in each stage was measured and is illustrated in Figure 10.1. The highest recovery, of about 99.5%; was achieved after stage four at a phase ratio of 3.25:1. The slight difference in the optimum phase ratio with that found when using the synthetic reformat is attributable to the difference in concentration of aromatics in the two feeds. The synthetic reformat used was 55% aromatics while the concentration of the aromatics in the actual reformat was 56%. Moreover as already explained there were differences in the concentration of each individual aromatics component. The composition of the actual reformat is shown in Table 10.1; by comparison the earlier synthetic reformat was taken as typical based upon reference (5). The component with the highest distribution coefficient (benzene) was present in smaller quantity in the actual than in the synthetic reformat.

Figure 10.2, shows that the recovery of aromatics increased with phase ratio to reach a maximum of 99.9% at 3.25:1. The percentage recovery of each individual aromatic component at the different phase ratios is shown in Figure 10.3. The percentage recoveries were in the order benzene > toluene > xylenes > and C<sub>3</sub>-benzene > C<sub>4</sub>-benzene. This is due to the distribution coefficient of benzene being greater than that of toluene, which is in turn greater than that of xylene as shown in Chapter 8.

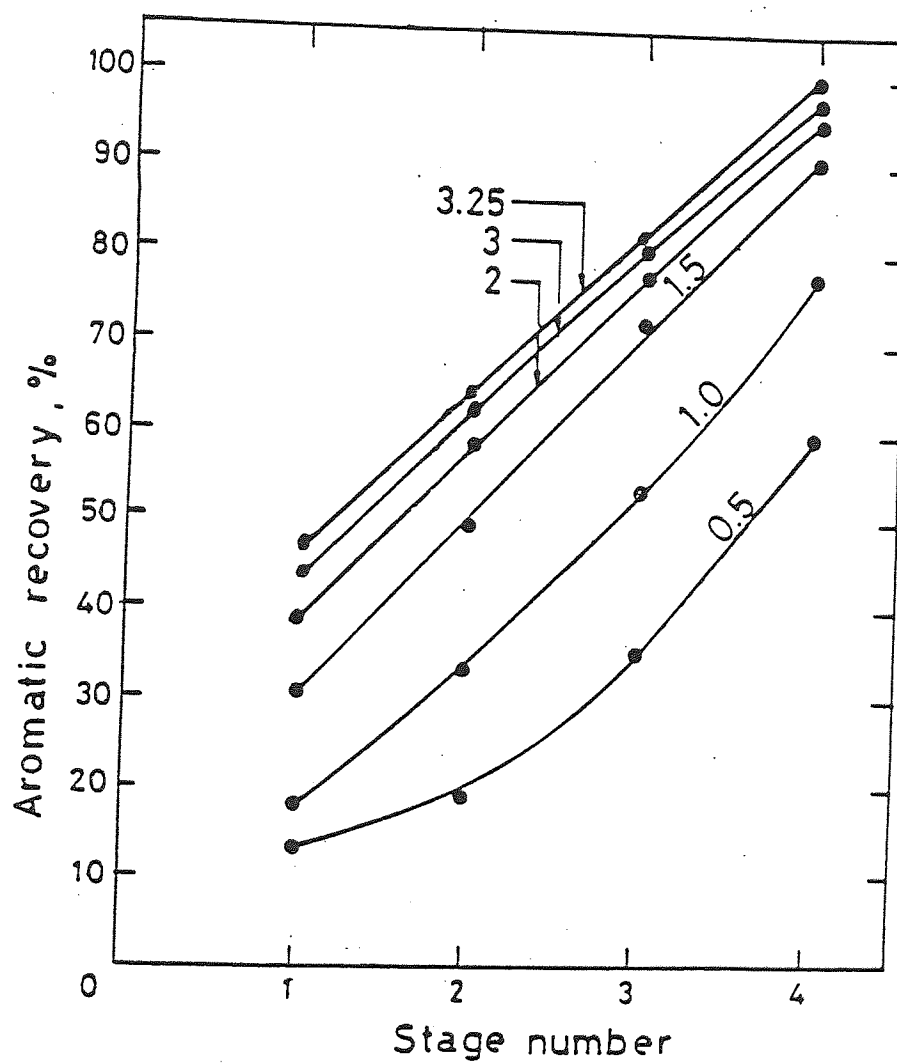


FIG. 10-1 PERCENTAGE AROMATIC RECOVERY VS STAGE NO  
AT DIFFERENT PHASE RATIOS.

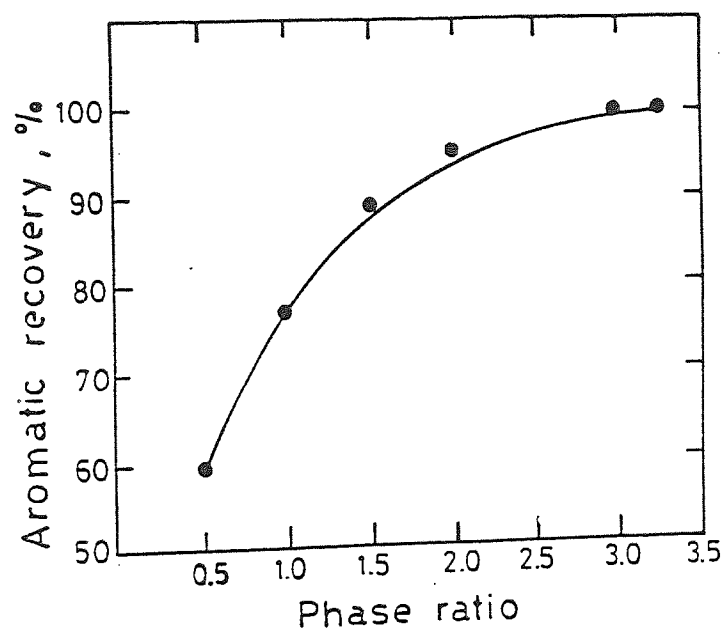


FIG. 10-2 PERCENTAGE RECOVERY OF AROMATICS VS PHASE RATIO

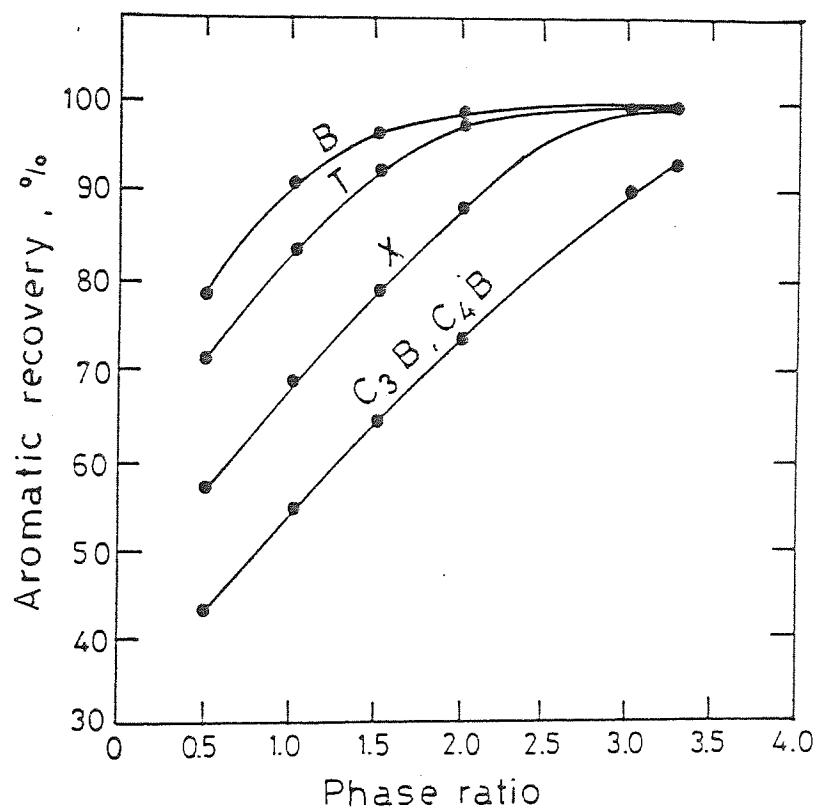


Fig 10.3 PERCENTAGE RECOVERY OF AROMATIC COMPONENTS VS PHASE RATIO.



As described previously hold-ups were again measured, in the presence of mass transfer only, by the rapid shut-off method. The drop sizes were measured using a graduated capillary tube inserted in the mixer and through which samples were withdrawn. As shown in Figure 10.4 for stage 4 the Sauter mean drop diameter  $d_{32}$  increased linearly with hold up. The range of drop sizes observed in the mixer was generally between 0.42 and 0.62 mm i.e comparable with those for the synthetic feed. The hold up range was between 0.125 and 0.193, and not directly comparable with earlier results because of the increased phase ratio .

The hold up was related to the corresponding flow rate of dispersed phase and is illustrated in Figure 10.5. This demonstrates the decrease in hold up with decreasing dispersed phase flow rate through the stages from four to one . The practical significance of this is that (other than with oversized settlers) the facility for dispersed phase-interface coalescence, i.e the settler size, would need to be 50% greater at the feed inlet end. Figure 10.6 illustrates the change of dispersed flowrate at each stage to exemplify this point.

The difference between the composition of synthetic and real reformat had some effect on diameter of drops; this is shown in Figure 10.7. and partly explains the variation in hold-up . Clearly in an industrial situation it would be important to cover the complete range of possible reformat compositions because of the dependence of mass transfer efficiency on  $d_{32}$  and  $X$  and of  $\Delta c$  on the distribution coefficient.

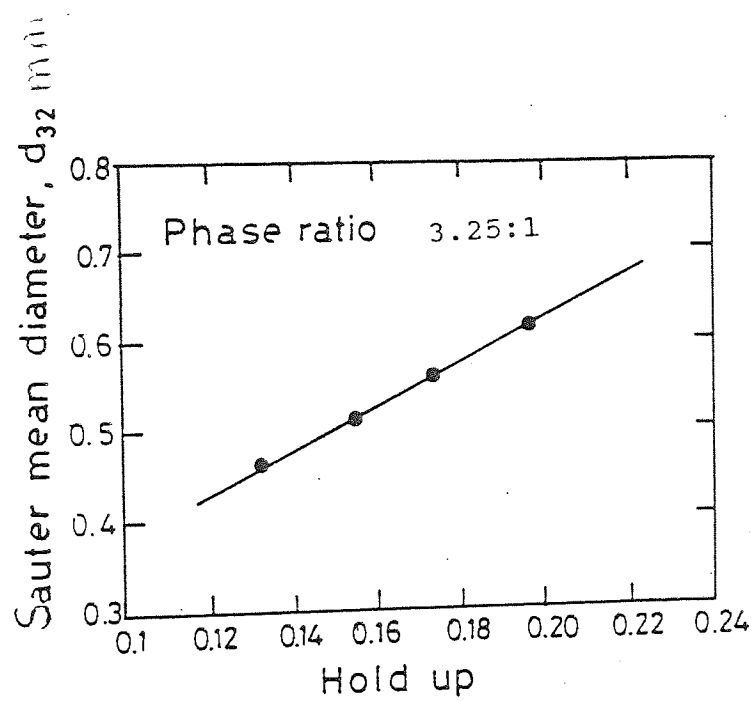


Fig 10.4 SAUTER MEAN DIAMETER  $d_{32}$  vs HOLD UP

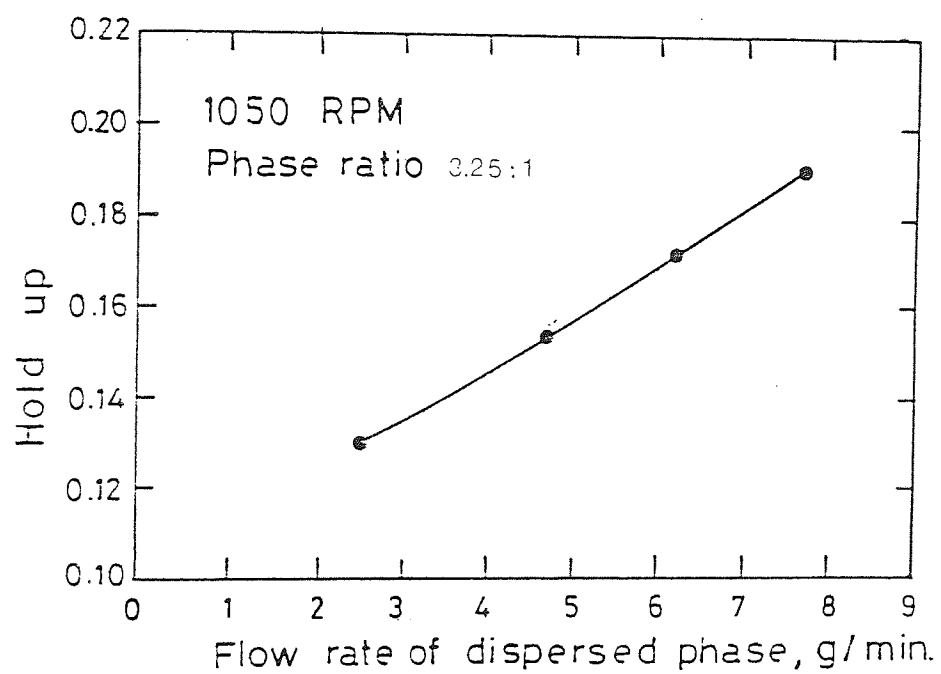


FIG. 10-5 HOLD UP VS FLOW RATE OF DISPERSED PHASE

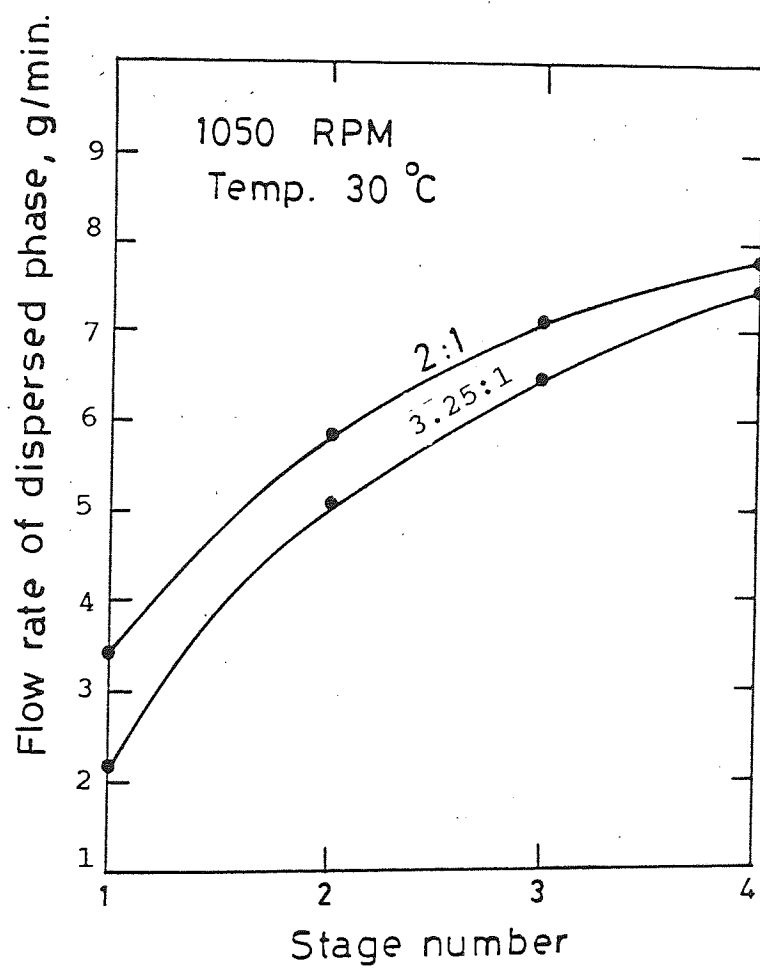
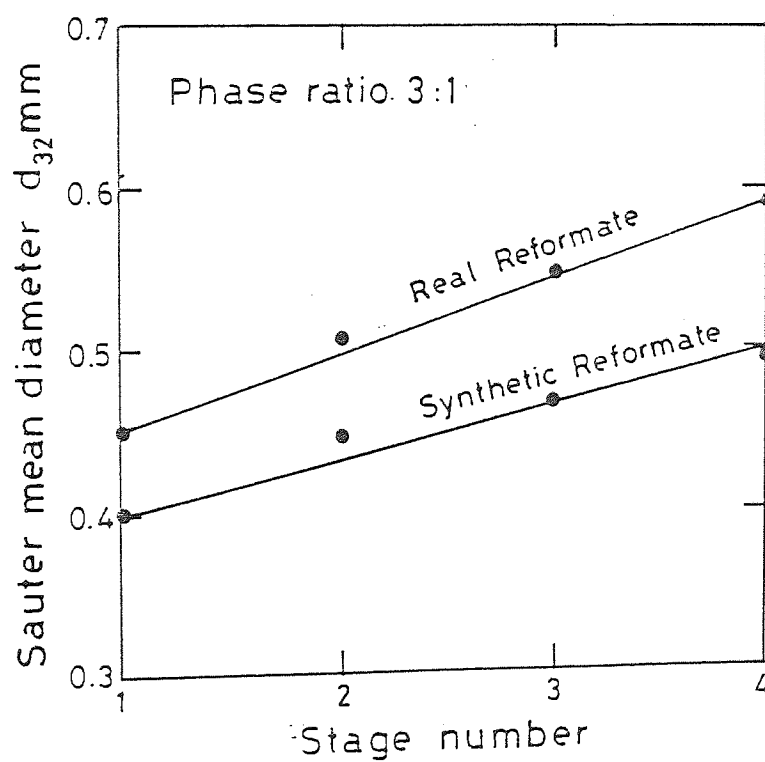


Fig 10.6 FLOW RATE of DISPERSED PHASE vs STAGE NUMBER



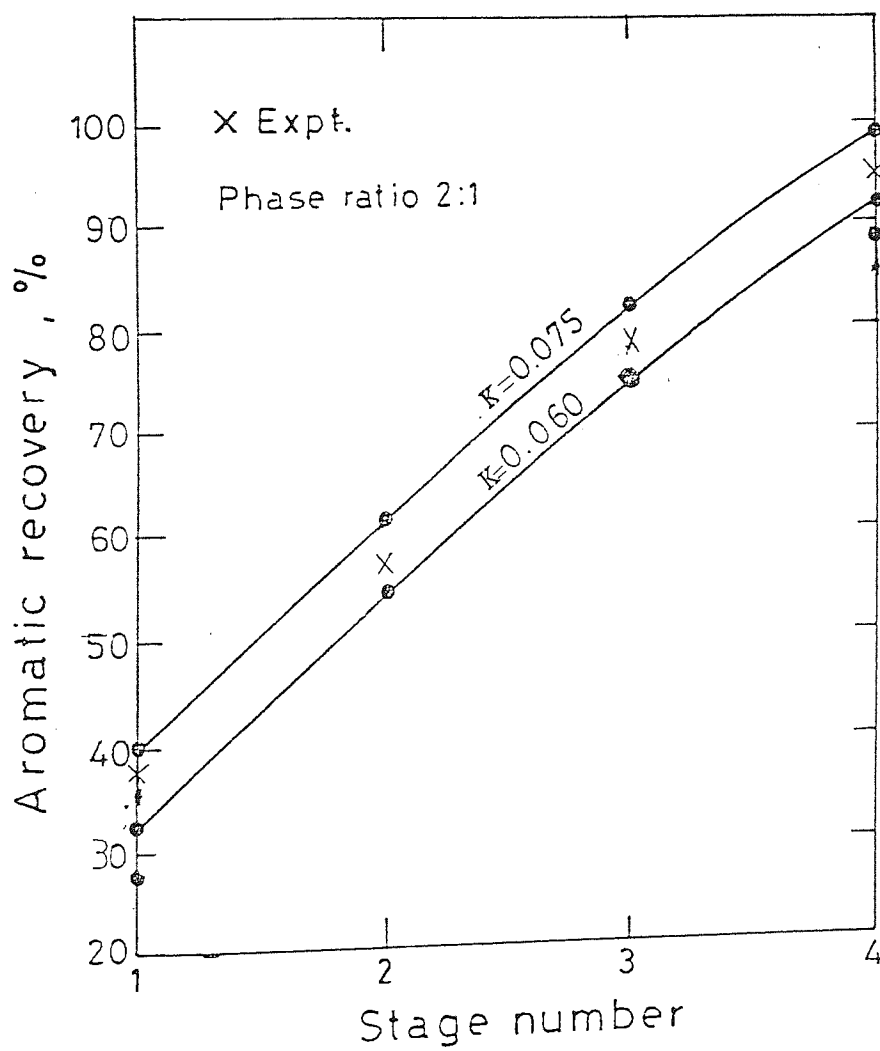
10-7 SAUTER MEAN DIAMETER  $d_{32}$  VS STAGE NO FOR REAL AND SYNTHETIC REFORMATE.

Prediction of overall mass transfer coefficient, in the way described in section 9.6.3 , was not possible with the actual reformat because the equilibria of the multicomponent system were not predictable .

#### 10.5 Mathematical Modelling Results

The detailed results obtained by applying Model No.3 in Chapter 7, are given in Appendix VII . The results are shown in Figures 10.8 and 10.9 together with the experimental results obtained from the previous Figures 10.1 and 10.2. Comparing these results it is clear that the overall mass transfer coefficient which would most-closely fit the experimental result ranges from  $0.06 \text{ sec}^{-1}$  to  $0.085 \text{ sec}^{-1}$  for the phase ratio 3:1, and from  $0.05 \text{ sec}^{-1}$  to  $0.075 \text{ sec}^{-1}$  for phase ratio 2:1. Interestingly these compare well with the experimentally determined coefficients for the synthetic reformat ( $0.06 \text{ sec}^{-1}$  at 3:1 and  $0.04 \text{ sec}^{-1}$  at 2:1).

The slight differences between the experimental and mathematical models results are probably attributable to the assumptions used in the model, especially those of linearity of the equilibrium relationship and constant phase flow rates throughout all the mixer-settler stages. However the reduction in overall coefficient with stage number is in agreement with experimental results .



10-8 EXPERIMENTAL AROMATIC RECOVERY VS MODEL RESULTS  
 AT PHASE RATIO (2:1).

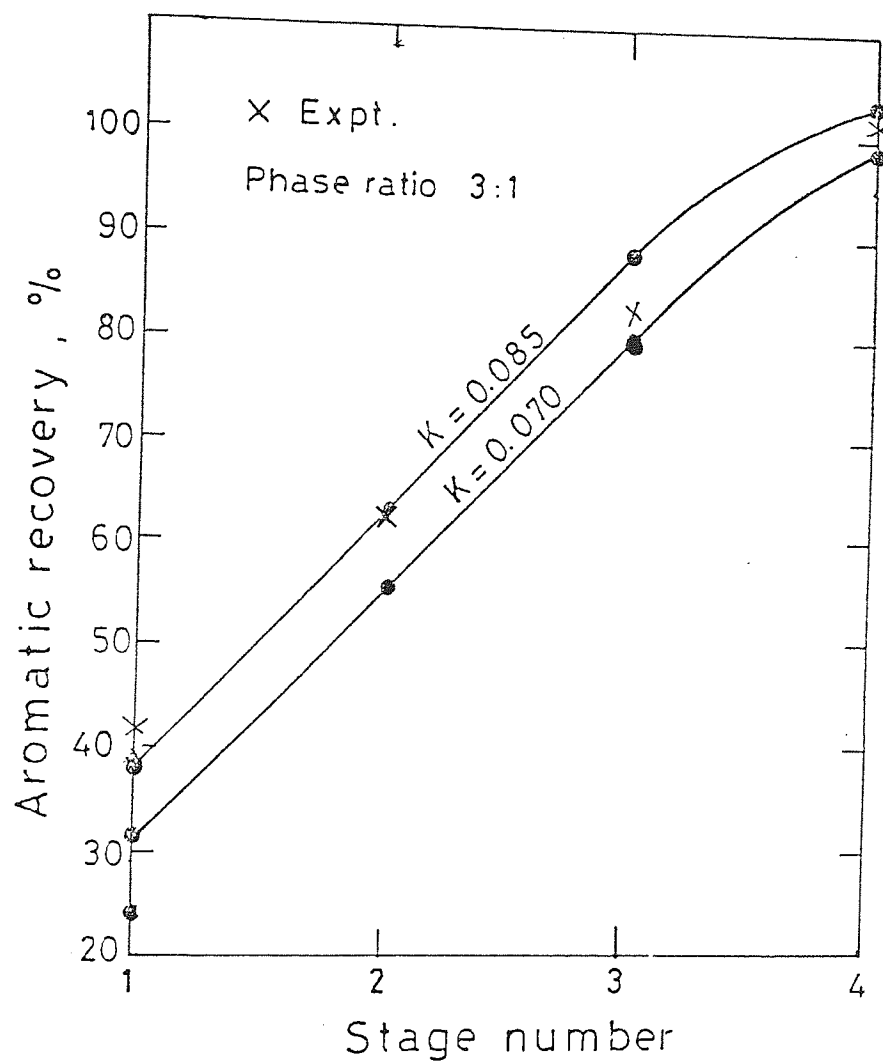


FIG. 10-9 EXPERIMENTAL AROMATIC RECOVERY VS MODEL  
RESULTS AT PHASE RATIO 3:1



## Chapter 11

---

### CONCLUSIONS AND RECOMMENDATIONS FOR FUTURE WORK

## 11.1 Conclusion

### 11.1.1 Sulfolane as a Solvent

As described in Chapter 2, a comparison of miscellaneous physical properties of available solvents with the corresponding properties of sulfolane shows that sulfolane is the best solvent to extract aromatics. Its specific gravity, viscosity, and interfacial tension are within the ranges which make for high extraction efficiency and volumetric capacity in extraction equipment .

Data were obtained in this study on the properties of sulfolane as an extractive agent of aromatic hydrocarbons from mixtures composed of aromatic and aliphatic hydrocarbons .The selectivity and the distribution coefficient did not have constant values over the complete heterogeneous area .

The selectivity of sulfolane decreased with an increase in temperature , since the heterogeneous area decreased with an increase in temperature . The best recovery of aromatics was achieved at a temperature of 30°C at which the distribution coefficient was the highest ( Chapter 10 ) .

### 11.1.2 Mixer-Settler Characteristics

#### 11.1.2.1 General

As would be expected, because of the range of interfacial tension (20-29 dyne/cm) the mixer settler cascade worked well e.g. with stage efficiencies of about 100% . Operation was stable and startup easy except at the highest phase ratio of 7:1 ( solvent:feed ) when injection of the dispersed phase was difficult .No

secondary haze formation occurred at reasonable levels of agitation (  $<1050$  rpm ) . However the ratio of settler to mixer volume was 50:1, so a realistic test for the settler arrangement was not possible .

The work confirmed that for systems of reasonably high interfacial tension and significant density difference between the phases ( e.g. 0.56 ) a mixer-settler cascade with simple gravity settlers is a viable alternative to continuous differential columns .

#### 11.1.2.2 BTX Extraction in a Mixer-Settler Cascade

As summarized in Chapter 9 , BTX extraction was efficiently accomplished in the mixer-settler cascade at a solvent to feed ratio of approximately 3:1 . By comparison the ratio used commercially in an RDC is 10:1 (5) . Therefore, despite the increased inventory associated with interstage gravity settling , which was not minimized in the present study, a mixer-settler cascade is technically a viable alternative for BTX extraction .

Under the optimum conditions used in the present work  $< 5$  stages would be adequate .

#### 11.1.3 Prediction and Modelling of Mass Transfer

##### Performance

Comparison of the experimental overall mass transfer coefficients with predicted coefficients (based upon the correlations in Chapter 9 ) for the synthetic reformat showed that the experimentally-determined values were always greater by a factor of 1.5 to 3.1 depending on the stage number i.e. the prevailing hold-up . Since the predicted values were calculated on

the assumption that all the drops were in the oscillating regime ( because of the relatively large agitator diameter and small agitator to wall clearance ) the enhanced mass transfer in practice can only be explained by a coalescence-redispersion mechanism (175).

Because the real reformat comprised many components it was difficult to predict the overall mass transfer coefficient from theory or to evaluate  $\Delta C$  to calculate experimental values . The model applied in this case involved prediction by assuming a value and checking the concentration profile by trial and error until a match was obtained with the experimental data . These predictions indicated that the overall mass transfer coefficient was in the range of  $0.05 \text{ sec}^{-1}$  to  $0.075 \text{ sec}^{-1}$  for a phase ratio of 2:1 , and  $0.06 \text{ sec}^{-1}$  to  $0.085 \text{ sec}^{-1}$  for a phase ratio of 3.25:1 .

By comparison with the synthetic reformat the experimentally-determined overall mass transfer coefficients under similar operating conditions were between  $0.02 \text{ sec}^{-1}$  ,  $0.04 \text{ sec}^{-1}$  at in phase ratio of 2:1 , and  $0.03 \text{ sec}^{-1}$  to  $0.06 \text{ sec}^{-1}$  at a phase ratio of 3:1, which considering the circumstances, was good agreement.

However whilst the predicted values are therefore of the right order of magnitude, the limitations imposed in the use of the model were insertion of a single value of overall coefficient whereas in fact it would be expected to vary between stages, because  $m$  and the physical properties vary . Therefore a good fit was not possible between the predicted and actual concentration profiles .

Despite the differences between the results for the synthetic and actual reformates, the simplification of basing the main part of the study on the synthetic reformat appears justified . It enabled a comparison with theory which is not possible with a complex multi-component feed .Moreover it yielded phase equilibria of general application.

#### 11.2 Recommendations for Future Work

The following areas of further work would logically follow-on from the present investigation ;

1. An investigation could be made into the increase in selectivity of sulfolane achievable by the addition of water as antisolvent . The selectivity is thus improved by increasing the  $X_{AA}/X_{AB}$  ratio rather than by attempting to improve  $m$  ,the distribution coefficient of solute, which may actually be lowered. The dosage of water in a solvent for a particular feed-stock can be adjusted in such a way that maximum selectivity is obtained for the required recovery of the aromatics. However, the use of water in the solvent recovery step is disadvantageous since more thermalenergy is required, and, in addition, water can cause corrosion.

An alternative approach would be to use a combination of solvents so as to balance the selectivity and solvency functions. Such a combination (such as NMP and DEG ) of solvents has the advantage of lower consumption of energy, and lower solvent: feed ratio, with consequent reduction in the dimensions of the extractor.

2. An economic study would be useful into the application of a mixer settler cascade instead of an RDC for the Sulfolane process. Whilst the processes for solvent and solute recovery would be identical, the variables to be considered include the solvent: feed ratio and the power consumption during agitation and interstage pumping.

3. An investigation could be made of any limitations on settler design, e.g. employing a standard gravity settler with a settler:mixer ratio of 1:5, and of the improvement obtainable with coalescence aids .

4. Although the laboratory mixer-settler used had a high efficiency, it had a low volumetric throughput. Therefore for further work the design of this mixer settler should be improved. This could be done by application of centrifugal force to the settler . This yields many times the forces available under normal gravity conditions thereby enhancing the separation. By rapid rotation of the entire mass of liquids involved in extraction, as in a centrifuge , the pressure

head available to force the liquids through the equipment could be greatly increased. This results in much higher liquid throughput with a shorter time of contact between the liquids. Such centrifugal extractor require smaller floor space and headroom compared to conventional units of equal capacity.

5. A thermodynamic package based on UNIFAC can be developed, and introduced into the model given in Chapter 7 to handle complex petroleum fractions .The object

would be to evaluate distribution coefficients for each cut . An investigation would also be useful to improve prediction near the plait point by improving the interaction parameters of UNIFAC .

6. Based on this study a computer package could be developed to evaluate the performance of a mixer-settler in the extraction of any particular system of industrial importance in which  $m$  varies with concentration . The model used in this study applied the experimentally-determined overall mass transfer coefficient to determine the rate of mass transfer in each stage. However, a useful approach would be to introduce UNIFAC to predict the distribution coefficient in each stage and hence , using equation 4-1 ,the overall mass transfer coefficient ,which otherwise requires experimental determination .Conversion of the model to a basis of solute-free flowrates would also avoid the limitation associated with unpredictable variation of flowrates with stage number.

## APPENDICES



## APPENDIX (I)

### Refractive Indices, and Densities of Hydrocarbon Components

	REFRACTIVE INDEX	DENSITY (g/ml)
N-HEXANE	1.372	0.65
N-HEPTANE	1.385	0.68
N-OCTANE	1.395	0.70
BENZENE	1.498	0.87
TOLUENE	1.494	0.86
XYLENE	1.493	0.86

APPENDIX (II)  
UNIFAC Computer Program

U SAID.UNIFAC  
 16R10. SAT-11/16/85-11:31:06-(52,53)

```

1:C   PROGRAM UNIFAC
2:C
3:C   *****
4:C
5:C   PROGRAM UNIFAC (INPUT,OUTPUT,TAPES=INPUT,TAPES=OUTPUT)
6:C
7:C   PURPOSE
8:C     CALCULATE ESTIMATES OF ACTIVITY COEFFICIENTS IN NON-
9:C     ELECTROLYTE LIQUID MIXTURES.
10:C
11:C   METHOD
12:C     COMBINES THE SOLUTION-OF-FUNCTIONAL-GROUPS CONCEPT WITH
13:C     A MODEL FOR ACTIVITY COEFFICIENTS BASED ON AN EXTENSION
14:C     OF THE QUASI-CHEMICAL THEORY OF LIQUID MIXTURES (UNIQUAC).
15:C
16:C   REFERENCES
17:C     (1)FREDENSLUND,A.,JONES,R.L.,PRAUSNITZ,J.M./AICHE J.
18:C        21,1086(1975).
19:C     (2)ABRAMS,D.S.,PRAUSNITZ,D.M./AICHE J.21,116(1975).
20:C     (3)SKJOLD-JORGENSEN,S.,KOLEB,F.,OMERLING,J.,PASMUSSEN,P..
21:C        I.E.C.PROC.DES.DEV.,10(4),714(1979)
22:C     (4)ZARKARIAN,J.A.,ANDERSON,F.E.,BOYD,J.A.,PRAUSNITZ,J.M.,
23:C        I.E.C.PROC.DES.DEV.,18(4),657(1979)
24:C
25:C   PROGRAMED BY R.L.JONES MAY 75.
26:C   REVISIONS AND MODIFICATIONS BY T.F.ANDERSON OCT 76.
27:C   FURTHER REVISIONS AND MODIFICATIONS BY F.E. ANDERSON NOV. 79
28:C
29:C   *****
30:C
31:C   DIMENSION MOL(5,11),XMOL(11),COMLN(11),RESLN(11),ALGAC(11),
32:C      1 ACTCF(11),IDGP(6,11),NOGP(6,11),NGMOL(11),AL(11),
33:C      2 RI(11),GI(11),QGPI(6,11),QGP(11),PARAM(11,11),ID(11),
34:C      3 GSUM(11),G(11),TNAM(3,11)
35:C   DIMENSION GNAM(3,81),QQ(81),RP(81),PARAM(42,42),NKTAB(81),
36:C      * KODE(42,42)
37:C   dimension xf(7),xe(7),xks(7),xrn(7),actfr(7),actfe(7),xr(7)
38:C   DATA LNK /
39:C
40:C   NOTE: DIMENSION OF KODE AND PARAM HAVE BEEN SET TO 42X42
41:C   BECAUSE OF INPUT BY AN IMPLIED DO-LOOP AND FORMAT
42:C   # 4003.
43:C
44:C   LUI=5
45:C   LUO=6
46:C   LUD=10
47:C   nnn=0.0
48:C   mmm=0
49:C   phi=0.1
50:C   delta=0.10
51:C
52:C   READ DATA BANK.
53:C

```

```

54:      READ (LUD,4001) NMG,NSG
55:C      READ (LUD,4002) (QQ(I),RR(I),NKTAB(I),GNAM(I),I=1,NSG)
56:      READ (LUD,4002) (QQ(I),RR(I),NKTAB(I),GNAM(J,I),J=1,3),I=1,NSG)
57:C      WRITE (6,1)
58:C      1 FORMAT ('1')
59:C      WRITE (6,*) NSG
60:C      DO 10 I=1,NSG
61:C      WRITE (6,5) I,QQ(I),RR(I),NKTAB(I),GNAM(J,I),J=1,3)
62:C      5 FORMAT (15,5X,2F10.4,11D,10X,PA4,A2)
63:C      10 CONTINUE
64:C      WRITE (6,1)
65:C      WRITE (6,*) NMG
66:C      DO 15 I=1,NMG
67:C      WRITE (6,*) I
68:C      READ (LUD,4003) (KODL(I,J),PARAM(I,J),J=1,NMG)
69:C      DO 14 J=1,NMG
70:C      14 WRITE (6,*) J,KODL(I,J),PARAM(I,J)
71:      15 CONTINUE
72: 4001 FORMAT (D12)
73: 4002 FORMAT (3(2F7.4,12,A10),2X)
74: 4002 FORMAT (3(2F7.4,12,2A4,A2),2X)
75: 4003 FORMAT (7(11,F9.2),10X)
76:C
77:C      READ COMPONENTS AND NUMBER OF GROUPS PER COMPONENT.
78:C
79:C      LNK = 10H
80:      25 J = 1
81:C      30 READ (5,1001) MOL(1,J),MOL(2,J),NGMOL(J)
82:      30 READ (5,1001) NGMOL(J),MOL(K,J),K=1,5)
83:      IF (MOL(1,J).EQ.LNK) GO TO 35
84:      J = J + 1
85:      GO TO 30
86:      35 IF (J.EQ.1) STOP
87:      NSPS = J - 1
88:      DO 40 J=1,NSPS
89:      NN = NGMOL(J)
90:C      40 READ (5,1002) (NGGP(I,J),IDGP(I,J),I=1,NN)
91:      40 READ (5,*) (NGGP(I,J),IDGP(I,J),I=1,NN)
92:      NGPT = 0
93:      DO 60 J=1,NSPS
94:      NN = NGMOL(J)
95:      DO 55 I=1,NN
96:      IF (NGPT.EQ.0) GO TO 50
97:      DO 45 K=1,NGPT
98:      IF (IDGP(I,J).NE.ID(K)) GO TO 45
99:      IDGP(I,J) = K
100:      GO TO 55
101:      45 CONTINUE
102:      50 NGPT = NGPT + 1
103:      ID(NGPT) = IDGP(I,J)
104:      IDGP(I,J) = NGPT
105:      55 CONTINUE
106:      60 CONTINUE
107:C
108:C      PRINT SUMMARY OF INPUT DATA.
109:C
110:      WRITE (6,2001)

```

```

111:      DO 62 J=1,NSPS
112:C      WRITE (6,2002) MOL(1,J),MOL(2,J)
113:      WRITE (6,2002) (MOL(K,J),K=1,5)
114:      K = NGMOL(J)
115:      DO 61 I=1,K
116:      L = LIDGP(I,J)
117:      L = ID(L)
118:      M = NKTAB(L)
119:      NUM = NOCP(I,J)
120:C      61 WRITE (6,2003) GNAM(L),M,L,NUM,GQ(L),PR(L)
121:      61 WRITE (6,2003) (GNAM(LL,L),LL=1,3),M,L,NUM,GQ(L),PR(L)
122:      62 CONTINUE
123:C
124:C      READ TEMPERATURE AND NUMBER OF MIXTURES TO BE CALCULATED.
125:C
126:C      63 READ (5,1003) TEMP,NMIX
127:      63 READ (5,*) TEMP,NMIX
128:      IF (NMIX.EQ.0) NMIX = 1
129:      IF (TEMP.LT.200.) GO TO 25
130:      DO 65 I=1,NGPT
131:      K = ID(I)
132:      K = NKTAB(K)
133:      DO 65 J=1,NGPT
134:      L = ID(J)
135:      L = NKTAL(L)
136:      IF (L.EQ.K) GO TO 65
137:      IF (KODE(K,L).EQ.0) GO TO 64
138:      WRITE (6,2009)
139:      IF (KODE(K,L).EQ.1) WRITE (6,2010) K,L,ID(I),ID(J)
140:      IF (KODE(K,L).EQ.2) WRITE (6,2011) K,L,ID(I),ID(J)
141:      IF (KODE(K,L).EQ.3) WRITE (6,2012) K,L,ID(I),ID(J)
142:      64 CONTINUE
143:      IF (ABS(PARAM(K,L)).GT.1.E-3) GO TO 65
144:      WRITE (6,3001) K,L
145:      3001 FORMAT (1X,'INTERACTION PARAMETER FOR THE ',12,'-',12,
146:      1 ' NOT AVAILABLE')
147:      STOP
148:      65 PARAM(I,J) = EXP(-PARAM(K,L)/TEMP)
149:C
150:C      PRINT GROUP INTERACTION PARAMETER DATA.
151:C
152:      DO 70 I=1,NGPT
153:      K = ID(I)
154:      DO 70 J=1,3
155:C      70 TNAM(I) = GNAM(K)
156:      70 TNAM(J,I)=GNAM(J,K)
157:      WRITE (6,2004) NMIX,TEMP
158:C      WRITE (6,2005) (TNAM(I),I=1,NGPT)
159:      WRITE (6,2005) ((TNAM(J,I),J=1,3),I=1,NGPT)
160:      DO 75 I=1,NGPT
161:C      75 WRITE (6,2006) TNAM(I), (PARAM(I,J),J=1,NGPT)
162:      75 WRITE (6,2006) (TNAM(J,I),J=1,3), (PARAM(I,J),J=1,NGPT)
163:      222 nnn=nnn+1
164:C
165:C      READ SET OF COMPOSITIONS.
166:C
167:      DO 170 II=1,NMIX

```

```

168:      if(nnn.eq.1)then
169:C      READ (5,1004) (XMOL(J),J=1,NSPS)
170:      READ (5,*) (XMOL(J),J=1,NSPS)
171:      else
172:      read (5,*) (xf(i),i=1,7)
173:      do 112 I=1,7
174:      xr(I)=(xf(I)-phi*xmol(I))/(1-phi)
175:      xmol(I)=xr(I)
176: 112 continue
177:      endif
178:C
179:C      COMPUTE COMBINATORIAL PORTION AND RELATED SUMS.
180:C
181: 333 mmm=mmm+1
182:      RSUM = 0.
183:      QSUM = 0.
184:      DO 80 I=1,NGPT
185: 80  QGP(I) = 0.
186:      DO 95 J=1,NSPS
187:      RI(J) = 0.
188:      QI(J) = 0.
189:      K = NGMOL(J)
190:      DO 85 I=1,K
191:      A = NOGP(I,J)
192:      L = IDGP(I,J)
193:      M = ID(L)
194:      RI(J) = RI(J) + A*RR(M)
195:      QI(J) = QI(J) + A*QG(M)
196:      QGPI(I,J) = A*QG(M)
197: 85  QGP(L) = QGP(L) + QGPI(I,J)*XMOL(J)
198:      RSUM = RSUM + RI(J)*XMOL(J)
199:      QSUM = QSUM + QI(J)*XMOL(J)
200:      DO 90 I=1,K
201: 90  QGPI(I,J) = QGPI(I,J)/QI(J)
202: 95  CONTINUE
203:      DO 100 I=1,NGPT
204: 100 QGP(I) = QGP(I)/QSUM
205:      SUML = 0.
206:      DO 105 J=1,NSPS
207:      AL(J) = 5.*(RI(J) - QI(J)) - RI(J) + 1.
208: 105 SUML = SUML + AL(J)*XMOL(J)
209:      DO 120 J=1,NSPS
210:      CON1 = RI(J)/RSUM
211:      CON2 = QI(J)/QSUM
212: 120 COMLN(J) = ALOG(CON1) + 5.*QI(J)*ALOG(CON2/CON1)
213:      + AL(J) - CON1*SUML
214:C
215:C      COMPUTE RESIDUAL PORTION.
216:C
217:      DO 125 I=1,NGPT
218:      GSUM(I) = 0.
219:      DO 125 K=1,NGPT
220: 125 GSUM(I) = GSUM(I) + PARM(K,I)*QGP(K)
221:      DO 135 I=1,NGPT
222:      SUM = 0.
223:      DO 130 K=1,NGPT
224: 130 SUM = SUM + QGP(K)*PARM(I,K)/GSUM(K)

```

```

225: 135 G(I) = 1. - ALOG(GSUM(I)) - SUM
226: DO 155 J=1,NSPS
227:   RESLN(J) = 0.
228:   K = NGMOL(J)
229:   DO 140 I=1,K
230:     M = IDGP(I,J)
231:     GSUM(I) = 0.
232:     DO 140 N=1,K
233:       L = IDGP(N,J)
234: 140 GSUM(I) = GSUM(I) + PARM(L,M)*QGPI(N,J)
235:     DO 150 I=1,K
236:       SUM = 0.
237:       M = IDGP(I,J)
238:       DO 145 N=1,K
239:         L = IDGP(N,J)
240: 145 SUM = SUM + QGPI(N,J)*PARM(M,L)/GSUM(N)
241:       JJ = ID(M)
242:       CONST = FLOAT(NGGP(I,J))*QG(JJ)*(G(M) - (1.-ALOG(GSUM(I))-SUM))
243: 150 RESLN(J) = RESLN(J) + CONST
244:       ALGAC(J) = COMLN(J) + RESLN(J)
245: 155 ACTCF(J) = EXP(ALGAC(J))
246:       if(mmm.eq.1)then
247:         do 111 j=1,7
248:           actfe(j)=actcf(j)
249: 111 continue
250:         else
251:           do 113 j=1,7
252:             actfr(j)=actcf(j)
253: 113 continue
254:           endif
255:           if(nnn.eq.1)go to 222
256:           if(mmm.eq.1)then
257:             do 216 i=1,7
258:               xr(i)=(xf(i)-phi*xr(i))/(1.-phi)
259:               xmol(i)=xr(i)
260: 216 continue
261:             go to 333
262:             endif
263:             sum1=0
264:             do 114 i=1,7
265:               xks(i)=actfr(i)/actfe(i)
266:               xrn(i)=xf(i)/(1+phi*(xks(i)-1.))
267:               sum1=sum1+(xr(i)-xrn(i))*2
268: 114 continue
269:             if(sum1.gt.10e-8)then
270:               do 115 i=1,7
271:                 xe(i)=xks(i)*xrn(i)
272:                 xmol(i)=xe(i)
273: 115 continue
274:               mmm=0
275:               go to 333
276:               endif
277:               sum2=0
278:               do 117 i=1,7
279:                 sum2=sum2+xrn(i)
280: 117 continue
281:               write(c,*)phi,sum2

```



```

282:      if(abs(sum2-1.).gt.1(e-5))then
283:      phi=phi+delta
284:      do 118 i=1,7
285:      xmol(i)=xe(i)
286: 118 continue
287:      mmm=0
288:      go to 333
289:      endif
290:      do 119 i=1,7
291:      write(6,*)xf(i),xr(i),xe(i)
292: 119 continue
293:      write(6,*)xf(i),xr(i),xe(i)
294:c
295:c      PRINT RESULTS OF MIXTURE CALCULATIONS.
296:c
297:      WRITE (6,2007)
298:      DO 160 J=1,NSPS
299:c 160 WRITE (6,2008) MOL(1,J),MOL(2,J),XMOL(J),ALGAC(J),ACTCF(J)
300: 160 WRITE (6,2008) (MOL(K,J),K=1,5),XMOL(J),ALGAC(J),ACTCF(J)
301: 170 CONTINUE
302:      GO TO 63
303:c
304:c 999 CALL EXIT
305:      STOP
306:c
307:c1001 FORMAT (2A10,I2)
308: 1001 FORMAT (I2,5A4)
309:c1002 FORMAT (16I5)
310:c1003 FORMAT (F10.0,I5)
311:c1004 FORMAT (EF10.0)
312: 2001 FORMAT (1H1,"UNIFAC CALCULATION OF ACTIVITY COEFFICIENTS")
313:c2002 FORMAT (1H-,2A10//EX,"GROUP",4X,"PRI",2X,"SEC",3X,"NUM",7X,
314: 2002 FORMAT (1H0,5A4//EX,"GROUP",4X,"PRI",2X,"SEC",3X,"NUM",7X,
315: 1 "q",9X,"R"/)
316:c2003 FORMAT (6X,A10,"(",I2,")",1X,"(",I2,")",4X,I2,4X,F6.4,4X,F6.4)
317: 2003 FORMAT (6X,2A4,A2,"(",I2,")",1X,"(",I2,")",4X,I2,4X,F6.4,4X,F6.4)
318: 2004 FORMAT (1H1,"ACTIVITY COEFFICIENTS FOR ",I2," COMPOSITIONS AT ",
319: 1 F6.2," DEGREES KELVIN"/1X,"PARAMETERS"/)
320:c2005 FORMAT (14X,11A10)
321: 2005 FORMAT (14X,11(2A4,A2))
322:c2006 FORMAT (/1X,A10,11F10.5)
323: 2006 FORMAT (/1X,2A4,A2,11F10.5)
324: 2007 FORMAT (1H1,5X,"COMPONENT",9X,"MOLE FRAC",2X,"LOG ACTCF",4X,
325: 1 "ACTCF"/)
326:c2008 FORMAT(1X,2A10,4X,F7.4,4X,F7.5,4X,F7.4)
327: 2008 FORMAT(1X,5A4,4X,F7.4,4X,F7.5,4X,F7.4)
328: 2009 FORMAT(/,5X,"...PARAMETER BACKGROUND NOTE")
329: 2010 FORMAT(7X,"PARAMETERS FOR THE ",I2,"-",I2," INTERACTION HAVE BEEN
330: 1OBTAINED FROM METHANOL DATA, SEE REF. 3",/,
331: 27X,"THESE PARAMETERS ARE USED FOR THE ",I2,"-",I2," SECONDARY GROU
332: 3P INTERACTION",/)
333: 2011 FORMAT(7X,"PARAMETERS FOR THE ",I2,"-",I2," INTERACTION MAY NOT BE
334: 1RELIABLE IN WHOLE CONCENTRATION RANGE, SEE REF. 3",/,
335: 27X,"THESE PARAMETERS ARE USED FOR THE ",I2,"-",I2," SECONDARY GROU
336: 3P INTERACTION",/)
337: 2012 FORMAT(7X,"PARAMETERS FOR THE ",I2,"-",I2," INTERACTION WERE OBTAI
338: 1NED FROM GAS CHROMATOGRAPHIC DATA, SEE REF. 4",/,

```

```
339: 27X, THESE PARAMETERS ARE USED FOR THE ",12,"-","12," SECONDARY GROU
340: 3P INTERACTION",/)
341: END
EOF:341
0:
END ED. LINES:341 ASCII
KSC41A=SAID(1).UNIFAC(53)

&ASG,T PUNIFAC.
FACILITY WARNING 10000000000
```

## APPENDIX (III)

### Diffusivities

# Diffusivities of dispersed and continuous phase

Phase Ratio					1:1					1.5:1				
Stage number		1	2		3	4	Stage number		1	.2	3	4		
$D_{Ar.nAr}$		$9.9 \times 10^{-7}$	$3.9 \times 10^{-7}$		$2.0 \times 10^{-7}$	$1.6 \times 10^{-7}$	$D_{Ar.nAr}$		$1.4 \times 10^{-6}$	$4.7 \times 10^{-7}$	$2.3 \times 10^{-7}$	$1.6 \times 10^{-7}$		
	$D_{Ar.S}$	$1.5 \times 10^{-5}$	$6.9 \times 10^{-6}$		$3.7 \times 10^{-6}$	$2.3 \times 10^{-6}$		$D_{Ar.S}$	$1.5 \times 10^{-5}$	$7.9 \times 10^{-6}$	$4.9 \times 10^{-6}$	$3.4 \times 10^{-6}$		
Phase Ratio		2:1					3:1							
Stage number		1	2		3	4	Stage number		1	2	3	4		
$D_{Ar.nAr}$		$1.9 \times 10^{-6}$	$5.1 \times 10^{-7}$		$2.3 \times 10^{-7}$	$1.6 \times 10^{-7}$	$D_{Ar.nAr}$		$3.2 \times 10^{-6}$	$7.3 \times 10^{-7}$	$2.5 \times 10^{-7}$	$1.6 \times 10^{-7}$		
	$D_{Ar.S}$	$1.5 \times 10^{-5}$	$8.9 \times 10^{-6}$		$5.7 \times 10^{-6}$	$4.2 \times 10^{-6}$		$D_{Ar.S}$	$1.5 \times 10^{-5}$	$1.1 \times 10^{-5}$	$7.6 \times 10^{-6}$	$5.8 \times 10^{-6}$		

	NMP	DMF	DMSO	Sulfolane	TEG	DPG	DGA	NPM
Molecular weight	99.13	73.15	78.13	120.16	194	134	105	115
Boiling point at 760 mm Hg	202°C	150-153°C	189°C (372°F)	285	dec.	231	206	117.8
Melting point °C	-24.4	-61	18.55°C (65.4°F)	28.86	-39	-8	-9	20
Specific gravity at 20°C (68°F)	1.0278	0.9445 (25°C)	1.1014 (9.18 lbs. per gal.)	1.2625 (30°C)	1.13	1.02	1.06	1.53
Refractive index at 20°C (68°F)	1.4680	1.4269 (25°C)	1.483	1.4830 (25°C)				
Surface tension at 25°C			42.85 dynes per cm	50-53 (30°)				
at 50°C			40.35 dynes per cm	47.79				
at 140°C			31.6 dynes per cm					
Toluene dilution ratio			5.75	-	55 cst (50°C)	32 cst (50°C)	90 cst (50°C)	30 cst (50°C)
Viscosity 25°C (77°F)		7.96	1.98 cps	10.3 (30°C)	0.29	0.36	0.38	0.24
Specific heat at 29.4°C			0.47±0.015 cal/gm°C (30°C)	0.31 (30°C)				
at 96.0°C			0.48±0.02 cal/gm°C (110°C)	0.36 (110°C)				
at 149.0°C			0.52±0.03 cal/gm°C					
Heat of vaporization at 70°C		11.37	260 BTU/lb 11.3 Kcal/mole	15 (100°C)		240. Btu/lb		220 Btu/lb
Heat of solution at 20°C			60 cal/gm					
Heat of fusion			44 cal/gm	2.84				
Heat combustion at 25°C			6050 cal/gm					
Flash point (open cup)			95°C (203°F)					
Auto ignition temperature in air			300-302°C					
Flammability limits in air lower (100°C) upper			3-3.5% by vol. between 42.64% by vol.					
Coefficient of expansion			0.00068 per 1°C	0.00383				
Dielectric constant (8 mc)	32.0	36.71	48.9 (20°C) 45.5 (40°C)	41.8 (10 mc)				
Solubility parameter			13					
Dipole moment		3.86	4.3 Debye Unit	4.81				
Conductivity 20°C			3x10 <sup>-8</sup> (ohm <sup>-1</sup> cm <sup>-1</sup> )	1x10 <sup>-8.4</sup>				
80°C			7x10 <sup>-8</sup> (ohm <sup>-1</sup> cm <sup>-1</sup> )					

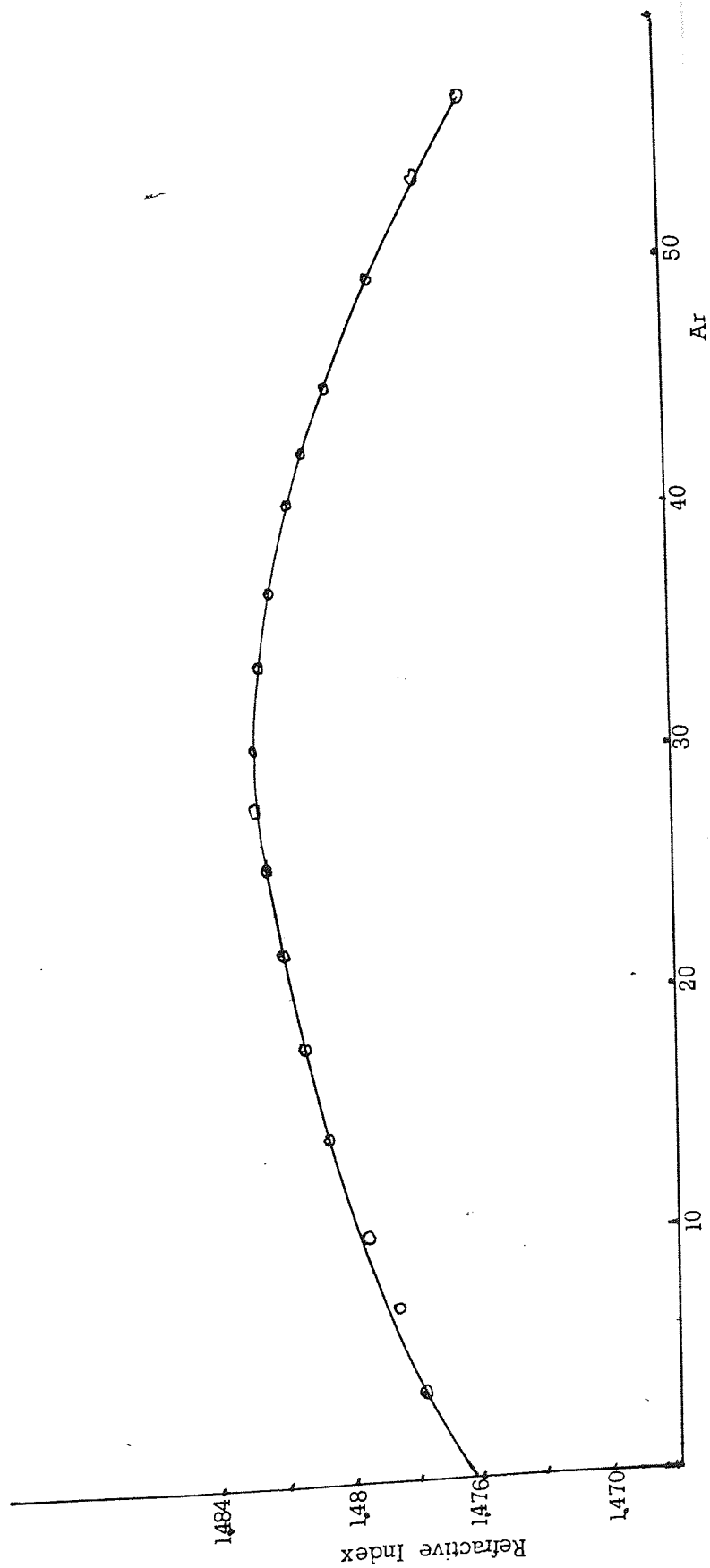
NMP = N-Methyl-2-pyrrolidinone; DMF = Dimethylformamide

DMSO = Dimethylsulfoxide; TEG = Tetraethylene glycol

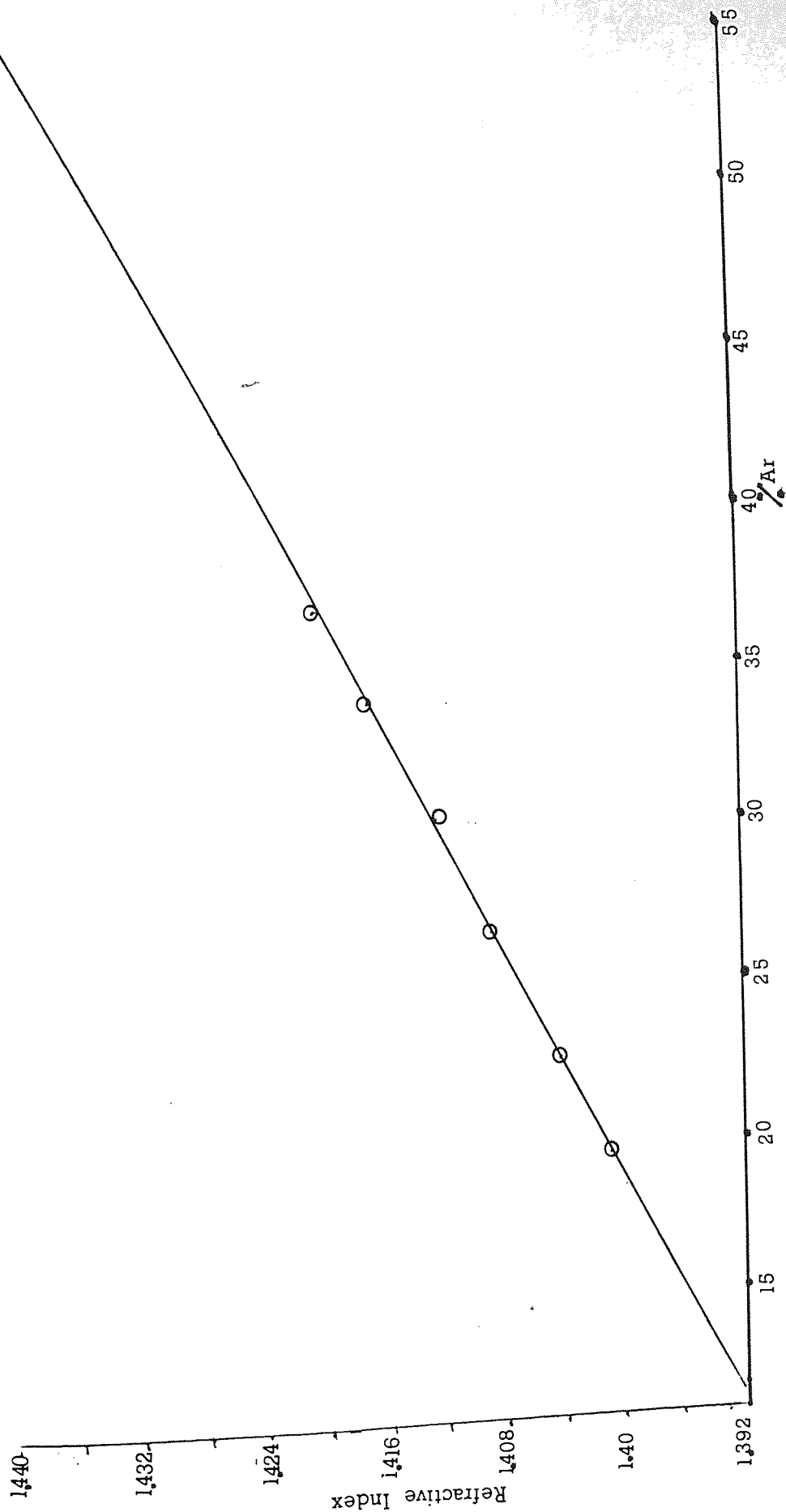
DEG = Diethylene glycol; DPG = Dipropylene glycol

DGA = Diglycolamine; NFM = N-formylmorpholine

APPENDIX (IV)  
Concentration Calibration Curves



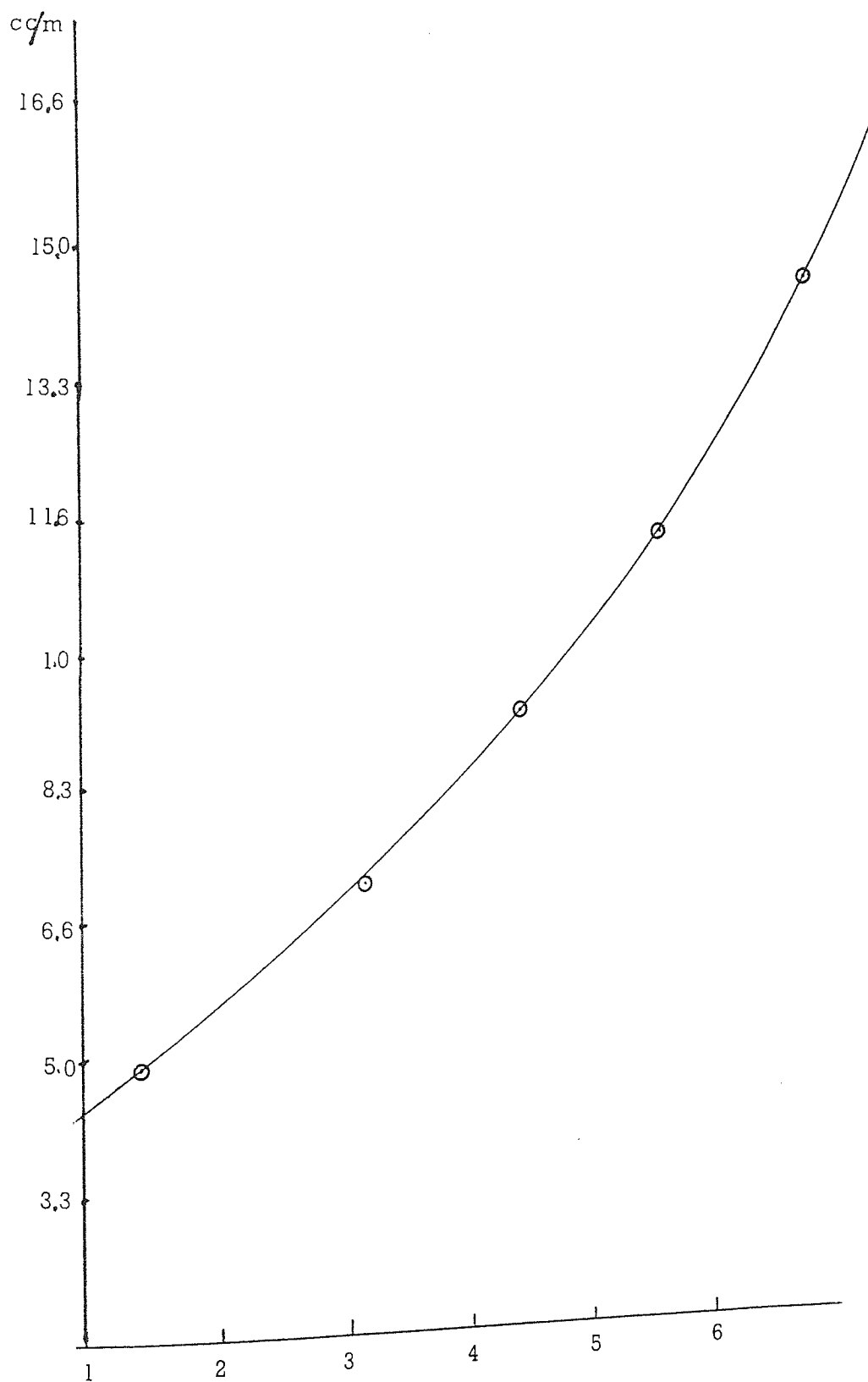
Calibration curve of aromatics in Sulfolane phase



Calibration curve of aromatics in Rafinate phase

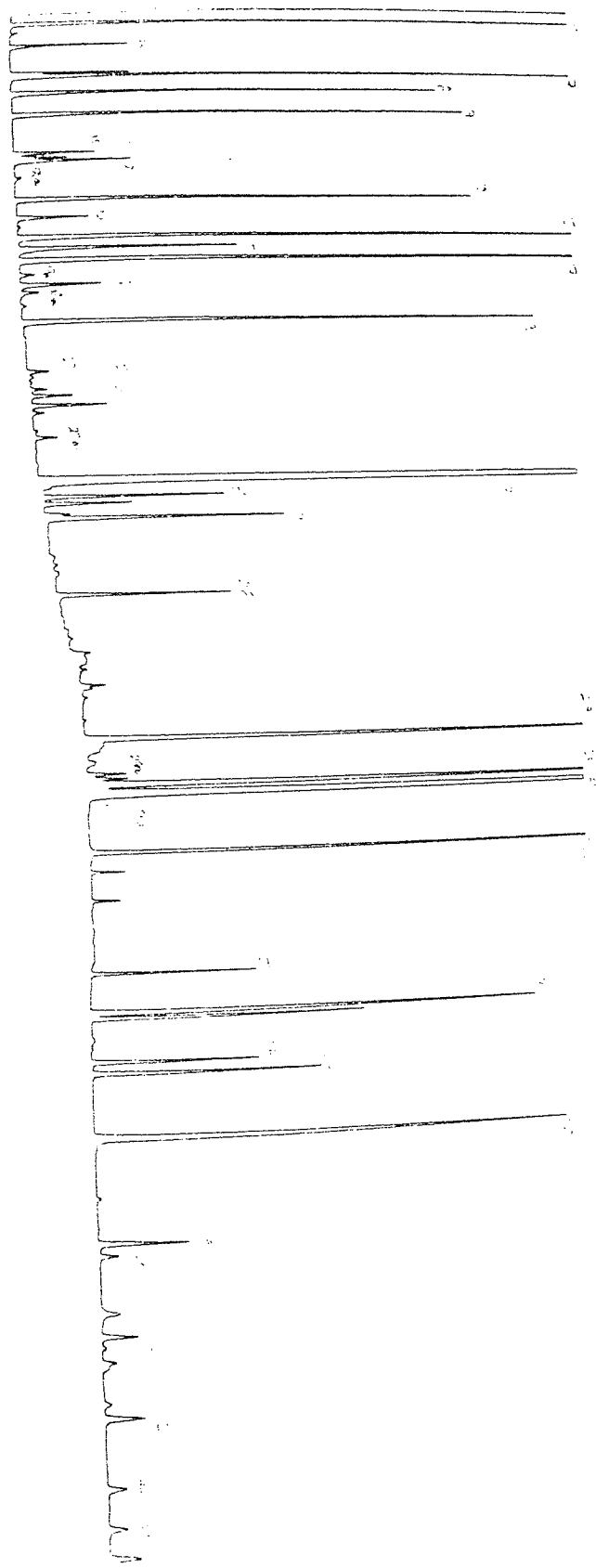


APPENDIX (V)  
Rotameter Calibration Curve



Calibration Curve Of Theflowmeter

APPENDIX (VI)  
Reformat GLC Analysis Results



## APPENDIX (VII)

### Model (3) Results

\*\*\*\*\*  
 \* RESULTS \*  
 \*\*\*\*\*

S T A R T   S T E A D Y - S T A T E   V A L U E S

STAGE NR	1	2	3	4
X-PHASE	.3923	.3341	.2443	.1035
Y-PHASE	.3617	.2313	.1844	.1119

NUMBER OF ITERATIONS 3  
 TIME CONSUMPTION START STEADY-STATE CALCULATIONS .000 SECONDS

S T E A D Y - S T A T E   V A L U E S

STAGE NR	1	2	3	4
X-PHASE	.3920	.2510	.3068	.2601
Y-PHASE	.1370	.1071	.0742	.0336
MT-RATE	.0004	.0004	.0004	.0005

NUMBER OF ITERATIONS 117  
 TOTAL TIME CONSUMPTION STEADY-STATE CALCULATIONS .000 SECONDS

\*\*\*\*\*  
\* RESULTS \*  
\*\*\*\*\*

START STEADY-STATE VALUES

STAGE NR	1	2	3	4
X-PHASE	.4143	.3033	.3130	.1865
Y-PHASE	.2767	.2378	.2227	.1972

NUMBER OF ITERATIONS 10  
TIME CONSUMPTION START STEADY-STATE CALCULATIONS .000 SECONDS

STEADY-STATE VALUES

STAGE NR	1	2	3	4
X-PHASE	.3998	.3650	.3247	.2791
Y-PHASE	.1674	.1348	.0964	.0518
RT-RATE	.0003	.0003	.0004	.0005

NUMBER OF ITERATIONS 119  
TOTAL TIME CONSUMPTION STEADY-STATE CALCULATIONS .000 SECONDS

\*\*\* MAXIMUM CELLS ( 606 ) AVAILABLE FOR SAVING TIME-DELAYED VALUES EXCEEDED \*  
FOR A NEW RUN WITH THE SAME D E L T THE FOLLOWING ALTERNATIVES ARE AVAILAB

- A. CHANGE THE MAXIMUM ALLOWED VALUE OF VARIABLE MAXM TO AT LEAST 667 .  
THIS REQUIRES A CHANGE OF THE PROGRAMS DIMENSION. SEE USER'S MANUAL.
- B. GIVE THE VARIABLE SAVINT A VALUE GREATER THAN .0553 VIA INPUT DATA.  
A VALUE GREATER THAN .100 GIVES BAD ACCURACY. CHOOSE ALTERNATIVE A

\*\*\*\*\*

\*\*\*\*\* THE RUN IS TERMINATED \*\*\*\*\*

\*\*\*\*\*  
 \* RESULTS \*  
 \*\*\*\*\*

S T A R T S T E A D Y - S T A T E V A L U E S

STAGE NR	1	2	3	4
X-PHASE	.4254	.4119	.3723	.2558
Y-PHASE	.2808	.2734	.2517	.1878

NUMBER OF ITERATIONS  
 TIME CONSUMPTION START STEADY-STATE CALCULATIONS 05 .000 SECONDS

S T E A D Y - S T A T E V A L U E S

STAGE NR	1	2	3	4
X-PHASE	.4289	.3820	.3473	.3039
Y-PHASE	.2027	.1698	.1283	.0745
MT-RATE	.0002	.0003	.0003	.0004

NUMBER OF ITERATIONS  
 TOTAL TIME CONSUMPTION STEADY-STATE CALCULATIONS 118 .000 SECONDS

\*\*\* MAXIMUM CELLS ( 606 ) AVAILABLE FOR SAVING TIME-DELAYED VALUES EXCEEDED \*.  
 FOR A NEW RUN WITH THE SAME D E L T THE FOLLOWING ALTERNATIVES ARE AVAILABLE

A. CHANGE THE MAXIMUM ALLOWED VALUE OF VARIABLE MAXP TO AT LEAST 968 .  
 THIS REQUIRES A CHANGE OF THE PROGRAMS DIMENSION. SEE USER'S MANUAL.

B. GIVE THE VARIABLE SAVINT A VALUE GREATER THAN .0002 VIA INPUT DATA.  
 A VALLE GREATER THAN .100 GIVES BAD ACCURACY. CHOSE ALTERNATIVE A .

\*\*\*\*\*

\*\*\*\*\* THE RUN IS TERMINATED \*\*\*\*\*



## APPENDIX (VIII)

...to with Sulfolane

# Correlation of Phase Equilibria of Naphtha Reformate with Sulfolane

Mohamed S. Hassan<sup>†</sup> and Mohamed A. Fahim

Department of Chemical Engineering, P.O. Box 5969, Kuwait University, Kuwait

Clive J. Mumford\*

Department of Chemical Engineering and Applied Chemistry, University of Aston in Birmingham, Birmingham, U.K.

Liquid-liquid equilibria of the ternary systems *n*-hexane-benzene-sulfolane, *n*-heptane-toluene-sulfolane, and octane-xylene-sulfolane have been determined at temperatures of 30, 35, and 40 °C. The equilibria were measured with a thermostatically controlled Smith-Bonner cell. The work was then extended to a multicomponent system. A feed with a composition typical of a reformate containing 55% aromatics was extracted with sulfolane and the phase equilibria were determined. The data were correlated by using Hand's method and were found to be in good agreement with theoretical predictions using the UNIFAC method.

## Introduction

The excellent performance of sulfolane as a solvent for the extraction of aromatics has been demonstrated by commercial operation of the sulfolane process over several years in a large number of units (1). Simultaneous extraction of BTX from both reformate and hydrotreated pyrolysis naphthas yields aromatic products of 99% purity (2). In the present investigation the liquid-liquid equilibria of four systems containing sulfolane have been determined and the data correlated by using Hand's equation. The UNIFAC method was subsequently applied to predict comparable data.

## Experimental Investigation

**Purity of Materials.** The toluene and benzene used had a minimum purity of 99.5%. Sulfolane, obtained from Fluka AG, Chemical Fabrickin, Switzerland, was predistilled in a packed column of 2 m length and 10 cm diameter and had a maximum water content of 0.05%. Hexane, heptane, octane, and xylene were obtained from BDH Ltd, UK.

**Equilibrium Measurements.** Measurements were made using a Smith-Bonner cell (3) controlled at a temperature of 30,

Table I. Experimental LLE Compositions for *n*-Hexane-Benzene-Sulfolane at 30 °C

wt fraction in raffinate			wt fraction in extract		
<i>n</i> -hexane	benzene	sulfolane	<i>n</i> -hexane	benzene	sulfolane
0.990		0.009	0.006		0.993
0.851	0.131	0.018	0.015	0.083	0.891
0.705	0.26	0.034	0.047	0.181	0.771
0.512	0.392	0.995	0.088	0.281	0.62

Table II. Experimental LLE Compositions for *n*-Heptane-Toluene-Sulfolane at 30 °C

wt fraction in raffinate			wt fraction in extract		
<i>n</i> -heptane	toluene	sulfolane	<i>n</i> -heptane	toluene	sulfolane
0.981		0.018	0.01		0.989
0.025	0.155	0.899	0.012	0.049	0.938
0.029	0.228	0.742	0.015	0.088	0.896
0.031	0.272	0.696	0.017	0.126	0.856

Table III. Experimental LLE Compositions for *n*-Octane-Xylene-Sulfolane at 30 °C

wt fraction in raffinate			wt fraction in extract		
<i>n</i> -octane	xylene	sulfolane	<i>n</i> -octane	xylene	sulfolane
0.983		0.017	0.005		0.994
0.865	0.123	0.021	0.008	0.085	0.907
0.812	0.161	0.026	0.019	0.125	0.855
0.675	0.289	0.036	0.029	0.185	0.785

Table IV. Experimental LLE Compositions for Nonaromatics-Aromatics-Sulfolane at 30 °C

wt fraction in raffinate			wt fraction in extract		
non-aromatic	aromatic	sulfolane	non-aromatic	aromatic	sulfolane
0.845	0.144	0.012	0.007	0.048	0.944
0.783	0.204	0.013	0.012	0.072	0.916
0.731	0.255	0.014	0.016	0.142	0.842
0.550	0.422	0.029	0.02	0.231	0.749

35, or 40 °C. Specific amounts of A (the nonaromatic) and the solute C (the aromatic) were introduced into the cell and agitated while maintained at a constant temperature by circulation

<sup>†</sup> College of Technical Studies, Kuwait.

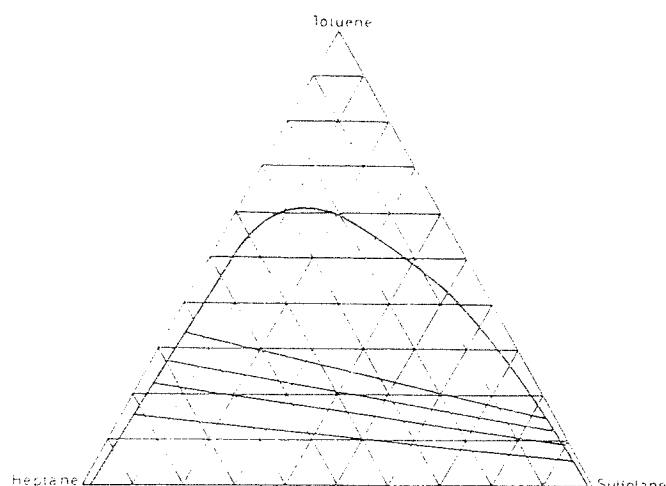


Figure 1. Ternary solubility diagram of the system toluene-heptane-sulfolane at 30 °C.

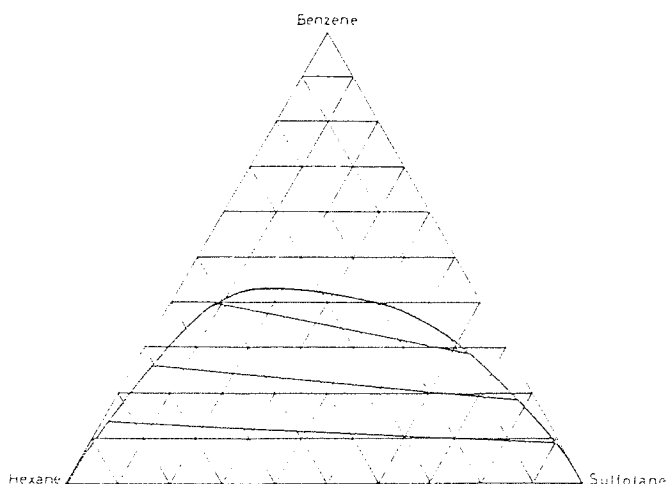


Figure 2. Ternary solubility diagram of the system benzene-hexane-sulfolane at 30 °C.

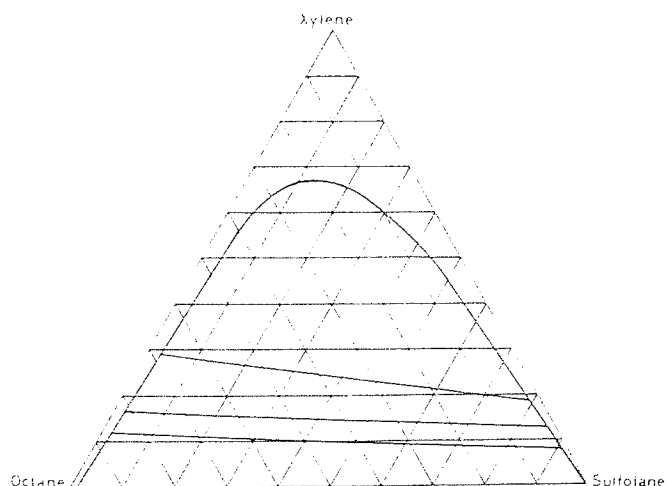


Figure 3. Ternary solubility diagram of the system xylene-octane-sulfolane at 30 °C.

of water through the external jacket from a thermostatic bath. The mixture was then titrated slowly against sulfolane until turbidity appeared, and continued until the turbidity disappeared. Repeating this procedure at various compositions enabled a complete set of curves to be obtained (4).

**Method of Analysis.** Analyses were performed using an Abbe refractometer supplied by American Optics. The solubility diagrams are shown in Figures 1–5, and the data are given in Tables I–VI.

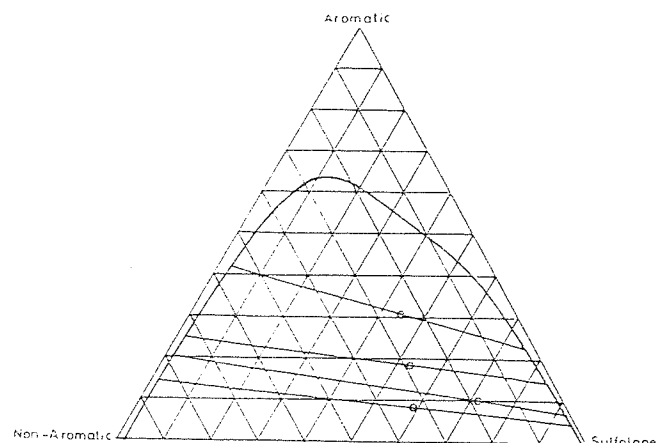


Figure 4. Solubility diagram of the system aromatics-nonaromatics-sulfolane at 30 °C.

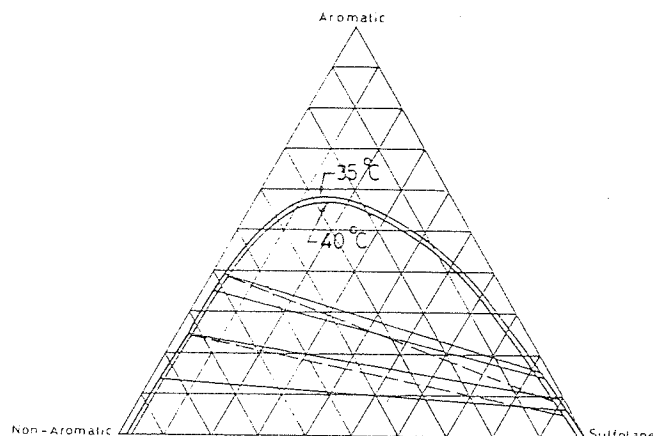


Figure 5. Solubility diagram of the system aromatics-nonaromatics-sulfolane at 35 and 40 °C.

Table V. Experimental LLE Compositions for Nonaromatics-Aromatics-Sulfolane at 35 °C

wt fraction in raffinate			wt fraction in extract		
non-aromatic	aromatic	sulfolane	non-aromatic	aromatic	sulfolane
0.842	0.135	0.023	0.017	0.06	0.923
0.73	0.245	0.025	0.02	0.09	0.88
0.66	0.313	0.027	0.025	0.115	0.86
0.58	0.39	0.03	0.035	0.145	0.82

Table VI. Experimental LLE Compositions for Nonaromatics-Aromatics-Sulfolane at 40 °C

wt fraction in raffinate			wt fraction in extract		
non-aromatic	aromatic	sulfolane	non-aromatic	aromatic	sulfolane
0.912	0.06	0.028	0.015	0.025	0.95
0.822	0.149	0.029	0.022	0.052	0.92
0.675	0.282	0.037	0.027	0.088	0.88
0.6	0.36	0.04	0.03	0.11	0.86

#### Correlation of Data

Geometrical methods for interpolation and extrapolation of tie line data have been devised by Brancker et al. (5), Sherwood (6), and Hand (7). While they are entirely graphical, these methods are useful for extrapolation. The first empirical equation describing the distribution of components in a three-component, two-phase liquid system was due to Bachman (8)

$$X_{BS} = r + b(X_{BB}/X_{AA}) \quad (1)$$

where  $r$  and  $b$  are constants.

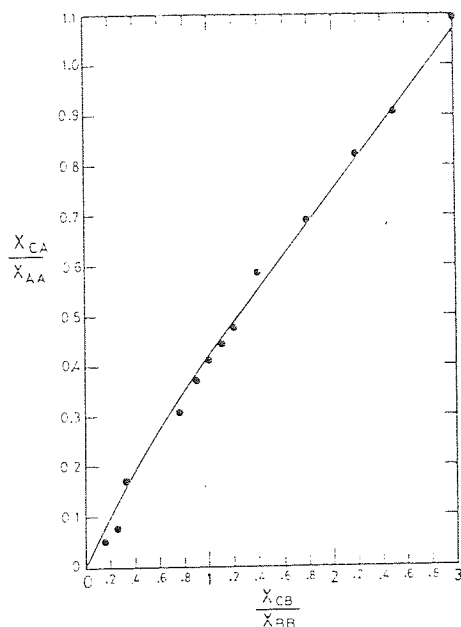


Figure 6. Equilibrium curve for the system aromatic-nonaromatic-sulfolane at 30 °C.

Othmer and Tobias (9) showed that this correlation is of limited use, because it is based on ternary systems composed of practically immiscible, nonconsolute components in the absence of the consolute component. They therefore proposed that

$$\frac{1 - X_{AA}}{X_{AA}} = K \left[ \frac{1 - X_{BB}}{X_{BB}} \right]^n \quad (2)$$

On logarithmic coordinates this equation gives a straight line.

However, the method of Othmer and Tobias is also limited by the fact it does not include the concentration of the distributed component. Therefore, the most useful formula appears to be that of Hand which correlates the concentration of the solute in the two conjugate solutions. Hand's equation is represented by

$$\frac{X_{CA}}{X_{AA}} = K \left[ \frac{X_{CB}}{X_{BB}} \right]^r \quad (3)$$

i.e., the logarithmic plot of  $X_{CA}/X_{AA}$  against  $(X_{CB}/X_{BB})$  is rectilinear.

A regression analysis of the solubility data for the system aromatics-nonaromatics-sulfolane, based on Hand's correlation, resulted in the equation

$$\frac{X_{CA}}{X_{AA}} = 0.414 \left[ \frac{X_{CB}}{X_{BB}} \right]^{0.865} \quad (4)$$

where A, B, and C refer to sulfolane, nonaromatics, and aromatics, respectively.

Figure 6 plotted that the results predicted by Hand's correlation, when plotted against the experimental values, gave good agreement. The results of regression analysis of the data for this system at 35 °C resulted in the equation

$$\frac{X_{CA}}{X_{AA}} = 0.23 \left[ \frac{X_{CB}}{X_{BB}} \right]^{0.64} \quad (5)$$

and at 40 °C

$$\frac{X_{CA}}{X_{AA}} = 0.188 \left[ \frac{X_{CB}}{X_{BB}} \right]^{0.73} \quad (6)$$

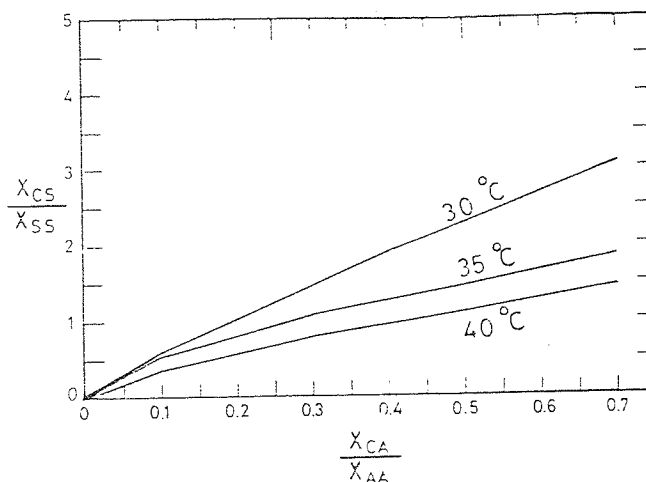


Figure 7. Hand's correlation for the system aromatic-nonaromatic-sulfolane at 30, 35, and 40 °C.

Table VII. Predicted LLE Compositions at 30 °C for the Aromatics-Nonaromatics-Sulfolane System<sup>a</sup>

wt fraction in raffinate			wt fraction in extract		
non-aromatic	aromatic	sulfolane	non-aromatic	aromatic	sulfolane
0.843	0.142	0.015	0.009	0.052	0.938
0.781	0.199	0.019	0.014	0.075	0.910
0.725	0.254	0.020	0.020	0.149	0.840
0.549	0.420	0.035	0.025	0.239	0.735

<sup>a</sup> Compositions of aromatics: benzene 46.80, toluene 32.29, xylene, 20.91 vol. %; nonaromatics: *n*-hexane 21.47, *n*-heptane 40.6, *n*-octane 37.91 vol. %.

Figure 7 represents Hand's correlation for the multicomponent system nonaromatics-aromatics-sulfolane at 30, 35, and 40 °C.

**Computation of LLE Data by UNIFAC.** Computation of the liquid-liquid equilibrium phase compositions involves solving eq 7 with material balance eq 8, 9, and 10, using an iterative procedure based on the Newton-Raphson method (10)

$$(\gamma X_i)^I = (\gamma X_i)^{II} \quad (7)$$

$$X_i^F = \theta X_i^I + (1 - \theta) X_i^{II} \quad (i = 1, 2, \dots, N) \quad (8)$$

$$\sum_{i=1}^N X_i^I = 1 \quad (9)$$

$$\sum_{i=1}^N X_i^{II} = 1 \quad (10)$$

$\theta$  is the fraction extracted. The procedure involves estimation for  $\theta$  and  $X_i^I$  and successive iteration until eq 7 is satisfied; the  $\gamma_i^I$  and  $\gamma_i^{II}$  are next calculated, using the compositions just obtained from the UNIFAC (11). New values of  $X_i^I$  and  $X_i^{II}$  are then calculated from the eq

$$X_i^{II} = \frac{X_i^F}{1 + (K_i - 1)\theta} \quad (11)$$

$$X_i^I = K_i X_i^{II} \quad (12)$$

where  $K_i = X_i^I/X_i^{II}$  and  $\theta$  are improved upon successive iter-

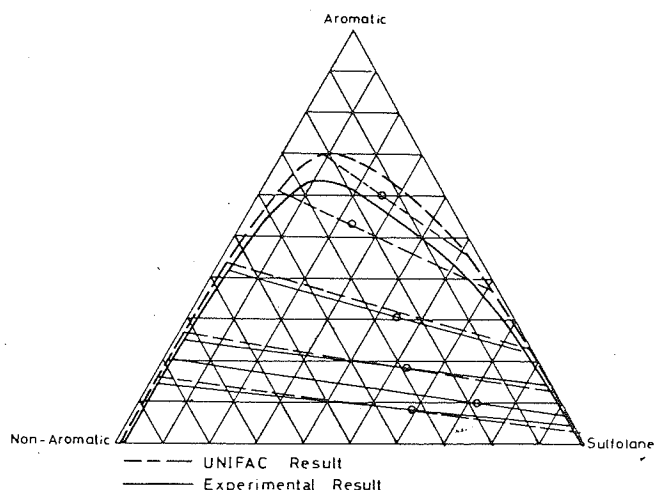


Figure 8. Comparison of predicted and experimental phase compositions of the system aromatics-nonaromatics-sulfolane at 30 °C.

ation until  $\sum (X_i^{II_{old}} - X_i^{II_{new}}) < 10^{-8}$ .

### Results and Discussion

Figure 8 and Table VII demonstrate that the predicted phase compositions are in good agreement with the corresponding experimental values for the system aromatic-nonaromatic-sulfolane. The deviation of the predicted compositions near the plait point is characteristic of any prediction method but is of little consequence since practical extractions are never carried out near the plait point.

With regard to the effect of temperature on the selectivity and distribution coefficient, the selectivity of sulfolane will decrease with temperature since the heterogeneous area decreases with temperature. The slope of the tie lines is inclined toward the solvent, but the selectivity is greater than one; thus the extraction is possible.

### Conclusions

It is concluded from the above results that the temperature had a modest effect on the miscibility range of the systems studied. On balance, considering both capacity and selectivity of sulfolane, with the systems studied better results were achieved at the lowest temperature of 30 °C.

Good agreement was obtained between data predicted by the UNIFAC method and experimental results as shown in Figure 8. The UNIFAC method is presently being applied to predict phase equilibria for actual naphtha cuts. The predicted values will be used to correlate data obtained on the extraction of naphtha by sulfolane, using a mixer-settler cascade. Work is also in progress to improve prediction near the plait point by improving the interaction parameters of UNIFAC.

### Glossary

- $X_{BB}$  concentration of solvent B in B phase in eq 1, 2, and 3
- $X_{AA}$  concentration of solvent A in A phase in eq 1, 2, and 3
- $X_{CA}/X_{AA}$  concentration of aromatics in nonaromatics phase per concentration of nonaromatics in nonaromatics phase in eq 4
- $X_{CB}/X_{BB}$  concentration of aromatics in sulfolane phase per concentration of sulfolane in sulfolane phase in eq 4
- $r, b, n$  constants
- $X_i^F$  concentration of component  $i$  in feed
- I extract phase
- II raffinate phase
- $\gamma$  activity coefficient

Registry No. Hexane, 110-54-3; benzene, 71-43-2; heptane, 142-82-5; toluene, 108-88-3; octane, 111-65-9; xylene, 1330-20-7; sulfolane, 126-33-0.

### Literature Cited

- (1) Voethtr, H.; Kusters, W. C. G. Presented at The Sixth World Petroleum Congress, 1963; Section III, paper 11.
- (2) Broughton, D.; Asselin, G. F. *7th World Pet. Congr.* 1967, 65.
- (3) Smith, T. E.; Bonner, R. F. *Ind. Eng. Chem.* 1950, 42, 896.
- (4) Alders, L. *Liquid-Liquid Extraction*; Elsevier: London, 1959.
- (5) Branner, A. V.; Hunter, T. G.; Nash, A. W. *Ind. Eng. Chem. Anal. Ed.* 1940, 35, 12.
- (6) Sherwood, T. K. *Absorption and Extraction*, 1st ed.; McGraw-Hill: New York, 1937.
- (7) Hand, P. B. *J. Phys. Chem.* 1930, 34, 1961.
- (8) Bachman, I. *Ind. Eng. Chem. Anal. Ed.* 1940, 12, 38.
- (9) Othmer, D. F.; Tobias, P. E. *Ind. Eng. Chem.* 1942, 34, 690.
- (10) Fredenslund, A.; Jones, R. L.; Prausnitz, J. M. *AIChE* 1975, 21, 1086.
- (11) Skojold-Jorgensen, S.; Kolbe, B.; Gmehling, J.; Rasmussen, P. *Ind. Eng. Chem. Process Des. Dev.* 1979, 18, 714.

Received for review October 27, 1986. Accepted October 18, 1987.

## Ultrasonic Velocity and Adiabatic Compressibility of Monochloroacetic Acid in Aqueous Ethanol at Various Temperatures

Pandharinath S. Nikam\* and Mehdi Hasan

P. G. Department of Physical Chemistry, M.S.G. College, Malegaon Camp 423 105, District Nashik, India

Ultrasonic velocities of solutions of monochloroacetic acid in aqueous ethanol were measured at 25, 30, 35, and 40 °C by using a single-crystal interferometer at a frequency of 1.5 MHz. The ultrasonic velocity, density, and concentration were used to calculate adiabatic compressibility, intermolecular free length, and apparent molal compressibility. Bachem's relation has been found to be obeyed and the constants  $A$  and  $B$  of this relation of various solvents have also been reported.

### Introduction

Accurate thermodynamic data on dilute electrolyte solutions are frequently needed. The sound velocity is a purely thermodynamic function. Many other thermodynamic properties of electrolyte solutions are determined from sound velocity (1, 2). In recent years ultrasonic velocity studies in many of the aqueous and nonaqueous electrolytic solutions have led to new insights into the process of ion-ion and ion-solvent interactions (3-11). Ultrasonic velocity and adiabatic compressibility are quite sensitive to changes in ionic concentrations. Either or

## NOMENCLATURE

A	: Constant.
A	: Coefficient in equation 4-36.
A	: Matrix defined in equation 7-103.
A	: Interfacial area.
A	: Area of contact.
A	: Horizontal cross section area of the settler in equation 6-19.
$A_n$	: Eigen Value.
$A_f$	: Area of rest drop
a	: Constant.
a	: Horizontal radius of spheroid, m.
a	: System constant in equation 6-11.
a	: Superfacial Area of contact of the phases.
$a_{av}$	: Average Interfacial Area.
$a_d$	: Drop surface .
$a_{mn}$	: UNIFAC binary group interaction parameter for groups m,n related to $a_{nm}$
$a_{nm}$	: UNIFAC binary group interaction parameter for groups n,m related to $a_{mn}$ .
$a_o$	: Initial Horizontal radius in equation 4-31.
$a_p$	: Amplitude in x-axis in equation 4-31 .
B	: Constant in equation 4-35.
B	: Matrix defined in equation 7-103.
B	: Constant.
b	: Vertical radius of spheroid, m.in equation 4-30.
b	: Liquid molar volume constant $\text{cm}^3/\text{gmole K}$ .
b	: Constant.
$b_o$	: Initial vertical radius in equation 4-30.
C	: Concentration mole/l .

$C_2$  : constant.  
 $C_f$  : Final concentration .  
 $C_o$  : Initial concentration .  
 $C^*$  : Equilibrium concentration .  
 $cri$  : Critical .  
 $c$  : Concentration mole/l .  
 $c$  : Combinatorial part of the activity coefficient .  
 $C_1$  : Constant.  
 $D$  : Distribution coefficient .  
 $D$  : Molecular diffusivity.  
 $D_{AB}$  : Molecular diffusion coefficient of solute A at very low concentration in solvent B.  
 $D_{AB}^o$  : Infinite dilution diffusion coefficient.  
 $D_c$  : Diffusivity of Continuous phase,  $m^3/sec$  .  
 $D_d$  : Diffusivity of Dispersed phase,  $m^3/sec$  .  
 $D_E$  : Effective diffusivity.  
 $d_f$  : Diameter during formation.  
 $dM$  : Amount transfer during time  $dt$ .  
 $d_T$  : Tank diameter,  $m$  .  
 $d_p$  : Drop diameter,  $mm$  .  
 $d_i$  : Impeller diameter.  
 $d_o$  : Drop size at zero hold-up,  $mm$ .  
 $d_{32}$  : Sauter mean diameter,  $mm$  .  
 $d_e$  : Equivalent diameter of droplet,  $mm$  .  
 $E$  : Extraction factor,  $mU_X/U_Y$  .  
 $E$  : Energy.  
 $E$  : Efficiency.  
 $E$  : Dimensionless number given by  $E_m < E < E_r$  .  
 $E_i$  : Intercept of the equilibrium line. in Equation 7.75  
 $E$  : eccentricity.

$E_f$  : Combined end effect .  
 $E_j$  : Effective longitudinal diffusion coeff. in jth phase .  
 $E_m$  : Fraction approach to equilibrium in steady fall period.  
 $E_m$  : Mean efficiency  
 $E_r$  : Total efficieny, defined in equation 4.5  
 $E_{t1}$  : Fraction approach to equilibrium in drop formation period.  
 $E_{t2}$  : Fraction approach to equilibrium in coalescence period  
 $E_x$  : Axial mixing coefficient of raffinate phase.  
 $E_y$  : Axial mixing coefficient of extract phase.  
 $F_j$  : Volumetric flow rate of the jth phase .  
 $Fr$  : Froud number  $v^2/dg$   
 $f_1(t)$  : Function of time in equation 4.27.  
 $Ga$  : Galileo number  $d_e V/D$   
 $g, g_c$  : Acceleration due to gravity  $m/sec^2$  .  
 $H$  : Hold-up of aqueous phase .  
 $H$  : Height of Liquid in Agitated Tank.  
 $HCL$  : Hydrocarbon Loading.  
 $h$  : Hold-up of organic phase .  
 $J$  : The rate of mass transfer to a forming drop.  
 $K$  : Constant.  
 $K_1$  : Proportionality constant characterized of the agitator.  
 $K_2$  : Geometric constant in equation 6-14.  
 $K_C$  : Overall Mass Transfer Coefficient Based on Dispersed Phase.  
 $K_d$  : Overall Mass Transfer Coefficient Based on Continuous Phase.  
 $K_3$  : Combined constant in drop size in equation 6-16.  
 $K_{HB}$  : Coeff. calculated from Handlos and Baron's model  $cm/sec$  .



$K_{od}$  : Overall mass transfer coefficient Based on Dispersed Phase.

$K_{ox}$  : Overall mass transfer coefficient based on x phase.

$K_{oy}$  : Overall mass transfer coefficient based on y phase.

$k_1, k_2, k_3$  : Constant .

$k_c$  : Individual mass transfer coefficient. dispersed phase.

$k_{co}$  : Mass transfer coefficient based on continuous phase of oscillation drops

$k_d$  : Individual mass transfer coeff. continuous phase.

$k_d$  : Actual transfer coefficient.

$k_{do}$  : Mass transfer coefficient based on dispersed phase of oscillation drops

$k_{df}$  : Mass transfer Coeff. during drop formation.

L.L.E : Liquid-Liquid Equilibrium.

$M$  : Molecular weight.

$m$  : Coefficient.

$m$  : Distribution coefficient.

$N$  : Last number of actual stages required .

$N$  : Mass transfer rate.

$N$  : Number.

$N$  : Impeller speed .

$N_p$  : Power number  $Pg_c / N^3 d^5$ , dimensionless.

$N_c$  : Number of components .

$N_g$  : Number of groups .

$(No)_x$  : Number of true overall mass transfer units based on x phase  $(K_{ox} a L / U_x)$  .

$(No)_y$  : Number of True overall mass transfer units based on y phase  $(K_{oy} a L / U_y)$  .

$n$  : Total number of actual stages required.

$n$  : Mode of oscillation.

$n$  : Constant.

$n$  : Number of drops.  
 $P$  : Power input N.m/sec .  
 $(Pe)_x$  : Peclet number  $U_x d_c / E_x$  .  
 $q_i$  : Total surface area parameter for group  $i$  .  
 $q_x$  : Organic phase flow rate.  
 $q$  : Aqueous phase flow rate.  
 $Q$  : Volumetric flow rate in equation 6-20,  $m^3/sec$ .  
 $Q_k$  : Surface group parameter for group  $k$ .  
 $Q_{mn}$  : Group surface area fraction for  $m$ .  
 $Re$  : Reynold number  $vd_e \rho / \mu$ .  
 $\tilde{Re}$  : Modified Reynold Number  $\rho_c \omega d_e^2 / \mu_c$ .  
 $R$  : Constant effective diffusivity in equation 4-17  
 $R_k$  : Total group volume parameter for group  $k$  .  
 $r$  : Radius of sphere of volume equal to that of a drop, mm .  
 $r$  : Velocity ratio of phases (  $V_d/V_c$  ) .  
 $r$  : Constant.  
 $r_o$  : Initial radius of drop .  
 $S$  : Solvent .  
 $S_c$  : Schemdit number .  $\mu/\rho d$   
 $Sp$  : Solvent power.  
 $S_i$  : Solute transferred to the organic phase in stage  $i$ .  
 $(Sh)_n$  : Contribution of sherwood number due to natural convection.  
 $T_k$  : Activity coefficient of group  $k$ .  
 $T_k^i$  : Activity coefficient of group  $k$  in pure component  $i$ .  
 $T_{mk}$  : Group interaction parameter given in equation 8-15.  
 $T$  : Absolute temperature.  
 $t$  : Equilibrium time of contact, sec .  
 $t_e$  : Time of contact of solute transfer .

$t_f$  : Time of drop formation, sec .  
 $U$  : Superfacial velocity .  
 $\overline{U}^2$  : Mean of Turbulence fluctuating velocities.  $c. \left( \frac{\rho d_p}{\mu f_m} \right)^{2/3}$   
 $U_t$  : Terminal velocity .  
 $U_x$  : Volumetric flow rate of raffinate phase.  
 $U_y$  : Volumetric flow rate of extract phase.  
 $V$  : Phase velocity, m/sec .  
 $V$  : Characteristic velocity.  
V.L.E : Vapour-Liquid Equilibrium.  
 $V_A$  : Molal volume of solute at its normal boiling point.  
 $v$  : Volume of Liquid in equation 6-2, cu m.  
 $W_A$  : Extraction rate of component A in equation 4-51.  
 $W$  : Fractional oscillation drop characteristics.  
 $W_A, W_B$  : Flux referred to stationary point gmole/sec cm<sup>2</sup>.  
 $w$  : Blade width in fig.6.8  
 $We$  : Weber number  $\rho d_i^3 N^2 / \sigma$   
 $X$  : Mass fraction of solute in raffinate phase.  
 $X$  : Inversion hold up in equation 6-12  
 $X$  : Solute volume fraction.  
 $X_{A1}$  : Concentration of component A at position 1.  
 $X_{A2}$  : Concentration of component A at position 2.  
 $X_{AA}$  : Concentration of solvent A in A phase.  
 $X_{BB}$  : Concentration of solvent B in B phase.  
 $X_{CA}/X_{AA}$  : Concentration of aromatics in sulfolane phase  
per concentration of sulfolane sulfolane phase.  
 $X_{CB}/X_{BB}$  : Concentration of aromatics in nonaromatic phase  
per concentration of nonaromatics in nonaromatic  
phase.  
 $X_m$  : Mole fraction of group m in the solution.

- $x^O$  : Matrix containing the steady state organic phase concentration.  
 $x_O$  : Initial drop diameter.  
 $x$  : Hold up of the dispersed phase, fraction.  
 $x$  : Total concentration in the system.  
 $x$  : Mole fraction in the liquid hydrocarbon phase in equation 3.1.  
 $x$  : Association factor, dimensionless.  
 $x_e$  : Defined in Fig 6.13.  
 $x_i$  : Volume fraction of the dispersed phase in the initial charge to the vessel,  $V_d/V_d+V_c$ .  
 $y$  : Mass fraction of solution extract phase  
 $y$  : Mole fraction in the liquid solvent phase in equation 3-1.  
 $y$  : Constant in equation 6-20.  
 $y_e$  : Defined in Fig 6.13.  
 $\bar{Z}$  : Coordination Number .  
 $Z_c$  : Height of mixing Vessel ,m.  
 $Z_i$  : Aqueous phase solute concentration in stage i.

### Subscripts

- $1,2$  : Phases 1,2. *b. Bulk*  
 $C$  : Continuous phase.  
 $c$  : Continuous phase.  
 $D$  : Dispersed phase.  
 $d$  : Dispersed phase.  
 $E$  : Extract phase.  
 $f$  : Final , Feed.  
 $e$  : Equivalent.

$i$  : Stage number.  
 $i$  : Initial.  
 $M$  : Murfree.  
 $N$  : Last stage number.  
 $n$  : Stage within contactor.  
 $n$  : Number of assumed droplet size group.  
 $o$  : X phase inlet end, within contactor.  
 $o$  : Oscillation.  
 $s$  : Saturated phase.  
 $x$  : Concentration in raffinate phase.  
 $y$  : Concentration in extract phase.

#### Superscripts

$C$  : Combinatorial part of activity coefficient.  
 $R$  : Residual part of activity coefficient.  
 $*$  : Equilibrium value.  
 $I, II$  : Phases 1, 2.

#### Greek Letters

$\alpha_x$  : Back mixing coefficient in continuous phase.  
 $\alpha_y$  : Back mixing coefficient in dispersed phase.  
 $\alpha$  : Constant.  
 $\beta$  : Light-Heavy selectivity.  
 $\beta$  : Group selectivity.  
 $\beta$  : Constant.  
 $\gamma$  : Activity coefficient of component  $i$  in solvent phase  
 $\bar{\gamma}$  : Activity coefficient of component  $i$  in hydrocarbon phase  
 $\gamma$  : Constant.  
 $\gamma_i^C$  : Combinatorial part of activity coefficient.

$\gamma_i^R$	: Residual part of activity coefficient.
$\xi$	: Murphree efficiency.
$\xi$	: Dimensionless group.
$\xi_0$	: Overall stage efficiency.
$\xi_n$	: Combined overall efficiency for n stages.
$\theta_i$	: Surface area fraction for component i.
$\theta$	: Residence time, sec.
$\theta$	: Fraction extracted in equation 8-17
$u_i$	: UNIFAC constant for component i , related to $r_i$ and $q_i$ .
$\mu$	: Viscosity.
$\rho$	: Density.
$\Delta\rho$	: Positive difference in Density.
$\rho_m$	: Average Density.
$\Phi_0$	: Holdup of dispersed phase, fraction.
$\Phi$	: Volume fraction dispersed phase, average for the vessel.
$\Phi$	: Constant asymptotic in inversion concentration.
$v_k^{(i)}$	: Number of groups of type k in component i.
$\psi_i$	: Segment fraction of component i.
$u_i$	: UNIFAC constant for component i, related to $r_i$ and $q_i$
$\lambda$	: Eigen value.
$\lambda$	: Ratio of phase flows.
$\omega$	: Mode of oscillation.
$\epsilon$	: Amplitude of oscillation.
$\sigma$	: Interfacial tension.
$\varpi$	: $0.5 \omega$ .
$\Gamma_k$	: Residual activity coefficient of the functional group k in the actual mixture.

# REFERENCES.

1. Encyclopedia of Chemical Technology, Vol. 4, 65-78, Third edition (1967).
2. Fujiyama, F., and coworkers, U.S. Pat. 3, 948, 998 (Dec. 5, 1974) (to Mitsubishi Gas Chemical Co.)
3. Gresham, W. F., and Taber, G. E., U.S. Pat. 2, 485, 37 (Nov. 8, 1966) (to E.I. du Pont de Nemours Co.)
4. Somekh, G. S., and Friedlander, S. K., Sym. Refining Petroleum for Chemicals, New York, September 7-12, (1969).
5. Broughton, D. B., Asselin, G. F., 7th World Petrol. Cong. 4, 65-72 (1967).
6. Strobaugh, R. B., Hydrocarbon Process, 45 (5), 205-214 (1966).
7. Kenny, E., Chemistry and Industry, p. 518-522, (1973).
8. Asselin, G. F., and Pensak, R. A., Petrolieri international, 49-72, (1978).
9. Smith, T. E., Bonner, R. F., Ind. Eng. Chem., 42, 896, (1950).
10. Ali, G., and Jernquist, A., Chemistry and Industry, 1046-1048 (1971).
11. Hand, D. B. J., Phys. Chemistry, 34, 1961 (1930).
12. Licht, W. J., and Pensing, W. F., Ind. Eng. Chem., 45, 1885 (1953).
13. Krishnamurti, S., Nature J., 128, 639 (1931).
14. Smith, C. P., and Rogers, H. E., Am. Chem. Soc. 52, 1824 (1930).
15. Marek, J., and Standart, G., Collection Czech. Chem. Cummun 19, 1074 (1954).
16. Marek, J., and Standart, G., Collection Czech. Chem. Cummun. 20, 1490 (1955).
17. Johnson, E. W., and Nash, L. K., J. Am. Chem. Soc., 72, 547 (1950).
18. Farmer, W. S., U.S. Atomic Energy Com. Tech. Infor. Div Oak Ridge, Tenn. Rept. ORNL-635 (1949).
19. Perry, R. H., and Chilton C. H., "Chemical Engineer's Hand book" 5th edition, McGraw-Hill, NY (1973).
20. Joy, S. D., and Kyle, B. G., AIChEJ, 15, (2), 298 (1969)

21. Boberg, T. C. , Ph.D. Thesis, Univ. Michigan, Ann-Arbor (1960) .
22. Techo, R. , Ph.D. Thesis, Georgia Inst. Tech., Atlanta (1961) .
23. Renon, H. M. , Ph.D. Thesis, Univ. California, Barkely (1966) .
24. Coplan, BV., Davidson, T. K., and Zebrozi, E. L., Chem. Eng. Prog., 50, 8, 403 (1954) .
25. Renon, H. , and , Prausnitz, J. M. , Local composition in thermodynamic excess functions for liquid mixtures, AIChEJ. 14 (1) 135 (1968) .
26. Anderson, T. F., Prausnitz, J. M., Application of UNIQUAC equation to calculation of multicomponent phase equilibria, I, EC process Des. Dev., 17, (4), 561 (1978) .
27. Fredenslund, A. , Jones, R. L., Prausnitz, J.M., Group contribution estimation of activity coefficients in non ideal mixtures, AIChE J., 21, 60 , 1086 (1976).
28. Dakshinamurthy, Chiranjivi, Rao and Subrahmanyam, Chem. Eng. Data , 17, (3), 379 (1961) .
29. Treybal, R. E., Liquid Extraction, Second edition, McGraw Hill (1963) .
30. Griffith, R., Chem. Eng. Sci., 12, 198 (1960) .
31. Lewis, W. B., and, Pratt, H., Nature, 171, 1155 (1953) .
32. Sherwood, T. K., Evans, J. E., Longcore, J. V. , Ind. Eng. Chem., 31, 1144 (1939) .
33. Sherwood, T. K. , Evans, J. E. , Longcore, J.V., Trans. Am. Inst. Chem. Engrs. , 35, 597 (1939) .
34. West, F. B., Robinson, P. A. , and , others. Ind. Eng. Chem., 43, 234 (1951) .
35. Johnson, A. T., and, Hamielec, A. E., AIChEJ, 6 (1), 145 (1960) .
36. Nadi, S., and , Viswanathan, S., Current Science (India) , 15 (1946) .
37. Marsh, B.D., and, Heideger, W.J., Ind. Eng. Chem. Fund., 4, 129 (1965).
38. Heertjes, P. M., Holve, W. A. , and , Talsma, H. , Chem. Eng. Sci., 3, 122 (1954) .
39. Higbie, R., Trans. Am. Inst. Chem. Eng., 31, 365 (1935) .



40. Licht, W., J., Conway, J., Ind. Eng. Chem. 42, 1151 (1950) .
41. Salem, A. S. , Ph.D. Thesis, University of Aston (1975) .
42. Skelland, T. V., Minhas, S. P., Chem. Soc., 18, 219 (1960) .
43. Heertjes, P. M., and De Nie, L. H., "Mass transfer to Drops", Recent advances in liquid-liquid extraction , Hanson, C., Pergamon Press, (1971) .
44. Coulson, Z. M., and Skinner, S. E., Chem. Eng. Sci., 1971(1952) .
45. Garner, F. H. , and Grafton, R. W., Proc. R. Soc., 224, 64 (1954) .
46. Kinard, G.E., Manning, F. S., and Manning, W. P., Brit. Chem. Eng. 8, 326, (1963) .
47. Laddha, G. S., and Degalessan ,T. E., Transport Phenomena in liquid Extraction, Tata McGraw Hill, New Delhi, (1976) .
48. Hadmard, J. R., Hebd. Seanc. Acad. Sci., Paris, 152. 1753 (1911) .
49. Sawistowski, H., and Goltz, G.E., Trans. Inst. Chem. Engrs. 41, 174 (1963) .
50. Al-Hassan, T. S., Ph.D. Thesis, University of Aston in Birmingham, U.K., (1979) .
51. Newman, A. B., Trans. Am. Inst. Chem. Engrs. 27, 310 (1931) .
52. Vermeulen, T. et al, Chem. Eng. Progress, 51, 85 (1955) .
53. Boussinesq, M. J. , Ann. Chem. Phys. , 29, 364 (1913) .
54. Garner, F.H., and , Hale, A. R., Chem. Eng. Sci, 2, 157 (1953) .
55. Sideman, S., and , Shabatia, H., Can. J. Chem. Eng., 42, 107 (1964) .
56. Kronig, R., and Brink, J. C. , Appl. Sci. Res. A2, 142 (1960) .
57. Olander, D. R., AIChE J., 12, 1018 (1966) .
58. Calderbank , P.H., and Moo Young, M., Chem. Eng. Sci. 16, 39 (1961) .
59. Handlos, A.E., and Baron, T. AIChE J., 3, 127 (1957) .
60. Skelland, A. H., and Wellek, R. M., AIChE J., 10, 491 (1964) .

61. Rose, P. M., and Kinter, R. C. AIChE J., 12, 530 (1960) .
62. Lamb, H., cited in Ellis, W. B., Ph.D Univ. of Maryland, (1966) .
63. Angelo, J. B. , Lightfoot , E. N. , and Howard, D. W., AIChEJ , 12, 751, (1966) .
64. Braunson, R. J., and Wellek, R. M., Can. Chem. Eng. J. , 48 , 266, (1970) .
65. Yamaguchi, M. , Fujimoto, F., and Katayama, T. , Chem. Eng, Japan , 8, 361, (1975) .
66. Griffith, R. M., Chem. Eng. Sci., 12, 198 (1980) .
67. Linton, W. H. , and Sherwood, T. K. , Chem. Eng. Prog. 46, 258 (1950) .
68. Garner, F. H., Jenson, V. C., and Keey, R., AIChE J. 37, 197 (1957) .
69. Linton, M., and Sutherland, K. I., Chem. Sci., 17, 214 (1960) .
70. Rowe, P. N. et al., Trans. Inst. Chem. Eng. 43, 14 (1965).
71. Treybal, R. E., AIChE J., P. 202 (1958) .
72. Friedlander, S. K. AIChE J., 3, 43 (1957) .
73. Gaffney, B. J., and Drew, T. B., Ind. Engng. Chem., 42, 1120 (1950) .
74. Boussinesq , M., J. Math. Pures, Appl., 11, 285 (1905)
75. Baird, M. H. I., and Hamielec, A. E., Can. J. Chem. Eng., 40, 119 (1962) .
76. Garner, F. H., Foord, A., and Tayeban, M., J Appl. Chem., 9, 315 (1959) .
77. Hugmark, G. A. , Ind. Engng. Chem. Fund., 6, 408 (1967).
78. Garner, F. H., and Skelland, A. H. P. and, Ind. Eng. Chem., 46, 1225 (1955) .
79. Garner, F. H. , and Tayeban , M. , Anal. R. Soc. Esp. Fis. Quim. (Madrid) B 56, 479 and 491 (1960) .
80. Yamaguchi, M., Yabuta S., and Nagata, S. K., Chem. Eng. (Japan) 27, 576 (1963) .
81. Mekasut, L., Molinier, J., and Angelino, H., Chem. Eng. Sci. 33, 821 (1978).
82. Mumford, C. J., Ph.D. Thesis University of Aston , (1970) .

83. Olander, D. R., and, Redd, L. B., Chem. Eng. Sci., 19, 67 (1964) .
84. Glasstone, S. K., Laidler, and, Eyring, H., The Theory of rate processes, first ed. McGraw Hill, New York (1941) .
85. Edwards, C. A., and Himmelbau, D.M., Ind. Eng. chem. 53, 229 (1961) .
86. Overcashier, R. H., Kingsley, JR., and, Olney, R. B., AIChEJ. 2, 529 (1956) .
87. Othmer, D. F., White, A.M., and, Trager, E., Ind. Eng. Chem. 33, 1240 (1941) .
88. Jeffreys, G. V., and, Ellis, E.M., Chisa, 65 (1962) .
89. Marangoni, C., Ann, Inst. Phys. 143, 337 (1871) .
90. Sterling, C. V., and, Scriven, L.E., AIChEJ, 5, 514 (1959) .
91. Schindler, D. S., Treybal, R. E., AIChEJ, 790 (1968) .
92. Calderbank, P. H., Trans. Inst. Chem. Eng., 36, 443 (1958) .
93. Vermeulen, T., et al, Chem. Eng. Progress, 51, 85 (1955) .
94. Fick, J. L., Rea, H. E., and Vermeulen, T., US. Atomic Energy Com. OrNL-2545 (1954) .
95. Bird, R. B., Stewart, W. E., and Lightfoot, E. N. "Transport Phenomena", John Wiley, New York (1960) .
96. Nagata, S. k., Yamama, M. , and, Vjihaza, L., Chem. Eng. , (Japan) 23, 130 (1959).
97. Patel, J. M., and, Wellek, R. M., AIChE J., 13, 289 (1967) .
98. Hanson, C., Brit. Chem. Eng. 10, 1, 34 (1965).
99. Davis, M. W., Hicks, T.E., and, Vermeulen, T., Chem. Eng. Prog, 50, 4, 188 (1954) .
100. Oldshue, J. Y., and, Rushton, J. H., Chem. Eng. prog, 48, 297 (1952) .
101. Roberts, F., and, Bell, B. T., Trans. Inst. Chem. Eng. , 35, 7 (1957) .
102. Holmes, J.H., and , Schafar, A. C., Chem. Eng. Prog., 52, 5, 201 (1956) .
103. Mumford, C. J., British. Chemical. Eng. July. 13, 981 (1968) .

104. Akell, R. B., Chem. Eng. Progress, 62, 9, 50 (1966) .
105. Hanson, C., "Recent Advances in Liquid Extraction " , first ed. , (1971), Pergamon Press .
106. Sterbacek, Z., and, Tausk, P., "Mixing in the Chemical Industry ", Pergamon press Ltd.
107. AIChE , "Standard Testing Procedure, Impeller-Type Mixing Equipment ", AIChE., New York, (1960) .
108. Olney, R. B., AIChE J., 10, 827 (1964) .
109. Miller, S. A., and, Mann, C. A, Trans. Am. Inst. Chem. Eng., 40, 707 (1944) .
110. Martin, J. J., Trans. AIChE J., 42, 777 (1946) .
111. Brown, G. G., "Unit Operations" P 507 Wiley, New York, (1950) .
112. Quinn, J. A., and, Sigloh, D. B., Can. J. Chem. Eng., 41, 15 (1963) .
113. Chen, H. T., and, Middleman, S., AIChE J., 13, 989 (1976) .
114. Ali, F. A., MSc. Thesis, Univ. of Manchester (1969) .
115. Yeh, G. C., Hayme, F. H., Moses, R. A., AIChE J., 10, 260 (1964) .
116. Hossain, K. T., Sarkar, S., Mumford, C. J., and, Phillips C. R., Ind. Eng. Chem. Process Des. Dev. 22, 553-556 (1983) .
117. Maclory, M. J., and, Mansori, G. A., Proper Presented to 79th Annual Meeting of AIChE, in Houston, Texas, March 1975.
118. Coulaloglou, C. A., Tavaridles, L. L., "Drop size Distribution and Coalescence Frequencies of Liquid-liquid Dispersions in Flow Vessels" AIChE J., 22, 289 (1976) .
119. Thornton, J. D., Bouyatiotis, B. A., I. Chem. E. Symp. Series 26, 43 (1967) .
120. Lawson, G. B., Ph.D Thesis University of Manchester (1967) .
121. Davies, G. A., and, Jeffreys, G. V., "Advances in Solvent Extraction Technology "Symposium, Bradford University, April (1970) .
122. Jeffreys, G. V., Davies, G. A., and, Pitt, K., AIChE J., Vol. 16, 5, 823 (1970) .

123. Mizrahi, J., and, Barnea, E., Process. Eng,  
60, 1 (1973) .
124. Vijayan, S., and, Ponter, A. B., Proc, I.S.E.C, 1, 3263  
(1974) .
125. Jeffreys, G. V., and, Pitt, K. I., Chem. Eng. Symposium  
Series, 26, 11 (1967) .
126. Williams, et al, cited in, Hitit, A., Ph. D. Thesis,  
Univ. of Aston, Birmingham (1972) .
127. Hanson, C., and, Kaye, D. A., British Patent  
Appl. 44707/63
128. Hossain, K.T., M.Sc., Thesis, University of Aston,  
Birmingham (1970) .
129. Jeffreys, G. V., and, Davies, G. A., C.14." Recent  
Advances in Liquid Extraction" Edited. Hanson, C.,  
Pergamon press (1973) .
130. Sareen, S. S., et al, AIChE J. 12, 1045 (1966) .
131. Davies G. A., and, Jeffreys, G. V., Filtration and  
Separation, July/August, 349 (1969) .
132. Davis, M. W., Hicks, T. E., and, Vermeulen, T.,  
- Chem. Eng. Prog. 50, 4, 188 (1954) .
133. Hanson C., and, Kaye, D. A., Chem and Press Eng.  
214, 413, (1964) .
134. Hartland, S., and, Horvath, M., Ind. Eng. Chem. Process.  
Des. Dev., 24, 1220-1225 (1985) .
135. McKittrick, D. S., U.S. Pat. 2, 164, 193  
(June, 27, 1939) .
136. Schoneborn, H., U.S. Pat. 1, 949, 496 (March 6, 1934) .
137. McConnell, E. B., U.S. Pat. 2, 091, 645 (August 31, 1947) .
138. Scheibel, E. G., Chem. Eng. Progr. 44, 681 (1948) .
139. Battaro, G., U.S. Pat. 1, 651, 328 , (November 29, 1947) .
140. Othmer, D. F., U.S. Pat. 2, 1000, 606 , (May 7, 1935) .
141. Van Dijk, W. D., Pat. 2, 266, 521 , (December 16, 1941) .
142. Holley, A. E., et al., U.S. Pat. 1, 953, 651, (April  
3, 1934) .
143. Mensing, E., U.S. Pat. 2, 176, 899, ( Oct. 24, 1939) .
144. Edeleanu, L., et al, U.S. Pat. 1, 651, 328 ,  
(Nov. 29, 1927) .

145. Standard Oil Department Co., Report SSOD-21,  
(July 29, ( 1949) .
146. Gordon, J.J., and, Cuckney, M., Trans. Inst. Chem.  
Engrs., 24, 90 (1946) .
147. I.M.I., Institute for Research and Development, Israel  
U.S. Pat.3, 489, 526 (1947) .
148. Windscale Mixer-Settler, UK. A.E.A., ISEC , (1971) .
149. Warwick, G. C. I., Scuffham, J. B., and Lott, J. B., (PGC  
Ltd., U.K.) ISEC Vol. 11 (1971) .
150. Ryan, A.D., Daley, F.L., and Lowrie, R.S., Chem. Eng. Prog.  
, 55 (10), 70 (1959) .
151. Dupex Process, Cited in Ref. 154.
152. Mattila, T. K., I.S.E.C., Vol. I., Session 2 (1974) .
153. Stonner, H. M., and Wohler F., I Chem E Symposium Series  
No. 42 Paper 14, Inst. Chem. Engrs. London, (1975) .
154. Mehner, W., et.al, Proceedings International Solvent  
Extraction Conference ISEC', 71 Vol 2, P 1265, Society  
of Chemical Industry, London , (1971)
155. Sleicher, C. A., AIChE J., 5, 145 (1959) .
156. Flynn, A. W., and Treybal R. E., AIChE J., 1, 324 (1955) .
157. Yamaguchi, M., Ind. Eng. Chem. Fund., 2, 113 (1963) .
158. Sleicher, C. A., AIChE J., 6, 529 (1960) .
159. Ricker, N. l., Nakashio F., and King C. J., AIChE J.  
27, 277 (1981) .
160. Stobaugh, R. B., Hydrocarbon Process, 45 (5), 205-214  
(1960) .
161. Gutmann, V. Co-ordination Chemistry in Non-Aqueous  
Solutions, Springer-Verlag, Wein,  
New York, 19, (1968) .
162. Desbanes, J., Pichet P., and Benoit, R. L., Electro  
Chemical Acta. ,13, 1899 (1968) .
163. Geotzee, J. F., Simon, J. M., Bertozzi, R. J., Anal.Chem.  
41 , 766 (1969) .
164. Spurgeon, J. C., Ph.D. Thesis. Univ. of Pittsburg (1972).
165. Brodwell, F. G., Imes R. H., and Steiner F. J., Am. Chem.  
Soc. 89, 3905 (1967) .
166. Fernandez, R., Prue, J. E., Trans. Faraday Soc., 62, 1257

167. Jones, J. Tetrahedron Letters, 31, 2116 (1964) .
168. Goetzee, J. F., and Bertozzi R. J., Anal. Chem. 45, 1064 (1973) .
169. Goetzee, J. F., Simon J. M., Anal. Chem. 44, 1129 (1972).
170. Alders, L. Liquid-liquid Extraction, Elsevier, London, (1959) .
171. Brancker, V. A., Hunter T. G., Ind. Eng. Chem., Anal. Ed. 12, 35 (1940) .
172. Bachman, I., Ind. Eng. Chem. Anal., Ed. 12, 38 (1940) .
173. Othmer, D. F., Tobias, P. E., Ind. Eng. Chem., 34, 690 (1942) .
174. Fredenslund, R., Jones R. L., and Prausnitz J. M., AIChE J., 21, 1086 (1975) .
175. Skojoid-Jorgensen, S., Koibe, B., Gmehling, J., and Rasmussen, P., Ind. Eng. Chem. Process. Dev., 18, 714 (1974) .
176. Wilke, E. R., Chang, P., AIChE J., 1, 264 (1955) .
177. Anderson, J. L., Hall, J. R., and Babb, A. L., Phys. Chem., 62, 404 (1958) .
178. Bonnet, J. C., Ph.D. Thesis, University of Aston, UK (1982) .
179. Hassan, M. S., Fahim, M. A. and Mumford, C. J. Chem. Eng. Data, 23, 2, 162-165 (1988).
180. Arnold, D., Ph.D., Thesis University of Aston (1974) .
181. Hitit, A., Ph.D., Thesis University of Aston (1977) .
182. Scheibel, E. G., AIChE J., 2, 74-78 (1956) .
183. Milos, H., Stanley, H., Ind. Eng. Chem. Process Des., 24, 1220-1225 (1985) .
184. Al-Aswad, K.K., Mumford, C.J., Jeffreys, G.V., AIChE J., 31, 9 (1983).